OCS Study
MMS 2007-061

Study of Barite Solubility and the Release of Trace Components to the Marine Environment

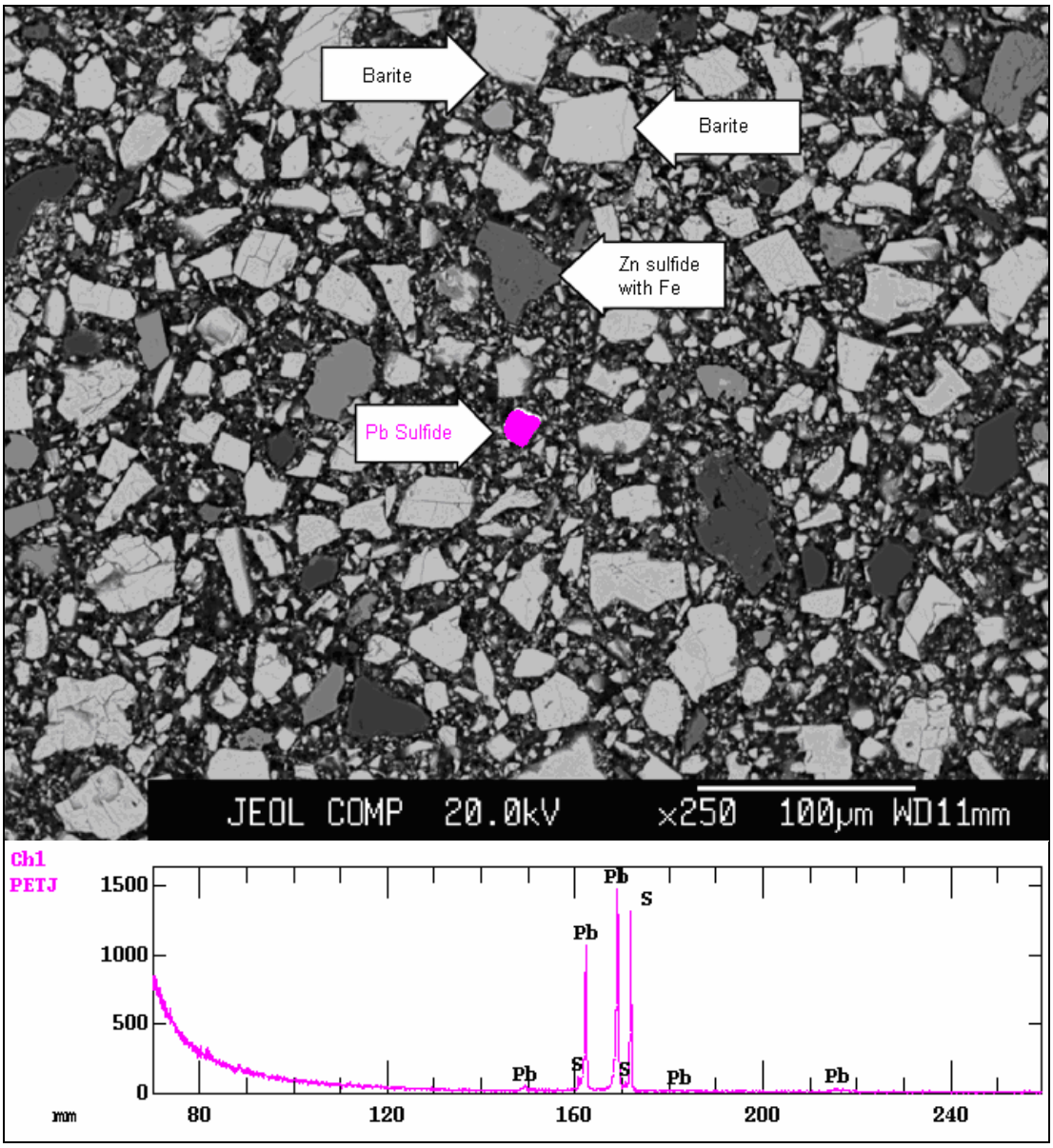

MMS U.S. Department of the Interior
Minerals Management Service
Gulf of Mexico OCS Region

OCS Study
MMS 2007-061

Study of Barite Solubility and the Release of Trace Components to the Marine Environment

Authors

Eric Crecelius
Battelle Northwest Division
Sequim, Washington

John Trefry
Florida Institute of Technology
Melbourne, Florida

James McKinley
Battelle Northwest Division
Richland, Washington

Brenda Lasorsa
Battelle Northwest Division
Sequim, Washington

Robert Trocine
Florida Institute of Technology
Melbourne, Florida

Prepared under MMS Contract
1435-01-02-RP-70000 (M03PC00001)
by
Battelle Northwest Division
1529 West Sequim Bay Road
Sequim, Washington 98323

Published by

U.S. Department of the Interior
Minerals Management Service
Gulf of Mexico OCS Region

New Orleans
December 2007

DISCLAIMER

This report was prepared under contract by Battelle Northwest Division. This report has been technically reviewed by Battelle Northwest Division and the Minerals Management Service (MMS) and it has been approved for publication. Approval does not signify that the contents necessarily reflect the views and policies of Battelle Northwest Division or MMS, nor does mention of trade names or commercial products constitute endorsement of recommendation for use. It is, however, exempt from review and compliance with MMS editorial standards.

REPORT AVAILABILITY

Extra copies of this report may be obtained from the Public Information Office (Mail Stop 5034) at the following address:

U.S. Department of the Interior
Minerals Management Service
Gulf of Mexico OCS Region
Public Information Office (MS 5034)
1201 Elmwood Park Boulevard
New Orleans, Louisiana 70123-2394

Telephone: (504) 736-2619 or
1-800-200-GULF

CITATION

Suggested citation:

Crecelius, E., J. Trefry, J. McKinley, B. Lasorsa, and R. Trocine. 2007. Study of barite solubility and the release of trace components to the marine environment. U.S. Dept. of the Interior, Minerals Management Service, Gulf of Mexico OCS Region, New Orleans, LA. OC5 Study MMS 2007-061. 176 pp.

ACKNOWLEDGMENTS

A special thanks to Carolynn Suslick for report preparation. Your dedication to this report and positive attitude was much appreciated. The authors would like to thank the members of the quality review board (Nicolas Bloom of Studio Geochimica, Dr. James McManus of Oregon State University, Dr. Jerry Neff of Neff and Associates, and Dr. James Ray of Ocean Environmental Solutions) who provided valuable technical reviews of the draft report.

ABSTRACT

Laboratory tests conducted on several fine-grained industrial barite samples indicate that mercury (Hg) and other trace metals are not released in significant quantities into seawater or the pore water of marine sediment. Mercury, cadmium (Cd), copper (Cu), lead (Pb), and zinc (Zn) are the primary metals of marine environmental concern in barite because these metals can be enriched by more than an order of magnitude compared to marine sediment. In addition, the USEPA water quality criteria for these metals are relatively low.

A relatively small amount of these five metals in barite are soluble in seawater in the pH range of 7.3 to 8.3. During one week exposure of barite in seawater, less than 1 percent of the Cu, Hg and Pb, 3 percent of the Zn, and 15 percent of the Cd dissolved from the barite. However, at acidic conditions, simulating the gut of deposit feeding benthic animals, a major portion of the Cd, Cu, Pb and Zn are soluble; and, less than 1 percent of the Hg and barium (Ba) are soluble in 48 hours. The relationships between the soluble trace metals supports their occurrence as Zn and iron (Fe) sulfide mineral phases in the barite mineral. The analysis of the location of trace metals in barite minerals by x-ray microprobe further confirms the occurrence of Cu, Hg, Pb and Zn in minute sulfide mineral inclusions dispersed in a barite matrix.

When barite is added to oxic surface sediment (2 cm thick) and aged for months, the concentrations of Cd, Cu, Hg, Pb, and Zn in the overlying seawater and pore water are considerably lower than for barite alone in seawater. When barite is added to anoxic sediment, the concentrations of Ba, Fe, and manganese (Mn) in pore water increase dramatically as the barite dissolves. The concentrations of methylmercury, Hg, Cd, Cu, and Pb are not elevated compared to the same anoxic sediment without the addition of barite, however, the concentration of Zn in pore water increases by as much as a factor of four in anoxic sediment that contains 10 percent barite.

TABLE OF CONTENTS

PAGE

TABLE OF CONTENTS (continued)

PAGE

TABLE OF CONTENTS (continued)

PAGE

LIST OF FIGURES

PAGE

List of Figures (continued)

PAGE

List of Figures (continued)

PAGE

LIST OF TABLES

PAGE

LIST OF TABLES (continued)

PAGE

LIST OF ACRONYMS

AFIT	Acid leached FIT-Blend barite
Amal.-AFS	Amalgamation atomic fluorescence
AMIH	Acid leached MI-High barite
BSE	Backscatter electron
CVAAS	Cold vapor atomic absorption spectrometry
CVAF	Cold vapor atomic fluorescence
DOI	Department of the Interior
DQO	Data quality objective(s)
EDS	Energy-dispersive x-ray spectroscopy
EMP	Electron microprobe
FAAS	flame atomic absorption spectrometry
FIT	Florida Institute of Technology
FIT-Blend	FIT blended barite
GFAAS	Graphite furnace atomic absorption spectrometry
GOM	Gulf of Mexico
GOMA GOM	GOM sediment with algae
GOMS	GOM sediment
GOMSW	GOM seawater
HCl	Hydrochloric acid
HTMB	High trace metal barite
ICP-MS	Inductively coupled plasma-mass spectrometry
ICP-OES	Inductively coupled plasma optical emission spectroscopy
MDL	Method detection limit
MI-High	High metal barite
MI-Low	Low metal barite
MMS	Minerals Management Service
NIST	National Institute of Standards and Technology
NPDES	National Pollution Discharge Elimination System
NORBAR	North Sea barite sample
OCS	Outer Continental Shelf
OCSLA	Outer Continental Shelf Lands Act
ORPS	Oxidation reduction potential standard
OSPAR	Oslo and Paris Commission
QC	Quality control
SBSW	Sequim Bay seawater
SEI	Secondary electron detector
SEM	Scanning electron microscopy
SRM	Standard reference material
US	United States
USEPA	United States Environmental Protection Agency
WQC	Water quality criteria
XMP	X-ray microprobe

1.0 Introduction

Barite is a weighting agent used extensively in drilling mud in the Gulf of Mexico. In 1989, the use of barite as a weighting material in drilling fluids accounted for 90 percent of the total United States consumption. Barite is mined around the world and the purity of the raw material varies with the source. Trace metals are one of the impurities within barite and mercury (Hg) and cadmium (Cd) are the impurities of the greatest concern.

The US Environmental Protection Agency (USEPA) studied the trace metals impurities in barite in the 1980's (USEPA 1993). Their analysis of the range of impurities in bedded versus veined barite deposits and the availability of 'clean' barite led to regulations that the barite used in drilling mud and permitted for discharge to the Gulf of Mexico must contain less than 1 part per million (ppm) Hg and 3 ppm Cd. Because the various metals in barite are typically present together, limitations on those two metals also limited the levels of other metals. The insolubility of barite, a quality which suited its use in drilling, was also thought to prevent the release of trace metals into the Gulf of Mexico (GOM). The documenting scientific literature was of a general nature, and in some cases, considered proprietary to the company which performed the research.

Through the Outer Continental Shelf Lands Act (OCSLA), the Department of the Interior (DOI) is responsible for the orderly management of Outer Continent Shelf oil and natural gas resources while maintaining the protection of the human, marine, and coastal environment. The Minerals Management Service (MMS) within the DOI is tasked to conduct studies to monitor the offshore environment impacted by oil and gas exploration and production. MMS works with the USEPA which regulates all discharges to waters through the Clean Water Act, National Pollutant Discharge Elimination System (NPDES).

During the 1990's the Gulf Coast States analyzed fish tissue Hg concentrations and set consumption advisories as needed (Ache 2000). The main source of Hg is considered to be fossil fuel combustion which releases Hg to the atmosphere which is then deposited through rainfall (Neff 2002). Other regional sources that have been investigated by state agencies include discharges from chemical plants such as chloralkali plants and naturally occurring Hg. When the first advisory in state offshore waters for king mackerel was issued, concerns arose that more localized sources, such as drilling mud discharged around offshore platforms could be an additional source of Hg that ultimately accumulates in fish tissue (*Mobile Register* 2001a). The *Mobile Register* published a *Special Report* on Hg in seafood which began in July 2001 and was reprinted in newspapers Gulf-wide (*Mobile Register* 2001b). The Mercury Forum meeting was held in Mobile, Alabama in May 2002 to share information about the latest science in Hg sources, health effects, methylmercury (methyl-Hg) formation, and fish tissue sampling. The Mississippi-Alabama Sea Grant Consortium, a partnership between universities and the federal government, planned the Forum. In addition to and subsequent to the Forum, a special task force was organized at the national level with the representation of many federal agencies to determine the state of knowledge and research needs regarding methyl-Hg in the environment with focus on the gulf coast (NSTC 2004).

1.1 Concentrations and Forms of Hg and Cd in Barite

Previous research reported by Trefry and Smith (2003) and Trefry (1998) provides a synthesis that addresses the issues of the forms of Hg and Cd in barite and the solubility of these metals. The chemical form of Hg in barite is a key factor in assessing the fate in the marine environment. Mercury in barite deposits could occur as a substitution in the crystal lattice of barium (Ba) sulfate (Kramer et al. 1980; Goldschmidt 1954; and Wedepohl 1978), as a separate mineral phase associated with barite (Kramer et al. 1980), or in fluid inclusions in barite (Komov et al.1987).

Candler et al. (1990) reported arithmetic mean concentrations of Hg and Cd of 1.2 and 1.1 µg/g, respectively, for their set of 113 representative samples of barite available in the drilling fluids market from 1975 to 1985. Concentration distributions of both metals were skewed, with a few high concentrations in the presence of many smaller concentrations. As a result, the geometric mean concentrations of 0.38 and 0.40 µg/g, for Hg and Cd, respectively, are more representative of the most frequently observed values. Within their data set, Candler et al (1990) found that concentrations exceeded 5 µg/g in three samples for Hg and seven samples for Cd. The ranges of concentrations reported by Candler et al. (1990) are consistent with concentrations reported by Kramer et al. (1980) for 39 barite samples.

Regulations in the United States (US) limit the Hg and Cd content of barite used in drilling fluids or cuttings to be discharged into the oceans to 1 and 3 µg/g respectively (USEPA 1993). The Oslo and Paris Commission (OSPAR) sets no specific limits on the metal content of barite used internationally. However, OSPAR states that discharge of "barite with lower level of trace metal impurities" does not need to be strongly regulated because this practice poses "little or no risk to the environment" (Oslo and Paris Commission 1995). The OSPAR countries have implemented this provision by requiring quality control measures on barite to exclude sources with high trace metal content. Although concentrations of Hg and Cd in a few barite deposits may be as high as 10 to 30 µg/g relative to levels of <0.10 µg/g in average crustal rock, average Hg and Cd levels in drilling fluid barite are much lower as discussed above. Overall, nine of the 113 barite samples (8 percent) analyzed by Candler et al. (1990) would have exceeded the US regulatory limit for Cd in barite and 29 of 113 samples (26 percent) would have exceeded the US limit for Hg.

The chemical forms of Hg and Cd in barite are a key factor in assessing their environmental fate following marine discharges of drilling fluids. Mercury and Cd could occur in barite deposits as substituted elements in the crystal lattice of barium sulfate or associated with other minerals. Kramer et al. (1980) stated that Hg and Cd found with barite are predominantly present in sulfide phases, especially with sphalerite (ZnS). This statement is consistent with an abundance of sulfides in vein-filling barite deposits and some sulfides in residual barite deposits as discussed below. However, Goldschmidt (1954) stated that Hg was reported to substitute in the barite structure. Conclusive confirmation of Goldschmidt's statement, even with modern methods, would be difficult;

however, substitution of Hg and Cd in the lattice of barite should occur only at low levels.

Barite usually occurs as orthorhombic crystals containing sulfate as a tetrahedral group with Ba present in 12-fold coordination with oxygens (O) belonging to seven different sulfate groups (Gaines et al. 1997). Strontium (Sr), calcium (Ca), and lead (Pb) are the most commonly substituted elements for Ba in the barite structure. These metals form sulfates of low solubility with Ksp values at 25°C as follows: $BaSO_4 = 10^{-10.0}$, $PbSO_4 = 10^{-7.7}$, $SrSO_4 = 10^{-6.5}$, $CaSO_4 = 10^{-4.1}$ (Hogfeldt 1982). Mercury II also forms a sulfate of relatively low solubility (Ksp value at 25°C for $HgSO_4$ is $10^{-6.1}$); a fact that may have influenced Goldschmidt's (1954) statement that Hg may substitute in the barite structure. In contrast, other sulfates, including $CdSO_4$ have much higher solubilities with equilibrium K values at 25°C as follows: $CdSO_4 = 10^{2.5}$; $ZnSO_4 = 10^{2.6}$; $FeSO_4 = 10^{2.2}$ (Hogfeldt 1982). The difference in sulfate solubility for Hg versus Cd suggests a preference for Hg incorporation into the barite structure relative to Cd. However, the basic question remains as to whether Hg and Cd occur primarily in sulfate, sulfide, or other phases. Indisputably, both Hg and Cd have strong affinities for sulfide (Ksp values, $HgS = 10^{-53.3}$; $CdS = 10^{-27}$).

In geological formations, barite occurs in three different types of deposits: (1) metalliferous vein and cavity fillings, (2) bedded deposits in sedimentary rock and (3) residual deposits resulting from the weathering of limestone or dolomite (Kier 1972; Gaines et al. 1997). The nature of the deposit directly influences the amounts and chemical forms of impurities such as Hg and Cd associated with barite. All three types of deposits (vein, bedded, and residual) contain quartz and sulfides. However, vein deposits have abundant sulfide minerals and fluorite, whereas bedded deposits are richer in carbonates with minor amounts of pyrite (FeS_2) and secondary iron (Fe) oxides. Residual deposits also contain minor amounts of sulfides. Bedded deposits generally contain Hg and Cd at levels that are close to levels in average continental crust. This distinction has been generally ascribed to the abundance of sulfide minerals in vein deposits and the enrichment of Hg and Cd in sulfides (Kramer et al. 1980; Candler et al. 1990).

Extensive literature on the geologic setting of barite deposits shows that the general sequence of mineral deposition in many barite deposits is pyrite (FeS_2), marcasite (FeS_2 replacement mineral), galena (PbS), sphalerite (ZnS), barite ($BaSO_4$), and calcite ($CaCO_3$) (Lamey 1966; Hanor 1968; Carr and Smith 1977; Leach 1980; Hutchison 1983; Edwards and Atkinson 1986; Komov et al.1987; Clark and Poole 1989; Ramos and de Brodtkorb 1989; Lottermoser and Ashley 1996; Gaines et al. 1997; Barnes 1997). This trend has been documented for vein deposits from a volcanic/sedimentary sequence in Japan (Oshima et al. 1974) and for a slightly metamorphosed sedimentary sequence in Australia (Carr and Smith 1977). The barite is located at the top of ore veins in both of these cases because it is stratigraphically the last of the S-containing minerals to be deposited. The close proximity and/or co-occurrence of barite with sphalerite, pyrite and/or galena in vein deposits increase the probability for metal-rich, sulfide impurities to be mined along with barite.

The Hg- and Cd-rich barites are clearly those where sphalerite, galena and pyrite are admixed with or adjacent to the barite vein. Cinnabar (HgS) is not commonly reported with barite deposits; however, in those cases where cinnabar was observed, it was in closest proximity to barite (e.g. Komov et al. 1987). No mention of pure CdS phase such as greenochite was found in association with barite ores. Thus, when Hg or Cd is associated with barite as sulfides, they most likely occur as trace components of more abundant sulfide minerals such as sphalerite, pyrite, and galena.

The process of fractionation of sulfides, including sphalerite, pyrite, and galena, separately from barite in vein deposits, favors removal of Hg and Cd with various sulfide phases before the barite phase forms. Data for the Hg and Cd content of sulfides show the higher concentrations of these metals with sulfide minerals rather than iron oxides. Sphalerite is the most Cd-rich of the common sulfides, mainly due to similarities in ionic radii and charge between zinc (Zn) and Cd. Mercury, with its extremely low solubility as a sulfide, is found enriched to similar levels in the three major sulfides. The association of elongated halos of Hg around barite deposits has been used as an effective indicator while prospecting for barite (Komov et al. 1987). At a distance of 20 to 30 m from barite ore bodies, contact ore bodies were found to contain Hg at levels as high as 0.20 μg/g relative to background levels of about 0.075 μg/g. However, a key point made by Komov et al. (1987) is that Hg levels decreased to 0.030 μg/g at the point of contact and inside the barite vein. These trends support the contention that high Hg levels are associated with phases such as sulfides that contact or mix with barites, rather than with the barite phase itself.

Komov et al. (1987) also report a value for Hg in gas-liquid inclusions in barite of 1 μg/g. This Hg value is 25 times higher than the Hg level of 0.04 μg/g in crustal rock. Separation of Hg into the inclusion, rather than incorporation into the barite mineral structure strengthens the case for limited substitution of Hg into the barite lattice. In addition, concentrations of Zn at 200 μg/g were reported for gas-liquid inclusions in barite (Komov et al. 1987). Because Zn and Cd behave similarly in geochemical rock cycles (the mole ratio of Zn/Cd in crustal rock is about 1000 for Zn/Cd weight ratio of 600), the estimated Cd levels in barite gas-liquid inclusions would be 0.3 μg/g, about three times greater than in the average crustal rock. The main point of introducing inclusions here is to support the position that even when Hg and Cd are present during barite formation, they tend to be excluded from the barite lattice by partitioning more strongly into inclusions. However, such inclusions are generally a minor fraction (<10 percent by volume) in barite ores (Leach 1980) and thus these inclusions do not lead to Hg- or Cd-rich barite.

1.2 Goal of this Study

The solubility of barite in oxygenated seawater is fairly well understood (Monnin et al. 1999; Monnin 1999; Rushdi et al. 2000; Church and Wolgemuth 1972). However, unique redox conditions in sediments and the associated biota may have a profound effect on the solubility of barite and the trace metal impurities within the barite matrix. This can result in availability of trace metals that cannot be predicted by theoretical modeling. The conditions under which barite might dissolve (i.e., sulfate reduction) would stabilize the sulfide phases containing Hg and Cd as well as other trace metals that form insoluble sulfides, such as Cu, Pb, and Zn. Conversely, an oxidizing environment would be more favorable for the release of Hg and Cd. This scenario is certainly plausible. The important point for the present study was to carry out research that focuses on dissolution of both Ba and metals in oxygenated water and in anoxic sediment.

This study was designed to gather data to describe trace metals concentrations in barite and the environmental conditions that would cause their release from the barite to the environment. The goal was to produce a document that is specific to barite use in the offshore oil industry in drilling mud, in the Gulf of Mexico. The study includes the species of the metals within the barite, the solubility of the metals under various conditions, including static and flowing conditions, oxygenated and anaerobic conditions, and under acidic conditions.

2.0 Selection of Materials

Five different barite samples were chosen for this study. Two of the samples were made available by Stephen Rabke of M-I SWACO, Houston, Texas. These included a high metal barite (MI-High) from Morocco and a low metal barite (MI-Low) from China. In addition, a blend of two barites (FIT-Blend) was prepared at Florida Institute of Technology (FIT). One barite sample, coded HTMB for high trace metal barite, was also supplied by FIT and was previously used in experiments conducted by Dr. Trefry (Trefry et al. 1986a). The barite sample coded NORBAR, provided by Dr. Stig Westerlund of Rogaland Research, Randaberg, Norway, is typical of barite used in the North Sea. The surface area of three of the barite samples was determined by a gas adsorption technique called BET specific surface area analysis at Porous Materials, Inc., Ithaca, New York. The surface areas (4.5 m^2/g for MI-High, 4.8 m^2/g for MI-Low, and 5.7 m^2/g for FIT-Blend) were similar and indicate the particle size of these three barites are similar.

Total metal concentrations for the five barite samples (Table 1) span a broad range. Concentrations of Hg in three of the barite samples exceed the 1 µg/g limit set for Hg in barite by the USEPA (USEPA 1993). The Cd level in two barite samples exceeded the USEPA limit of 3µg/g. Barite samples with high levels of Hg and Cd were included in the overall study design to provide data for extreme conditions or possibly for barite discharged to the ocean prior to the USEPA 1993 regulation. The MI-Low barite is believed to be representative of that used in the GOM since 1993.

Gulf of Mexico surface sediment (GOMS) was collected with a box core in 20m water depth from the Louisiana continental shelf (28°55'N and 90° 10'W) in February 2004 and stored in plastic buckets at 4°C. The sediment grain size was 4 percent sand, 47 percent silt, and 49 percent clay and contained 46 percent solids and 1.5 percent total organic carbon. The concentrations of metals in GOMS, shale, and fine-grained marine sedimentary rock are included in Table 1. The solubility of barite in sediment included some experiments with mixtures of sediment, barite, and algae (*Ulva sp.*). The algae, a green seaweed collected from a rocky beach in Sequim Bay, Washington, was ground in the blender and stored refrigerated. The dry weight of the algae was 13.6 percent and the total volatile solids were 61 percent of the dry algae.

Table 1

Concentration of elements in barite samples, GOMS, and shale (µg/g).

	Hg	Cd	Ba	Cr	Cu	Fe	Mn	Pb	Zn
MI-Low	0.44	0.35	538,000	15	98	6,603	625	318	35
MI-High	5.9	0.77	524,000	6.5	88	9,267	541	243	167
FIT-Blend	6.7	7	507,000	11	189	29,623	1,321	1,368	1,211
HTMB[a,b]	8.4	9.9	424,000	NA	54	9,200	38	450	2,030
NORBAR	0.05	0.05	NA	40	86	25,300	2,420	18	85
GOMS[c]	0.05	0.33	713	55	17	27,300	442	21	86
Shale[d]	0.4	0.3	580	100	57	47,000	850	20	80

a Trefry et al. 1986a
b Trefry and Smith 2003
c surface sediment from the Gulf of Mexico
d Krauskopf 1967
NA Not analyzed

Gulf of Mexico seawater (GOMSW) was collected from 10m depth at the same location and at the same time as the sediment collection. The GOMSW was collected and filtered using an acid-cleaned all plastic pump, tubing, and in-line 0.45µm pore size disposable filter cartridge. The filtered seawater was stored in acid cleaned polyethylene carboys in the dark at room temperature. Sequim Bay surface seawater (SBSW) was also collected in northwestern Washington State, and filtered using 0.45µm pore size acid cleaned membrane filters, then stored in clean polyethylene containers at room temperature in the dark. The salinity and pH of GOMSW was 31.2 ppt and 8.1, while the salinity and pH of SBSW was 31.1 ppt and 8.0, respectively.

Table 2

Concentration of dissolved metals (less than 0.45µm) in GOMSW and SBSW used for barite solubility.

Metal	**GOMSW (µg/L)**	**SBSW (µg/L)**
Ba	18	10.5
Cd	0.2	0.4
Cu	<0.9	<0.9
Hg	0.009	0.001
Pb	0.1	0.3
Zn	<0.3	4.9

3.0 Trace Metal Species Within the Barite Structure

Barite particles were prepared for mineralogical analysis then analyzed by several instruments in order to identify which of the minerals in the barite contained trace elements such as Cd, copper (Cu), Hg, Pb, and Zn. The barites were known to contain trace contaminants of heavy metals. These were presumed to occur, as previously reported for barites, as sulfide mineral inclusions (Trefry and Smith 2003, Trefry et al. 2003)

Three barite samples of different provenance, designated FIT-Blend, MI-High, and MI-Low, were examined. Also, samples FIT-Blend and MI-High were processed by pH 2.2 acid leaching at FIT, and were designated AFIT and AMIH. The samples were gram quantities of uniform-appearing powders. The samples were of known bulk composition, and included trace impurities of several elements, including Cd, chromium (Cr), Cu, Fe, Hg, manganese (Mn), Pb, and Zn. The distribution of the impurities, either as substitutions in the barite, as substitutions in distinct minor phases, or as major components of discrete mineral phases was determined through the use of several bulk or micro-analytical methods. These methods included x-ray diffraction, scanning electron microscopy (SEM), electron microprobe analysis (EMP), and x-ray microprobe analysis (XMP).

3.1 Method of Analysis

3.1.1 X-ray Diffraction

Samples were ground with a mortar and pestle to a visually homogeneous particle size, and then packed into a zero background slide in a 9 mm well. The slides were mounted into a Phillips X'Pert MPD x-ray diffractometer, and against Cu Kα x-rays over the range 2 – 75º theta.

3.1.2 Electron and X-ray Beam Analysis

The samples were divided, and a sub-sample was prepared for analysis using electron and x-ray beam methods. Each powder sample was dispersed in petrographic epoxy (Epo-Thin), and air was removed by evacuation in a bell jar. The hardened grain blocks were cut and re-mounted in blocks containing quartz grains, then slabbed and mounted onto glass microscope slides. The mounted slabs were milled, then ground to uniform 30 μm thickness using the quartz interference colors as a gauge. The sample surfaces were diamond-polished and carbon-coated for electrical conductivity. All processing was done without contact with an aqueous phase to avoid dissolution or alteration. For grain size determinations, powder samples were dispersed directly onto an adhesive substrate on a microscope planchette, and carbon-coated for electrical conductivity.

3.1.3 Scanning Electron Microscopy Analysis

For particle morphology and sample imaging, the samples were examined in a JEOL 6340f scanning electron microscope, using a backscattered electron detector (BSE) for atomic-number contrast imaging and a secondary-electron detector (SEI) for morphological imaging. The SEI images were used only for particle size determinations

from grain mounts after analysis by an Adobe Photoshop plug in, Reindeer Graphic Fovea Pro 3.0 (Reindeer Graphics). The BSE images provided a ready means for detecting clasts that were compositionally distinct, particularly oxides and sulfides of metals.

Qualitative compositional information, and confirmation of phase identities for minerals, including contaminant metals, was done using energy-dispersive x-ray spectroscopy (EDS). The identity of the mineral phases was deduced from the major-element compositional information provided by EDS spectra, which could be rapidly collected from μm-scale regions on the sample surface.

3.1.4 Electron Microprobe Analysis

For phase relationships, the samples were examined using a JEOL 8200 electron microprobe in a manner similar to that for other materials (McKinley et al. 2004). Wavelength spectrometers were calibrated against mineral standards, and elemental abundance maps were constructed for elements of interest. For each map, an area of interest was defined, 400 μm x 400 μm, and the sample was positioned under the focused electron beam over this area by rastering the stage in two μm steps (each map included 160,000 analysis points.) At each point, the characteristic x-ray flux for each element was measured for 100 msec; a complete set of maps for each sample required 21 h of instrument time.

3.1.5 X-ray Microprobe Analysis

For x-ray microprobe analysis, samples FIT-Blend and MI-High were mounted on an optical bench stage at the Advanced Photon Source, Argonne National Laboratory. The x-ray beam was focused using Kirkpatrick-Baez mirrors and tuned using a silicon-crystal monochrometer, providing an intense 5 μm x-ray 'spot' on the sample surface. The method provides elemental detection limits of approximately 1 μg/g, two orders of magnitude lower than available using EMP, but provides a lesser optical resolution (Heald et al. 1999, McKinley et al. 2004). For comparison with high-resolution BSE images and location of associated phases, the XMP images were superimposed on BSE images using Adobe Photoshop.

3.2 Results

The comprehensive set of results is presented in Appendices A through F, which include sections organized as follows:

- Appendices A and B include detailed EMP results for sample FIT-Blend, including elemental abundance maps, BSE images, EDS spectra of selected mineral inclusions, and full wavelength scans of selected inclusions showing complete qualitative compositions.
- Appendix C includes EMP elemental abundance maps for samples MI-High, MI-Low, AFIT, and AMIH.
- Appendix D includes combined BSE images and XMP elemental abundance maps for sample FIT-Blend.

- Appendices E and F include XMP elemental abundance maps, alone, for sample MI-High and FIT-Blend.

X-ray diffraction analysis was not able to distinguish any mineralogical differences between the barite samples. When the diffraction patterns were overlain, each sample included the same peaks in x-ray scattering (Figure 1). Close comparison showed that peaks were similar between samples.

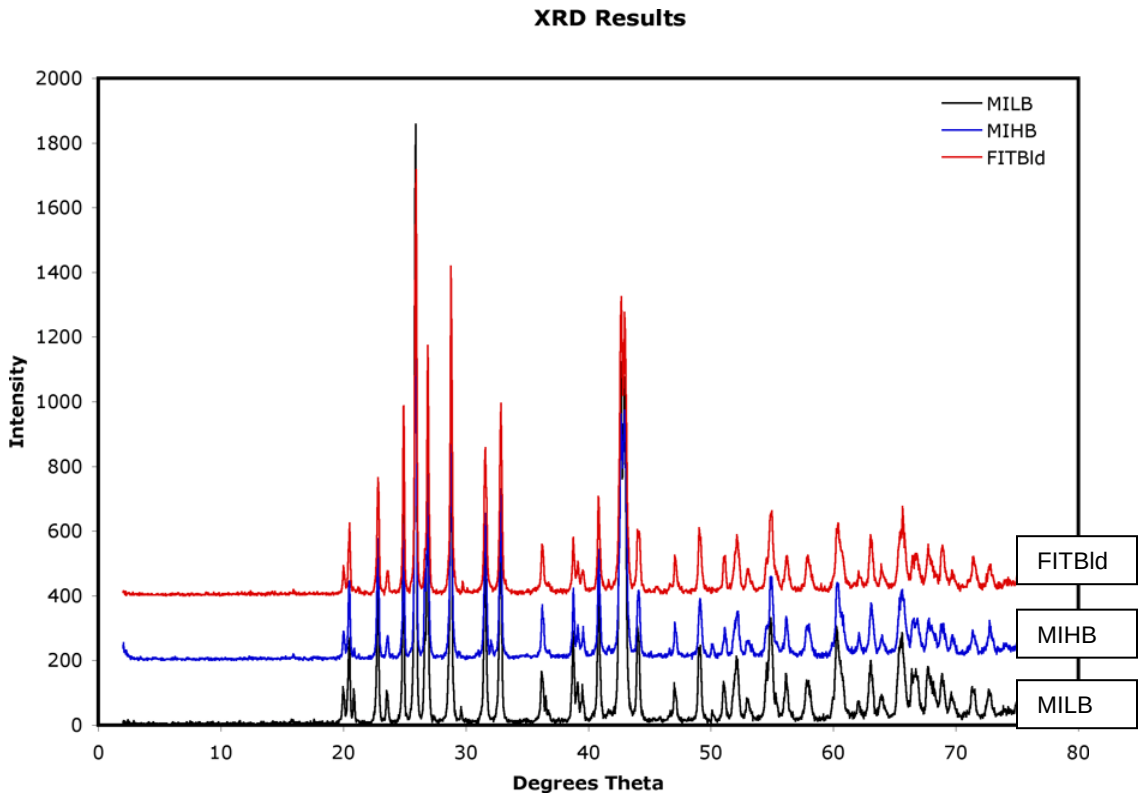

Figure 1. X-ray diffraction patterns for three barites.

Particle size determinations indicated that FIT-Blend and MI-High had similar particle size distributions, with equivalent particle diameters of 5.6 µm and 4.8 µm, respectively (Table 3). Sample MI-Low was finer, with an equivalent particle diameter of 1.4 µm.

The sample FIT-Blend was treated as representative of barites, and was subjected to the most complete analyses (see Appendix A and Appendix B). In addition to barite, BSE imaging and EDS analyses showed the presence of quartz; iron oxides; Fe, Zn, and Mn sulfides; silicate minerals; and phosphate minerals. Lead and Hg were found to be associated as components of sulfide mineral inclusions. Copper was associated with Pb sulfides, but also occurred rarely as Cu sulfide. Strontium was detected as a minor component of some barite clasts. X-ray microprobe analysis provided more sensitive detection of Hg, Pb, and Sr (Section 3.2.2). Strontium was found to reside in minute inclusions of an unidentified phase, where it was much more concentrated, as well as a

trace component of barite. Mercury and Pb were observed to occupy separate high-concentration phases, also as minute inclusions.

The MI-High sample included Pb and Zn associated in sulfide inclusions, and discrete inclusions of minute phases containing unassociated Zn, arsenic (As), Hg, Pb, and Sr. The minor phase abundances were not noticeably different from the FIT-Blend sample. The MI-Low sample was examined only by EMP. Minute discrete inclusions of Pb, Cu, Mn, and Sr were observed, but the abundance of heavy-metal mineral inclusions was apparently less than for FIT-Blend and MI-High. Quartz was more abundant in this sample.

The acid-leached samples were examined only by EMP (see Appendix C). They included the same minor phases as their unleached counterparts. Although these phases may have been less abundant after leaching, their rarity prevented quantification of differences in abundance between the two sample sets.

Table 3

Particle size distributions determined by image analysis.

Sample	Area, μm^2	Equiv. Diam, μm	Standard Deviation
FIT-Blend	35	5.6	3.5
MI-High	20	4.8	1.9
MI-Low	5	1.4	0.5

3.2.1. EMP

Results from EMP analyses are presented as a series of figures with explanatory captions in Appendix A and Appendix B. The FIT-Blend sample was shown to be predominantly barite, as was known. A number of trace elements were detected as discrete included particles of oxide and sulfide mineralogy. In particular, Pb sulfides were widely detected, and these apparently included Hg. Minute discrete particles that contained Zn, phosphorus (P), Mn, Cu, and Cr were found. Cadmium was expected from bulk analysis, but not observed, and Sr was detected, associated with barite.

Figures A-2 through A-7 present elemental abundance maps for elements of interest from an area included in Figure A-1. Included in each figure for reference is a pixel-by-pixel backscatter electron (BSE) image collected along with the abundance maps. Each map was collected by tuning an individual spectrometer to the x-ray wavelength for the element of interest, using an appropriate standard material. The maps were then made by moving the sample under the electron beam in a 400 x 400 pixel array, stepping the sample 2 μm between steps, and collecting the characteristic x-rays at each point for 100 msec. Four iterations were required to map 14 elements on four spectrometers; total collection time was approximately 21 hours. The false-color maps are accompanied by

keys that indicate the characteristic x-ray flux (intensity) associated with each color, and the percent of the image occupied by each intensity. They thus map the distribution over the sample of each element. The false-color maps are self-normalizing, so that each image ranges from blue to white regardless of the maximum x-ray flux. When an image is collected for an element that is not detectable (e.g., for Cd, Figure A-5), the map is speckled because the full false-color range is assigned to random background. An apparently dark image contains points for which the characteristic x-ray flux is high due to inclusions of the element of interest, and the element of interest is of low or zero abundance elsewhere (e.g., Mn, Figure A-5). Figure A-7 presents abundance maps for Pb, Cu, Cr, and Zn that were manipulated to enhance the apparent distribution.

3.2.2 XMP

Backscatter electron detection images of sample FIT-Blend, overlain by XMP abundance maps are presented in Appendix D, Figures D1 through D4. Figures E1 through E6 (Appendix E) and Figures F1 through F7 (Appendix F) include XMP elemental abundance maps for MI-High and FIT-Blend samples, respectively. There were a few particles with detectable concentrations of Hg, Pb, and Zn in these XMP elemental abundance maps, and these metals did not appear to be co-located. There was a strong overlap of Cr and Ba. Basically, the Cr could not be imaged except at very strong hotspots. There was As in the glass substrate. Mercury was difficult to find, but the near edge confirmed that some of the hotspot in FIT-Blend (QGZ3) contained Hg.

3.3 Summary

The barite minerals contained minute inclusions of sulfide minerals of Cu, Fe, Hg, Mn, Pb, and Zn. Other minerals present were quartz, iron oxides, silicate minerals, and phosphate minerals. Cadmium was not detected in the barite minerals. Mercury was difficult to find, however, a few particles with detectable concentrations of Hg were present that did not appear to be co-located with other metals. It is possible that a significant quantity of Hg is dispersed throughout the barite mineral at concentrations below detection.

4.0 Solubility of Metals from Barite in Seawater

The solubility of metals from barite in seawater was determined under conditions that are expected to be present in the oxygenated water column on the continental shelf in the GOM. Initial range finding tests were conducted to determine pH, agitation, and the concentration of barite in seawater affecting the solubility of Ba and several other metals over an eight day period. The results of these range finding tests suggested that neither barite concentration nor agitation significantly change the solubility of metals; however, pH made a significant difference. Based on the results of the range finding tests, a series of static solubility tests were conducted for several months at three pH conditions. The affect that temperature and pressure have on solubility of Ba and trace metals was examined for a month and did not appear to differ from room temperature and ambient (atmospheric) pressure. Some solubility tests were conducted under flowing seawater conditions to compare with solubility rates of metals under static conditions.

4.1 Chemical Analysis Methods

4.1.1 pH

The pH of seawater, pore water and sediment was determined using a pH electrode. The electrode was calibrated at 3 points using commercial buffer solutions. To verify the accuracy of the pH measurements in seawater, three synthetic seawater buffers were prepared according to Dickson (1993) and measured at the same time. The pH of these buffers spanned the expected pH range of the study samples. Results for the three synthetic seawater buffers agreed to within 0.1 to 0.2 pH units of the published values.

4.1.2 Total Mercury

Sediment and barite samples were analyzed for total Hg concentration using cold vapor atomic absorption (CVAA) in accordance with modifications to EPA Method 245.5 and SW-846 7471A. Prior to analysis, samples were digested using a mixture of hydrochloric (HCl) and nitric acids. An approximately 200-mg (dry weight) aliquot of each sample was combined with nitric and hydrochloric acids in a Teflon bomb and heated in an oven at 130ºC (±10ºC) for a minimum of eight hours. After heating and cooling, deionized water was added to the sediment digestate to achieve analysis volume. Quality control samples included a blank, a standard reference material (SRM) and triplicate analysis. The method detection limit for sediment was 0.00432 µg/g dry weight.

Total Hg concentrations in water samples were determined using cold vapor atomic fluorescence (CVAF) in accordance with EPA Method 1631. Quality control samples included a blank, a blank spike, a matrix spike, a matrix spike duplicate, a SRM, and a duplicate analysis. Data quality objectives are provided in Table 4. The method detection limit for water was 0.000116 µg/L.

Table 4

Data quality objectives for total Hg by CVAA or CVAF.

Parameter	**Frequency**	**Data Quality Objective**
Initial Calibration Curve	Prior to Analysis	R2>0.997
ICV/CCV	One per batch of 10 samples	85-115%
Method Blank	One per batch of 20 samples	<5x MDL
Matrix Spike/MS Dup	One per batch of 10 samples	71-125%
SRM	One per batch of 20 samples	77-123%
Blank Spike	One per batch of 20 samples	77-123%
Replicate RPD	One per batch of 20 samples	21%

4.1.3 Methylmercury

Seawater samples were analyzed for methyl-Hg concentrations using CVAF in accordance with Draft EPA Method 1630. Water samples were acidified with HCl then distilled into a clean water matrix. An ethylating agent was added to form a volatile methyl-ethylmercury derivative, and then purged onto graphitized carbon traps as a means of preconcentration and interference removal. Samples were then isothermally chromatographed, pyrolitically broken down to elemental Hg and detected using CVAF. Because of limited sample volume, quality control samples included a blank and a SRM. Data quality objectives for methyl-Hg provided in Table 5. The method detection limit was 0.0000260 µg/L.

Table 5

Data quality objectives for methylmercury by CVAF.

Parameter	Frequency	Data Quality Objective
Initial Calibration Curve	Prior to Analysis	R^2>0.997
ICV/CCV	One per batch of 10 samples	80-120%
Method Blank	One per batch of 20 samples	<0.05ng/L
Matrix Spike/MS Dup	One per batch of 10 samples	65-135%
SRM	One per batch of 20 samples	67-133%
Blank Spike	One per batch of 20 samples	67-133%
Replicate RPD	One per batch of 20 samples	35%

4.1.4 Trace Metals Analysis

Prior to analysis, approximately 20 mg of barite or 200 mg of sediment (dry weight) aliquot of each sample was combined with hydrofluoric, nitric and HCl acids in a Teflon bomb and heated in an oven at 130ºC (±10ºC) for a minimum of eight hours. After heating and cooling, deionized water was added to the sediment digestate to achieve analysis volume.

During preliminary investigations, sediment samples were analyzed for trace element concentrations using Inductively Coupled Plasma Optical Emission Spectroscopy (ICP-OES) in accordance with EPA Method 200.7. Barium, Cr, Cu, Fe, Mn, and Zn concentrations were measured. Data quality objectives are presented in Table 6; method detection limits are provided in Table 7. Quality control samples included a blank, a matrix spike, a replicate analysis, and a SRM.

Trace element concentrations of Ba, Cd, Cr, Cu, Fe, Pb, Mn, and Zn in sediment, seawater, and pore water samples were determined by Inductively Coupled Plasma Mass Spectrometry (ICP-MS) using either the Perkin Elmer 5000 or 6100. ICP-MS analysis was conducted in accordance with modifications to EPA Methods 1638, 200.8, and SW6020. Prior to analysis, water samples were diluted by a factor of 10 or 20. Data quality objectives are outlined in Table 6; method detection limits are provided in Table 7. Quality control samples included a blank, a matrix spike, a matrix spike duplicate, a replicate analysis and a SRM.

Table 6

Data quality objectives for trace metals by ICP-OES or ICP-MS.

Parameter	**Frequency**	**Data Quality Objective**
Initial Calibration Curve	Prior to Analysis	R^2>0.995
ICV/CCV	One per batch of 10 samples	85-115%
Method Blank	One per batch of 20 samples	< 10x MDL
Matrix Spike/MS Dup	One per batch of 20 samples	75-125%
SRM	One per batch of 20 samples	<25%
Blank Spike	One per batch of 20 samples	75-125%
Replicate RPD	One per batch of 20 samples	<25%

Table 7

Method detection limits.

Element	**Seawater (µg/L)**	**Pore Water (µg/L)**	**Sediment (µg/g dry weight)**
Ba	0.02	0.02	0.1
Cd	0.05	0.05	0.01
Cr	0.4	0.4	0.06
Cu	0.9	0.9	0.2
Fe	14	14	1.3
Hg	0.0002	0.0002	0.005
Methyl-Hg	0.00001	0.00001	0.00001
Pb	0.01	0.01	0.03
Mn	0.03	0.03	0.04
Zn	0.3	0.3	0.6

4.2 Experimental Design

4.2.1 Range Finding Tests

It was necessary to determine both a sufficient concentration of barite in seawater and the duration of aging required to observe the solubility of barite as evidenced by the release of Ba and trace metals. The effect of pH and whether the samples remained static or were agitated was also investigated. These tests were conducted at room temperature (18-22° C) and pressure (760 mm). Three aliquots of seawater with a salinity of 31 ppt were adjusted to pH 7, 8 and 9 respectively to exceed the pH range typically found in oceanic environments.

High trace metal barite (HTMB) was added to seawater aliquots of each pH level at a concentration equal to 10 g/L, 20 g/L and 40 g/L and remained in static condition. HTMB barite was also added to seawater aliquots of each pH level at a concentration of 20 g/L and the bottles were agitated continually on a shaker table at 60 rpm. All bottles were stored in a dark cabinet at ambient temperature and sampled after one day, two days, four days, and eight days. At the prescribed time an aliquot was removed from each bottle and vacuum filtered through an acid-cleaned filter membrane of 0.45 µm pore size. The filtrate was decanted into acid-cleaned Teflon bottles, acidified with trace metal grade nitric acid to pH <2, and analyzed for trace metals.

4.2.2 Static Solubility Test at Ambient Pressure

The solubility of barite as a function of time (as evidenced by the release of Ba and trace metals) was determined under static conditions in the dark at three different pH levels, at room temperature and pressure. Three aliquots of filtered GOMSW were used. The pH of one aliquot was adjusted to 7.3; the second to 8.3; and, the third was unadjusted (pH was 8.1). One hundred milliliters of each aliquot was removed, filtered through a 0.45µm membrane filter, acidified to pH <2, and stored in Teflon bottles for analysis of metals to determine the concentrations of metals in the GOMSW.

A total of nine sample types were produced: three with barite at pH 7.3, three with barite at pH 8.3, one with barite at pH 8.1, one with sediment at pH 8.1, and one with sediment and barite at pH 8.1. MI-Low, MI-High and FIT-Blend were added to GOMSW of pH 7.3 and 8.3 at a concentration of 20 g/L (2 percent wt/vol). FIT-Blend was added to GOMSW at pH 8.1 at a concentration of 20 g/L. Gulf of Mexico sediment (GOMS) was added to GOMSW at a concentration equivalent to 75 g/L dry weight, resulting in a sediment layer about 2 cm thick in the bottom of the liter bottle. To an aliquot of GOMS, 20g FIT-Blend was added thus producing a liter bottle with a 2 cm layer of sediment that was 22 percent barite.

These nine sediment/seawater sample bottles were stored in a dark cabinet at room temperature and atmospheric pressure. After 2, 24, 168, 690 (1 month), 2160 (3 months), and 4320 (6 months) hours, a 100 mL aliquot was removed from each bottle, vacuum filtered through an acid cleaned filter membrane of 0.45 µm pore size, preserved with acid to pH <2, and stored in Teflon bottles. Sample aliquots were submitted for trace metal analysis. Mercury was not analyzed in any samples aged for more than 2160 hours

since Hg had increased dramatically in two of the seawater samples at the 2160 hour sampling.

4.2.3 Static Solubility Test at Elevated Pressure

The solubility of barite was also determined at elevated pressure and 4°C to simulate barite on the ocean floor. By inserting 125 mL Teflon bottles into a pressure chamber made of epoxy coated steel pipe that was pressurized with 500 psi ultra high purity nitrogen gas, the pressure at about 300m depth was simulated.

Test samples were created using 125 mL of GOMSW at a pH level of 8.1 and salinity of 31 ppt. To each seawater sample, 2.5 g of barite was added, producing a concentration of 20 g/L barite in GOMSW. Three different types of barite were investigated: MI-Low, MI-High and FIT-Blend.

Half of the samples were aged at 4°C and atmospheric pressure while the remaining half was aged at 4°C and 500 psi. Aliquots from each aging condition were collected after 24 hours and after one month. At the time of collection, each aliquot was vacuum filtered through an acid cleaned filter membrane of 0.45 μm pore size and the filtrate was decanted into acid cleaned Teflon bottles. Samples were acidified to pH<2 and analyzed for Ba and trace metals.

4.2.4 Flowing Solubility Test

Non-filtered SBSW of pH range 7.9 to 8.1 and salinity of 31 percent was pumped through a peristaltic pump at an average rate of 0.85 milliliters per minute. In-line Teflon filter units which contained filter membranes of 0.45 μm pore size were loaded with barite. The pump accommodated four separate lines so that varying types and amounts of barite could be used. Sequim Bay seawater continuously flowed over the barite for 24.5 hours and a sub-sample was collected at the 2.5, 6.5 and 24.5 hour time intervals. The three samples represent a composite of the metals released from the barite during 0 to 2.5 hours, 2.5 to 6.5 hours, and 6.5 to 24.5 hours. All tubing, filter units, filter membranes, and water containers were acid cleaned. In this way it was possible to identify the solubility rate of barite as evidenced in the release rates of trace elements from barite.

4.3 Results and Discussion

4.3.1 Range Finding Test

Initial experiments were conducted with HTMB barite in SBSW to determine what factors had a major affect on the solubility of barite and several trace metals. These factors included pH values of 7, 8, and 9; barite concentrations in seawater of 10, 20, and 40 g/L of dry barite powder in seawater; barite contact time in seawater of either one, two, four, and eight days; and, the affect of agitation on solubility. Samples were prepared and analyzed for Ba, Cd, Cu, Pb, Mn, and Zn.

Figure 2 shows the amount of trace metal released from barite after either one, two, four and eight days. The concentrations of barite in seawater investigated were 10, 20 and 40

g/L samples kept in a static condition. A fourth sample containing 20 g/L of barite was shaken continuously.

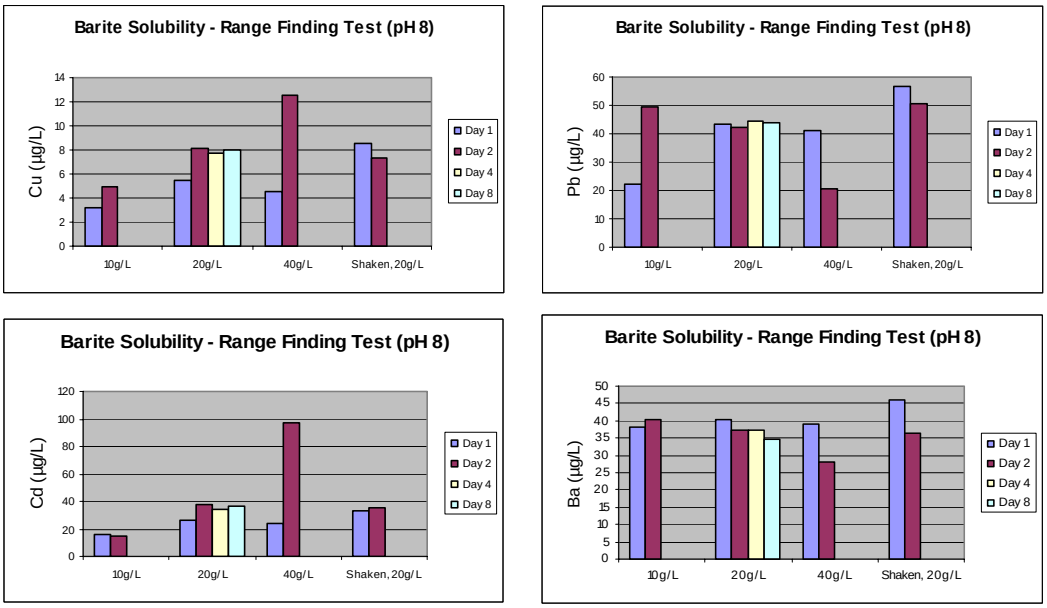

Figure 2. Release of trace metals from various times and concentrations of barite in pH 8 seawater.

Shaking the bottle did not appreciably increase the solubility of barite. The concentration equal to 20 g barite per liter of seawater was sufficient to observe the release of trace metals. For most metals, 10 g of barite per liter of seawater yielded appreciably lower concentrations of trace metals, and 40g barite per liter of seawater did not yield notably higher released concentrations. Thus it was determined that 20 g barite per liter of seawater would be used for the static solubility tests.

It can be seen in Figure 3 that the difference between aging the samples for one or two days is not significant. It can also be seen that the concentrations of trace metals released from barite are comparable at pH levels 7 and 8. At pH 9 the solubility decreased for all metals with the exception of Pb. Because the pH of seawater and pore water is usually in the range of 7 to 8, it was decided that pH levels of between 7 and 8 would be used for the static solubility tests.

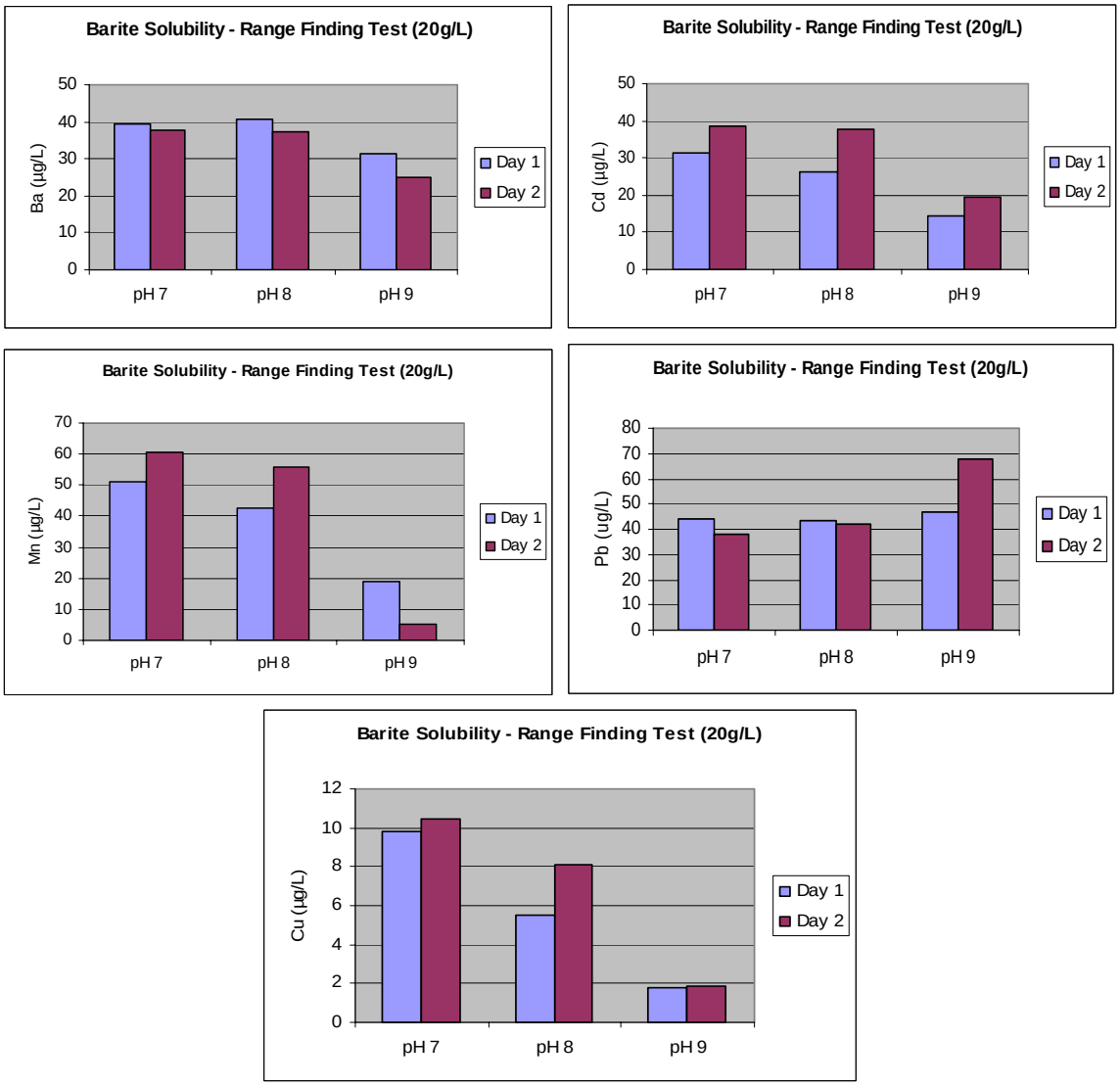

Figure 3. Release of trace metals from barite at various pH levels.

4.3.2 Static Solubility Test at Ambient Pressure

The static solubility testing used one liter of GOMSW, either at the natural pH of 8.1 or adjusted to either pH 7.3 or 8.3, placed in a Teflon bottle, and 20 g of barite or 163g wet weight (75g dry weight) of GOM sediment was added. Samples were aged in the dark, at room temperature and pressure. After different periods of time, seawater was filtered through a 0.45 µm filter and analyzed for total Hg, Ba, Cd, Cu, Pb, Mn, and Zn concentrations.

Figure 4 shows the concentration of trace metal released from barite over the sampling period of 4320 hours (6 months). Mercury was sampled over a period of 2160 hours at which time two of the static tests (pH 7.3 and pH 8.3) containing FIT-Blend show an unexplainable dramatic increase in Hg.

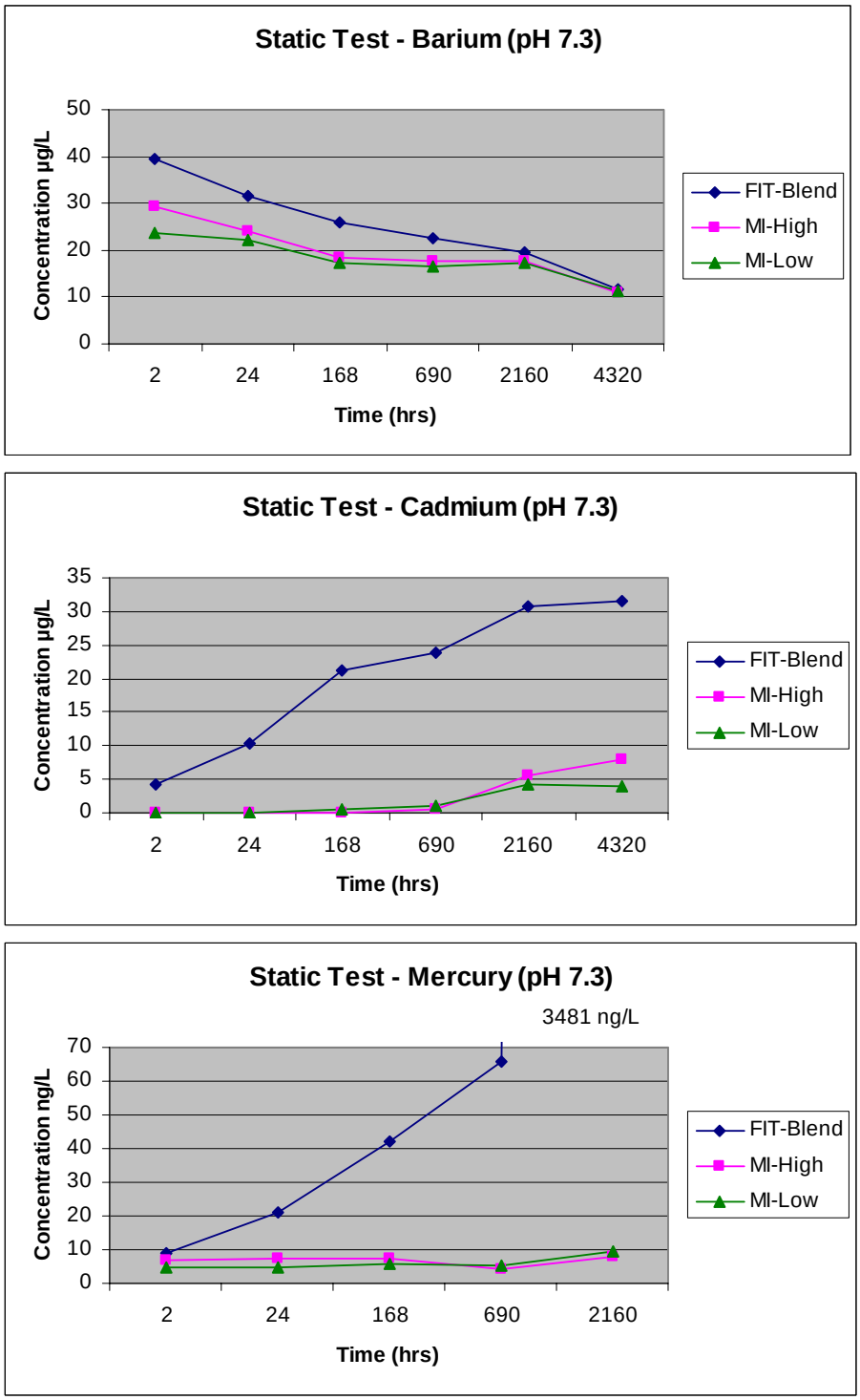

Figure 4. Trace metals released from barite in seawater at pH 7.3.

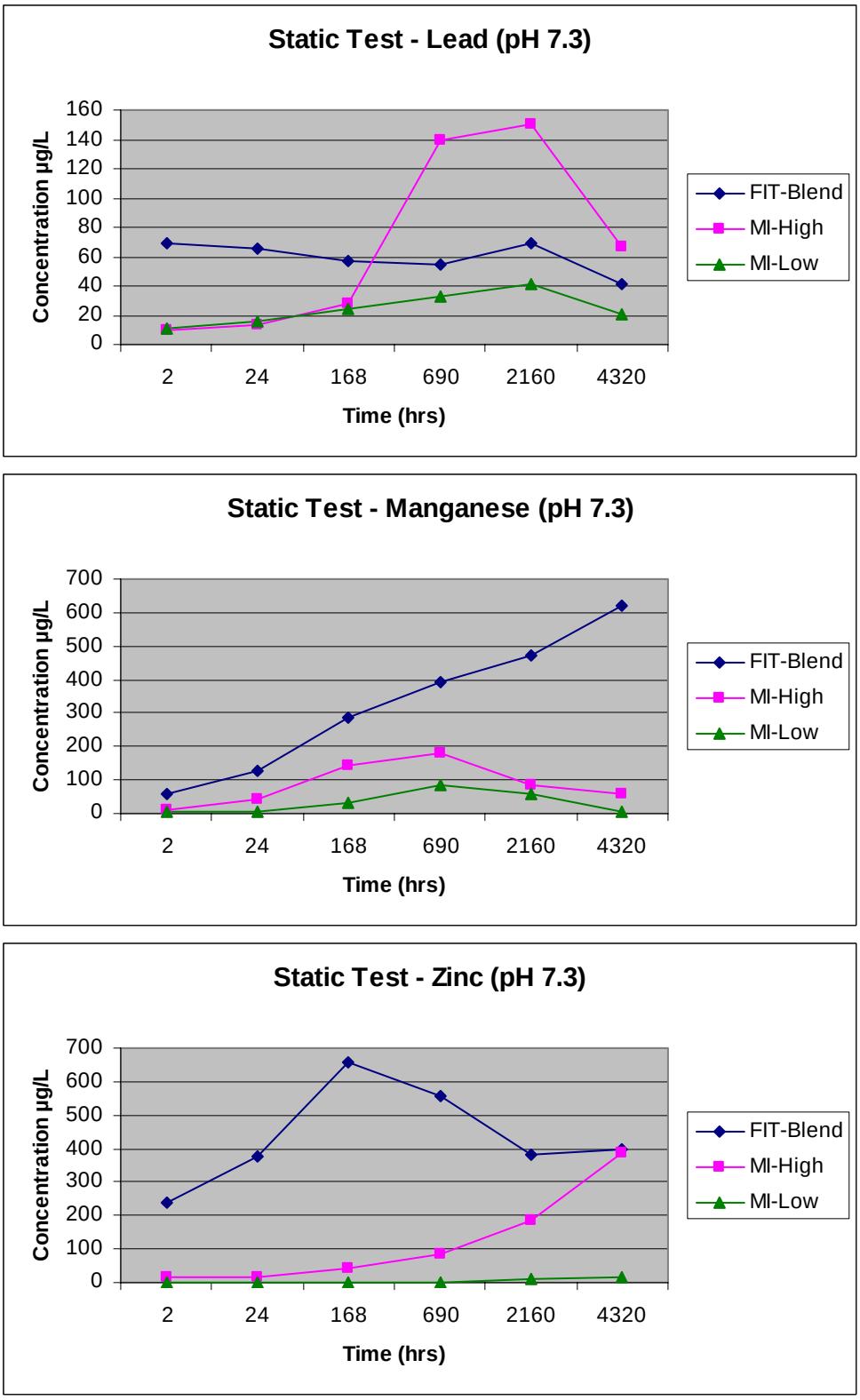

Figure 4. Trace metals released from barite in seawater at pH 7.3 continued.

The Cd, Mn, and Hg concentrations increase over time, most notably in FIT-Blend, which is the barite that has the highest trace metal concentration. Lead concentration increased until 2160 hours and then decreased. Barium and Cu concentrations decreased over time; however, it should be noted that Cu concentrations are not appreciably higher after 2160 hours than those found in coastal seawater.

The same trends are observed in samples created with GOMSW and with a pH adjusted to 8.3 in Figure 5. These samples were also aged at ambient temperature and pressure.

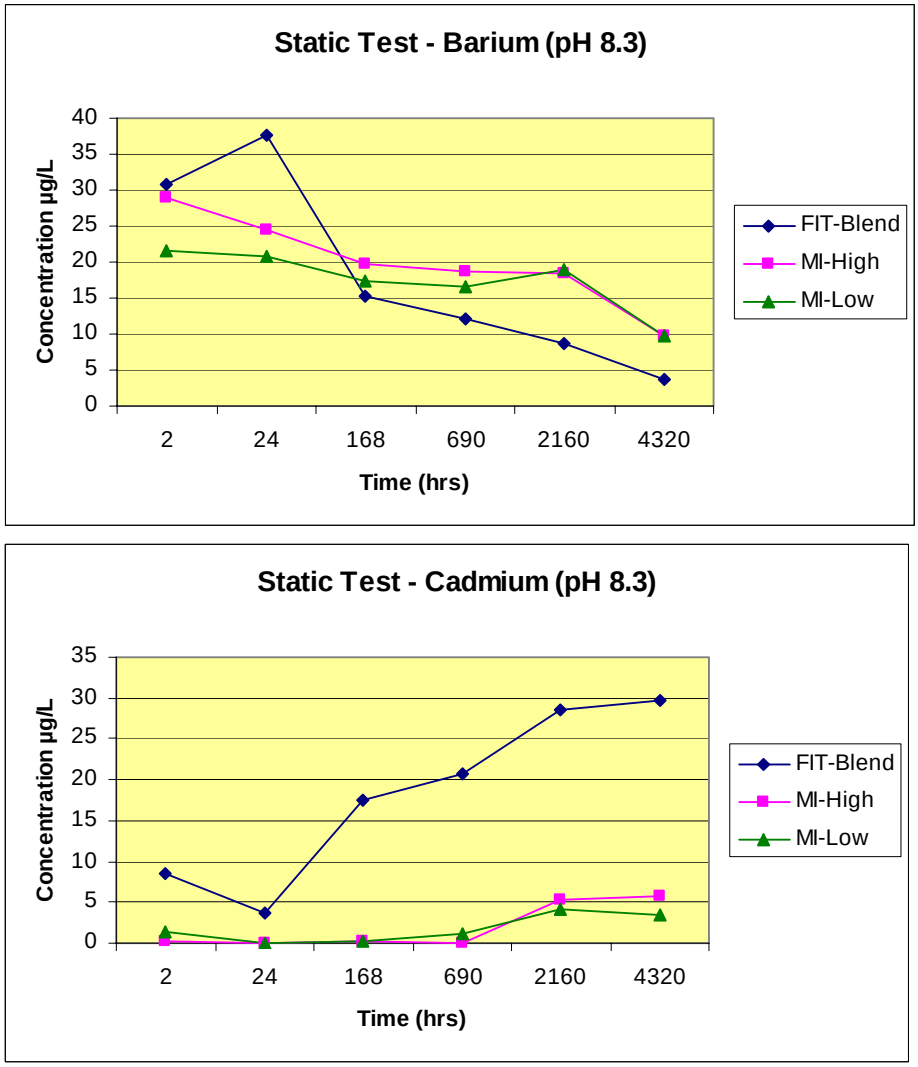

Figure 5. Trace metals released from barite in seawater at pH 8.3.

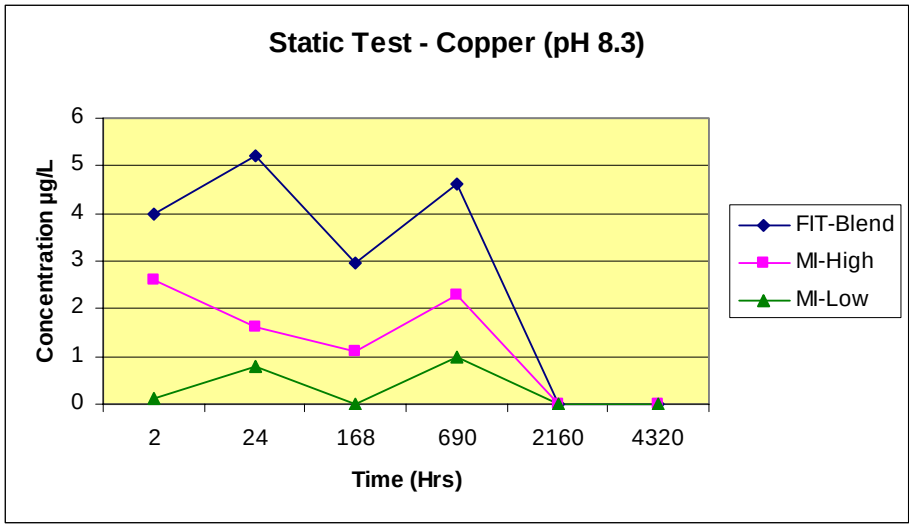

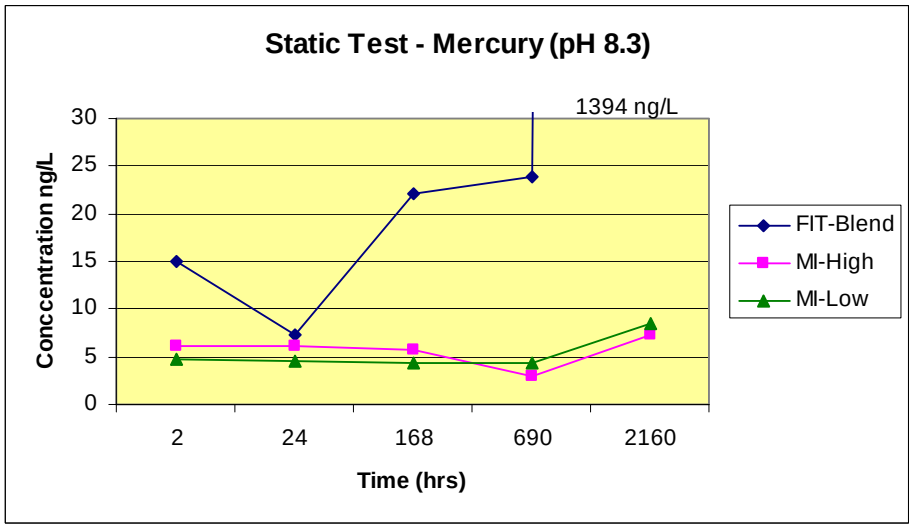

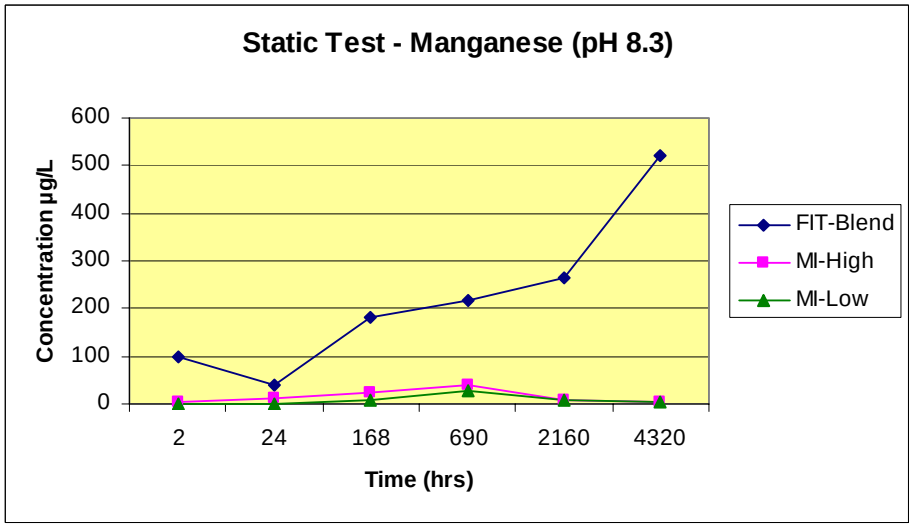

Figure 5. Trace metals released from barite in seawater at pH 8.3 continued.

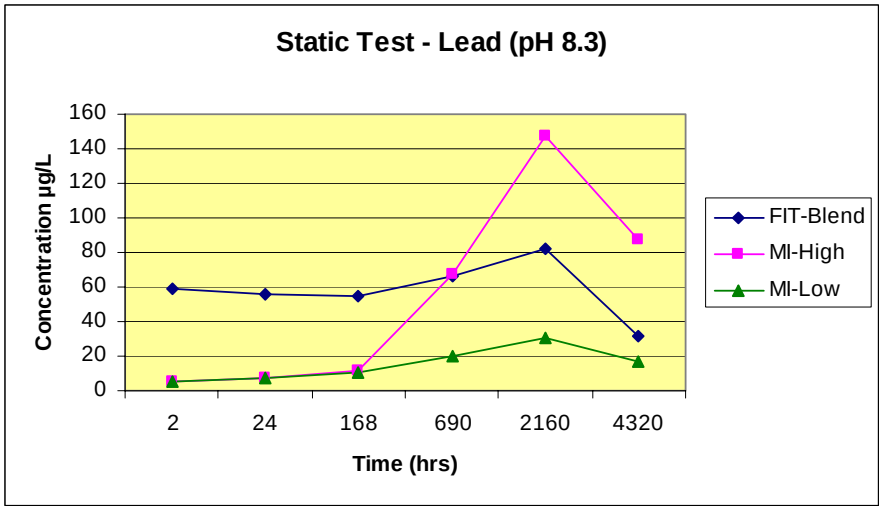

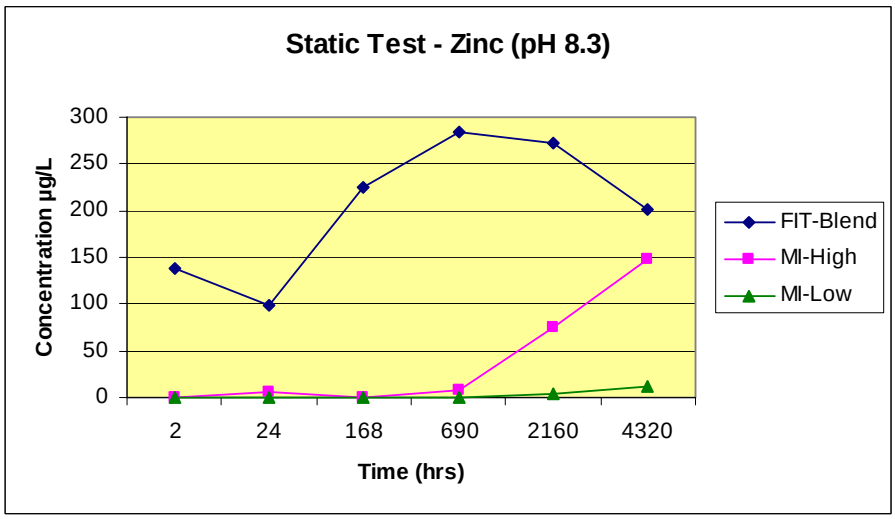

Figure 5. Trace metals released from barite in seawater at pH 8.3 continued.

Again, concentrations of Cd, Mn, and Hg increased over time, whereas Ba and Cu concentrations decreased. Lead showed the same increase until 2160 hours, then decreased. Mercury, Cu, and Zn concentrations measured in samples of pH 8.3 were approximately half the value observed at pH 7.3; but again, the Cu concentrations were found to decrease with time and approach those found in SBSW. This is the only notable difference observed between the two pH levels.

Three other static solubility tests were also conducted over the 6 month period: one with barite (FIT-Blend) in GOMSW at pH 8.1; one with GOMS in pH 8.1 GOMSW; and, the third with both FIT-Blend and GOMS in pH 8.1 GOMSW. These three tests were conducted to simulate the conditions at the sea floor when barite is mixed in surface sediment. The thickness of the barite containing sediment layer in the 1 L Teflon bottle was about 2 cm and contained 22 percent barite (20 g barite and 75 g GOMS) dry weight basis. The concentrations of dissolved metals in the overlying water versus time are shown in Figure 6. The results for FIT-Blend pH 8.1 are very similar to those for pH 8.3 and pH 7.3 except for Hg which increased to 42 ng/L after 2160 hours, remarkably less

than concentrations for similar static tests at pH 7.3 and 8.3 that for unexplainable reasons reach Hg concentrations of greater than 1000 ng/L at 2160 hours. When the mixture of sediment and barite was aged, the concentrations of metals were generally about the same as for sediment alone, indicating the sediment adsorbed the metals that were released from barite. Barium was the only metal that increases over time in the exposure of sediment alone.

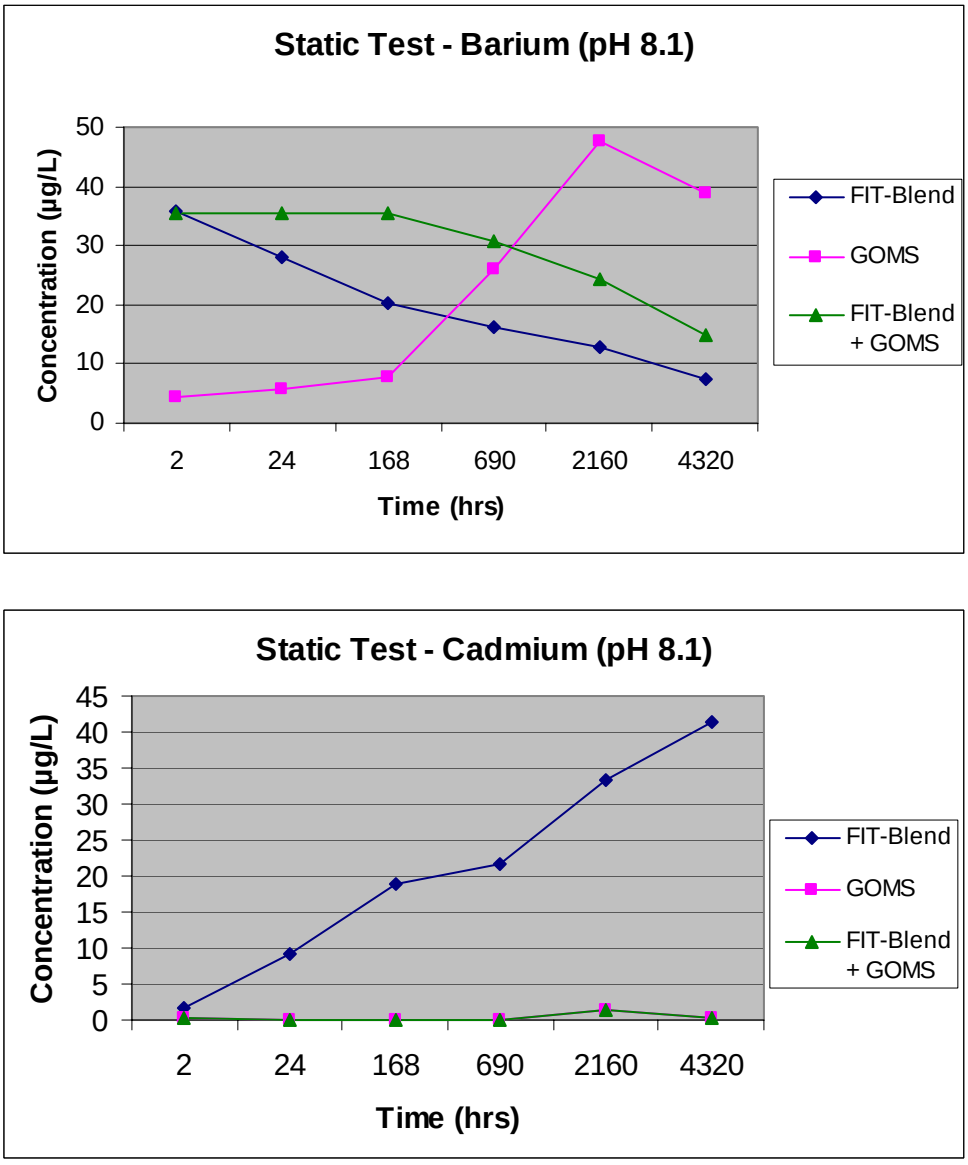

Figure 6. Trace metals released from barite and sediment at pH 8.1.

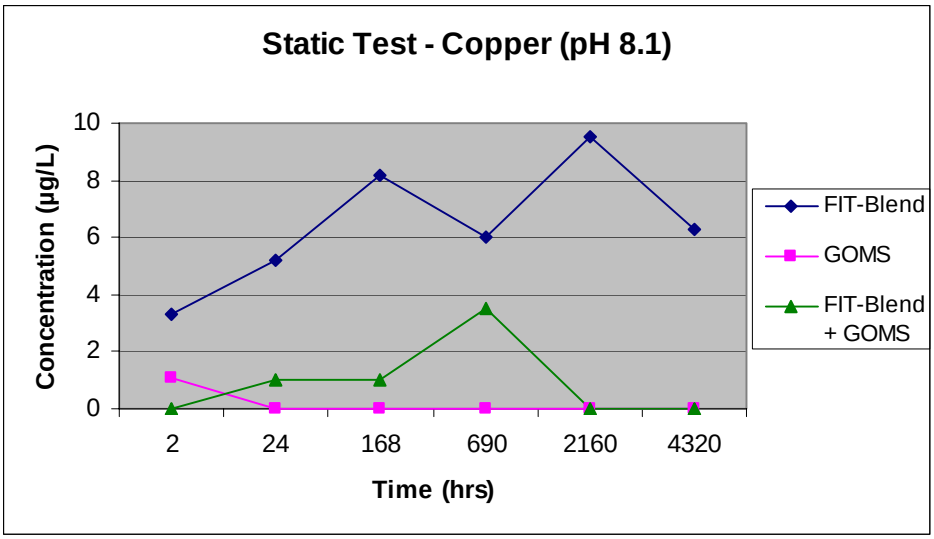

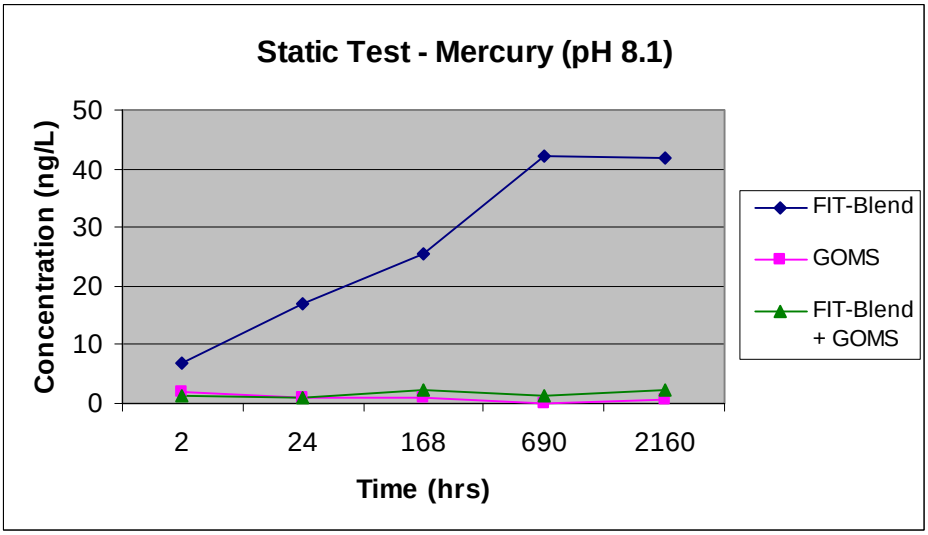

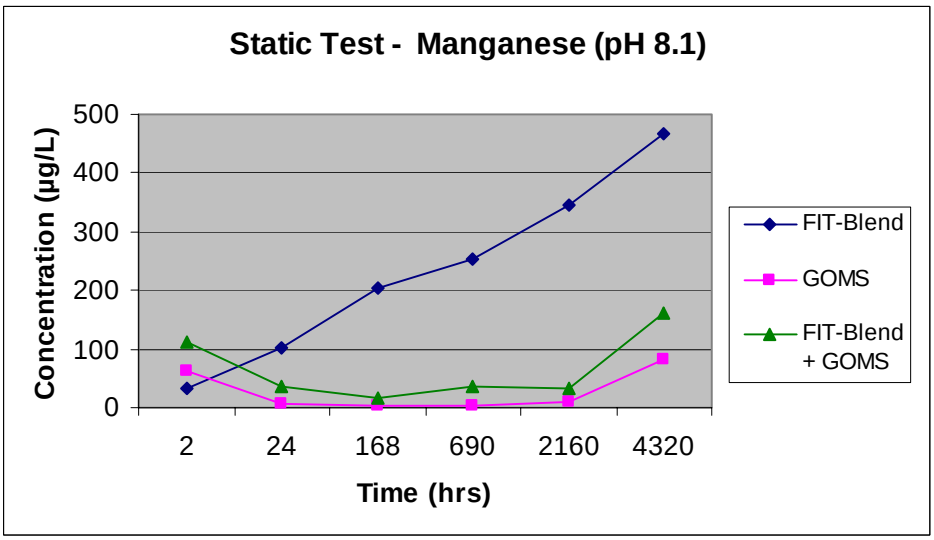

Figure 6. Trace metals released from barite and sediment at pH 8.1 continued.

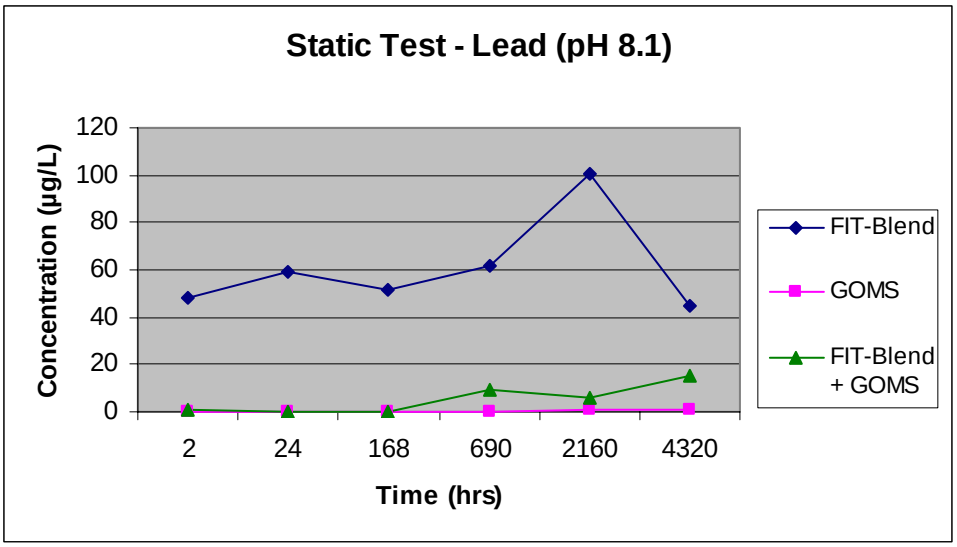

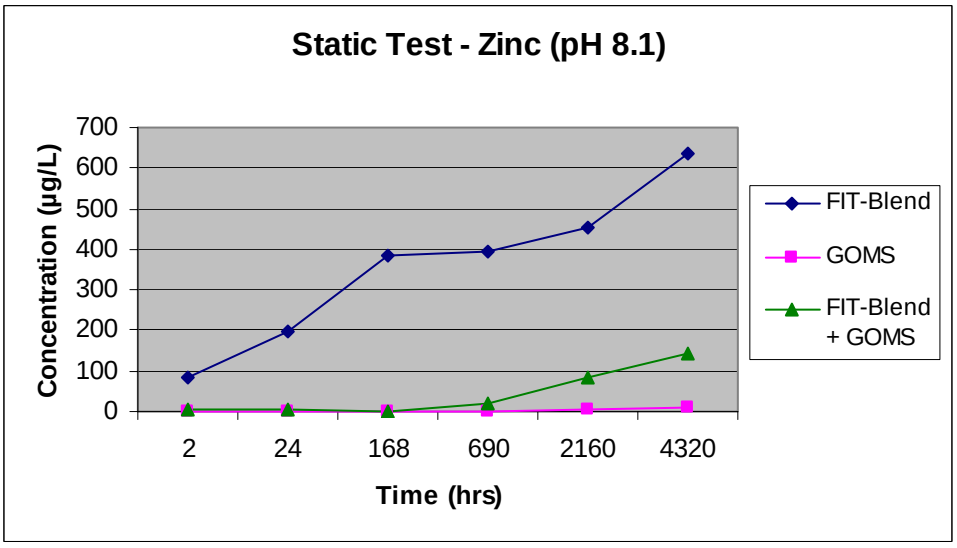

Figure 6. Trace metals released from barite and sediment at pH 8.1 continued.

4.3.3 Static Solubility at Elevated Pressure

The effect of increased pressure on the solubility of barite was also investigated under static conditions (see Figure 7). R1 and R2 identify the two experimental replicate containers of this barite. All samples were aged at 4°C, half at ambient pressure and half at 500 psi. An aliquot was collected after 24 hours and after one month.

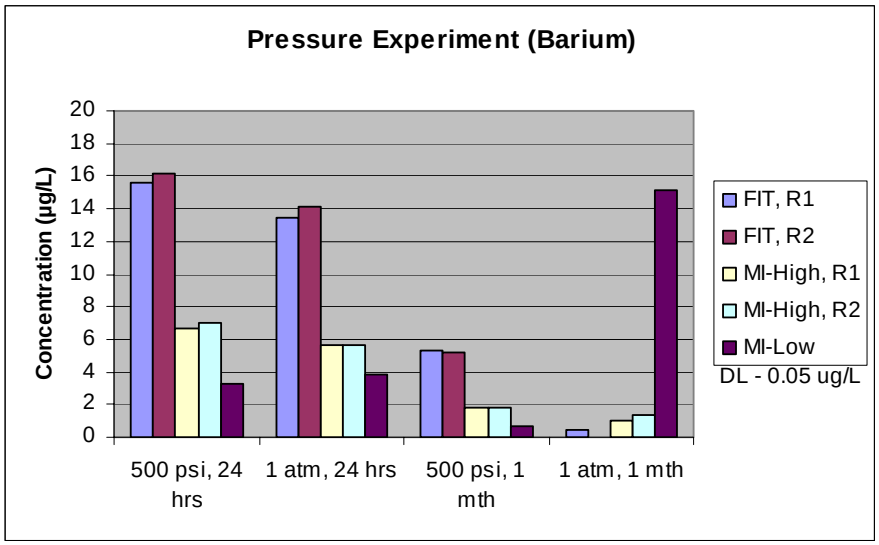

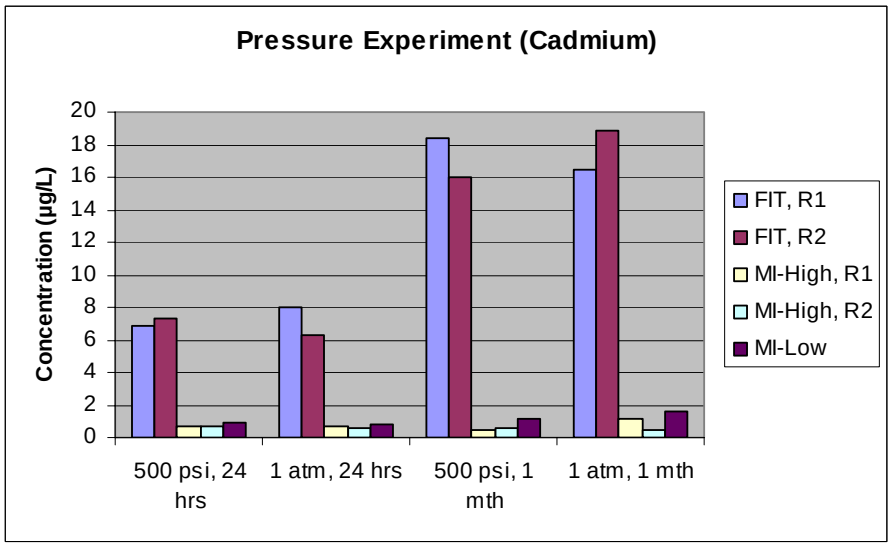

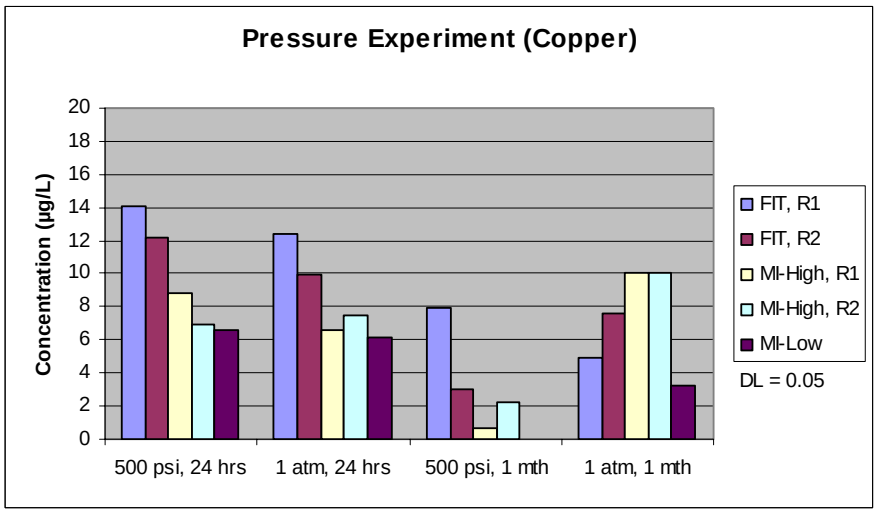

Figure 7. Trace metals released from barite at elevated pressure.

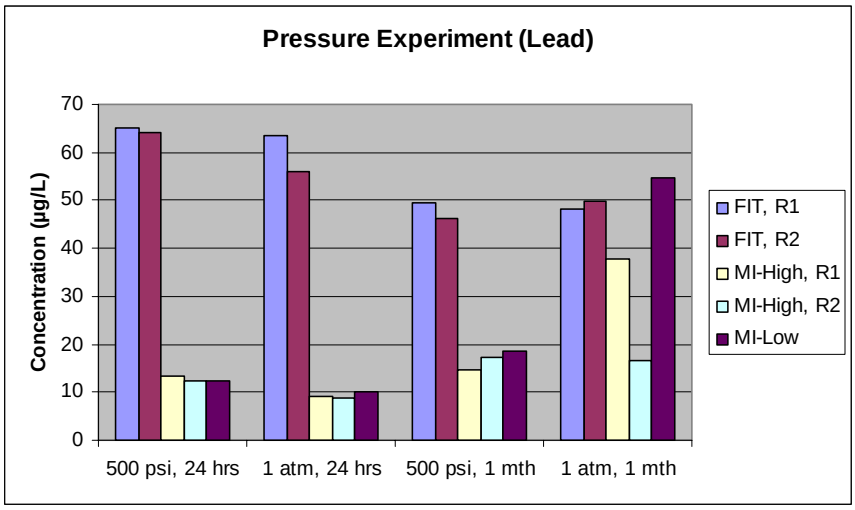

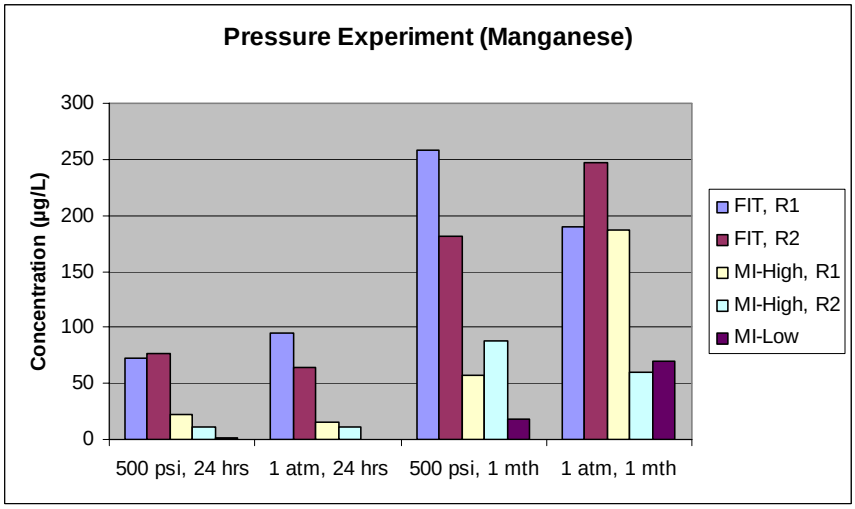

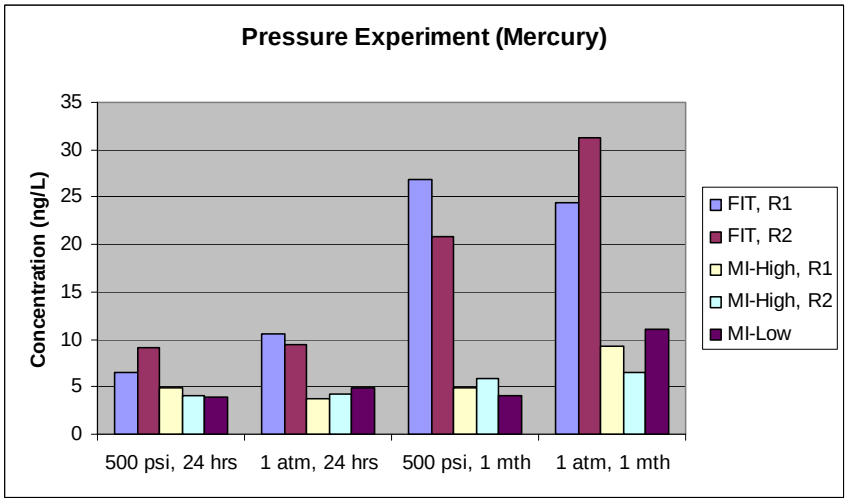

Figure 7. Trace metals released from barite at elevated pressure continued.

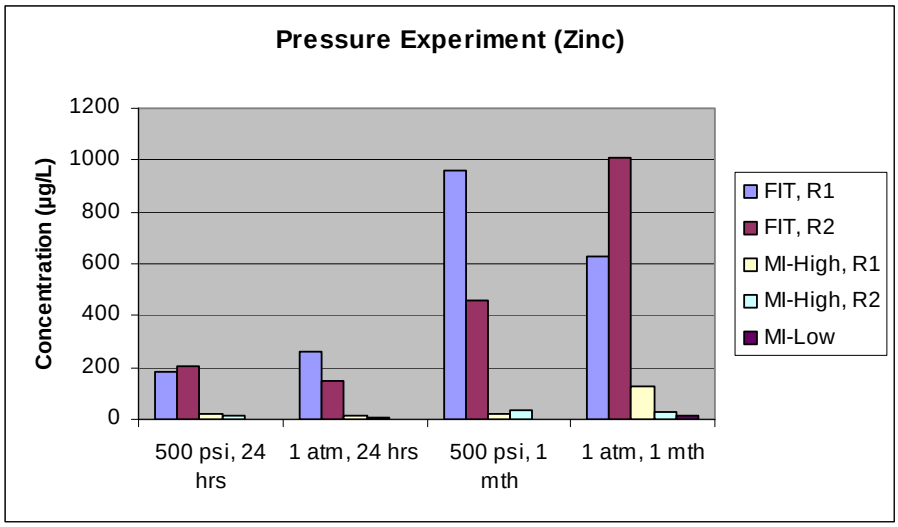

Figure 7. Trace metals released from barite at elevated pressure continued.

Barium, Cu, and Pb concentrations were higher in the sample collected after the first 24 hours regardless of pressure. There appears to be greater Ba solubility at elevated pressure, with the unexplained exception of the high Ba value after one month for MI-Low barite at atmospheric pressure. Concentrations of Cd, Hg, Mn, and Zn were higher after aging one month regardless of pressure. There appears to be no significant difference caused by increased pressure on the release of trace metals. The highest metal concentrations were usually from FIT-Blend barite. Replicate tests of FIT-Blend (R1 and R2) and MI-High (R1 and R2) are in agreement, usually not more than a 20 percent relative percent difference, except for Zn in FIT-Blend at one month.

The concentrations of metals are usually lowest in samples from MI-Low barite; however, in two cases the one month sample exposed at atmospheric pressure had Ba and Pb concentrations similar to those in FIT-Blend at 24 hours. At this time there is no apparent explanation for the two outliers for MI-Low.

4.3.4 Flowing Solubility Test

Samples were generated using the flow through apparatus described in Section 4.2.4. Two separate tests were conducted. In the first test 1g MI-Low and 1g MI-High were loaded onto separate in-line filters. A third empty filter was used as a blank. SBSW of pH 8.0 was pumped over the barite and the separate aliquots were collected after 2.5 hours, 6.5 hours and 24.5 hours. In the second test 0.5, 1.0, and 2.0g of FIT-Blend were eluted with SBSW. Separate aliquots were collected after 2.5 hours, 6.5 hours, and 24.5 hours. An aliquot of SBSW was also collected as a control blank. The samples produced were analyzed for Hg, Ba, Cd, Cu, Cr, Pb, Mn, and Zn. In all cases, Cr was not detected above the natural level observed in seawater and this trace element is excluded from discussion.

Figure 8 shows the rate at which barite dissolves as evidenced by the release of Ba from barite (in microgram trace element per gram barite per hour). The data are blank

corrected for the Ba in Sequim Bay seawater. Although the sample ID's for FIT-Blend indicate the amount of barite which was originally loaded onto the filter unit, the data have been normalized to one gram barite.

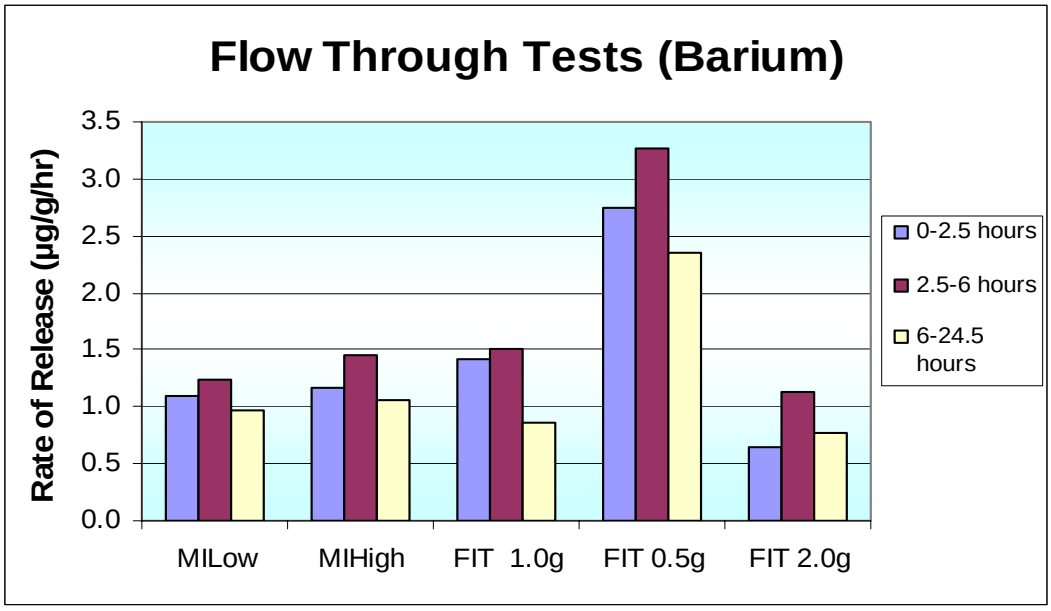

Figure 8. Release rate of Ba from barite.

In each sample the release rate of Ba remains fairly constant over time indicating that the saturation concentration (or a steady state condition) of Ba in seawater is achieved rapidly and remains uniform over the sampling period.

When comparing samples FIT-Blend 0.5g, FIT-Blend 1.0g, and FIT-Blend 2.0g in Figure 8, it can be seen that the maximum release rate of Ba is inversely proportional to the load of barite. When the load of barite was 0.5g, Ba was released at a rate of 2.0 to 3.3 µg/g/hr whereas barite at 1.0g and 2.0g load levels released Ba at a rate of 0.9 to 1.5 and 0.6 to 1.1 µg/g/hr, respectively. This seems to suggest that a greater dilution results in an increased release rate.

This phenomena was also observed for Cu, Pb, and Hg but not for Cd, Mn, or Zn (Figure 9) which may be indicative of the chemical phase in which these trace elements exist within the barite structure.

The highest release rate was observed during the time interval of 0 to 2.5 hours for Cd, Pb, Mn, Hg, and Zn. The maximum percent of each metal released over a 24 hour period was 0.013 percent of the total Ba, 1.6 percent of the total Mn, 0.17 percent of the total Hg, Cd (9 percent), Cu (7 percent), Pb (4 percent), and Zn (8 percent).

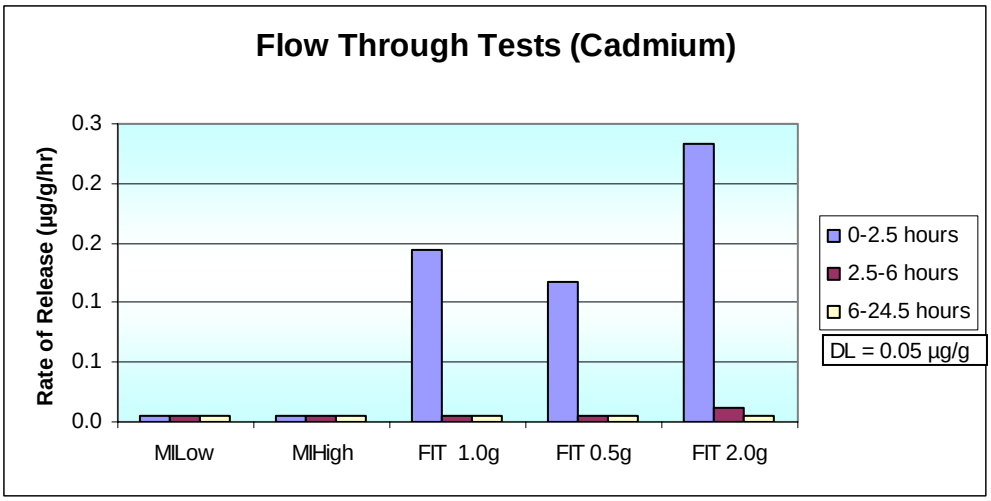

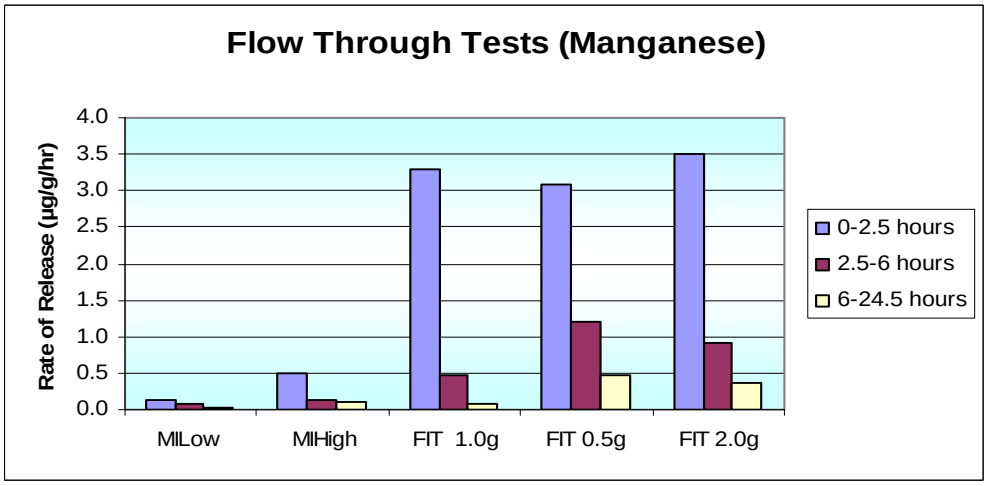

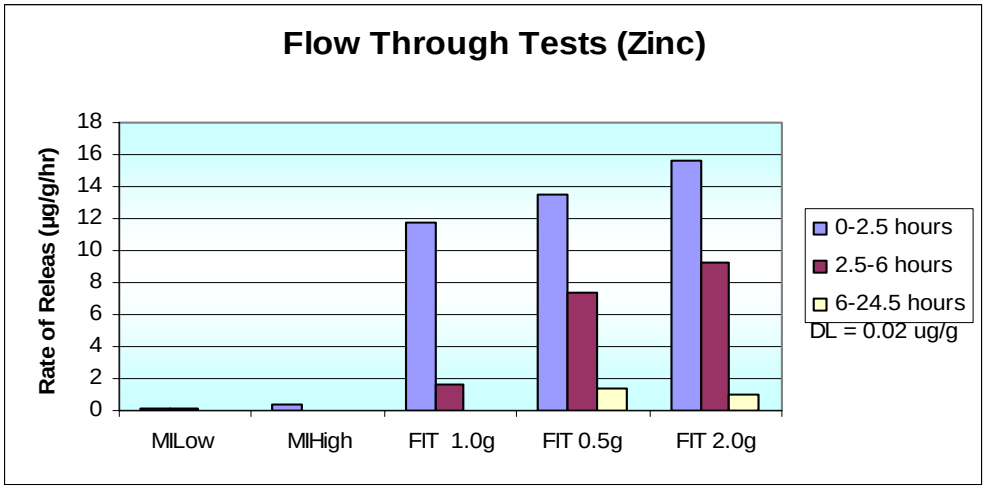

Figure 9. Release rate of trace metals from barite.

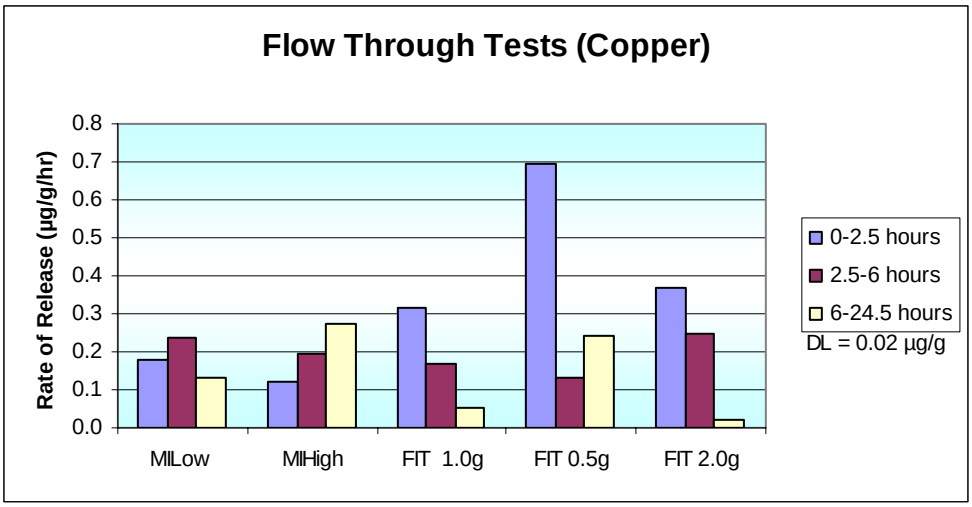

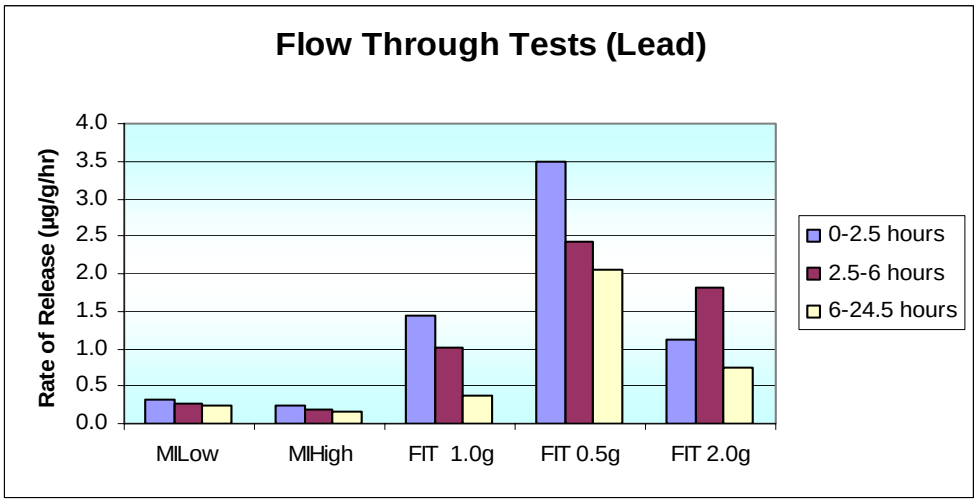

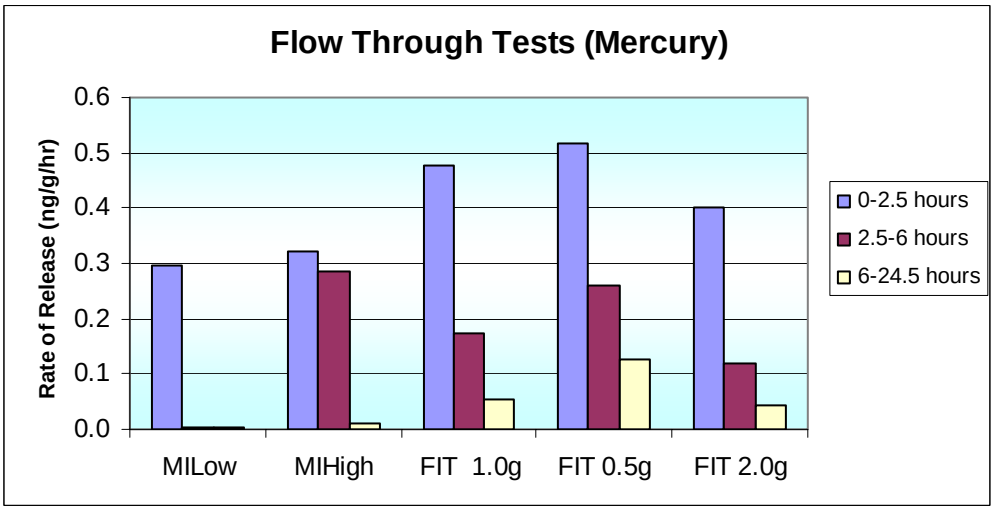

Figure 9. Release rate of trace metals from barite continued.

The maximum trace metal concentration in seawater was also calculated in microgram trace metal per liter seawater per one gram of barite over a 24 hour period. These data are shown in Table 8. When these concentrations are compared to the USEPA Marine Water Quality Criteria (USEPA 2004), only Cu and Pb exceed these criteria for the metal-rich barite samples, not MI-Low.

Table 8

Maximum dissolved trace metal concentrations in seawater flowing over 1g of barite at a rate of 1 L/day compared to USEPA WQC.

Metal (µg/L)	MI-Low	MI-High	FIT 1.0g	FIT 0.5g	FIT 2.0g	USEPA Marine Water (WQC) µg/L
Ba	20	23	18	46	15	NA
Zn	1.2	0.87	27	64	67	81
Mn	0.83	3.0	8.5	15	14	NA
Cu	3.0	5.0	1.7	4.9	1.4	3.1
Cd	0.49	NA	0.26	0.21	0.46	8.8
Pb	4.9	3.4	11	41	17	8.1
Hg	0.00059	0.0017	0.0015	0.0021	0.0012	0.94

NA Not available

4.4 Summary

The static solubility experiments provided an estimate of the maximum concentration of soluble metals that may occur in oxic seawater that is in contact with the barite for periods of hours to months. These concentrations would not be expected to occur in the field where currents and diffusion would dilute the metals.

The range of temperatures and pressures that were tested had little affect on the solubility of metals. However, both the pH and time had major affects on the concentrations of some metals. Mercury and Zn concentrations were about twice as high in pH 7.3 compared to pH 8.3 seawater, while Ba, Cd, Cu, Mn, and Pb were similar between the two pH levels tested. The concentrations of Pb, Mn, Hg, and Zn tended to increase with time for at least several months, while the concentration of Ba decreased with time. The dramatic increase in Hg in two static tests after one month cannot be explained.

The concentration of trace metals in the barite had a major affect on the soluble concentrations. MI-Low barite, which has acceptable concentrations of Hg and Cd for use offshore in the GOM, produced concentrations of Cd, Cu, Hg, Pb, and Zn that are below USEPA Chronic WQC of 8.8, 3.1, 0.94, 8.1, and 81 µg/L, respectively. However, barite that contains elevated concentrations of Hg, Cd, Pb, and Zn, such as MI-High and FIT-Blend, release these metals at concentrations which exceed the WQC.

A mixture of sediment and barite dramatically reduced the release of metals to the static water column compared to barite alone. The layer of oxic sediment (GOMS) containing

22 percent FIT-Blend barite was exposed to static seawater for six months resulting in concentrations of Cd, Cu and Hg below the WQC. However, after several months the concentrations of dissolved Pb and Zn exceeded the WQC by about a factor of two. The conclusion from these experiments is that oxic surface sediment contaminated with barite will cause minimal increases in the concentrations of these metals in bottom water.

5.0 Solubility of Metals from Barite in Marine Sediment

Laboratory experiments were conducted to determine the change in concentrations in Ba and the other trace metals in sediment amended with barite. These experiments were intended to simulate conditions that may occur on the continental shelf near a drilling platform where organic-rich sediment could contain between one and ten percent barite. The static experiments described in Section 4.3 demonstrated that when barite is incorporated in oxic surface sediment, there is almost no release of trace metals (<1 percent of total metal) to the overlaying water.

The following tests were conducted to determine if anoxic sediment will release dissolved trace metals from barite. First, a range finding test was conducted with barite and GOMS. However, the sediment did not become anoxic, evidently because of relatively low organic carbon content. Additional tests were conducted with GOMS that was amended with algae. The addition of algae caused the sediment to rapidly go anoxic.

5.1 Chemical Analysis Methods

5.1.1 Eh

The Eh of sediment samples were measured using a platinum electrode with a silver:silver chloride reference electrode (ThermoOrion model 96-78-00) and the resulting potential was read using an Orion model 701A potentiometer. The vessels containing the sediment/pore water mixture were centrifuged and the pore water decanted before Eh of the remaining sediment was measured. The electrode was inserted approximately two centimeters into the sediment and the potential was recorded after the electrode was allowed to equilibrate in an anoxic sediment for several minutes. Prior to sample measurements, the Eh measuring system was tested for accuracy using a ThermoOrion oxidation reduction potential standard (ORPS), a solution similar to Zobell's solution.

5.1.2 Sulfate

The concentration of sulfate in pore water was determined by ion chromatograph (EPA Method 300) after the pore water was treated to remove sulfide. Pore water was prepared for sulfate analysis by adding 100mg of activated Cu metal particles to remove the sulfide from a 2 mL aliquot.

5.2 Experimental Design

To determine the solubility of barite in sediment, a range finding test was conducted with North Sea Barite (NORBAR) mixed into GOMS at concentrations of 1 percent and 10 percent dry weight basis. NORBAR was used for the range finding test because there was a limited quantity of the other types of barite. GOMS control samples were also prepared. In all, three sample types were produced in triplicate in 50 mL centrifuge tubes: GOM control, GOM + 1 percent NORBAR and GOM + 10 percent NORBAR. Sample mixing was performed under a nitrogen atmosphere. Samples were aged in a dark nitrogen atmosphere at room temperature.

Pore water was sampled from each sample type after two, eight, and 32 days. At each sampling event, the tubes were centrifuged at 2500 rpm for one hour. Pore water was decanted and filtered using acid-cleaned vacuum filter units of 0.45 µm pore size. Each tube yielded approximately 12 mL of pore water. One milliliter was used for sulfate analysis and the remaining aliquot was acidified to pH <2 and stored in Teflon bottles at room temperature until metals analysis.

The data from the range finding tests in sediment revealed that the solubility of barite in oxic sediment was minimal. Barium concentrations in the pore water were low (26 to 45 µg/L) and sulfate was present indicating that the reducing environment necessary to dissolve barite had not occurred (Table 9).

In an attempt to dissolve barite in anoxic sediment, a mixture of sediment, barite and algae was prepared to produce an anoxic environment. Two batches of the sediment-barite mixture were prepared. The first used GOMS mixed with algae (*Ulva sp.*) in a proportion equal to 5 percent algae to sediment dry weight producing Gulf of Mexico sediment with algae (GOMA). FIT-Blend barite and MI-High were added to separate aliquots of GOMA in a concentration equal to 10 percent barite to GOMA dry weight. A GOMA control was also aged and processed. The sediment preparation was conducted under a nitrogen atmosphere and the containers were stored in a dark nitrogen atmosphere at room temperature.

A subset of samples was processed after aging for 39, 63, and 104 days. The 500 mL Teflon jars which contained the mixture were centrifuged at 2500 rpm for one hour. The pore water was decanted from the sediment and filtered under a nitrogen atmosphere using acid cleaned filter units of 0.45µm pore size. The filtrate was decanted into acid cleaned Teflon bottles. Samples were prepared for sulfate analysis. Eh of the sediment was measured. The remaining pore water was preserved at pH <2 and analyzed for trace metals.

The second batch of sediment, algae, and barite mixture was prepared using GOMS and algae in a proportion equal to 2 percent algae to sediment dry weight. To separate aliquots of the mixture, MI-High at concentrations of 1 percent and 10 percent were added. A GOMA control was also prepared, aged, and processed. The preparation of the sediment mixture was conducted under a nitrogen atmosphere and stored in Teflon jars in a dark nitrogen atmosphere at room temperature. A subset of these samples was processed after 43, 68, and 146 days of aging as described above.

5.3 Results and Discussion

The results from the range finding test showed that sulfate concentrations in all samples fall within the 125 to 135 mg/L range (Table 9), indicating that the anoxic environment required to dissolve barite by the reduction of sulfate to sulfide, was absent. This supposition was confirmed by the low levels of Ba in the pore water. With the exception of Fe in some pore water samples, the concentrations of other metals were very low.

Mercury was not analyzed in this pore water because of the very small volumes of pore water generated in the range finding test. Apparently, there was too little organic carbon in the GOMS to create anoxic conditions.

Table 9

Pore water chemistry results for the range finding test using mixtures of GOMS and NORBAR barite.

	Sulfate	Ba	Cd	Fe	Pb	Mn	Zn
Units:	*mg/L*	*µg/L*	*µg/L*	*µg/L*	*µg/L*	*µg/L*	*µg/L*
DAY 2:							
Control GOMS	127	41	*<0.05*	1350	*<0.01*	8.9	3.1
1% NORBAR	129	37	0.06	1450	0.08	8.7	7.2
10% NORBAR	126	41	*<0.05*	762	*<0.01*	8.5	5.2
DAY 8:							
Control GOMS	130	42	*<0.05*	2160	0.03	8.9	3.3
1% NORBAR	133	28	0.06	1310	*<0.01*	8.8	7.4
10% NORBAR	130	26	*<0.05*	2140	0.02	8.7	4.5
DAY 32:							
Control GOMS	130	45	*<0.05*	2490	*<0.01*	8.7	3.6
1% NORBAR	135	29	*<0.05*	2230	*<0.01*	8.6	3.4
10% NORBAR	125	31	*<0.05*	2170	*<0.01*	8.6	2.9

The experiments with algae demonstrated that barite will dissolve in anoxic sediment as sulfate reducing bacteria lower the sulfate concentration in pore water thus increasing the solubility of barite and at the same time producing significant quantities of sulfide. The sulfide should react with those metals that form highly insoluble sulfides such as Hg, Cd, Cu, Pb, and Zn. In this study, the experiments were designed to maximize the dissolution of barite by stimulating the sulfate reducing bacteria with the addition of algae, and by storing the sediment mixture under nitrogen at room temperature.

5.3.1 Batch One Sediment

Relatively high concentrations of Ba were present in pore water from sediment containing barite and 5 percent algae (Figures 10a and 10b). Even the Ba concentration in the control pore water (GOMA) is about 1000 µg/L compared to about 40 µg/L in the GOMS with the addition of algae. The same is true for Fe, Mn, and Zn indicating that these trace metals are released from the barite structure as the reduction of sulfate to sulfide dissolves the barite.

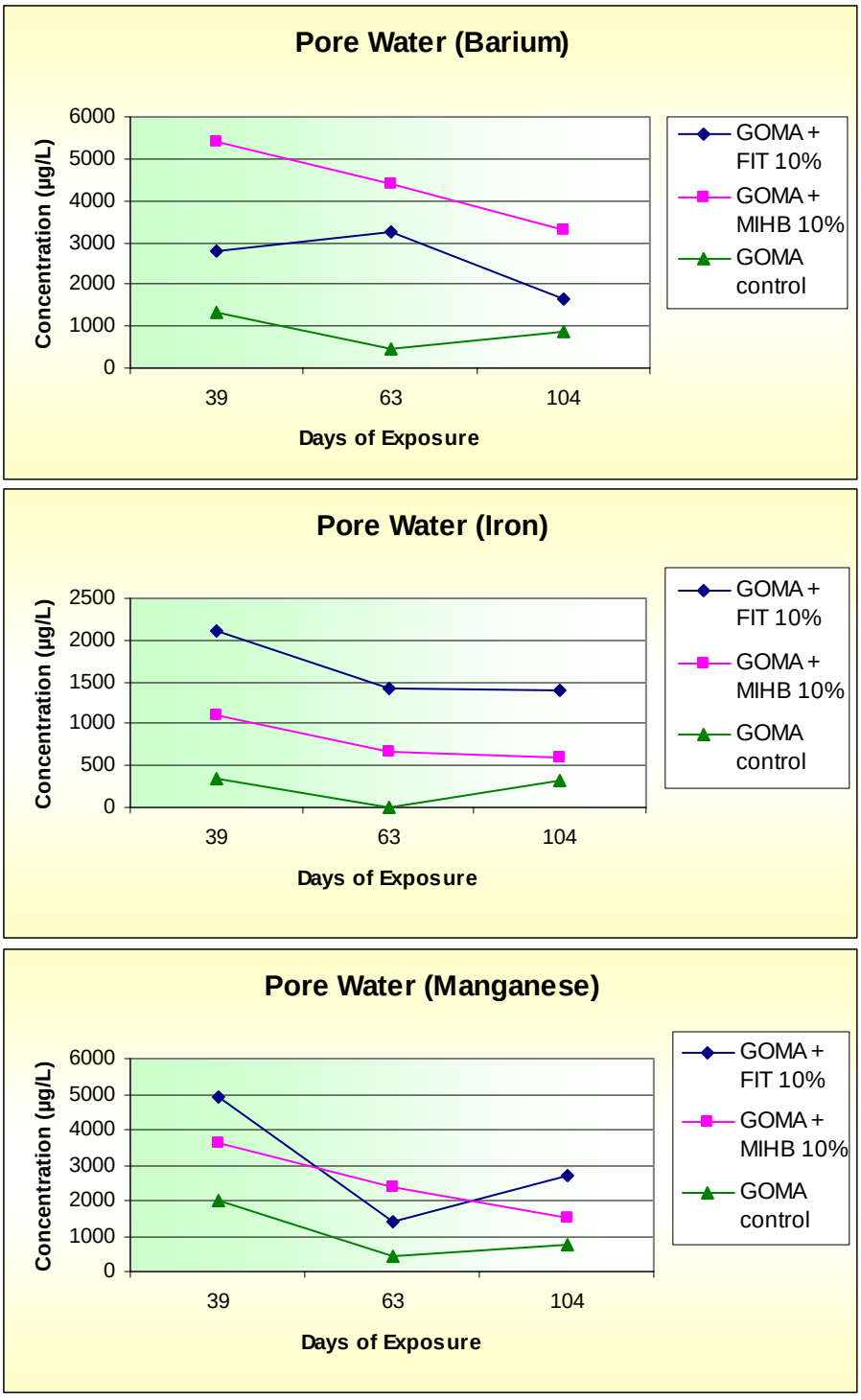

Figure 10a. Trace metals (Ba, Fe, and Mn) released from Batch One sediment.

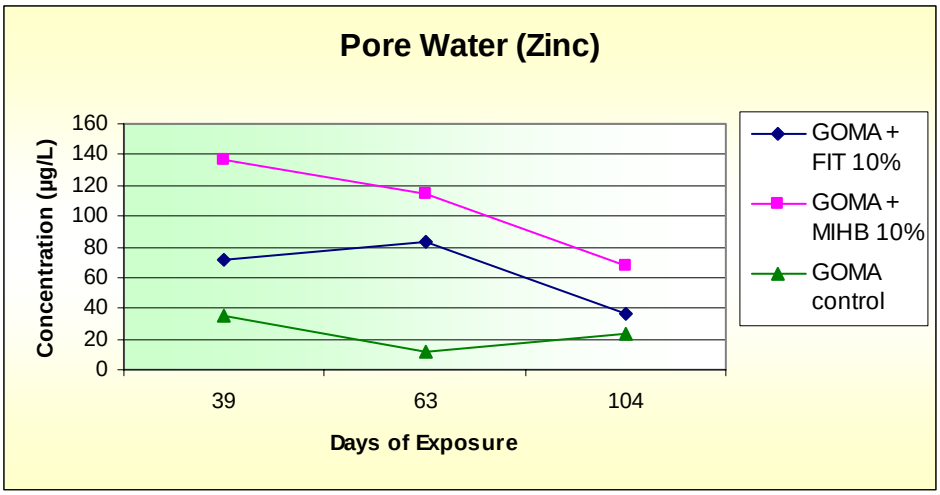

Figure 10b. Trace metal (Zn) released from Batch One sediment.

Figures 11a and 11b show that Cd, Cr, Pb, and Hg concentrations in pore water of barite containing sediment are similar to the control (GOMA). This suggests that if those metals are released from FIT-Blend and MI-High, they precipitate out of solution, most likely as insoluble sulfides. Copper was not detected in any sample.

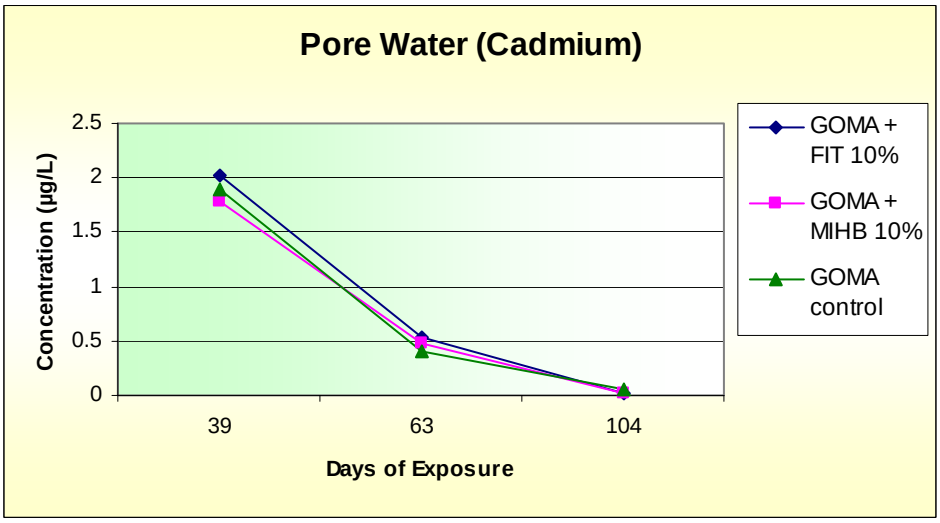

Figure 11a. Trace metal (Cd) released from Batch One sediment.

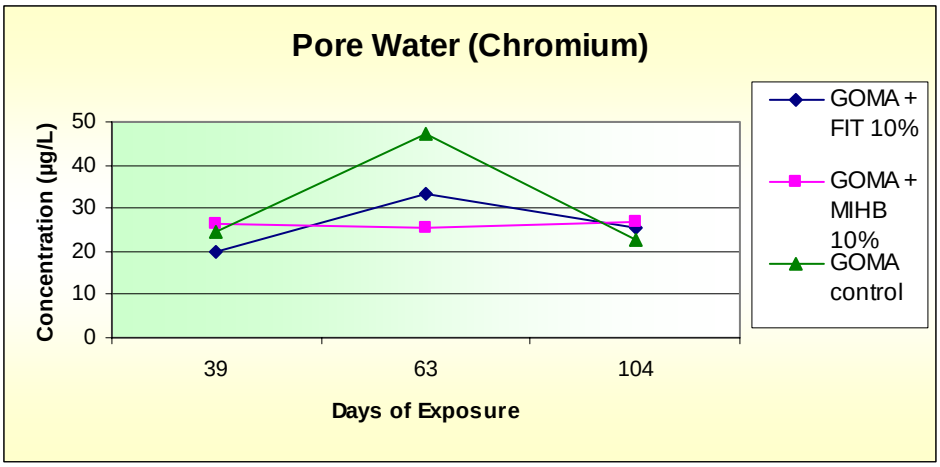

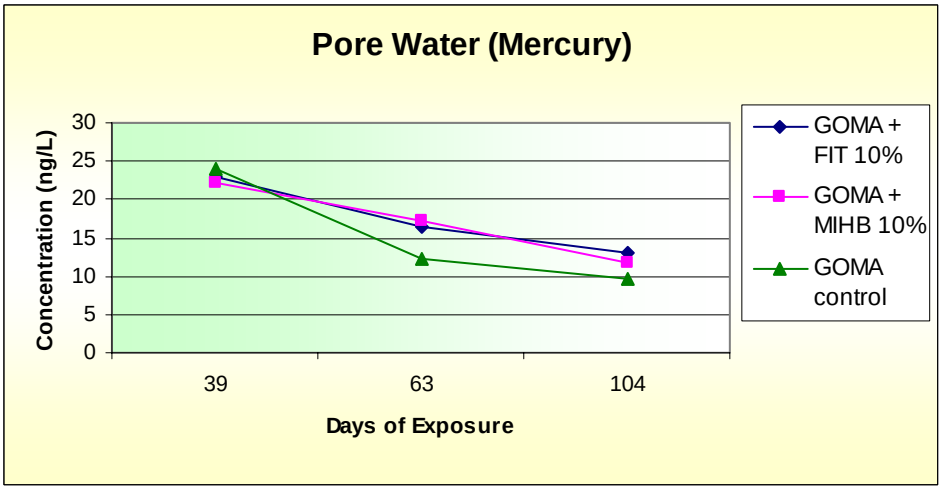

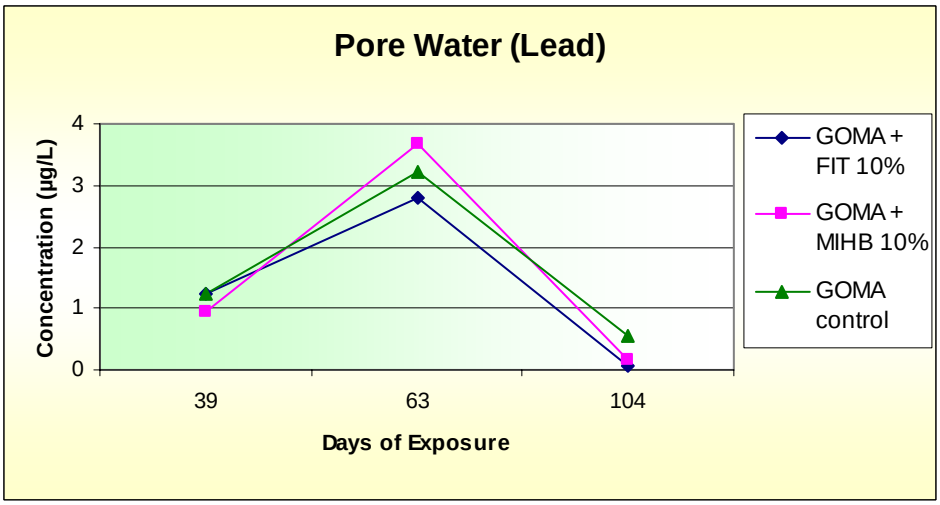

Figure 11b. Trace metals (Cr, Hg and Pb) released from Batch One sediment.

After 104 days exposure, methylmercury concentrations in the pore water samples from FIT-Blend, and MI-High, and the Control are in the range of about 1-3 ng/L (Table 10).

Table 10

Methylmercury concentrations in pore water from Batch One.

Sample Description	Days of Exposure	Methylmercury Concentration (ng/L)
GOMA + FIT-Blend 10%	104	3.15
GOMA + MI-High 10%	104	0.73
GOMA Control	104	2.77

Table 11 summarizes the Eh of sediment and dissolved sulfate in pore water. These data indicate the sediment samples were anoxic and that the sulfate had been reduced to sulfide.

Table 11

Eh in sediment and sulfate in pore water data for Batch One.

Sample Description	Days Aged	Eh (mV)	Sulfate (mg/L)
GOMA + FIT-Blend 10%	39	-15	<4
GOMA + FIT-Blend 10%	63	17	<4
GOMA + FIT-Blend 10%	104	-12	<4
GOMA + MI-High 10%	39	-27	<4
GOMA+ MI-High 10%	63	16	<4
GOMA + MI-High 10%	104	38	<4
GOMA Control	39	-109	<4
GOMA Control	63	-32	<4
GOMA Control	104	2.6	5.1

< =Less than the Method Detection Limit of 4 mg/L

5.3.2 Batch Two Sediments

Table 12 summarizes the Eh and sulfate data for Batch Two sediment containing 2 percent algae. These sediment samples were less reducing (positive Eh values) than Batch One yet the sulfate was reduced below detection indicating that a reducing environment existed.

Table 12

Eh and sulfate data for Batch Two sediment.

Sample Description	Days Aged	Eh (mV)	Sulfate (mg/L)
GOMA + MI-High 10%	43	92.4	<4
GOMA + MI-High 10%	68	38.2	<4
GOMA + MI-High 10%	146	342	NA
GOMA + MI-High 1%	43	66	<4
GOMA + MI-High 1%	68	86.7	<4
GOMA + MI-High 1%	146	394	NA
GOMA Control Batch 2	43	349	<4
GOMA Control Batch 2	68	83.4	<4
GOMA Control Batch 2	146	284	NA

< =Less than the Method Detection Limit of 4 mg/L
NA = Not analyzed

Barium concentrations in pore water from GOMA sediment containing barite MI-High 1 percent and MI-High 10 percent are at greater levels than the GOMA control (Figure 12). Interestingly, when compared to Figure 10a (pore water from a more anoxic sediment), Ba concentrations are higher in the less reducing sediment. This result is unexpected since it is believed that the more reducing the environment, the more barite would dissolve yielding higher Ba concentrations in the pore water.

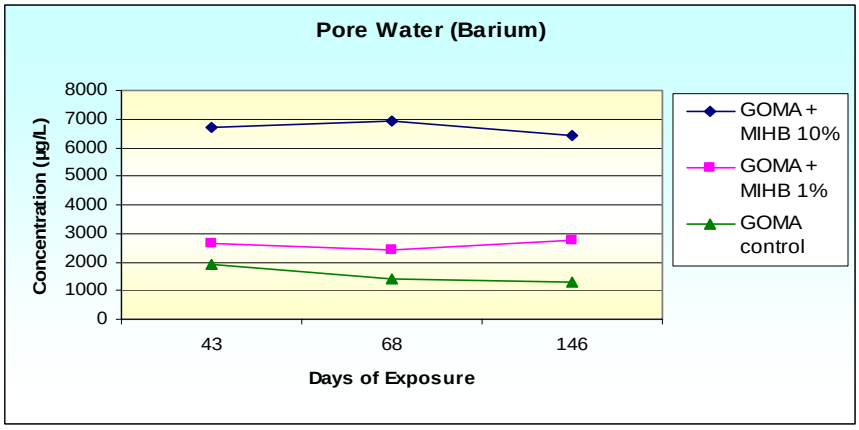

Figure 12a. Trace metal (Ba) released from Batch Two sediment (see Table 12)

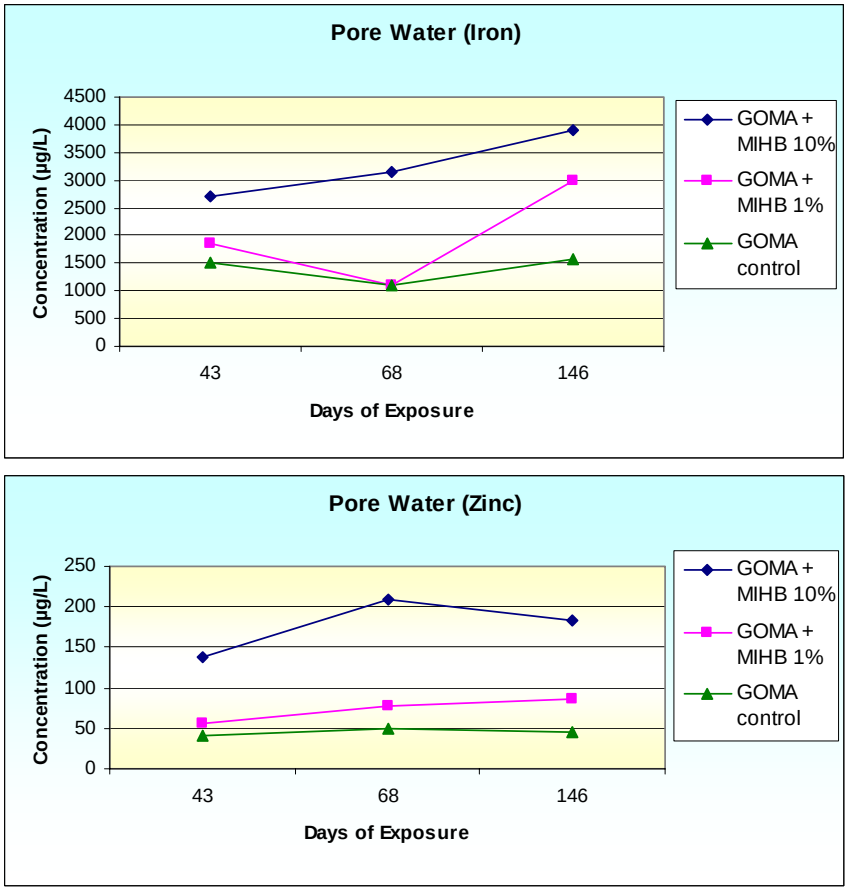

Figure 12b. Trace metals (Fe and Zn) released from Batch Two sediment.

This same trend is observed for Fe and Zn (Figure 12b). Again, these elements appear at higher concentrations from pore water containing MI-High 10 percent and MI-High 1 percent than the control but at greater concentrations than the more anoxic mixture used in Batch One.

Figure 13 shows that Mn concentrations in pore water from sediment containing MI-High 10 percent and MI-High 1 percent are higher concentrations than the control but at levels less than those from the more anoxic mixtures. This is to be expected since Mn concentrations are typically elevated in anoxic sediments and would indicate this trace element is not readily precipitated as a sulfide.

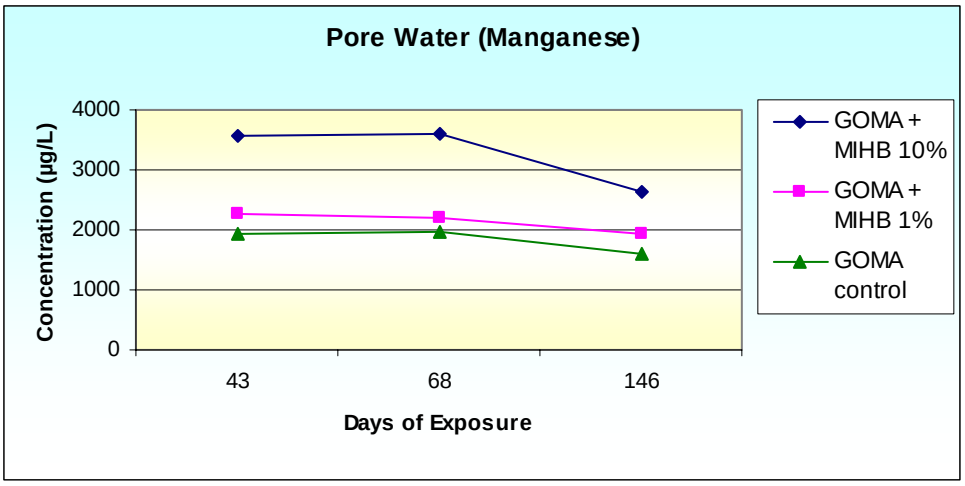

Figure 13. Manganese (Mn) released from Batch Two sediment.

Four trace metals, Cd, Cr, Pb, and Hg (Figures 14a and 14b) show less than a factor of five enrichment in pore water from barite containing sediment compared to control sediment. Copper was not detected in pore water.

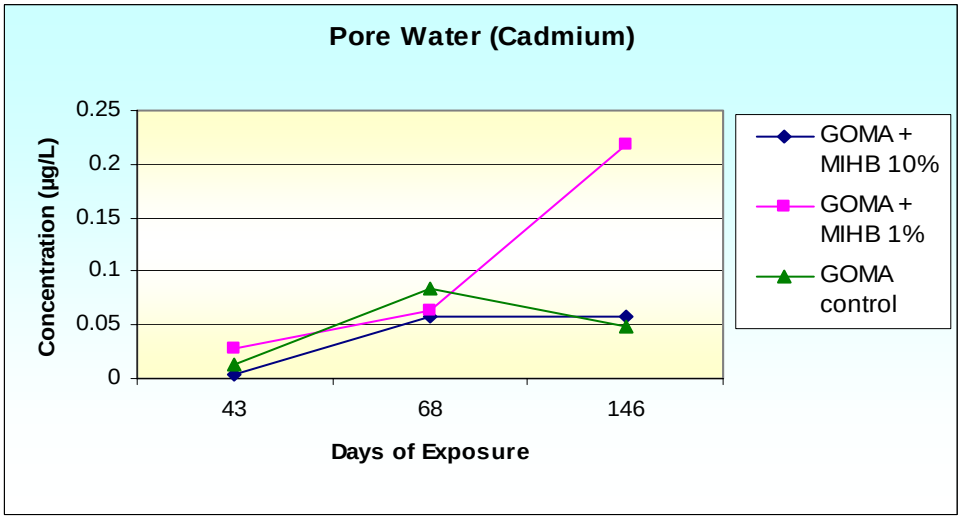

Figure 14a. Trace metal (Cd) released from Batch Two sediment.

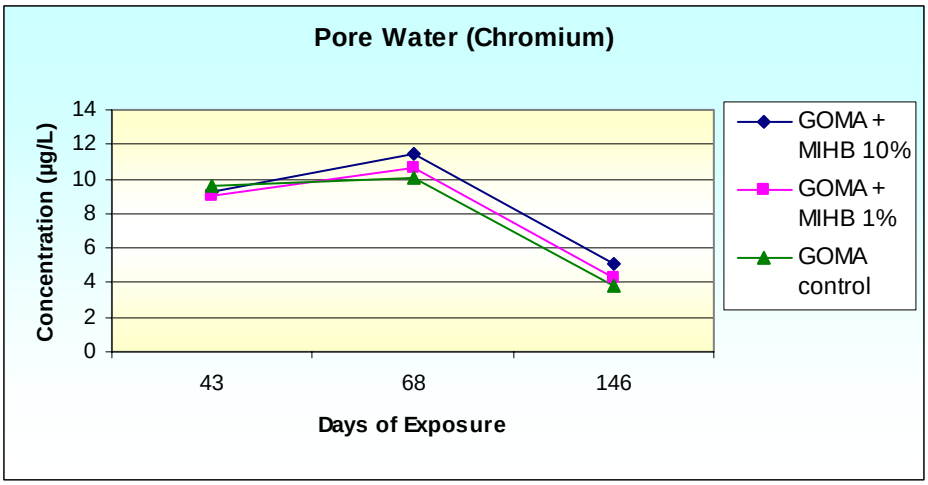

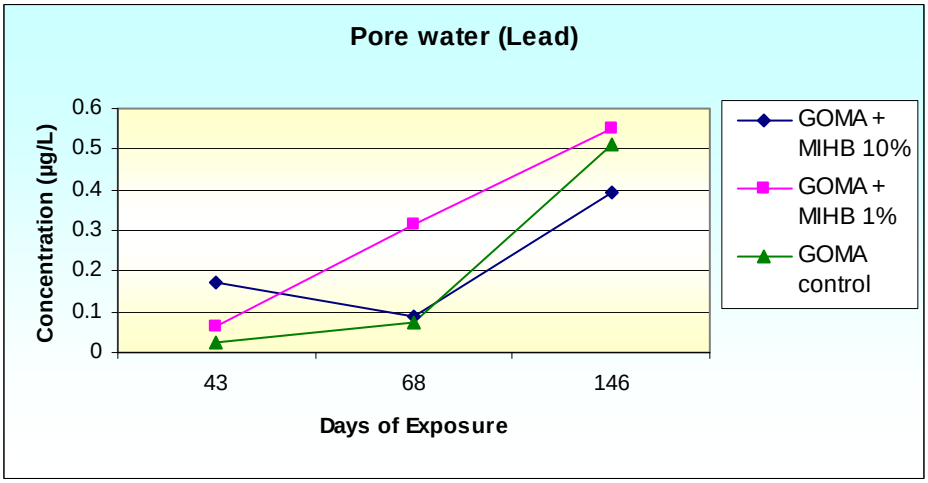

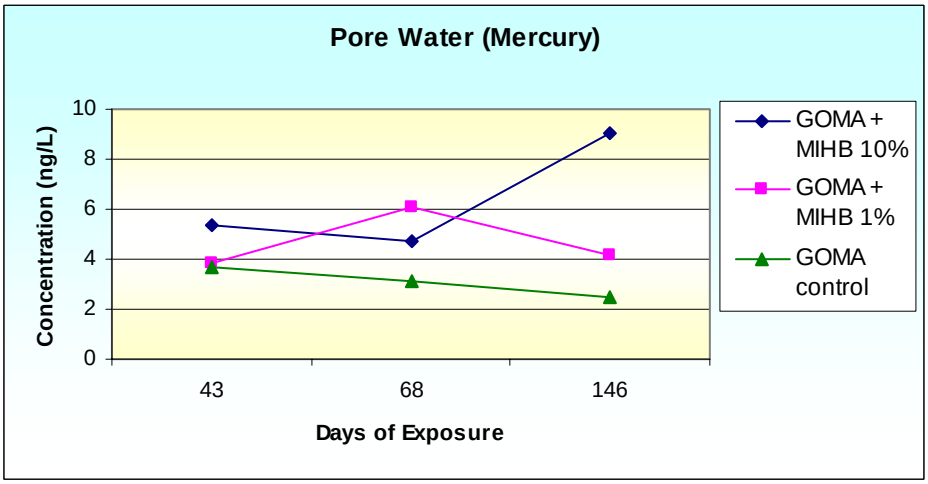

Figure 14b. Trace metals (Cr, Pb and Hg) released from Batch Two sediment.

Figure 15 shows the methyl-Hg concentration in pore water from sediment which contained 10 percent barite is appreciably higher than both the control and the sediment which contained 1 percent barite.

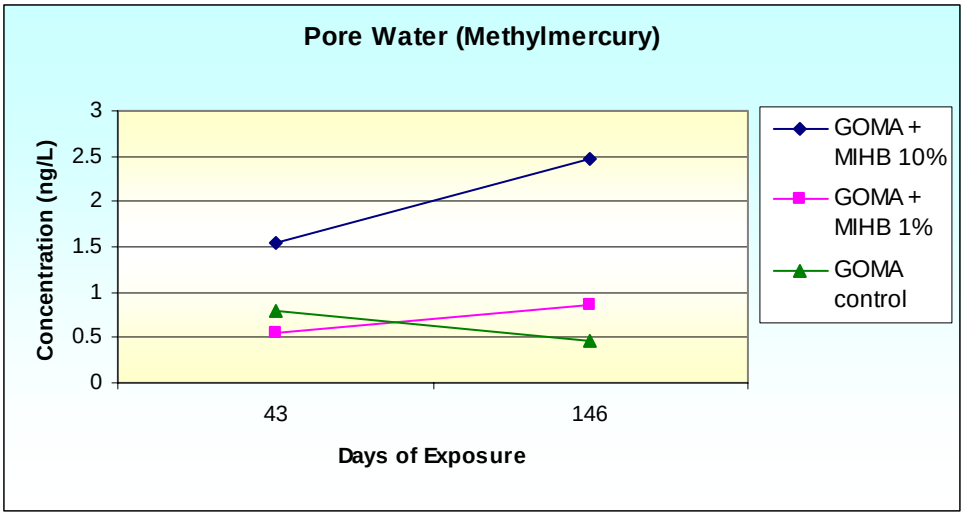

Figure 15. Methylmercury released from Batch Two sediment.

5.4 Summary

As described in Section 4.3, when barite was mixed in the oxic layer of GOMS, the results for anoxic sediment demonstrate that barite dissolves when sulfate reduction occurs in pore water. The anoxic pore water from sediment with and without barite was elevated in Ba, Fe, Mn, and Zn. However, the presence of barite increased the concentrations of these four metals by a factor of two to seven times above the concentrations in the un-amended anoxic sediment (Table 13).

Concentrations of Cd, Cu, Hg, methyl-Hg, and Pb in anoxic pore water were not significantly different from barite amended and un-amended sediment (Table 13). These results suggest that under anoxic conditions the sulfide minerals in barite are insoluble. Another explanation for the low concentrations of Cd, Cu, Hg, and Pb in anoxic pore water is these metals form insoluble sulfide minerals if released from the barite matrix. The low concentrations of methyl-Hg in the anoxic pore waters are consistent with field measurements made by Trefry et al. (2003) near offshore drilling sites in the GOM that indicate barite was not contributing to methyl-Hg in sediment.

The release of dissolved metals to the overlying water from an oxic layer of sediment (containing 22 percent FIT-Blend barite) caused very little increase in the water during a static exposure of several months. After several months the concentrations of Pb and Zn exceeded the WQC by about a factor of two, while the concentrations of Cd, Cu, and Hg were below the WQC.

Table 13

Maximum pore water concentrations of dissolved metals (μg/L) in GOMS, GOMA, and GOMA plus either 1% or 10% barite.

Metal	GOMS Control	GOMA Control	GOMA 1% MI-High	GOMA 10% MI-High	GOMA 10% FIT-Blend
Ba	45	1910	2660	6950	3230
Cd	0.01	1.9	0.1	1.8	2.0
Cu	<0.9	<0.9	<0.9	<0.9	<0.9
Hg	NA	0.024	0.006	0.022	0.023
MeHg	NA	0.003	0.001	0.002	0.003
Pb	0.03	<0.01	<0.01	<0.01	<0.01
Zn	4.0	49	77	209	83

NA Not analyzed

6.0 Solubility of Metals from Barite in Acidic Solutions

6.1 Chemical Analysis Methods of Metals in Acidic Solutions

Each of the three fine-grained barite samples were homogenized with a Teflon stirring rod and dried to constant mass. For each of the 150 experiments, 3 g or 6 g portions of barite were weighed out and placed in 50 mL plastic centrifuge tubes. Thirty or 24 mL of the appropriate pH solution were added to the 3 g and 6 g tubes, respectively, to prepare the 10:1 and 4:1 aqueous:solid mixtures. The solutions were prepared with Ultrex-grade, redistilled HCl. To achieve the range of pH values, the phthalate buffer system described in Trefry and Metz (1984) was used. The pH of each batch of leaching solution was determined at the start of the leaching experiment. The centrifuge tubes were sealed and placed on a wrist-action shaker for the assigned time. Following equilibration, the samples were centrifuged and the overlying fluid was filtered through a 0.4 μm, pore size polycarbonate, membrane filter. A filtration step is essential to separate the small particles from the dissolved fraction. The solutions were stored in low density polyethylene bottles. All samples were acidified to pH<2 to avoid adsorption on the walls of the plastic bottle by adding Ultrex HCl.

Analysis of samples, procedural blanks and reagent blanks was carried out by flame atomic absorption spectrometry (FAAS), Zeeman graphite furnace atomic absorption spectrometry (GFAAS), cold-vapor atomic absorption spectrometry (CVAAS) or amalgamation atomic fluorescence (Amal.-AFS) using available instruments at FIT. Detection limits are listed in Table 14. The methods used for each element and the corresponding MDL for the analytical techniques were chosen to minimize the number of non-detectable values. All analytical techniques followed manufacturers' specifications.

Table 14

Analytical method and method detection limits (MDL) for metals in sediment.

Metal	Method	MDL (μg metal/g dry sediment)
Ba	GFAAS or FAAS	1
Cd	ZGFAAS	0.02
Cr	GFAAS	1
Cu	GFAAS	2
Fe	FAAS	10
Hg	CVAAS	0.001
Hg	Amal.-AFS	0.0002
Pb	GFAAS	0.2
Zn	FAAS	2

6.2 Quality Assurance and Quality Control

For this project, QC measures included balance calibration, instrument calibration for FAAS, GFAAS, CVAAS, and Amal.-AFS, matrix spike analysis for each metal, duplicate sample analysis, and analysis of SRM, procedural blank analysis and standard checks. With each batch of samples, two procedural blanks, two SRMs, replicate samples and matrix-spiked samples were analyzed. Data quality objectives (DQOs) for these quality control measurements are provided in Table 15.

Electronic balances used for weighing samples and reagents were calibrated prior to each use with certified, National Institute of Standards and Technology (NIST) traceable standard weights. All pipettes (electronic or manual) were calibrated prior to use. Each of the spectrometers used for metal analysis was initially standardized with a three- to five-point calibration with a linear correlation coefficient of $r \geq 0.999$ required before experimental samples could be analyzed. Analysis of complete three- to five-point calibrations and/or single standard checks alternated every 5-10 samples until all the analyses were complete. The relative standard deviation (RSD) between complete calibration and standard check was required to be less than 15 percent or recalibration and reanalysis of the affected samples were performed.

Matrix spikes were prepared for a minimum of 5 percent of the total number of samples analyzed and included each metal to be determined. Results from matrix spike analysis using the method of standard additions provide information on the extent of any signal suppression or enhancement due to the sample matrix. If necessary (i.e., spike results outside 80-120 percent limit), spiking frequency was increased to 20 percent and a correction applied to the metal concentrations of the experimental samples.

Duplicate samples from homogenized field samples (as distinct from field replicates) were prepared in the laboratory for a minimum of 5 percent of the total samples. These laboratory duplicates were included as part of each set of sample digestions and analyses and provide a measure of analytical precision.

Two procedural blanks were prepared with each set of samples to monitor potential contamination resulting from laboratory reagents, glassware and processing procedures. These blanks were processed using the same analytical scheme, reagents, and handling techniques as used for the experimental samples.

A common method used to evaluate the accuracy of environmental data is to analyze reference materials, samples for which consensus or "accepted" analyte concentrations exist. The following SRM was used: NIST #1640 Trace Metals in Water. Metal concentrations obtained for the reference materials were required to be within 20 percent of accepted values for greater than 85 percent of other certified analyses. Results for the SRM were well within the limits set in the data quality objectives.

Table 15

Data quality objectives and acceptance criteria.

Element or Sample Type Criteria	Minimum Frequency	Data Quality Objective/Acceptance
Initial Calibration	Prior to every batch of samples Standard Curve	3-5 point curve depending on the element and a blank Correlation coefficient r ≥ 0.999 for all analytes
Continuing Calibration	Must end every analytical sequence; for flame, repeat all standards every 5 samples; for graphite furnace and AFS recheck standard after every 8-10 samples	RSD 15% for all analytes
Standard Reference Materials	Two per batch of 20 samples	Values must be within 20% of accepted values for >85% of the certified analytes and within 25% for Hg
Method Blank	Two per batch of 20 samples	No more than 2 analytes to exceed 5x MDL
Matrix Spike and Spike Method Blank	Two per batch of 20 samples	80-120%
Lab Duplicate	Two per batch of 20 samples	RSD <25% for 65% of analytes

6.3 Acidic Solubility Test

The metals included in the Acidic Solubility Test were selected by MMS and include Ba, Hg, Cd, Cr, Cu, Pb and Zn plus Fe. Concentrations of Cu and Zn, as well as Fe provide some perspective on the presence and behavior of possible sulfides present in the barite samples (pyrite, FeS_2; chalcopyrite, $CuFeS_2$, and sphalerite, ZnS). Therefore, Fe was included in the list of analytes.

The overall design for the pH leaching experiments for three different samples of industrial barite is outlined in Table 16. Incorporation of redox conditions into the pH leaching experiments also was considered. Data from Gambrell et al. (1976) showed that release of Cd is favored in a more oxidizing solution and release of Hg seems to be slightly more favored in a reducing environment. Because redox is addressed more directly and in a more environmentally meaningful manner in Section 6, the pH leaching

effort for this study was carried out under conditions open to the air. However, the Eh was measured in selected samples of the final leaching solution.

Table 16

Averages ± standard deviations for total metal concentrations in the three barite samples used for this study.

Metal	MI-Low Metal Barite	MI-High Metal Barite	FIT-Blend Barite
Ba (%)	53.8	52.4	50.7
Fe (%)	0.66 ± 0.01	0.93 ± 0.03	2.96 ± 0.05
Zn (µg/g)	35 ± 3	167 ± 1	1210 ± 10
Cd (µg/g)	0.35 ± 0.02	0.77 ± 0.08	7.0 ± 0.2
Pb (µg/g)	318 ± 3	243 ± 7	1370 ± 50
Hg (µg/g)	0.44 ± 0.02	5.9 ± 0.3	6.7 ± 0.4
Cu (µg/g)	98 ± 4	88 ± 4	189 ± 1
Cr (µg/g)	15 ± 1	6.5 ± 0.4	11 ± 1

Reaction times chosen for the experiments focus on both short-term release (15 minutes) and longer-term release (48 hours). In the Gambrell et al. study, the release rate for metals was found to be relatively fast with a significant fraction of total release observed within 15 minutes. Based on previous work, the leaching process comes to near completion/equilibrium in less than 3 hours. These short time periods suggest that metal release can be nearly complete during passage of sediment through the digestive tract of an organism.

One of the most significant changes in experimental design for the 2004 experiments was a decrease in the aqueous/solid ratio from 20:1 in the Trefry et al. (1986a) experiments to 10:1 and 4:1 in the proposed 2003-2004 design. This change was introduced because the lower ratios are more typical of those found in sediments that can pass through the digestive tract of benthic infauna and because they present a worst-case scenario for leaching of metals.

6.4 Solubility of Metals from Barite in Acidic Solutions

6.4.1 Overview

Results from dissolution of Ba, Fe, Zn and various trace metals from barite as a function of pH are used in this portion of the study to (1) help identify the likely phases that contain the trace metals of interest and (2) provide one analog for assessing metal release from solids as sediment moves through the digestive tract of an organism.

Knowledge about the solid phase that contains potential metal pollutants is valuable because such information allows one to predict how a particular metal may react in the marine environment. As previously described by Kramer et al. (1980) and Trefry and Smith (2003), the key trace metal-bearing phases in industrial barite are barite ($BaSO_4$)

and selected sulfides, including sphalerite (ZnS) and pyrite (FeS_2). Plots showing the release of Cd, Pb, Hg, Cu and Cr versus Ba, Zn and Fe at varying pH values can be used to help support conclusions regarding the key phases that contain each metal. If Cu, for example, is held in a sulfide phase that is present as a trace impurity in barite, then one can predict that the Cu will be immobilized in reducing, sulfidic sediments and more susceptible to dissolution under oxidizing conditions. In contrast, if a metal is held in the barite phase, then that metal is less likely to be leached under oxic conditions when high levels of interstitial water sulfate are present and more likely to be leached under reducing conditions when the solubility of barite increases.

In general, only a small fraction of the total metal content of sediments is biologically available. However, determining the biologically available fraction of the total metal content is difficult. One way to mimic the release of metals from sediment as sediment moves through the digestive tract of an organism is by leaching sediment in solutions of varying pH (e.g., Trefry and Metz 1984). The pH of marine sediments (i.e., the interstitial water) varies between ~6.5 and 8, but is generally ~7. However, much larger variations and lower pH values are common to invertebrate digestive systems. Invertebrates have internal pH levels of 5 to 8 (Owen 1966) that are considerably higher than levels that are as low as 3 in vertebrate digestive systems (Barnard 1973). Luoma and Bryan (1979) stated that the pH of the digestive tract is a key factor in the uptake of metals from ingested particles. In contrast, Miller and Mackay (1980) noted a poor correlation between gut pH and metal uptake, possibly the result of the inhibition of metal uptake at low pH. In either case, many researchers agree that a pH leach provides one useful perspective on the potential fate of sediment-bound metals. For these reasons, the research on leach barite samples as a function of pH, as requested by MMS, provides a valuable component to the overall assessment of the potential impacts of metals associated with industrial barite.

In one previous study, leaching experiments were carried out at pH values of 2.2, 3, 4, 5 and 6 using four different barite samples with analysis for Ba, Cd, Cu, Fe, Mn, Pb and Zn (Trefry et al. 1986a). Results for leaching of Cd from that study showed that >50 percent of the total Cd was leached at all five pH levels for one barite sample with a total Cd concentration of 4.3 µg/g and >20 percent of the total Cd level of 9.9 µg/g was leached at each pH from another barite sample (Figure 16). No detectable leaching of Hg (<0.002 µg/g) was observed for all four barite samples at all pH values, including one sample with total Hg levels of 8.4 µg/g. Trefry et al. (1986a) also determined the rate of metal release at pH 3 and 5 by collecting samples after reaction times of 0.25, 0.5, 1, 3, 6, 12, 24 and 48 hours. Results for Cd showed that 74 percent of the Cd leached after 48 hours was leached within 15 minutes and that 92 percent of the Cd leached after 48 hours was leached within 3 hours (Figure 17). Results for leaching of Ba were a bit more variable; however, at all pH values, <0.05 percent of the total Ba was leached.

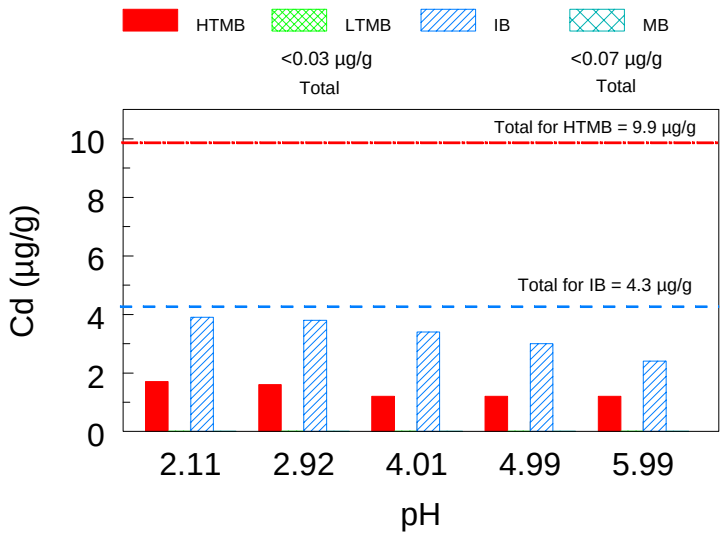

Figure 16. Amounts of leachable Cd in various barite samples as a function of pH.

Dashed lines show total metal concentrations in the barite samples. Filled and open bars show levels of Cd leached from HTMB and IB samples, respectively (HTMB = High Trace Metal Barite, IB = Italian Barite, MB = Moroccan Barite, LTMB = Low Trace Metal Barite (modified from Trefry et al. 1986a).

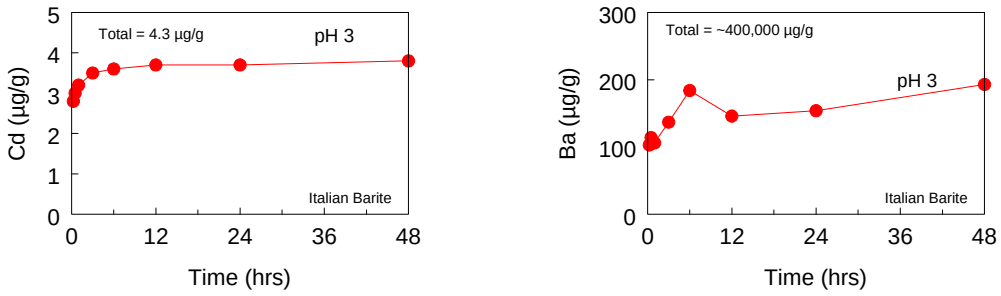

Figure 17. Amounts of leachable Cd and Ba at pH 3 versus time for samples of Italian barite (modified from Trefry et al. 1986a).

6.4.2 Barium

After 48 hours, <0.03 percent, <0.008 percent, and <0.002 percent of the total Ba was leached into solution for the MI-Low, MI-High and FIT-Blend samples, respectively (Table 17). Although no simple trends were observed as a function of pH, higher amounts of Ba were leached from samples when the final pH values were ≥4. In addition, the amount of Ba leached from barite was lower in samples with a 4:1

aqueous:solid ratio relative to a 10:1 aqueous:solid ratio at the same pH. This latter observation is consistent with the relatively uniform concentrations of dissolved Ba in each leach solution for a given barite sample (Table 18) and the smaller fraction of the total Ba that would be leached when the solid-aqueous ratio was lower.

Table 17

Concentrations of total Ba and Ba leached following different pH treatments after 48 hours.

Ba (µg/g)	Aqueous:Solid Ratio	MI-Low	MI-High	FIT-Blend
Total	-	538,000	524,000	507,000
pH 2.2	10:1	140 ± 5	17 ± 3	2.4 ± 0.1
pH 3	10:1	129 ± 3	25 ± 2	2.7
pH 3	4:1	60 ± 4	6	1.9
pH 4	10:1	143	31	3.7 ± 0.3
pH 5	10:1	130	39 ± 2	8.2
pH 5	4:1	58	5	2.3 ± 0.1
pH 6	10:1	146 ± 9	39 ± 3	7.8

Results from triplicate analyses are shown as mean ± standard deviation.

Maximum concentrations of dissolved Ba leached into solution for the MI-Low, MI-High and FIT-Blend samples of barite were 22.9 mg/L, 4.3 mg/L and 0.82 mg/L, respectively (Figures 18, 19 and 20). In the MI-Low sample, the highest amount of Ba release was observed after time periods of <4 hours (Figure 18). Then, after 48 hours, the concentration of Ba in solution at each pH and at each aqueous:solid ratio for the MI-Low sample ranged from only 13-15 mg/L. Thus, pH (at pH levels of 2.2-6) did not affect the amount of Ba in solution.

Table 18

Concentrations of dissolved Ba leached during different pH treatments after 48 hours.

Ba (mg/L)	Aqueous:Solid Ratio	MI-Low	MI-High	FIT-Blend
pH 2.2	10:1	14.2 ± 0.4	1.7 ± 0.3	0.24 ± 0.01
pH 3	10:1	13.2 ± 0.3	2.5 ± 0.2	0.27
pH 3	4:1	15 ± 1	1.5	0.47
pH 4	10:1	14	3.1	0.37 ± 0.03
pH 5	10:1	13	3.9 ± 0.3	0.82
pH 5	4:1	15	1.4	0.58 ±0.1
pH 6	10:1	15 ± 1	3.9 ± 0.4	0.78
All samples	-	14 ± 1	2.6 ± 1.1	0.5 ± 0.2

Results from triplicate analyses are shown as mean ± standard deviation.

In contrast with results for the MI-Low barite, concentrations of dissolved Ba in solutions from the MI-High and FIT-Blend barite samples were 3 to >30 times lower (Figures 19 and 20, Table 18). In all cases, the concentration of Ba in solution following leaching was greater than the solubility of Ba in seawater of 0.035 mg/L (Church and Wolgemuth 1972), but less than the solubility of Ba carbonate in pure water of about 24 mg/L. The relatively uniform concentrations of Ba in solutions from leaching of the MI-Low barite suggest that Ba levels are solubility controlled. Concentrations of dissolved Ba in the MI-High and FIT-Blend solutions (at 10:1 aqueous:solid ratio) also may have reached saturation at 3.9 mg/L and 0.8 mg/L, respectively (Table 18).

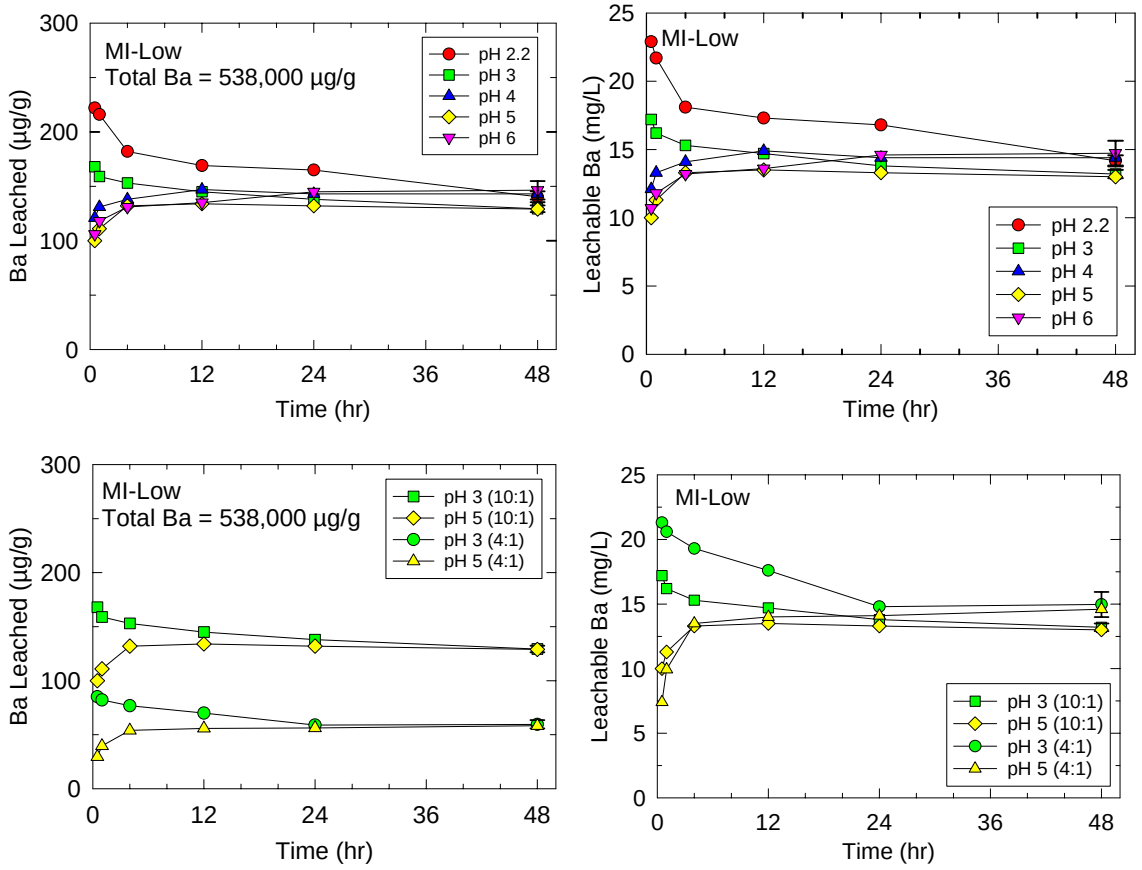

Figure 18. Amounts of Ba leached from the solid phase in µg/g and concentrations of Ba leached in mg/L at various pH values and times for the MI-Low barite sample.

In all cases, the fraction of the total Ba leached as a function of pH was less than 0.03 percent with an order-of-magnitude lower fraction of release for the FIT-Blend sample than for the MI-Low barite. The observed concentrations of dissolved Ba were higher than found in seawater where the concentration of dissolved sulfate is high (2.7 mg/L); however, concentrations of dissolved Ba in the pH leachates were less than the solubility in freshwater of 24 mg/L. The relative amounts of dissolved Ba in the pH solutions followed a trend of MI-Low (14 mg/L) greater than MI-High (2.6 mg/L) greater than

FIT-Blend (0.5 mg/L). This trend for dissolved Ba will be tracked through discussion of the various trace metals as one of several possible factors to explain the release of other metals.

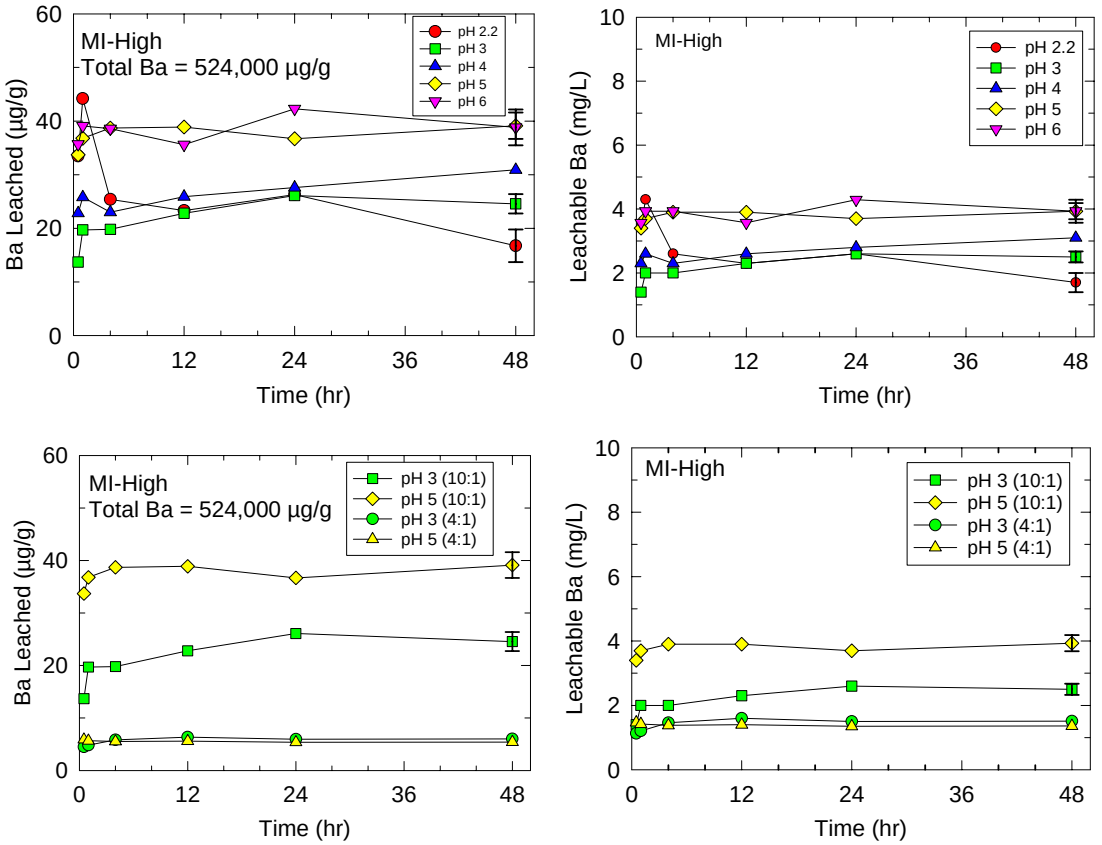

Figure 19. Amounts of Ba leached from the solid phase in µg/g and concentrations of Ba leached in mg/L at various pH values and times for the MI-High barite sample.

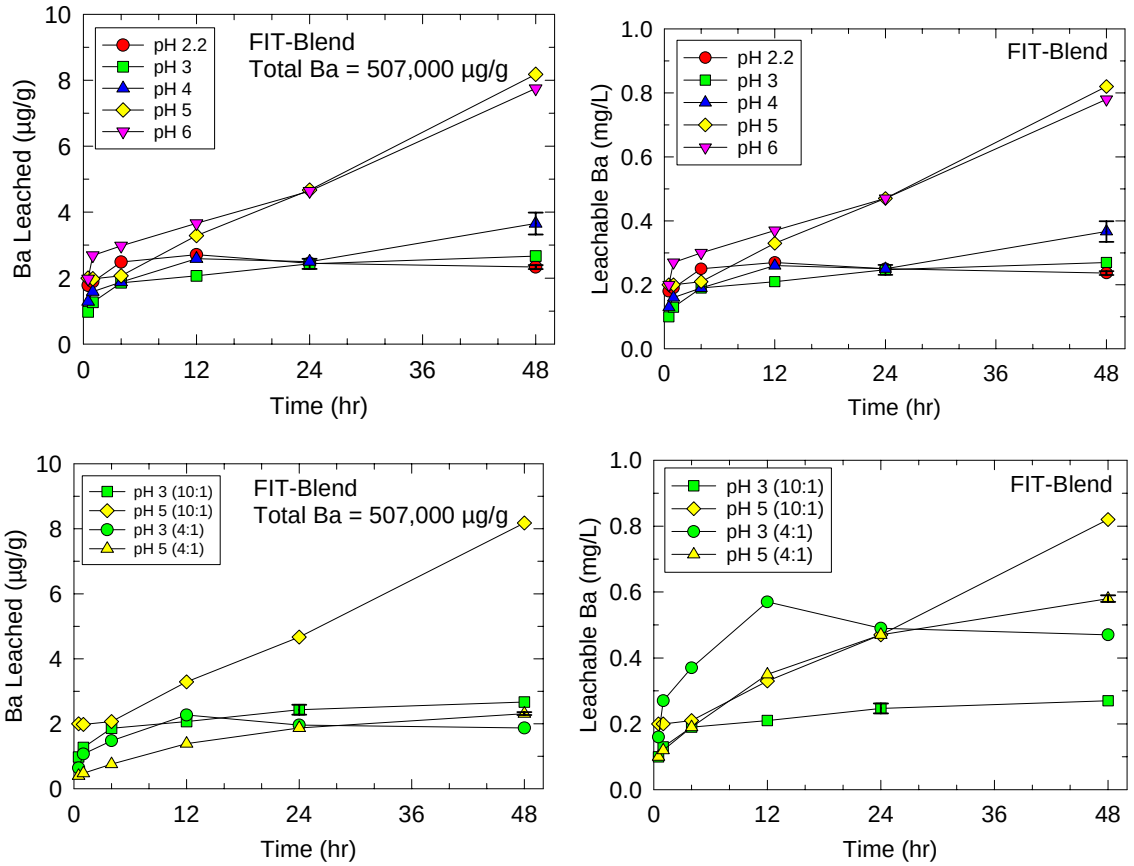

Figure 20. Amounts of Ba leached from the solid phase in µg/g and concentration of Ba leached in mg/L at various pH values and times for the FIT-Blend barite sample.

6.4.3 Iron

After 48 hours, 1.2 percent, 2.2 percent and 0.2 percent of the total Fe was leached into solution at pH 2.2 for the MI-Low, MI-High and FIT-Blend samples, respectively (Table 19). However, at pH 6, <0.02 percent of the total Fe was leached into solution for all three barite samples (Table 19).

Table 19

Concentrations of total Fe and Fe leached during different pH treatments after 48 hours.

Fe (µg/g)	Aqueous:Solid Ratio	MI-Low	MI-High	FIT-Blend
Total	-	6,600 ± 100	9,300 ± 300	29,600 ± 500
pH 2.2	10:1	80 ± 2	205 ± 5	48 ± 2
pH 3	10:1	52 ± 1	141 ± 2	10
pH 3	4:1	39 ± 1	74	5.9
pH 4	10:1	33	88	4.5 ± 0.2
pH 5	10:1	10	21.1 ± 0.4	4.1
pH 5	4:1	4	7	1.4 ± 0.1
pH 6	10:1	1.0 ± 0.2	1.28 ± 0.01	6.5

Results from triplicate analyses are shown as mean ± standard deviation.

Thus, for each sample, the fraction of Fe leached decreased by 16 to 162 fold as a function of pH, with lower amounts of Fe leached with increasing pH (Table 19, Figures 21 and 22). Similar to the observation for Ba, the fraction of Fe leached from each barite was consistently lower in the sample with a 4:1 aqueous:solid ratio.

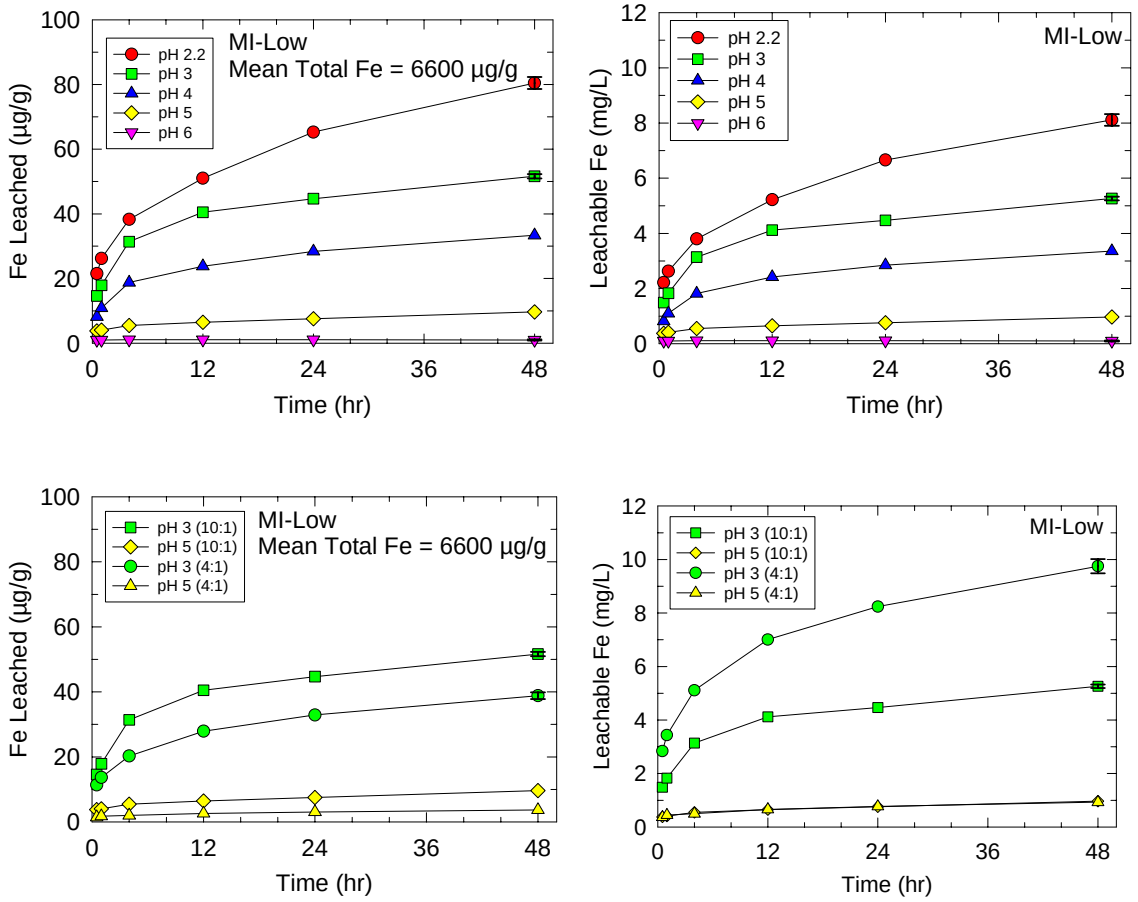

Figure 21. Amounts of Fe leached from the solid phase in µg/g and concentrations of Fe leached in mg/L at various pH values and times for the MI-Low barite sample.

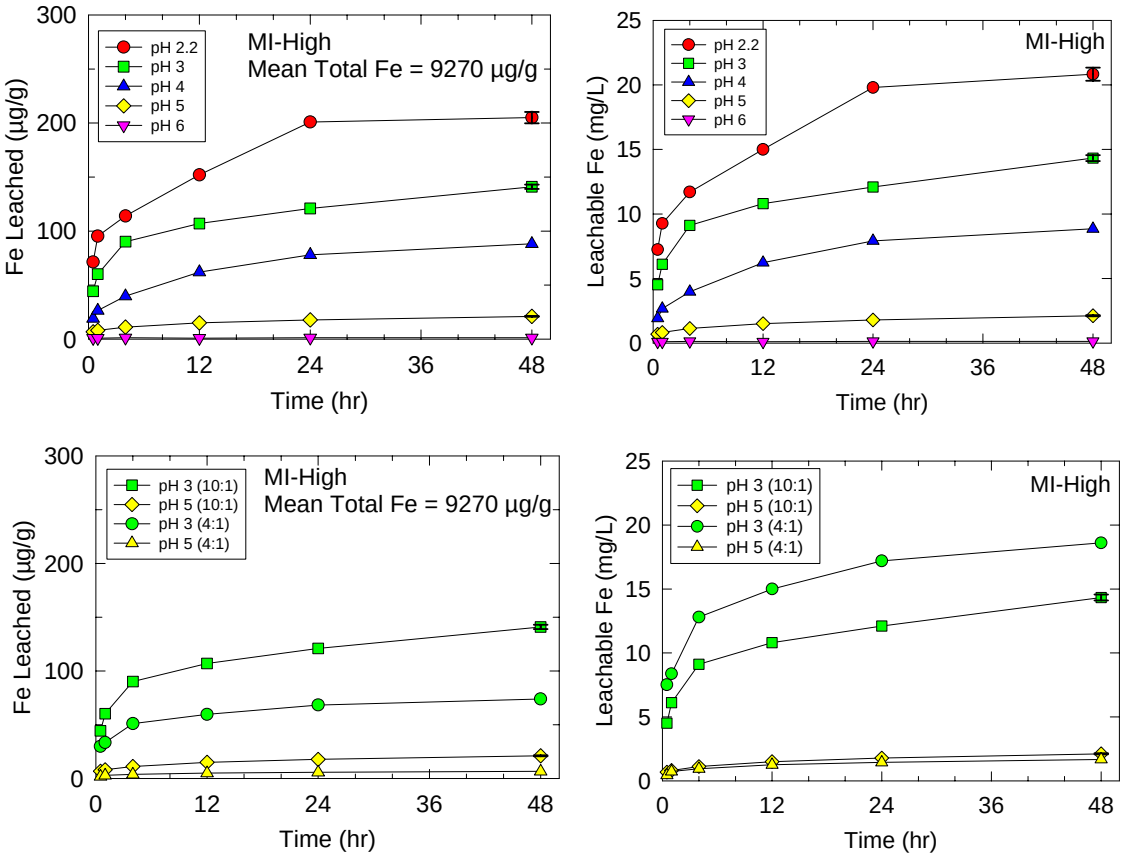

Figure 22. Amounts of Fe leached from the solid phase in µg/g and concentrations of Fe leached in mg/L at various pH values and times for the MI-High barite sample.

Maximum concentrations of dissolved Fe leached into pH 2.2 solutions for the MI-Low, MI-High and FIT-Blend samples of barite were 8.1, 21 and 4.9 mg/L, respectively (Table 20; Figure 23). The pH effect for Fe is strong with 74-, 162- and 16-fold higher concentrations of Fe in solutions from the MI-Low, MI-High and FIT-Blend at pH 2.2 than at pH 6. Thus, in contrast to Ba, pH played a significant role in the amount of Fe leached.

Table 20

Concentrations of dissolved Fe following different pH treatments for 48 hours.

Fe (mg/L)	Aqueous:Solid Ratio	MI-Low	MI-High	FIT-Blend
pH 2.2	10:1	8.1 ± 0.2	20.8 ± 0.5	4.9 ± 0.1
pH 3	10:1	5.3 ± 0.1	14.3 ± 0.2	1.0
pH 3	4:1	9.8 ± 0.3	19	1.5
pH 4	10:1	3.4	9	0.45 ± 0.02
pH 5	10:1	1.0	2.1 ± 0.1	0.4
pH 5	4:1	0.9	1.7	0.35 ± 0.03
pH 6	10:1	0.11 ± 0.02	0.13 ± 0.01	0.6

Results from triplicate analyses are shown as mean ± standard deviation.

At all pH values and for all three barite samples, the highest concentrations of Fe were observed in solution after 48 hours. This trend of increased release of Fe over time was greater at lower pH values (Figure 23). Concentrations of dissolved Fe in the pH leachates were much greater than observed in typical seawater ($0.01\text{-}0.05 \times 10^{-3}$ mg/L; Quinby-Hunt and Turekian, 1983; Donat and Bruland, 1995), but lower than natural values of dissolved Fe as high as 15 mg/L in anoxic interstitial water (Elderfield et al. 1981; Trefry and Presley 1982).

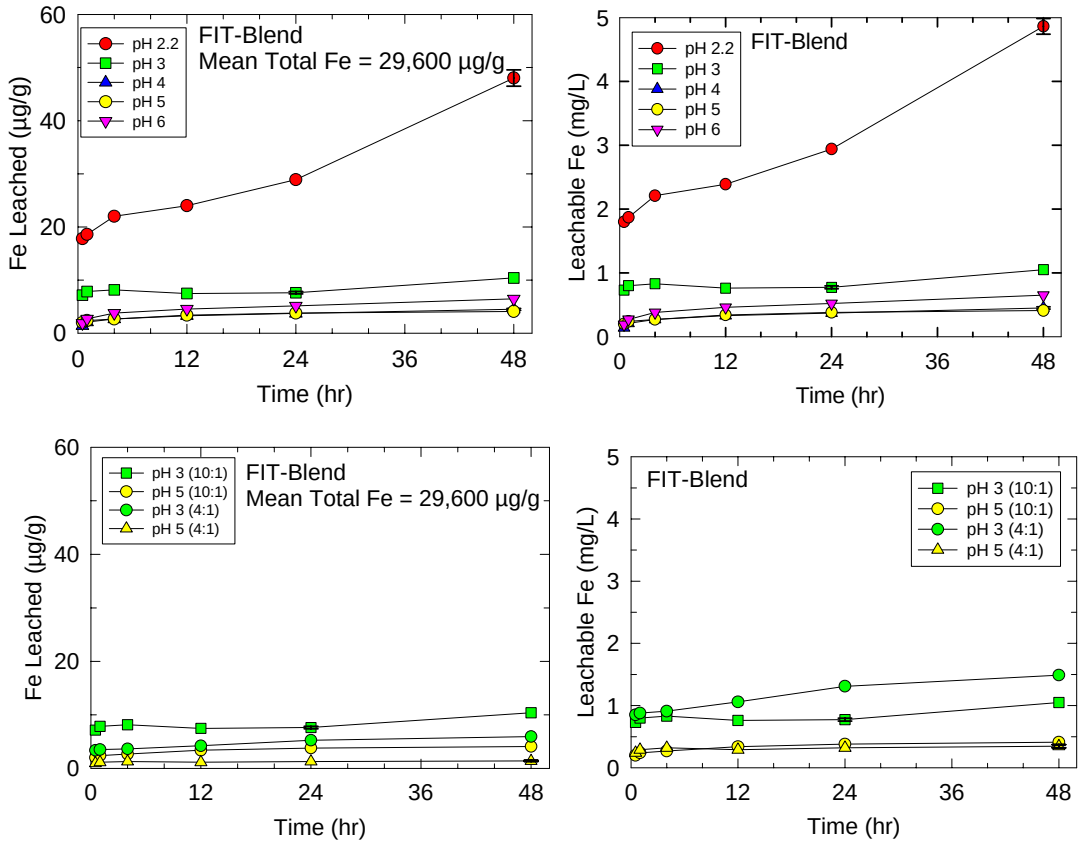

Figure 23. Amounts of Fe leached from the solid phase in µg/g and concentration of Fe leached in mg/L at various pH values and times for the FIT-Blend barite sample.

No strong relationships between concentrations of leachable Ba and Fe were observed for the three barite samples; and in two of three cases an indirect trend was found (Figure 24). Thus, the Ba and Fe are most likely contained in separate phases. As described above, the concentrations of Ba in the various pH leaches for each barite varied only slightly relative to larger ranges in concentrations of Fe. The smallest fraction of total Fe leached was found for the barite sample with the highest total concentration of Fe (FIT-Blend).

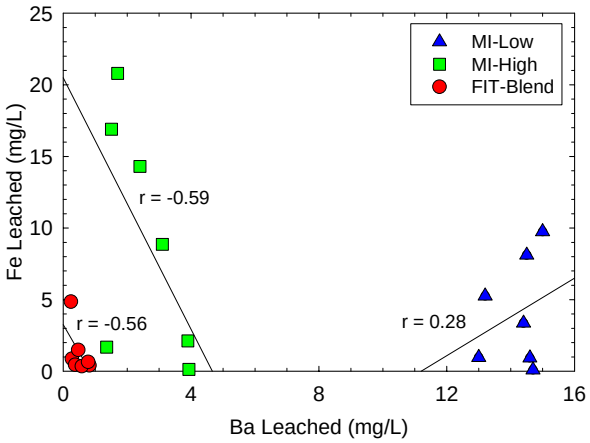

Figure 24. Concentrations of Ba versus Fe in solutions from pH-leaching of the three barite samples.

The solid lines show linear regression fit to the data and r indicates the correlation coefficients from the linear regressions.

6.4.4 Zinc

Approximately 20 percent, 35 percent and 22 percent of the total Zn was leached into pH 2.2 solutions over 48 hours for the MI-Low, MI-High and FIT-Blend samples, respectively (Table 21). For each barite sample, the fraction of Zn leached decreased by about three fold when the pH was increased to 6 (Table 21). However, the fraction of the total Zn leached from each barite differed by <20 percent in the samples with a 4:1 relative to the 10:1 aqueous:solid ratio.

Table 21

Concentrations of total Zn and Zn leached during different pH treatments after 48 hours.

Zn (μg/g)	Aqueous:Solid Ratio	MI-Low	MI-High	FIT-Blend
Total	-	35 ± 3	167 ± 1	1210 ± 10
pH 2.2	10:1	7.2 ± 0.1	59 ± 1	264 ± 4
pH 3	10:1	5.4 ± 0.1	52 ± 2	231
pH 3	4:1	5.9 ± 0.2	51	213
pH 4	10:1	5	50	211 ± 4
pH 5	10:1	3.4	38.7 ± 0.3	155
pH 5	4:1	3.5	34	131 ± 2
pH 6	10:1	1.99 ± 0.01	24.3 ± 0.4	100

Results from triplicate analyses are shown as mean ± standard deviation.

Maximum concentrations of dissolved Zn leached into the pH 2.2 solutions for the MI-Low, MI-High and FIT-Blend samples of barite were 0.73, 6.1 and 26.8 mg/L, respectively (Table 22; Figures 25 through 27). The pH effect yields about a three times lower release of Zn at pH 6 than at pH 2.2. The impact of leaching time also was much less than observed for Fe. Release of Zn from the MI-Low and MI-High samples was near completion in ~12 hours and within 1 hour for the FIT-Blend barite. Thus, the Zn-bearing phase seems to dissolve more rapidly than the Fe-bearing phase. Concentrations of Zn in the pH leachates are much greater than typical values of 0.01-0.45 x 10^{-3} mg/L in seawater (Quinby-Hunt and Turekian 1983, Donat and Bruland 1995) and 0.005-0.185 mg/L in interstitial water (Presley and Kaplan 1972).

Table 22

Concentrations of dissolved Zn following different pH treatments for 48 hours.

Zn (mg/L)	Aqueous:Solid Ratio	MI-Low	MI-High	FIT-Blend
pH 2.2	10:1	0.73 ± 0.02	6.1 ± 0.1	26.8 ± 0.4
pH 3	10:1	0.55 ± 0.01	5.3 ± 0.1	22.6
pH 3	4:1	1.5 ± 0.1	12.8	53.4
pH 4	10:1	0.52	5.0	21.2 ± 0.3
pH 5	10:1	0.35	3.89 ± 0.03	15.5
pH 5	4:1	0.88	8.5	32.8 ± 0.3
pH 6	10:1	0.20 ± 0.01	2.45 ± 0.03	10.1

Results from triplicate analyses are shown as mean ± standard deviation.

In addition to barite, possible phases that contain and can release trace metals include Fe and Zn sulfides such as pyrite (FeS_2) and sphalerite (ZnS) (Kramer et al. 1980; Trefry and Smith 2003). Trends for Ba versus Zn show no strong relationship for the MI-Low and

FIT-Blend samples and a negative relationship for the MI-High sample. Weak correlations between Zn and Fe for the MI-High and FIT-Blend samples suggest that the two phases are distinct, whereas the stronger correlation for the MI-Low sample may be due to the presence of some Zn as an impurity in an Fe phase. Overall, the results support the presence of Zn in a separate non-Ba and non-Fe bearing phase in MI-High and FIT-Blend samples, possibly sphalerite. Another less likely possibility is that Zn and Fe are together in one phase, but each dissolves at a different rate. The MI-Low barite contains 5 to 35 times less Zn than the other two samples and this Zn may be associated with an Fe phase or be in such low concentrations that no clear distinction appears on the Fe versus Zn plot.

Some more specific details based on Figure 25 through Figure 28 include the following: (1) 5 to 40 times more Zn than Fe is leached from the FIT-Blend, (2) at pH values of 2.2 to 4, about 10 times more Fe than Zn is leached from the MI-Low barite, (3) at pH 5 and 6, releases of both Fe and Zn are low with values that are within a factor of 2 to 3, and (4) release of Fe is 2 to 3 times greater than Zn at pH 2.2 to 4 for the MI-High barite; with a change to a 5 and 20 times greater release of Zn than Fe at pH levels of 5 and 6, respectively.

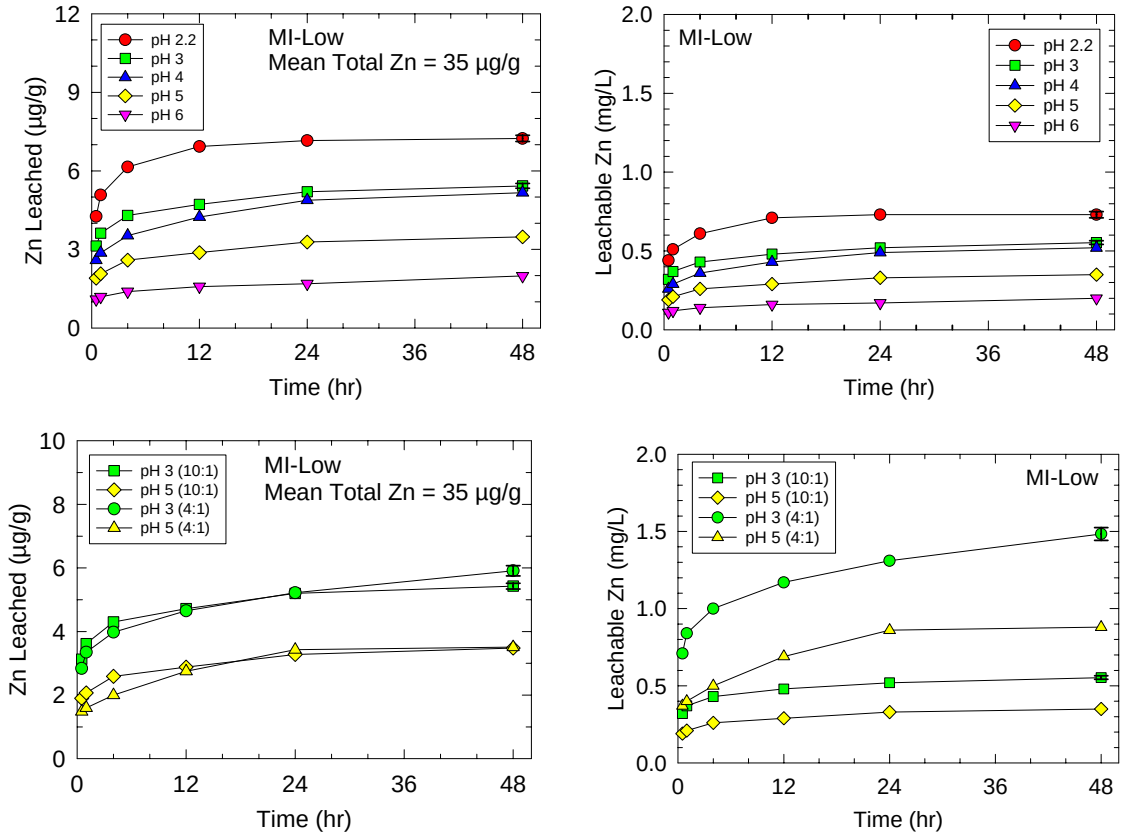

Figure 25. Amounts of Zn leached from the solid phase in µg/g and concentrations of Zn leached in mg/L at various pH values and times for the MI-Low barite sample.

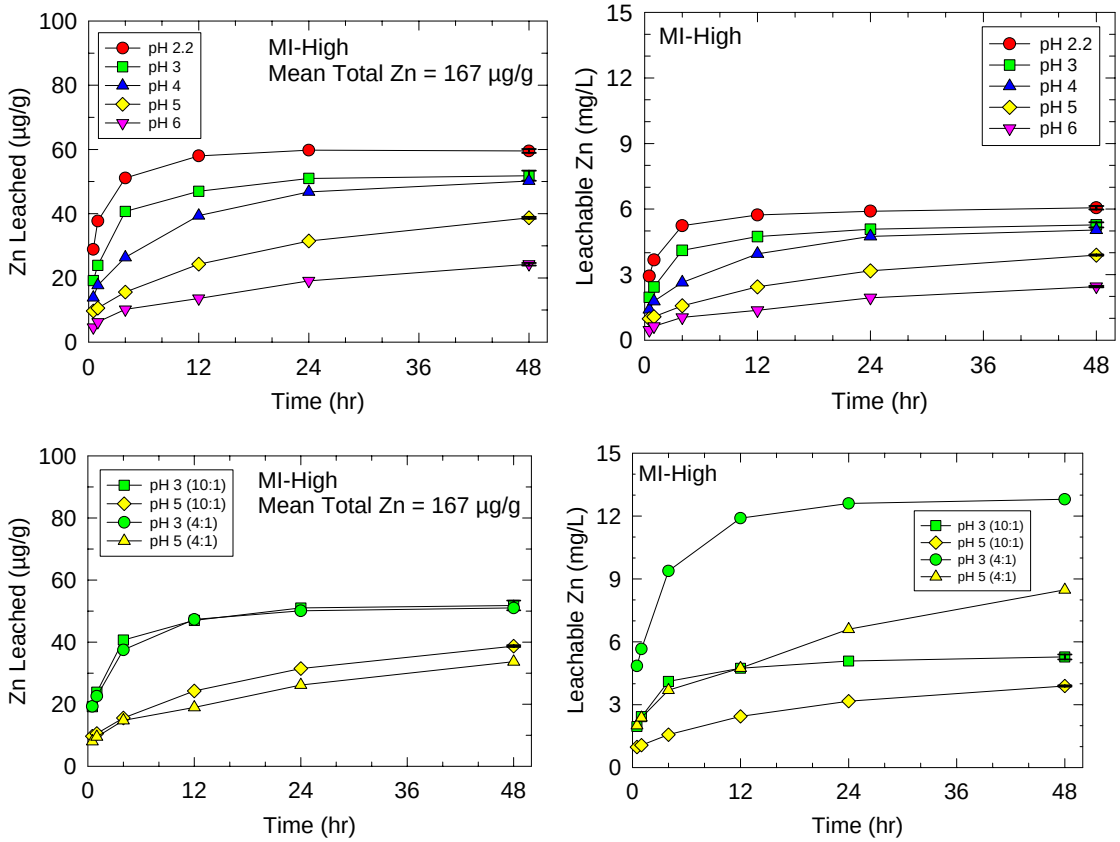

Figure 26. Amounts of Zn leached from the solid phase in µg/g and concentrations of Zn leached in mg/L at various pH values and times for the MI-High barite sample.

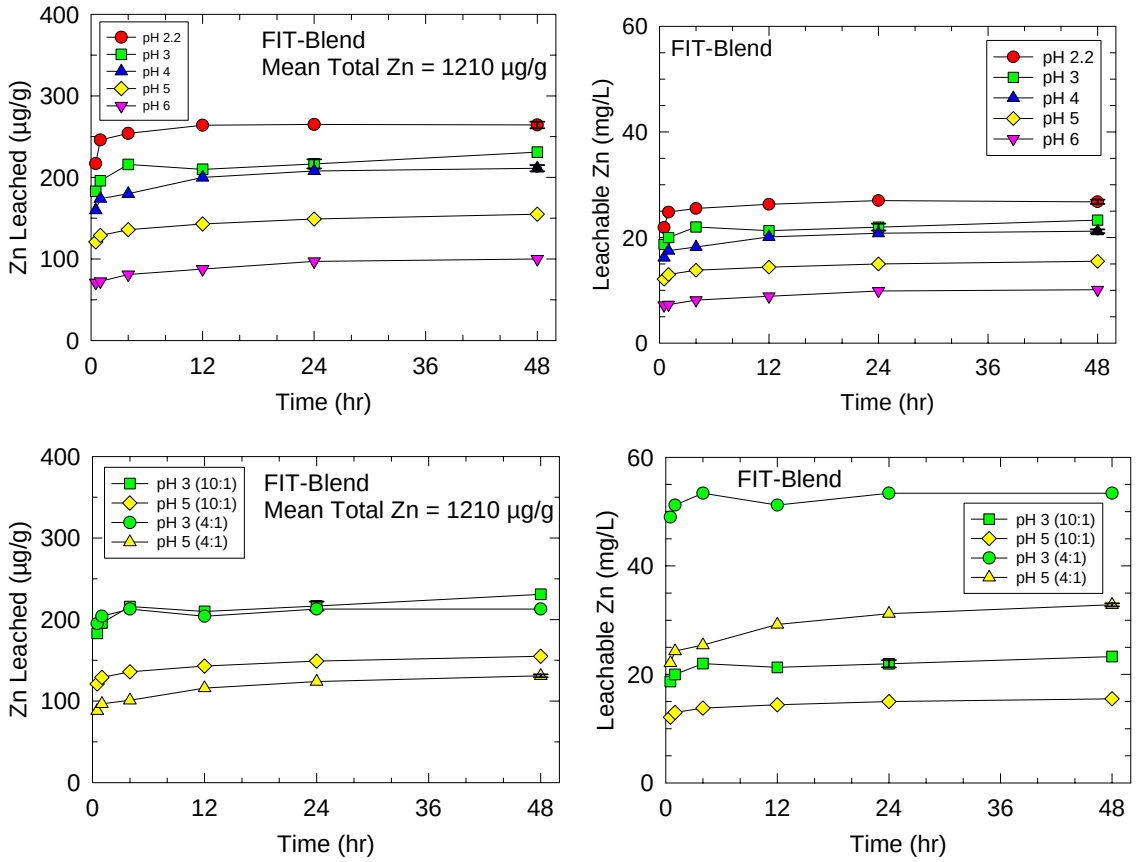

Figure 27. Amounts of Zn leached from the solid phase in µg/g and concentration of Zn leached in mg/L at various pH values and times for the FIT-Blend barite sample.

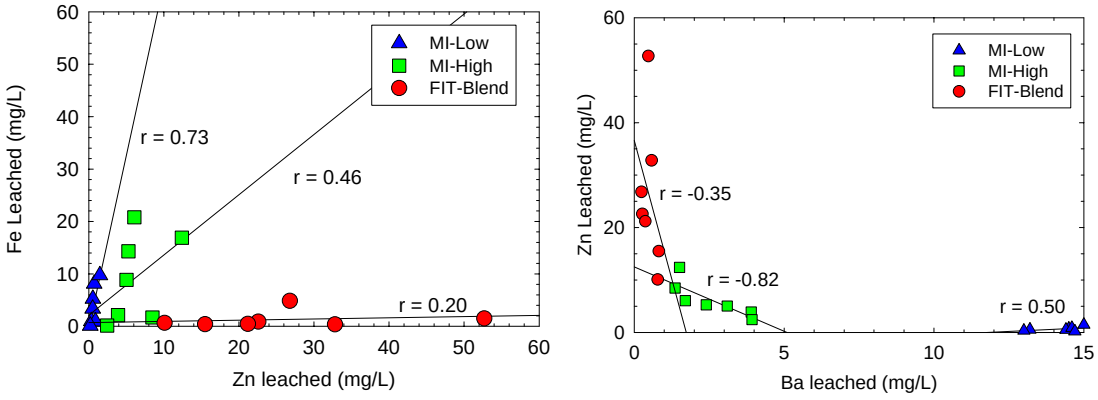

Figure 28. Amounts of Zn versus Fe and Ba versus Zn in solutions from pH-leaching of the three barite samples.

Solid lines show linear regression fit to the data and r indicates correlation coefficients from the linear regressions.

6.4.5 Cadmium

After 48 hours, all the Cd was leached at pH 2.2 from the MI-Low and MI-High samples and about half the Cd was leached at pH 2.2 from the FIT-Blend (Table 23). The fraction of Cd leached at pH 6 decreased to 34 percent, 21 percent and 10 percent of the total for MI-Low, MI-High and FIT-Blend samples, respectively.

Maximum concentrations of dissolved Cd leached into the pH 2.2 solutions for the MI-Low, MI-High and FIT-Blend samples of barite were 50, 82, and 341 µg/L, respectively (Table 24; Figures 29, 30 and 31). The pH effect yields about 4-5 times lower release of Cd at pH 6 than at pH 2.2. The impact of leaching time also was much less than observed for Fe and more similar to that observed for Zn.

Table 23

Concentrations of total Cd and Cd leached during different pH treatments after 48 hours.

Cd (µg/g)	Aqueous:Solid Ratio	MI-Low	MI-High	FIT-Blend
Total	-	0.35 ± 0.02	0.77 ± 0.08	7.0 ± 0.2
pH 2.2	10:1	0.50 ± 0.02	0.80 ± 0.01	3.37 ± 0.04
pH 3	10:1	0.41 ± 0.01	0.45 ± 0.01	3.0
pH 3	4:1	0.37 ± 0.02	0.47	1.7
pH 4	10:1	0.22	0.40	2.34 ± 0.03
pH 5	10:1	0.18	0.23 ± 0.01	1.4
pH 5	4:1	0.17	0.16	1.06 ± 0.03
pH 6	10:1	0.12 ± 0.01	0.16 ± 0.01	0.7

Results from triplicate analyses are shown as mean ± standard deviation.

Table 24

Concentrations of Cd leached during different pH treatments after 48 hours.

Cd (µg/L)	Aqueous:Solid Ratio	MI-Low	MI-High	FIT-Blend
pH 2.2	10:1	50 ± 1	82 ± 1	341 ± 3
pH 3	10:1	41 ± 1	46 ± 1	307
pH 3	4:1	93 ± 5	119	426
pH 4	10:1	22	40	235 ± 3
pH 5	10:1	18	23 ± 1	140
pH 5	4:1	44	41	265 ± 8
pH 6	10:1	12.2 ± 0.5	17 ± 1	72

Results from triplicate analyses are shown as mean ± standard deviation.

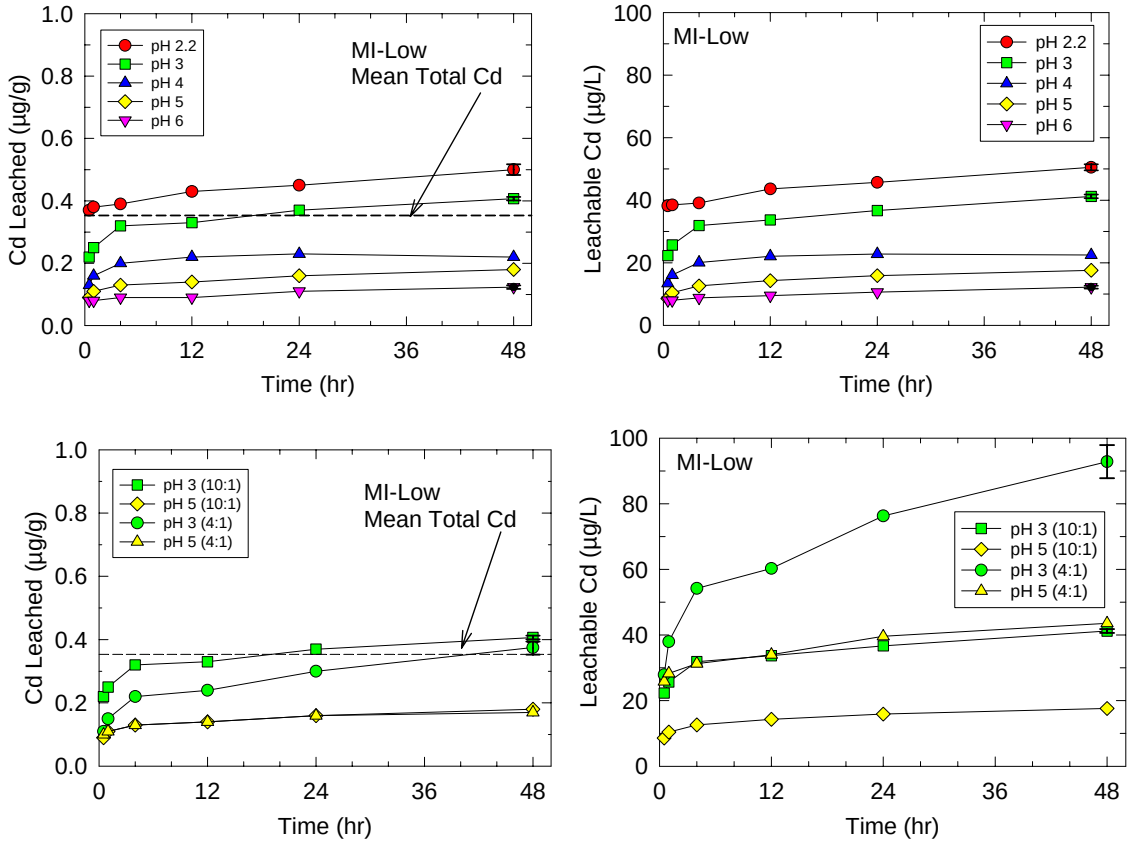

Figure 29. Amounts of Cd leached from the solid phase in µg/g and concentrations of Cd leached in µg/L at various pH values and times for the MI-Low barite sample.

Concentrations of dissolved Cd in the various pH solutions from this study were 2-3 orders of magnitude higher than the highest values reported for Cd in sediment interstitial water (0.07-0.27 µg/L, Klinkhammer et al. 1982; 0.01-0.35 µg/L, Trefry et al. 1986b).

Strong correlations ($r \geq 0.90$) were observed for Zn versus Cd for each barite sample (Figure 33) and for the grouped data (Figure 32). Good, but somewhat lower correlation coefficients were found for Fe versus Cd for the MI-High and MI-Low samples. A weaker correlation ($r = 0.48$) was found for Fe versus Cd for the FIT-Blend sample. The good fit for Zn versus Cd for the FIT-Blend and the weak fit for Fe versus Cd, coupled with the weak relationship between Fe and Zn (Figure 32) support the occurrence of Cd in a Zn phase, most likely sphalerite. The distinction is not as clear for the MI-High and MI-Low samples and Cd may be present in either a Zn or Fe or Zn-Fe phase. No significant relationships were observed for Ba versus Cd for the MI-Low and FIT-Blend samples and a negative relationship ($r = -0.73$) was found for the MI-High sample.

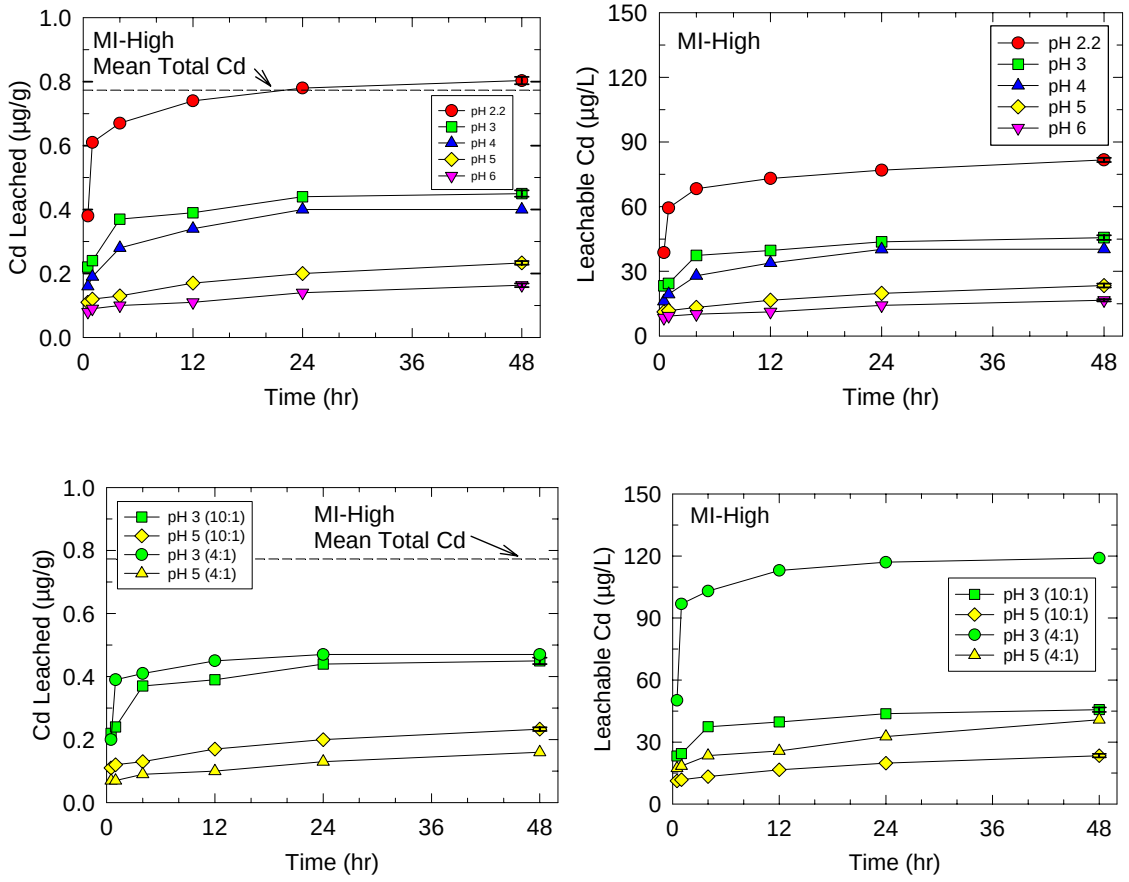

Figure 30. Amounts of Cd leached from the solid phase in µg/g and concentrations of Cd leached in µg/L at various pH values and times for the MI-High barite sample.

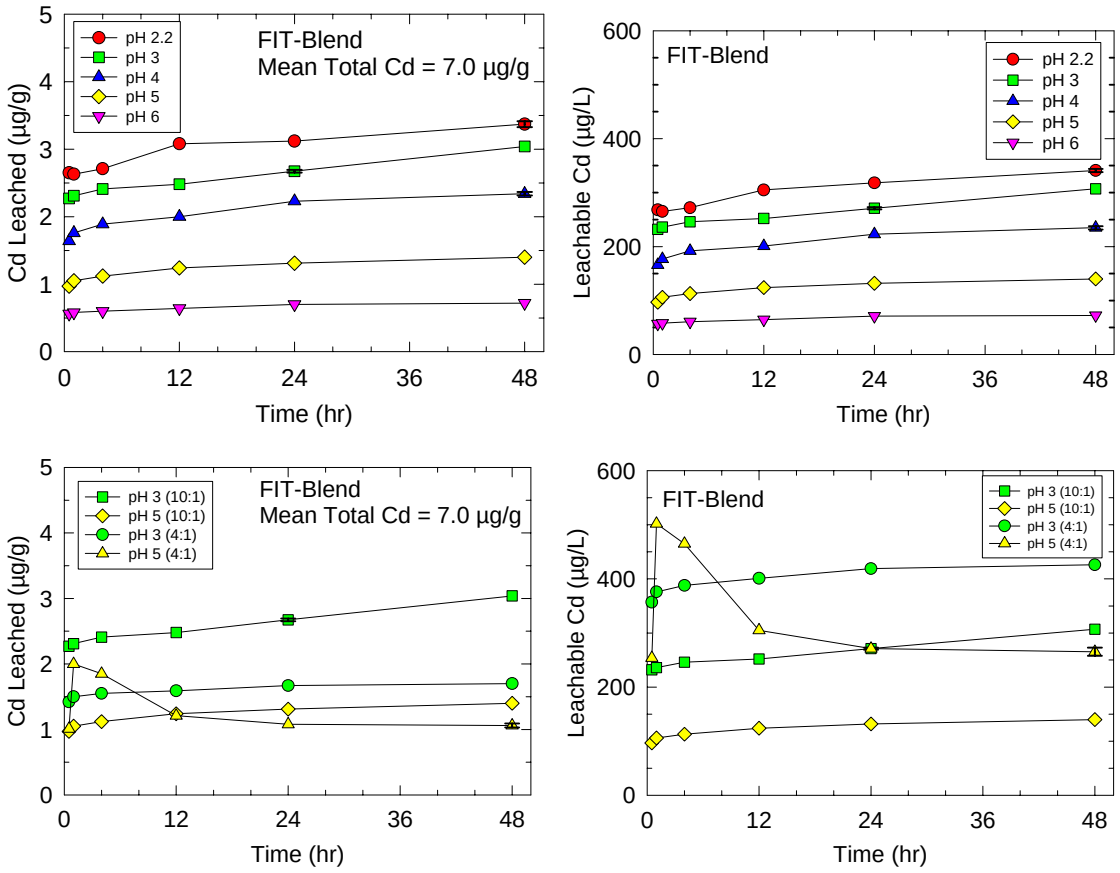

Figure 31. Amounts of Cd leached from the solid phase in µg/g and concentration of Cd leached in µg/L at various pH values and times for the FIT-Blend barite.

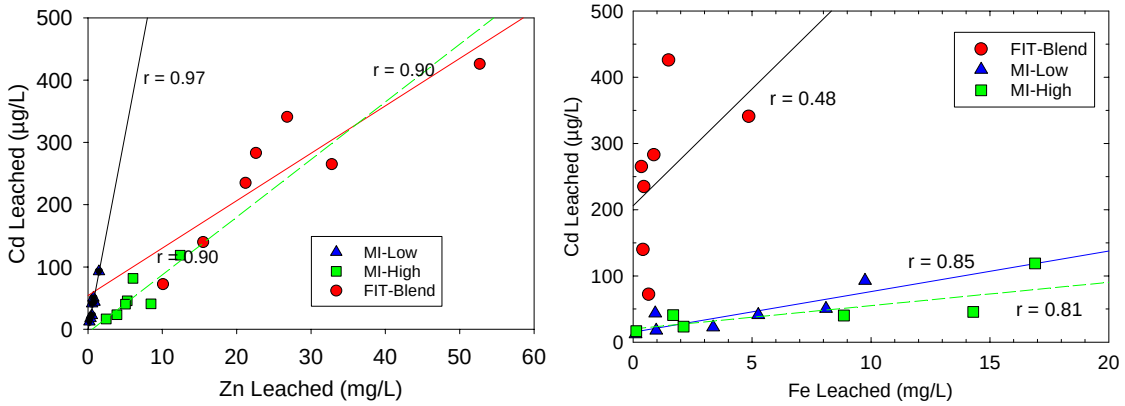

Figure 32. Amounts of Zn and Fe versus Cd leached after 48 hours at various pH values for each of the three barite samples.

The lines on each graph in Figure 32 show linear regression fits to the data for each barite sample with correlation coefficients (r). The dashed line on each figure represents the MI-High sample to avoid confusion with the nearby line.

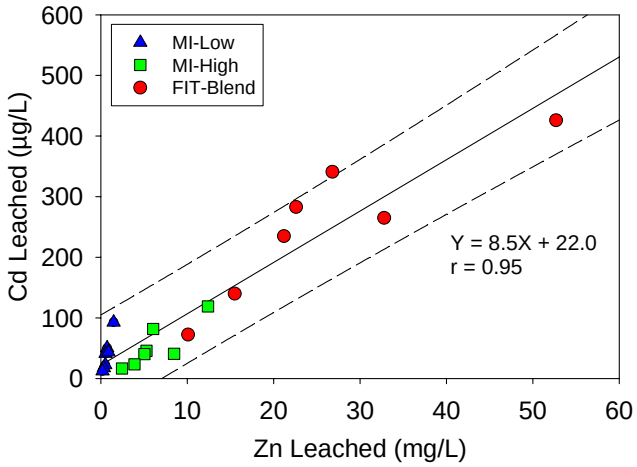

Figure 33. Amounts of Zn versus Cd leached after 48 hours at various pH values for each of the three barite samples.

The solid line shows linear regression fit to the data and dashed lines show 95 percent prediction interval. Equation and correlation coefficient (r) are from the linear regression.

6.4.6 Lead

Approximately 8 percent, 1.3 percent and 6.7 percent of the total Pb was leached over 48 hours into pH 2.2 solutions for the MI-Low, MI-High and FIT-Blend samples, respectively (Table 25). The fraction of Pb leached at pH 6 increased to 12 percent and 7 percent, respectively, for the MI-Low and MI-High samples. In contrast, the fraction of total Pb leached at pH 6 for the FIT-Blend decreased to 1 percent.

Table 25

Concentrations of total Pb and Pb leached during different pH treatments after 48 hours.

Pb (µg/g)	Aqueous:Solid Ratio	MI-Low	MI-High	FIT-Blend
Total	-	318 ± 3	243 ± 7	1370 ± 50
pH 2.2	10:1	24.7 ± 0.1	3.1 ± 0.1	92 ± 1
pH 3	10:1	41 ± 1	2.4 ± 0.1	72
pH 3	4:1	37 ± 2	4.4	43
pH 4	10:1	46	13	50 ± 1
pH 5	10:1	49	18.3 ± 0.4	28
pH 5	4:1	30	14	12.4 ± 0.2
pH 6	10:1	39 ± 1	17 ± 1	14

Results from triplicate analyses are shown as mean ± standard deviation.

Maximum concentrations of dissolved Pb leached into the pH 2.2 solutions for the MI-Low, MI-High and FIT-Blend samples of barite were 2.5, 0.32, and 9.3 mg/L, respectively (Table 26; Figures 33, 34, and 35). The impact of leaching time and pH for Pb was less than observed for Fe and similar to that observed for Zn for the MI-Low and MI-High samples (Figures 33 and 34). However, trends for Pb concentrations for the FIT-Blend barite were similar to those observed for Fe (Figure 35).

Table 26

Concentrations of Pb leached during different pH treatments after 48 hours.

Pb (mg/L)	Aqueous:Solid Ratio	MI-Low	MI-High	FIT-Blend
pH 2.2	10:1	2.5 ± 0.1	0.32 ± 0.01	9.3 ± 0.1
pH 3	10:1	4.2 ± 0.1	0.25 ± 0.02	7.3
pH 3	4:1	9.2 ± 0.6	1.1	10.9
pH 4	10:1	4.6	1.3	5.0 ± 0.1
pH 5	10:1	4.9	1.84 ± 0.04	2.8
pH 5	4:1	7.5	3.4	3.1 ± 0.1
pH 6	10:1	3.9 ± 0.2	1.7 ± 0.1	1.4

Results from triplicate analyses are shown as mean ± standard deviation

As observed for Cd, concentrations of dissolved Pb in the various pH solutions from this study were 1 to 2 orders-of-magnitude higher than the highest values reported for Pb in sediment interstitial water (0.05 mg/L, DelValls et.al. 1997).

Correlation coefficients of 0.77 were observed for Zn versus Pb for both the MI-Low and FIT-Blend samples (Figure 37) and 0.65 for Fe versus Pb in the FIT-Blend barite. Other relationships for Pb versus Zn, Fe and Ba were weak. These trends support the occurrence of Pb with a Zn phase for the MI-Low samples and a Zn-Fe phase for the FIT-Blend barite. These matches are also consistent with the trends for release of Pb versus time where the MI-Low sample follows the rates observed for Zn whereas release rates for Zn from the FIT-Blend barite more closely parallel the results for Fe. Concentrations of Pb leached from the MI-High barite averaged about 4 times less than that found for the other two samples and these low Pb releases did not correlate with levels of Ba, Fe or Zn; however, the rates of Pb release from the MI-High sample more closely match those observed for Zn.

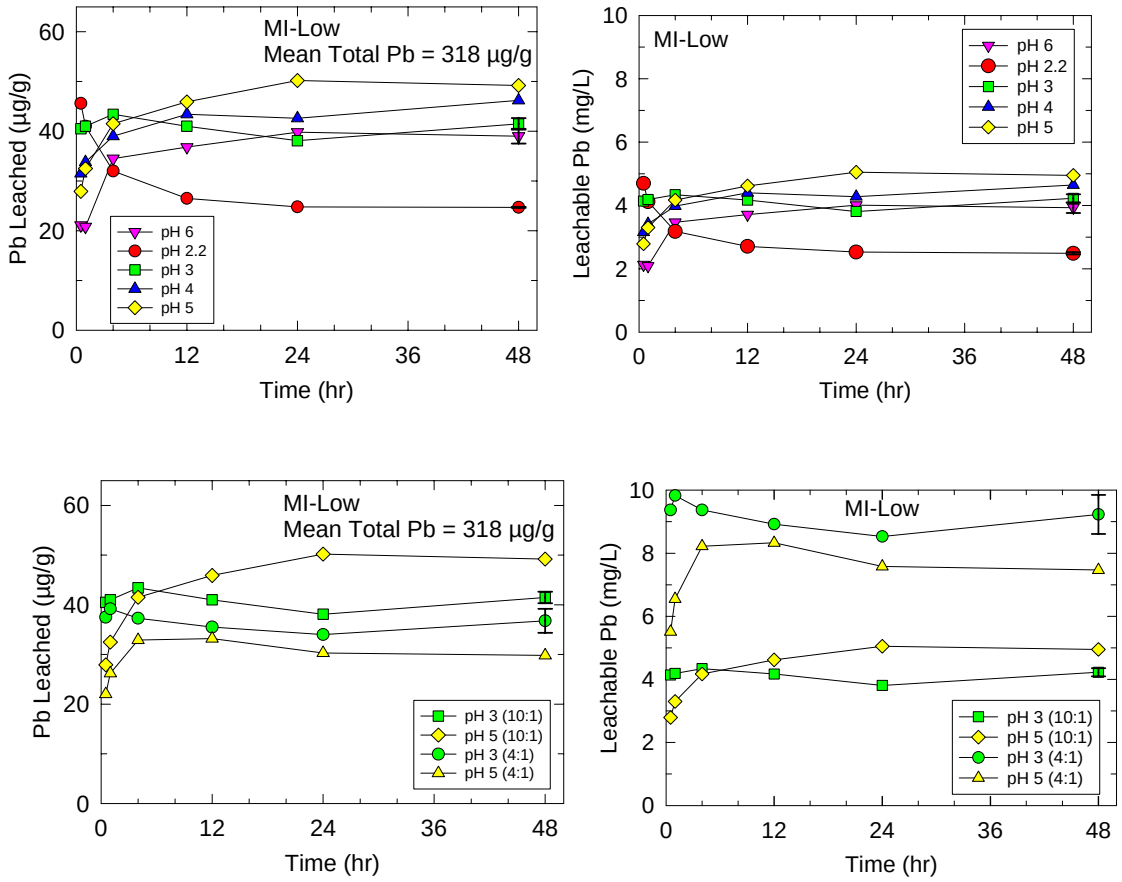

Figure 34. Amounts of Pb leached from the solid in µg/g and concentrations of Pb leached in mg/L at various pH values and times for the MI-Low barite sample.

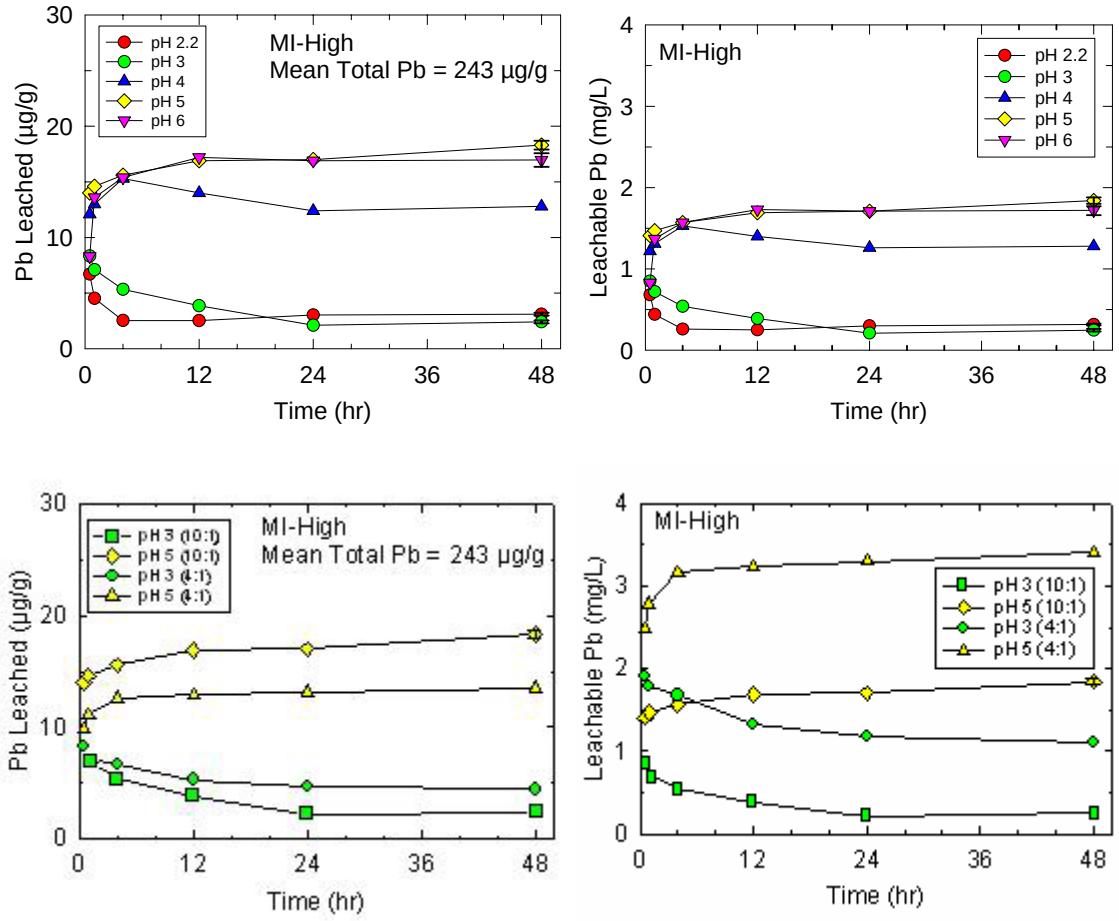

Figure 35. Amounts of Pb leached from the solid in µg/g and concentrations of Pb leached in mg/L at various pH values and times for the MI-High barite sample.

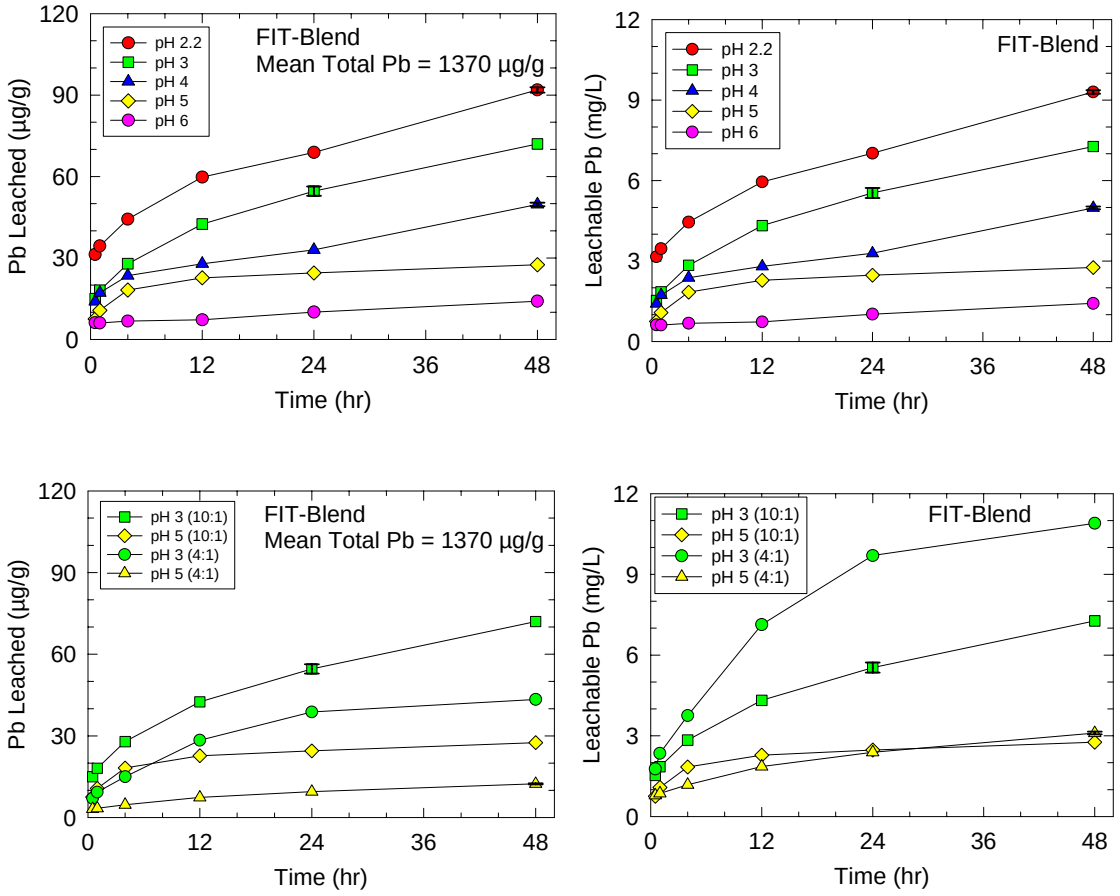

Figure 36. Amounts of Pb leached from the solid phase in µg/g and concentration of Pb leached in mg/L at various pH values and times for the FIT-Blend barite sample.

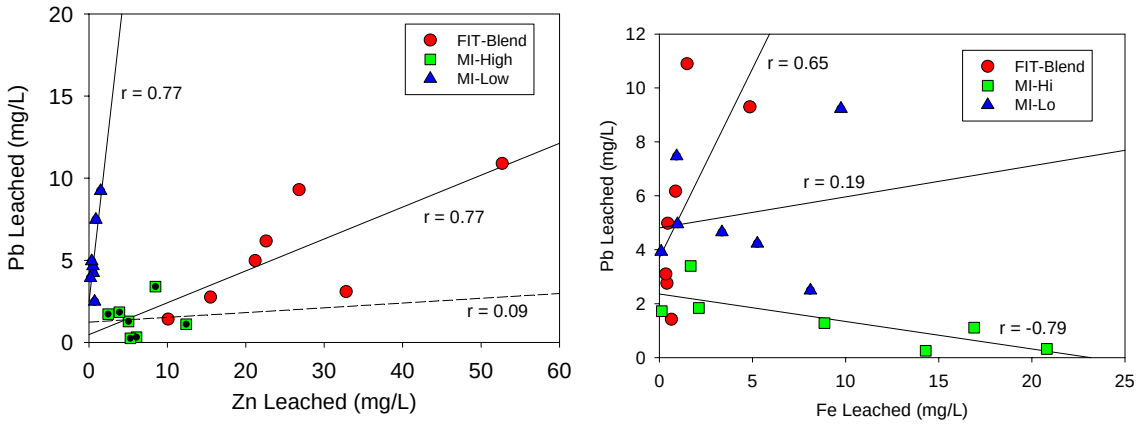

Figure 37. Amounts of Zn and Fe versus Pb leached after 48 hours at various pH values for each of the three barite samples.

The lines on each graph show linear regression fits to the data for each barite sample with correlation coefficients (r). The dashed line on each figure represents the MI-High sample to avoid confusion with the nearby line

6.4.7 Mercury

After 48 hours, the amount of Hg leached from the three barite samples at all pH values was <0.001 µg/g, the detection limit using CVAAS. This detection limit is equivalent to <0.2 percent, <0.02 percent and <0.02 percent of the total Hg being leached into solution for the MI-Low, MI-High and FIT-Blend samples, respectively (Table 27). Selected samples were analyzed by gold amalgamation and AFS (Tables 27 and 28). The result using the technique with lower detection limits shows that the maximum fraction of total Hg leached was at pH 2.2 and was 0.02 percent, 0.005 percent, and 0.006 percent for the MI-Low, MI-High and FIT-Blend samples, respectively (Table 27).

Concentrations of dissolved Hg in the various pH leachates for all three samples ranged from 0.004 to 0.040 µg/L (4-40 ng/L). These levels range from being comparable with to more than 50 times greater than found in ambient seawater. Leachable Hg concentrations from this study are much lower than values as high as 3 µg/L reported by Bothner et al. (1980) for anoxic interstitial water.

Table 27

Concentrations of total Hg and Hg leached during different pH treatments after 48 hours.

Hg (µg/g)	Aqueous:Solid Ratio	MI-Low	MI-High	FIT-Blend
Total	-	0.44	5.9	6.7
pH 2.2	10:1	0.00010	0.0003	0.0004
pH 3	10:1	0.00004	0.0003	0.0003
pH 3	4:1	0.00002	0.0001	0.0001
pH 4	10:1	-	-	-
pH 5	10:1	-	-	-
pH 5	4:1	-	-	-
pH 6	10:1	0.00010	0.0001	0.0002

Table 28

Concentrations of Hg leached during different pH treatments after 48 hours.

Hg (µg/L)	Aqueous:Solid Ratio	MI-Low	MI-High	FIT-Blend
pH 2.2	10:1	0.010	0.033	0.040
pH 3	10:1	0.004	0.029	0.032
pH 3	4:1	0.004	0.020	0.036
pH 4	10:1	-	-	-
pH 5	10:1	-	-	-
pH 5	4:1	-	-	-
pH 6	10:1	0.007	0.010	0.020

Concentrations of Hg in the pH leachates did not correlate well with Ba concentrations for the MI-Low sample and were inversely correlated with Ba for the MI-High and FIT-Blend barites (Figure 38). These observations are consistent with previous studies that conclude that Hg is not bound in the barite phase (Kramer et al. 1980, Trefry and Smith 2003). Strong positive correlations were found for Hg versus Fe for the MI-High and Hg versus Zn for the FIT-Blend samples (Figure 38). Hg concentrations in the pH leachates for the MI-Low sample did not correlate with Ba, Zn or Fe, most likely a function of the very low levels of Hg leached from the MI-Low barite.

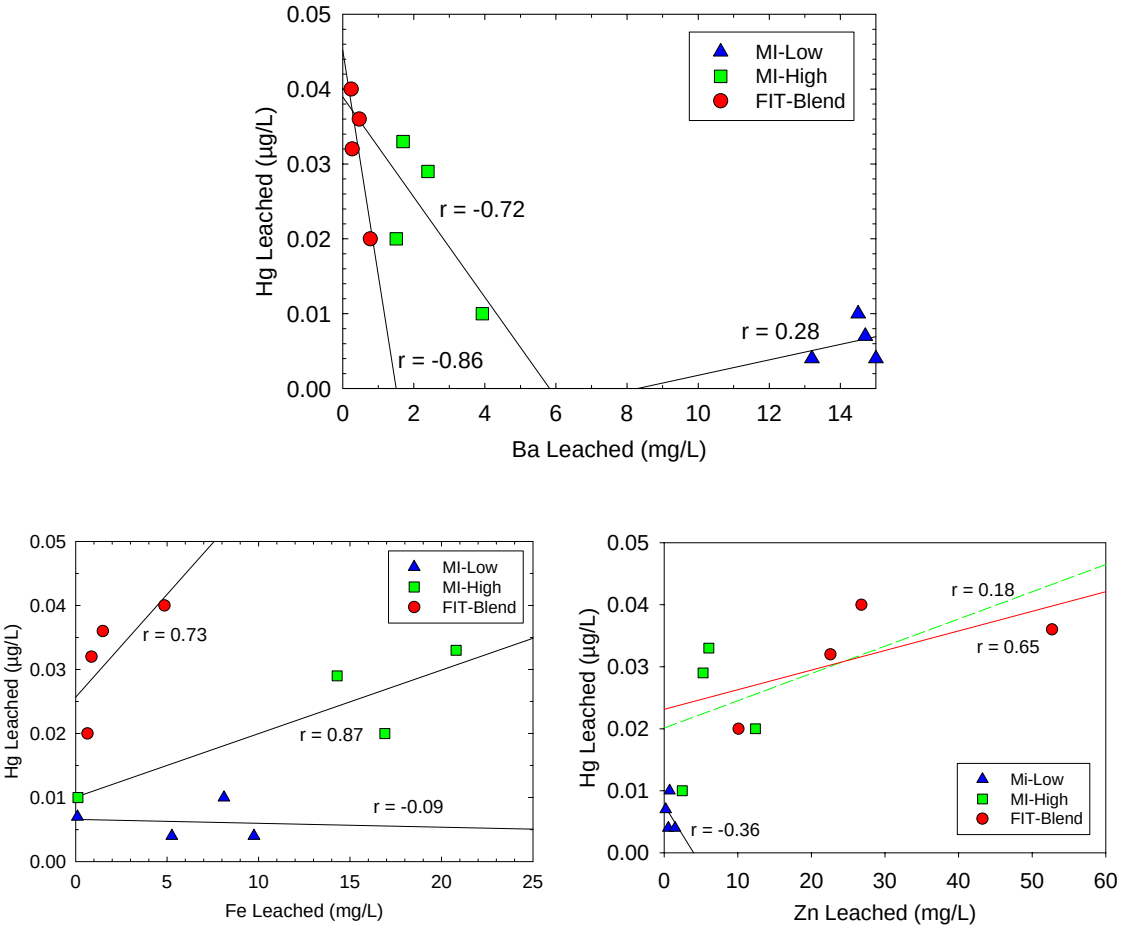

Figure 38. Concentrations of Ba, Fe and Zn versus Hg leached after 48 hours at various pH values for each of the three barite samples.

The lines on each graph show linear regression fits to the data for each barite sample with correlation coefficients (r). The dashed line was used in the Zn versus Hg figure to represent the MI-High sample to avoid confusion with the nearby line.

6.4.8 Copper

Approximately 20 percent, 45 percent and 30 percent of the total Cu was leached into pH 2.2 solutions over 48 hours for the MI-Low, MI-High and FIT-Blend samples, respectively (Table 29). The fraction of Cu leached at pH 6 decreased to 6 percent, 23 percent and 8 percent of the total for MI-Low, MI-High and FIT-Blend samples, respectively. The fraction of the total Cu leached from the barite in the sample with a 4:1 aqueous:solid ratio was within 25 percent of the amount removed when a 10:1 aqueous:solid ratio was used.

Maximum concentrations of dissolved Cu leached into the pH 3 solutions for the MI-Low, MI-High and FIT-Blend samples of barite were 4.1, 9.0, and 11.2 mg/L, respectively (Table 30; Figures 39 through 42). The pH effect causes a 2-3 times lower release of Cu at pH 6 than at pH 2.2. In all cases, the amount of Cu leached increased with time; however, >90 percent of the total amount leached over 48 hours was leached in 12 hours or less, similar to the rate observed for Zn.

Table 29

Concentrations of total Cu and Cu leached during different pH treatments after 48 hours.

Cu (μg/g)	Aqueous:Solid Ratio	MI-Low	MI-High	FIT-Blend
Total	-	98 ± 4	88 ± 4	189 ± 1
pH 2.2	10:1	20 ± 1	40 ± 1	56 ± 1
pH 3	10:1	15.5 ± 0.5	36 ± 1	46
pH 3	4:1	16.2 ± 0.3	36	45
pH 4	10:1	13	33	37.1 ± 0.3
pH 5	10:1	12	27 ± 1	26
pH 5	4:1	9	25	23 ± 1
pH 6	10:1	6.4 ± 0.2	19.9 ± 0.3	15

Results from triplicate analyses are shown as mean ± standard deviation.

Table 30

Concentrations of Cu leached during different pH treatments after 48 hours.

Cu (mg/L)	Aqueous:Solid Ratio	MI-Low	MI-High	FIT-Blend
pH 2.2	10:1	2.0 ± 0.1	4.1 ± 0.1	5.7 ± 0.1
pH 3	10:1	1.6 ± 0.1	3.6 ± 0.1	4.7
pH 3	4:1	4.1 ± 0.1	9.0	11.2
pH 4	10:1	1.3	3.3	3.72 ± 0.02
pH 5	10:1	1.2	2.8 ± 0.1	2.6
pH 5	4:1	2.4	6.4	5.8 ± 0.1
pH 6	10:1	0.64 ± 0.01	2.0 ± 0.1	1.5

Results from triplicate analyses are shown as mean ± standard deviation.

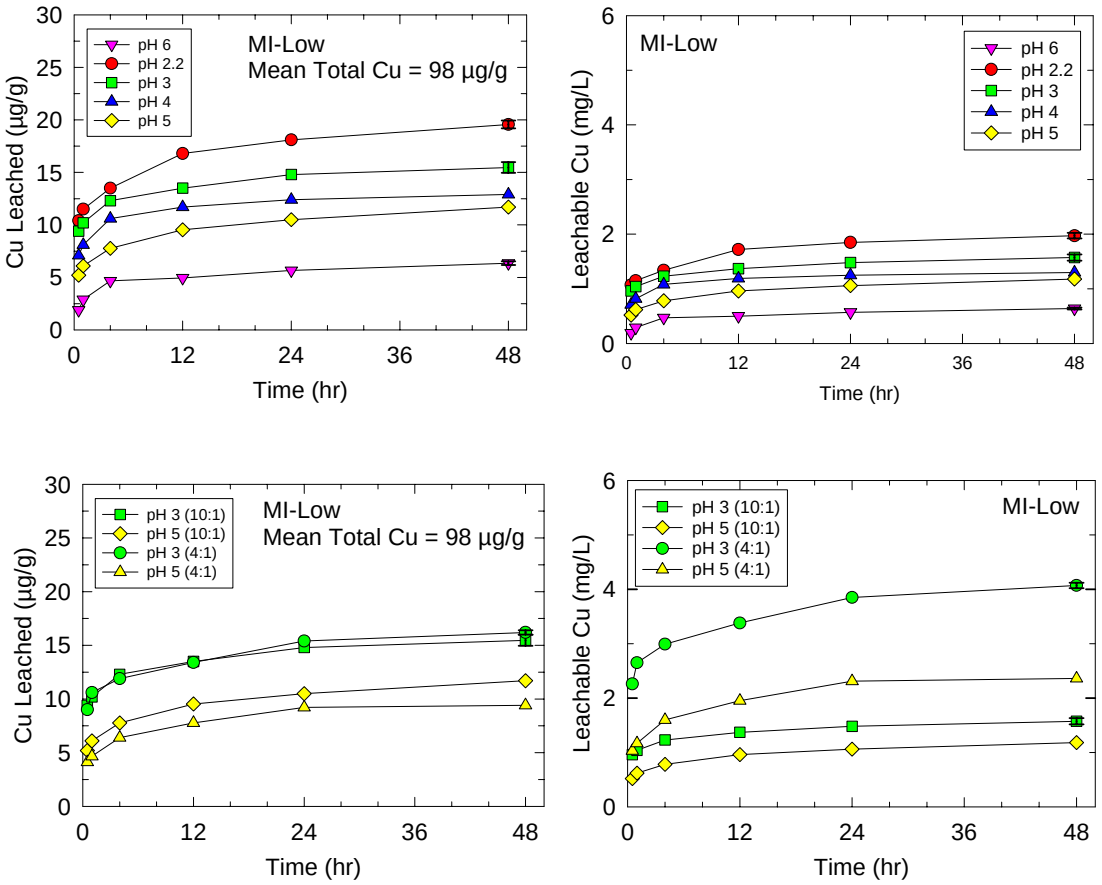

Figure 39. Amounts of Cu leached from the solid in µg/g and concentrations of Cu leached in mg/L at various pH values and times for the MI-Low barite sample.

Concentrations of Cu in the pH leachates were 3 to 40 times greater than values reported for sediment interstitial water (Klinkhammer et al. 1982). In each case, the correlation coefficient for the Zn versus Cu relationship was 0.99. This relationship strongly supports the presence of Cu in a Zn phase such as sphalerite.

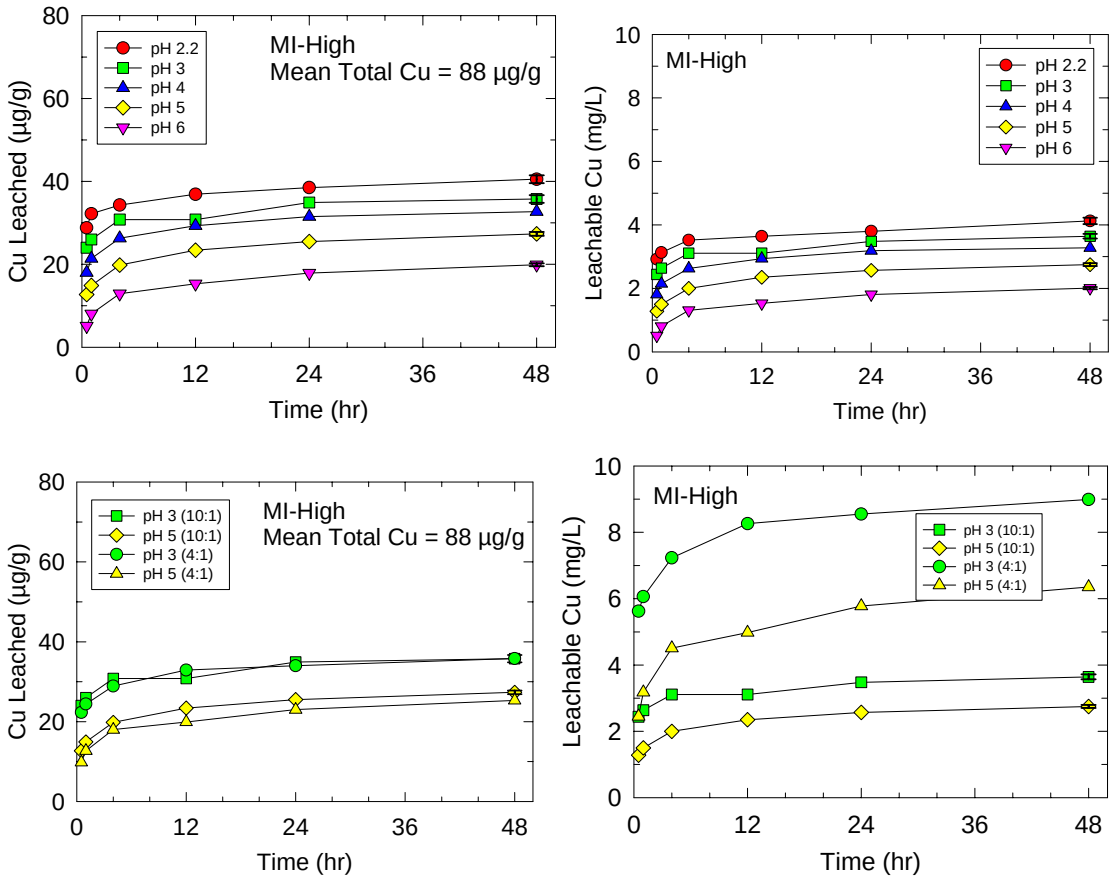

Figure 40. Amounts of Cu leached from the solid in µg/g and concentrations of Cu leached in mg/L at various pH values and times for the MI-High barite sample.

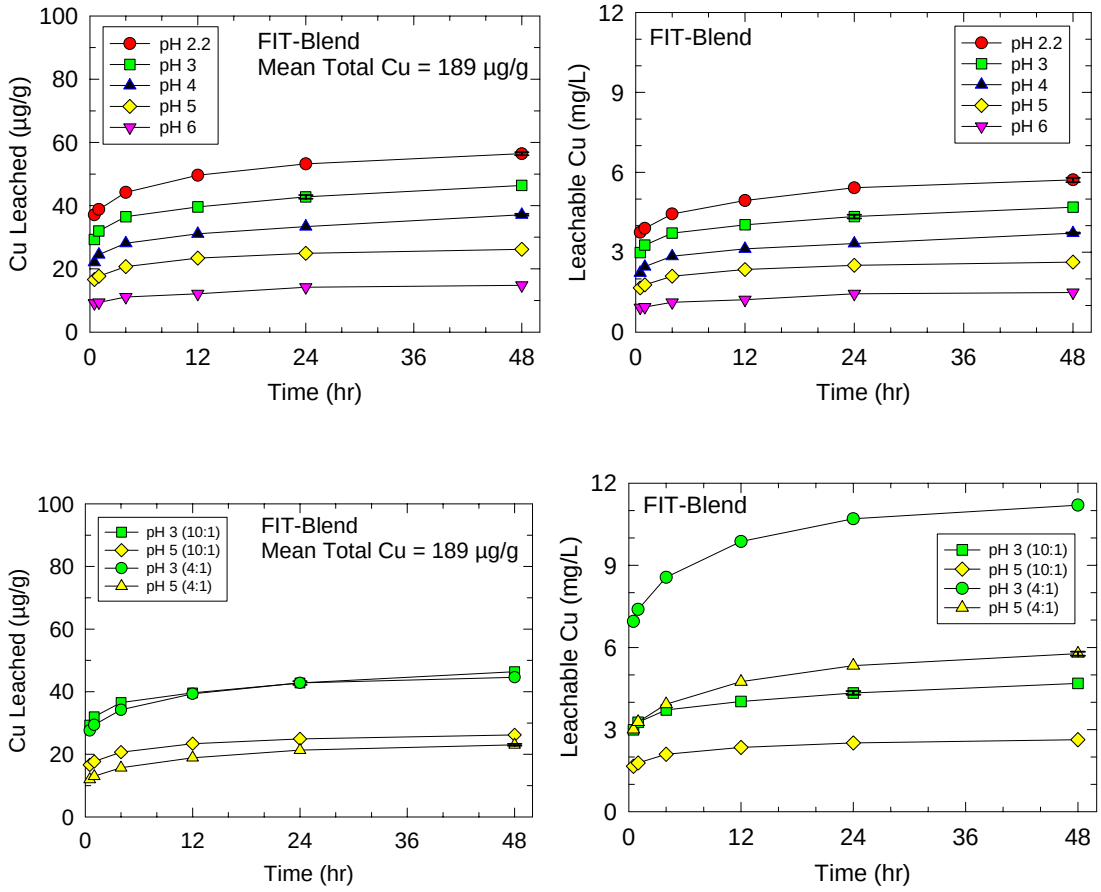

Figure 41. Amounts of Cu leached from the solid phase in µg/g and concentration of Cu leached in mg/L at various pH values and times for the FIT-Blend barite sample.

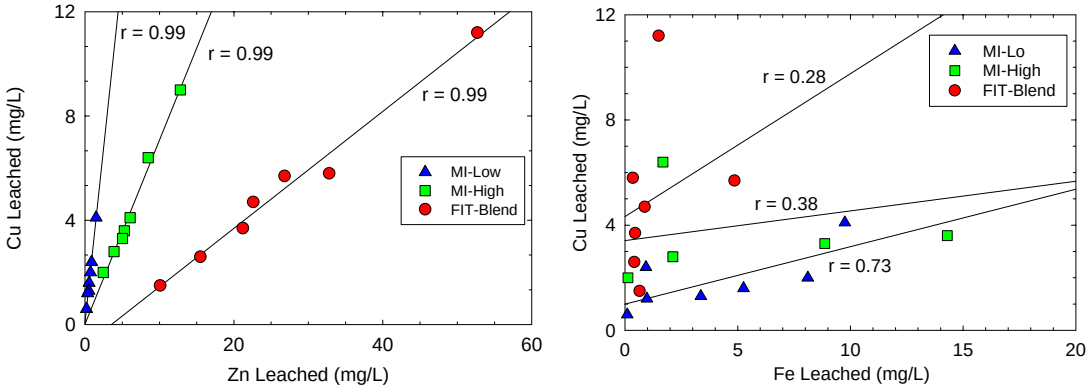

Figure 42. Amounts of Zn and Fe versus Cu leached after 48 hours at various pH values for each of the three barite samples.

The lines on each graph in Figure 42 show linear regression fits to the data for each barite sample with correlation coefficients (r). The r = 0.28 is the correlation coefficient for Fe versus Cu in FIT-Blend.

6.4.9 Chromium

After 48 hours, ~1.8 percent, ~6.8 percent and ~2.2 percent of the total Cr was leached into pH 2.2 solutions for the MI-Low, MI-High and FIT-Blend samples, respectively (Table 31). The fraction of Cr leached at pH 6 decreased to 0.1 percent, 0.3 percent and 0.5 percent of the total for MI-Low, MI-High and FIT-Blend samples, respectively. The fraction of the total Cr leached from the barite was less than 20 percent different in the sample with a 4:1 relative to the 10:1 aqueous:solid ratio.

Maximum concentrations of dissolved Cr leached into the pH 3 solutions for the MI-Low, MI-High and FIT-Blend samples of barite were 34, 44, and 45 µg/L, respectively (Table 32; Figures 43, 44 and 45). The pH effect yields about 4-20 times lower release of Cr at pH 6 than at pH 2.2. In all cases, the amount of Cr leached increased with time; however, greater than 90 percent of the total amount leached over 48 hours was leached in 12 hours or less.

Table 31

Concentrations of total Cr and Cr leached during different pH treatments after 48 hours.

Cr (µg/g)	Aqueous:Solid Ratio	MI-Low	MI-High	FIT-Blend
Total	-	15 ± 1	6.5 ± 0.4	11 ± 1
pH 2.2	10:1	0.27 ± 0.01	0.44 ± 0.02	0.24 ± 1
pH 3	10:1	0.12 ± 0.01	0.22 ±0.01	0.16
pH 3	4:1	0.14 ± 0.01	0.18	0.18
pH 4	10:1	0.09	0.13	0.13 ± 0.01
pH 5	10:1	0.06	0.06 ± 0.01	0.09
pH 5	4:1	0.05	0.05	0.09 ± 0.01
pH 6	10:1	0.02	0.02	0.06

Results from triplicate analyses are shown as mean ± standard deviation.

Table 32

Concentrations of Cr leached during different pH treatments after 48 hours.

Cr (µg/L)	Aqueous:Solid Ratio	MI-Low	MI-High	FIT-Blend
pH 2.2	10:1	27.5 ± 0.4	45 ± 1	23.9 ± 0.3
pH 3	10:1	12 ± 1	23 ± 1	16
pH 3	4:1	34 ± 2	44	45
pH 4	10:1	9	12	13.2 ± 0.03
pH 5	10:1	6	5.6 ± 0.1	9
pH 5	4:1	13	12	22± 1
pH 6	10:1	2	2	6

Results from triplicate analyses are shown as mean ± standard deviation.

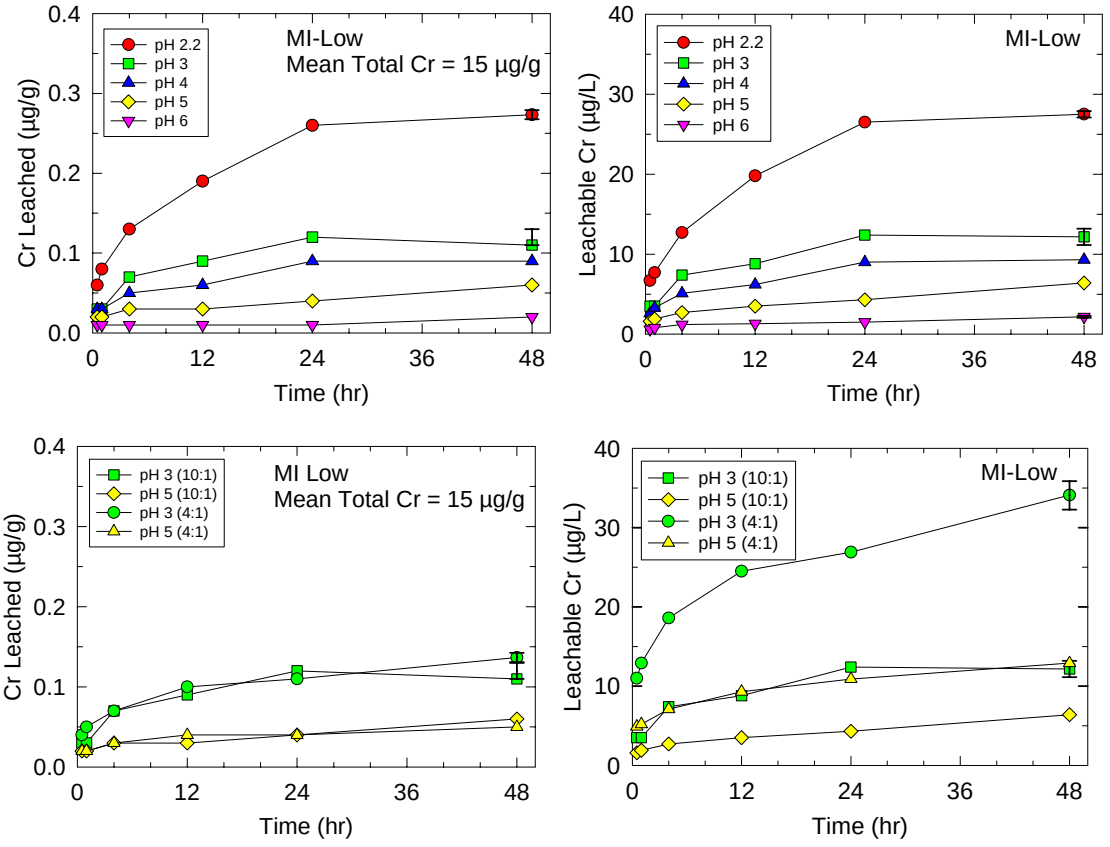

Figure 43. Amounts of Cr leached from the solid in µg/g and concentrations of Cr leached in µg/L at various pH values and times for the MI-Low barite sample.

Correlation coefficients of 0.88 and 0.98 were observed for Zn versus Cr for the MI-Low and FIT-Blend samples, respectively, and 0.93 and 0.94 for Fe versus Cr in the MI-Low and MI-High barite samples, respectively (Figure 46). Other relationships for Pb versus Zn, Fe and Ba were weak. These trends support the occurrence of Cr with a Zn phase for the FIT-Blend and a Zn-Fe phase the MI-Low and MI-High samples.

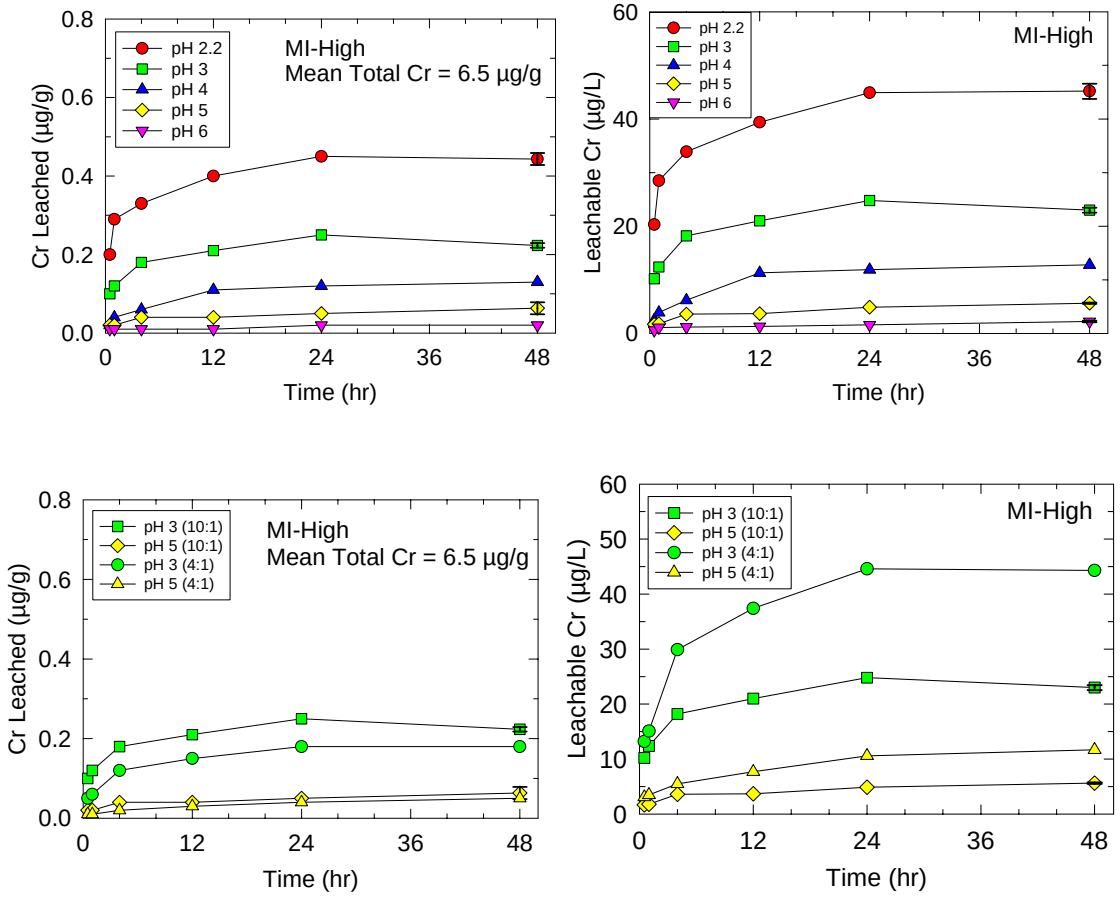

Figure 44. Amounts of Cr leached from the solid in µg/g and concentrations of Cr leached in µg/L at various pH values and times for the MI-High barite sample.

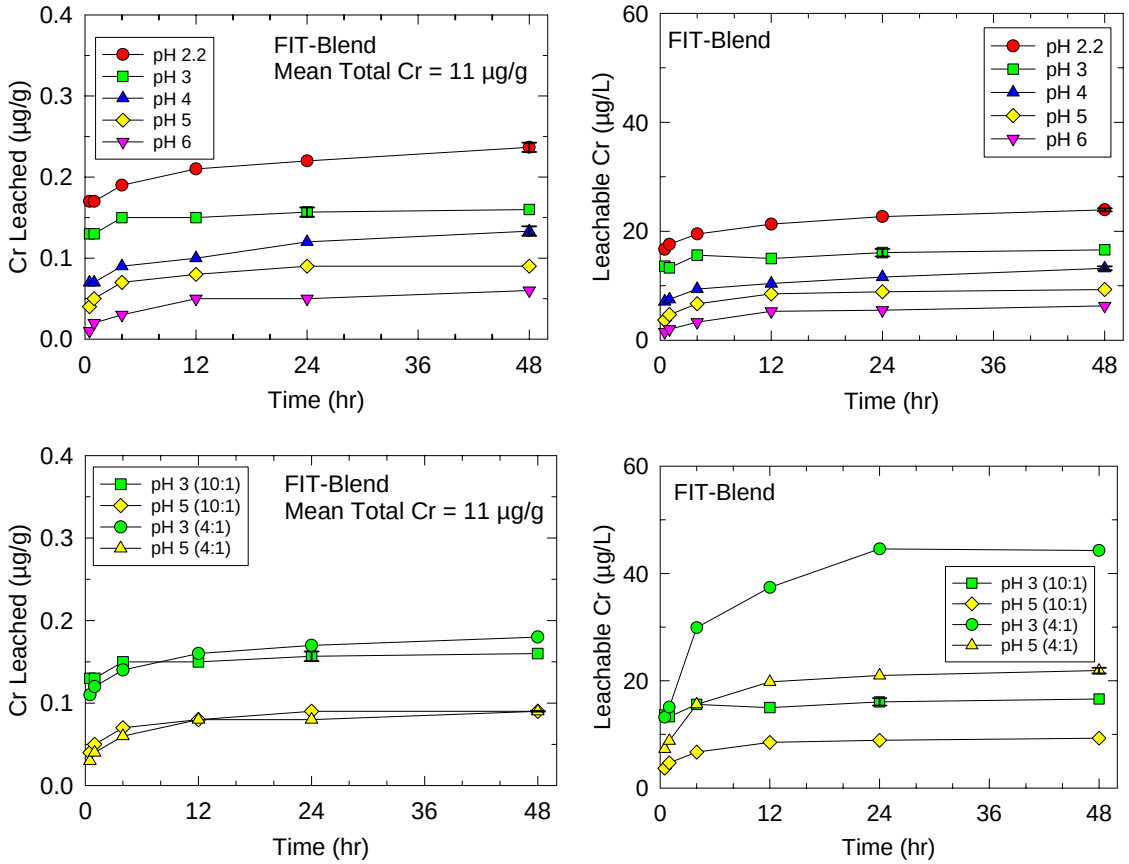

Figure 45. Amounts of Cr leached from the solid phase in µg/g and concentration of Cr leached in µg/L at various pH values and times for the FIT-Blend barite sample.

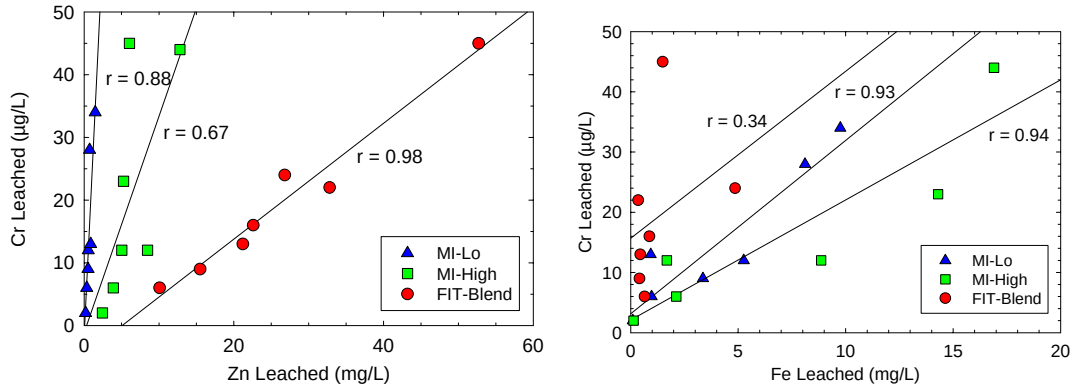

Figure 46. Amounts of Zn and Fe versus Cr leached after 48 hours at various pH values for each of the three barite samples.

The lines on each graph in Figure 45 show linear regression fits to the data for each barite sample with correlation coefficients (r).

6.4.10 Summary

Chemical leaching of three separate samples of industrial barite led to the release of <0.03 percent of the total Ba in each case (Table 33). Concentrations of Ba in solution following leaching were greater than the solubility of Ba in seawater of 0.035 mg/L, but less than the solubility of Ba carbonate in pure water of about 24 mg/L (Table 34). The relatively uniform concentrations of Ba in solutions from leaching of the barite samples suggest that Ba levels are solubility controlled.

After 48 hours, <2 percent of the total Fe present in the barite samples was leached into solution at pH 2.2 (Table 33). However, at pH 6, <0.02 percent of the total Fe was leached into solution for all three barite samples. Concentrations of dissolved Fe in the pH leachates were much greater than observed in typical seawater, but lower than natural values of dissolved Fe that are as high as 15 mg/L in anoxic interstitial water (Table 34). No strong relationships between concentrations of leachable Ba and Fe were observed for the three barite samples; and in two of three cases an indirect trend was found. Thus, the Ba and Fe are most likely contained in separate phases (Table 35).

Approximately 20-35 percent of the total Zn was leached from the barite samples into pH 2.2 solutions over 48 hours (Table 33). Furthermore, the Zn-bearing phase seems to dissolve more rapidly than the Fe-bearing phase. Overall, the results support the presence of Zn in a separate non-Ba and non-Fe bearing phase, possibly sphalerite (Table 35).

After 48 hours, all the Cd was leached at pH 2.2 from the two barite samples and about half the Cd was leached from the third sample (Table 33). Concentrations of dissolved Cd in the various pH solutions from this study were 2 to 3 orders-of-magnitude higher than the highest values reported for Cd in sediment interstitial water (Table 34). Strong correlations ($r \geq 0.90$) were observed for Zn versus Cd for each barite sample. Coupled with significant relationships between Cd and Fe for two of the barite samples, the Cd is most likely present in a Zn or Fe or Zn-Fe phase (Table 35).

Less than 8 percent of the total Pb was leached for all three samples over 48 hours at pH 2.2 (Table 33). The impact of leaching time and pH for Pb was less than observed for Fe and similar to that observed for Zn. The inter-element trends support the occurrence of Pb with a Zn or Zn-Fe phase (Table 35).

After 48 hours, the amount of Hg leached from the three barite samples at all pH values was <0.2 percent of the total Hg (Table 33). Concentrations of dissolved Hg in the various pH leaches for all three samples ranged from 0.004 to 0.040 µg/L (4-40 ng/L). These levels range from being comparable with to more than 50 times greater than found in ambient seawater. Leachable Hg concentrations from this study are much lower than values as high as 3 µg/L for anoxic interstitial water (Table 34). Strong positive correlations were found for Hg versus Zn. Hg concentrations in the pH leachates did not correlate with Ba. Thus, Hg is most likely present in a Zn or Zn-Fe phase (Table 35).

Table 33

Percent of total metal content leached at pH 2.2 and 6 after 48 hours.

Metal	pH of leaching solution	MI-Low Barite	MI-High Barite	FIT-Blend Barite
Ba	2.2	0.026	0.0032	0.00047
	6	0.027	0.0074	0.0015
Fe	2.2	1.2	2.2	0.16
	6	0.015	0.014	0.022
Zn	2.2	20	35	22
	6	5.7	14	8.3
Cd	2.2	100	100	49
	6	34	21	10
Pb	2.2	7.9	1.3	6.7
	6	12	7.0	1.0
Hg	2.2	0.023	0.051	0.006
	6	0.023	0.002	0.003
Cu	2.2	20	45	30
	6	6.1	23	8.0
Cr	2.2	1.8	6.8	2.2
	6	0.13	0.31	0.54

About 20-45 percent of the total Cu was leached into pH 2.2 solutions over 48 hours for each barite sample (Table 33). Concentrations of Cu in the pH leachates were 3 to 40 times greater than values reported for sediment interstitial water (Table 34). The correlation coefficient for the Zn versus Cu relationship was 0.99. This relationship strongly supports the presence of Cu in a Zn phase such as sphalerite (Table 35).

After 48 hours, <7 percent of the total Cr was leached into pH 2.2 solutions (Table 33). Metal versus metal plots support the occurrence of Cr with a Zn or Zn-Fe phase (Table 35).

Table 34

Average concentrations of metals in solution at pH 2.2 and 6 after 48 hours.

Metal (mg/L)	pH of leaching solution	MI-Low Barite	MI-High Barite	FIT-Blend Barite
Ba	2.2	14	1.7	0.24
	6	15	3.9	0.78
Fe	2.2	8.1	21	4.9
	6	0.11	0.013	0.6
Zn	2.2	0.73	6.1	26.8
	6	0.20	2.5	10.1
Cd	2.2	50	82	341
	6	12	17	72
Pb	2.2	2.5	0.32	9.3
	6	3.9	1.7	1.4
Hg	2.2	0.010	0.033	0.040
	6	0.007	0.010	0.020
Cu	2.2	2.0	4.1	5.7
	6	0.6	2.0	1.5
Cr	2.2	28	45	24
	6	2	2	6

Table 35

Likely metal-bearing phases for trace metals in industrial barite.

Metal	MI-Low	MI-High	FIT-Blend
Cd	Zn phase (r = 0.97) Fe phase (r = 0.85)	Zn phase (r = 0.90) Fe phase (r = 0.81)	Zn phase (r = 0.90)
Pb	Zn phase (r = 0.77)	None detected	Zn phase (r = 0.77) Fe phase (r = 0.65)
Hg	None detected	Fe phase (r = 0.87)	Zn phase (r = 0.65) Fe phase (r = 0.73)
Cu	Zn phase (r = 0.99)	Zn phase (r = 0.99)	Zn phase (r = 0.99)
Cr	Fe phase (r = 0.93) Zn phase (r = 0.88)	Fe phase (r = 0.94)	Zn phase (r = 0.98)

Samples with correlation coefficient (r) for linear relationship between trace metal and metal-bearing phase listed. None of the trace metals studied showed a significant relationship with a Ba phase.

7.0 Conclusions

In the process of drilling wells on the outer continental shelf (OCS), large quantities of barite are deposited on the sea floor. The primary environmental issue concerning barite discharges on the OCS is the potential for release of metals. For example, in the GOM, the USEPA requires that only barite containing less than 1 μg/g Hg and 3 μg/g Cd be used. This report describes results of experiments conducted on barite with the purpose of understanding how the environmental conditions on the OCS affect the solubility of barite and selected trace metals. The focus was on Cd, Cu, Hg, Pb, and Zn because these metals are frequently elevated in industrial barite compared to marine sediment, and the USEPA marine WQC are relatively low for these metals. Several barite samples were examined that included barite which meets the USEPA requirements for the GOM and barite that fails this regulation.

7.1 Mineralogy

Mineralogical analysis by EMP and XMP of the barite particles identified many small mineral inclusions including: quartz, iron oxide, iron sulfide, zinc sulfide, Mn sulfides, silicate minerals, and phosphate minerals. Copper, Pb, Hg, and Zn were associated with sulfide mineral inclusions. Mercury and Pb were also observed in separate minute inclusions. Cadmium was not detected within any minerals.

7.2 Solubility of Metals from Barite in Seawater

The solubility of Ba and selected metals in barite was examined over periods of hours to months under specific environmental conditions (salinity 30 ppt, temperature 4° and 20°C, pH 7-9, and pressure 14 and 500 psi). At a pH of 7.3, the solubility of Cu, Hg, and Zn was almost double of that at higher pH. Temperature and pressure had little affect on the solubility of trace metals. When barite was leached in static seawater for months, several metals (Cd, Cu, Hg, Mn, and Zn) gradually increased over time. Lead did not change significantly after the first 2 hours of contact and Ba decreased over the 6 months of leaching from approximately 35 μg/L to 10 μg/L.

Barite particles were exposed to flowing seawater at pH 8 for 24 hours. The release rate of Cd, Cu, Hg, Pb, and Zn from the particles into the seawater was greatest during the first several hours. After 24 hours, the concentrations of dissolved metals in the flowing seawater were similar to the concentrations found in coastal seawater.

7.3 Solubility of Metals in Oxic and Anoxic Sediment

When barite is mixed into oxic surface sediment, the release of metals to the water column and pore water is greatly reduced compared to that from barite alone. Barite dissolves in anoxic sediment resulting in high concentrations of Ba, Fe, and Mn in pore water. However, the anoxic pore water concentrations of Cd, Cu, Pb, Hg, methyl-Hg, and Zn are well below the USEPA WQC, presumably due to the formation of insoluble metal sulfides. Methylmercury concentrations in pore water were very low indicating the Hg in barite is not available for methylation. These results from laboratory experiments are consistent with studies of field samples taken near drilling sites in the GOM where

Trefry et al. (2003) reported that methyl-Hg was not elevated in anoxic sediment that contained barite.

7.4 Solubility of Metals in Acidic Solutions

The solubility of metals from barite in acidic solutions provides an indication of the bioavailability of metals if barite is ingested by deposit feeding animals. Several metals were relatively insoluble in acidic solutions including Ba, Fe, and Hg with only <0.03 percent, <2 percent, and <0.06 percent, respectively, of the total metal leached. In contrast, Cd, Cu, Pb, and Zn were relatively soluble with as much as 100 percent, 45 percent, 8 percent, and 35 percent respectively, of the total metal leached at pH 2.2. The correlation between the concentrations of these four metals in the leachates suggests these metals were present as a zinc phase such as sphalerite.

Table 36 compares the percentages of total metal content of barite leached by pH 6 buffer (48 hours, 10:1 aqueous:solid) with that leached in pH 7.3 seawater (1 week, 50:1 aqueous:solid). In most cases the pH 6 buffer leached about an order of magnitude more metal than pH 7.3 seawater.

In Table 37 the concentrations of dissolved metals in the leachates from pH 6 buffer and pH 7.3 seawater are compared with the USEPA WQC. Except for Hg, which is well below the WQC, all other metals exceed the WQC in the pH 6 leachates for three types of barite tested and also exceed the WQC for some of the pH 7.3 seawater leachates.

Table 36

Percent of total metal content leached from barite by either non-seawater solutions in pH 6 buffer or pH 7.3 seawater.

Metals	pH of Solution	MI-Low (%)	MI-High (%)	FIT-Blend (%)
Cd	pH 6[a]	34	21	10
	pH 7.3[b]	7.1	0.8	15
Cu	pH 6[a]	6.1	23	8.0
	pH 7.3[b]	0.05	0.38	0.28
Hg	pH 6[a]	0.023	0.002	0.003
	pH 7.3[b]	0.06	0.006	0.03
Pb	pH 6[a]	12	7.0	1.0
	pH 7.3[b]	0.37	0.57	0.21
Zn	pH 6[a]	5.7	14	8.3
	pH 7.3[b]	0.1	1.3	2.7

a pH 6 buffer, 48 hour leach, 10:1 g buffer: g barite
b pH 7.3 seawater, 1 week leach, 50:1 g seawater:g barite

Table 37

Concentrations of dissolved metals in either non-seawater solutions in pH 6 buffer or pH 7.3 seawater.

Metals (µg/L)	pH of Solution	MI-Low	MI-High	FIT-Blend	WQC
Cd	pH 6[a]	12	17	72	8.8
	pH 7.3[b]	0.5	0.1	21	8.8
Cu	pH 6[a]	600	2,000	1,500	3.1
	pH 7.3[b]	1	7	11	3.1
Hg	pH 6[a]	0.007	0.010	0.020	0.94
	pH 7.3[b]	0.006	0.007	0.042	0.94
Pb	pH 6[a]	3,900	1,700	1,400	8.1
	pH 7.3[b]	24	27	57	8.1
Zn	pH 6[a]	200	2,500	10,100	81
	pH 7.3[b]	<1	44	600	81

a pH 6 buffer, 48 hour leach, 10:1 g buffer:g barite
b pH 7.3 seawater, 1 week leach, 50:1 g seawater:g barite

7.5 Overall Summary

Laboratory tests conducted on low-metal industrial barite samples indicate that Hg and other trace metals are not released in significant quantities into seawater or the pore water of marine sediment. Mercury, Cd, Cu, Pb, and Zn are the primary metals of marine environmental concern in barite because these metals can be enriched by more than an order of magnitude compared to marine sediment. In addition, the USEPA water quality criteria for these metals are relatively low. A relatively small amount of these five metals in barite are soluble in seawater in the pH range of 7.3 to 8.3. During one week exposure of barite in seawater, less than 1 percent of the Cu, Hg and Pb, 3 percent of the Zn, and 15 percent of the Cd dissolved from the barite. Because low-metal barite releases little of these metals to seawater, it is not likely that low-metal barite will cause environmental effects to organisms living in the water column.

When barite is added to oxic surface sediment (2 cm thick) and aged for months, the concentrations of Cd, Cu, Hg, Pb, and Zn in the overlying seawater and pore water are considerably lower than for barite alone in seawater. Organisms living on or near the sediment would not be exposed to elevated concentrations of dissolved metals. However, at acidic conditions, simulating the gut of deposit feeding benthic animals, a major portion of the Cd, Cu, Pb and Zn are soluble and therefore could be bioavailable to benthic animals. When barite is added to anoxic sediment, the concentrations of Ba, Fe, and Mn in pore water increase dramatically as the barite dissolves. The concentrations of methylmercury, Hg, Cd, Cu, and Pb are not elevated compared to the same anoxic sediment without the addition of barite, however, the concentration of Zn in pore water increases by as much as a factor of four in anoxic sediment that contains 10 percent barite.

Literature Cited

Ache, B.W., J.D. Boyle, and E.E. Morse. 2000. A Survey of the Occurrence of Mercury in the Fishery Resources of the Gulf of Mexico. Prepared by Battelle for the U.S. Gulf of Mexico Program, Stennis Space Center, MS. January 2000.

Barnard, A.E. 1973. Comparative Animal Physiology. Philadelphia, Pennsylvania: W.B. Saunders. Pp138-139.

Barnes, H.L. 1997. Geochemistry of Hydrothermal Ore Deposits. New York: John Wiley & Sons. 972 pp.

Bothner, M.H., R.A. Jahnke, M.L. Peterson, and R. Carpenter. 1980. Rate of Hg loss from contaminated estuarine sediments. Geochimica et Cosmochimica Acta 44: 273-285.

Brown, J.S., ed. 1997. Genesis of stratiform lead-zinc-barite-fluorite deposits in carbonate rocks. Lancaster, Pennsylvania: The Economic Geology Publishing Co. 443 pp.

Candler, J., A. Leuterman, S. Wong, and M. Stephens. 1990. Sources of mercury and cadmium in offshore drilling discharges. In: Proceedings of 1990 SPE Annual Technical Conference and Exhibition. Society of Petroleum Engineers. Pp. 579-586.

Carr, G.R. and J.W. Smith. 1977. A comparative isotopic study of the Lady Loretta zinc-lead-silver deposit. Mineralim Deposita 12:105-110.

Church, T.M., and K. Wolgemuth. 1972. Marine barite saturation. Earth and Planetary Science Letters 15: 35-44.

Clarke, S.H.B. and F.G. Poole. 1989. Stratabound barite ore fields of North America (excluding Arkansas). M.K. De Brodtkorb, ed: Nonmetaliferous stratabound ore fields. New York: Van Nostrand Reinhold. Pp. 93 f.

Dickson, A.G. 1993. pH buffers for sea water media based on the total hydrogen concentration scale. Deep-Sea Research 40: 107-118.

Donat, J.R. and K.W. Bruland. 1995. Trace elements in the oceans. In: B. Salbu and E. Steinnes, eds. Trace Elements in Natural Waters. Boca Raton, Florida: CRC Press. Pp 247-281.

DelValls, T.A., L.M. Lubián, J.M. Forja, and A. Gomez-Parra. 1997. Comparative ecotoxicity of interstitial waters in littoral ecosystems using microtox® and the rotifer *Brachionus plicatilis*. Environmental Toxicology and Chemistry 16: 2323-2332.

Edwards, R. and K. Atkinson. 1986. Ore deposit geology. London: Chapman and Hall. 466 pp.

Elderfield, H., R.J. McCaffrey, N. Luedtke, M. Bender, and V.W. Truesdale. 1981. Chemical diagenesis in Narragansett Bay sediments. American Journal of Science 281: 1021-1055.

Gaines, R.V., H.C.W. Skinner, E.E. Ford, B. Mason, and A. Rosenzweig. 1997. Dana's new mineralogy. New York: John Wiley & Sons, Inc. 1819 pp.

Gambrell, R.P., R.A. Khalid, and W.H. Patrick, Jr. 1976. Physiochemical parameters that regulate mobilization and immobilization of toxic heavy metals. In: P.A. Krenkel, J. Harrison, and J. C. Burdick III, eds. Dredging and its Environmental Effects. American Society of Civil Engineers, New York. pp. 418-434.

Goldschmidt, V.M. 1954. Geochemistry. A. Muir, ed. Oxford University Press. 251 pp.

Hanor, J.S. 1968. Frequency distribution of compositions in the barite-celestite series. The American Mineralogist 53:1215-1222.

Heald, S. M., D.L. Brewe, E.A. Stern, K.H., Kim, F.C. Brown, D.T. Jiang, E.D. Crozier, and R.A. Gordon. 1999. XAFS and Micro XAFS at the PNC-CAT Beamlines, J. Syn. Rad. 6: 347-349.

Hogfeldt, E. 1982. Stability constants of metal-ion complexes, part A: Inorganic ligands. Oxford: Pergamon Press. 310pp.

Hutchison, C.S. 1983. Economic deposits and their tectonic setting. New York: John Wiley & Sons, Inc. 365 pp.

Kier, J.S. 1972. Barium: economic geology. In:R.W. Fairbridge ed. The encyclopedia of geochemistry and environmental sciences, |vol. IV A. New York: Van Nostrand Reinhold. Pp. 63-67.

Klinkhammer, G., D.T. Heggie, and G.W. Graham. 1982. Metal diagenesis in oxic marine sediments. Earth and Planetary Science Letters 61: 211-219.

Komov, I.L., A.N. Lukashev, and A.V. Koplus. 1987. Geochemical methods of prospecting for nonmetallic minerals. Utrecht, The Netherlands: VNU Science Press. 241 pp.

Kramer, J.R., H.D. Grundy, and L.G. Hammer. 1980. Occurrence and solubility of trace metals in barite for ocean drilling operations. In: Research on Environmental Fate and Effects of Drilling Fluids and Cuttings, Vol II. Washington, D.C.: Courtesy Associates. Pp. 789-798

Krauskopf, K.B. 1967. Introduction to geochemistry. New York: McGraw-Hill. 698 pp.

Lamey, C.A. 1966. Metallic and industrial mineral deposits. New York: McGraw-Hill Book Co. 567 pp.

Leach, D.L. 1980. Nature of mineralizing fluids in the barite deposits of central and southeast Missouri. Economic Geology 75:1168-1180.

Lottemoser, B.G. and P.M. Ashey. 1996. Geochemistry and exploration significance of ironstones and barite-rich rocks in the Proterozoic Willyama Subgroup, Orlay Block, South Australia. Journal of Geochemical Exploration 57: 57-73.

Luoma, S.N., and G.W. Bryan, G.W. 1979. In: E.A. Jenne, ed. Chemical Modeling - Speciation, Sorption, Solubility, and Kinetics in Aqueous Systems. Washington, D.C.: American Chemical Society. Pp. 577-611

McKinley, J.P., J.M. Zachara, S.M. Heald, A.Dohnalkova, M.G. Newville, and S.R. Sutton. 2004. Microscale distribution of cesium sorbed to biotite and muscovite. Environmental Science and Technology 38(4): 1017-1023.

Miller, T.G., and W.C. Mackay. 1980. The effects of hardness, alkalinity and pH of test water on the toxicity of copper to rainbow trout (*Salmo gairdneri*). Water Research 14: 129-133.

Mobile Register. 2001a. Gulf Rigs: Islands of Contamination. December 30, 2001. Internet website: http://www.al.com/specialreport/index.ssf?mobileregister/mercuryinthewater.html

Mobile Register. 2001b. Mobile Alabama. Special Report – Mercury Taints Seafood. various issues 2001-2003. Internet website: http://www.al.com/specialreport/index.ssf?mobileregister/mercuryinthewater.html

Monnin, C. 1999. A thermodynamic model for the solubility of barite and celestite in electrolyte solutions and seawater to 200°C and to 1 kbar. Chemical Geology 153(1999): 187-209.

Monnin, C., C. Jeandel, T. Cattaldo, and F. Dehairs. 1999. The marine barite saturation of the world's oceans. Marine Chemistry 65(1999): 253-261.

National Science and Technology Council (NSTC). June 2004. Methylmercury in the Gulf of Mexico: State of Knowledge and Research Needs. Committee on the Environment and Natural Resources, Interagency Working Group on Methylmercury. Internet website: http://www.masgc.org/mercury/051004.pdf

Neff, J.M. 2002. Fates and effects of mercury from oil and gas exploration and production operations in the marine environment. Washington, D.C.: American Petroleum Institute. 136 pp.

Oshima, T., T. Hashimoto, S. Kawabe, K. Suga, S. Tanimura, and Y. Ishikawa. 1974. Geology of the Kosaka mine, Akita Prefecture. Society of Mining Geologists of Japan, Special Issue 6: 89-100.

Oslo and Paris Commission. 1995. List of substances/preparations used and discharged offshore. Summary record of the meeting of the Programmes and Measures Committee. Oslo and Paris Conventions for Prevention of Marine Pollution, Oviedo. 20-24 February 1995.

Owen G. 1966. In: K.M. Wilbur and C.M. Younge, eds. Physiology of Mollusca. New York: Academic Press. Pp. 53-88.

Presley, B.J., and I.R. Kaplan. 1972. Interstitial water chemistry: deep sea drilling project, leg 11. In: C.D. Hollister et al. eds. Initial Reports. DSDP. Washington, D.C.: U.S. Govt. Printing Office. Pp. 1009-1012.

Quinby-Hunt, M.S., and K.K. Turekian. 1983. Distribution of elements in sea water. EOS, Transaction of the American Geophysical Union 64: 130-131.

Ramos, V.A. and M.K. de Brodtkorb. 1989. Clestite, barite, magnesite, and fluorspar: stratabound settings through time and space. In: M.K. de Brodtkorb, ed. Nonmetaliferous stratabound ore fields. New York:Van Nostrand Reinhold. Pp. 297 f.

Rushdi, A.I., J. McManus, and R.W. Collier. 2000. Marine barite and celestite saturation in seawater. Marine Chemistry 69(2000): 19-31.

Trefry, J.H. 1998. Forms of mercury and cadmium in barite and their fate in the marine environment: a review and synthesis. Final Report to Exxon Production Research Co., Houston, Texas. 32 pp.

Trefry, J.H., and S. Metz, S. 1984. Selective leaching of trace metals from sediments as a function of pH. Analytical Chemistry 56:745-749.

Trefry, J.H., and B.J. Presley. 1982. Manganese fluxes from Mississippi Delta sediments. Geochimica et Cosmochimica Acta 46: 1715-1726.

Trefry, J.H., and J.P. Smith. 2003. Forms of Hg in drilling fluid barite and their fate in the marine environment: A review and synthesis. SPE/DOE/EPA Exploration and Production Environmental Conference, 10-12 March 2003. San Antonio, Texas. Paper SPE 80571.

Trefry, J.H., R.P. Trocine, S. Metz, and M.A. Sisler. 1986a. Forms, reactivity and availability of trace metals in barite. Report prepared for the Offshore Operators Committee, Task Force on Environmental Science, 50 pp. plus appendices.

Trefry, J.H., T.A. Nelsen, R.P. Trocine, S. Metz, and T.W. Vetter. 1986b. Trace metal fluxes through the Mississippi River Delta system. Rapp. P.-v. Réun. Cons. Int. Explor. Mer 186: 277-288.

Trefry, J.H., R.P. Trocine, M. McElvaine, and R.D. Rember. 2003. Concentrations of total and methylmercury in sediment adjacent to oil platforms in the Gulf of Mexico. SPE/DOE/EPA Exploration and Production Environmental Conference, 10-12 March 2003, San Antonio, Texas. Paper SPE 80569.

U.S. Environmental Protection Agency (USEPA). 1993. Oil and gas extraction point source category, offshore subcategory; effluent limitations guidelines and new source performance standards. Federal Register, March 4, 1993 58(41): 12,454-12,512.

U.S. Environmental Protection Agency (USEPA). 2004. National recommended water quality criteria. Federal Register, July 9, 2004 69(131): 14,720-14,743.

Wedepohl, K.H., ed. 1978. Handbook of Geochemistry Vol II/5 Elements La(557) to U(92). New York: Springer Verlag. 80-D-1.

APPENDIX A

Backscatter electron (BSE) images of untreated FIT-Blend barite particles

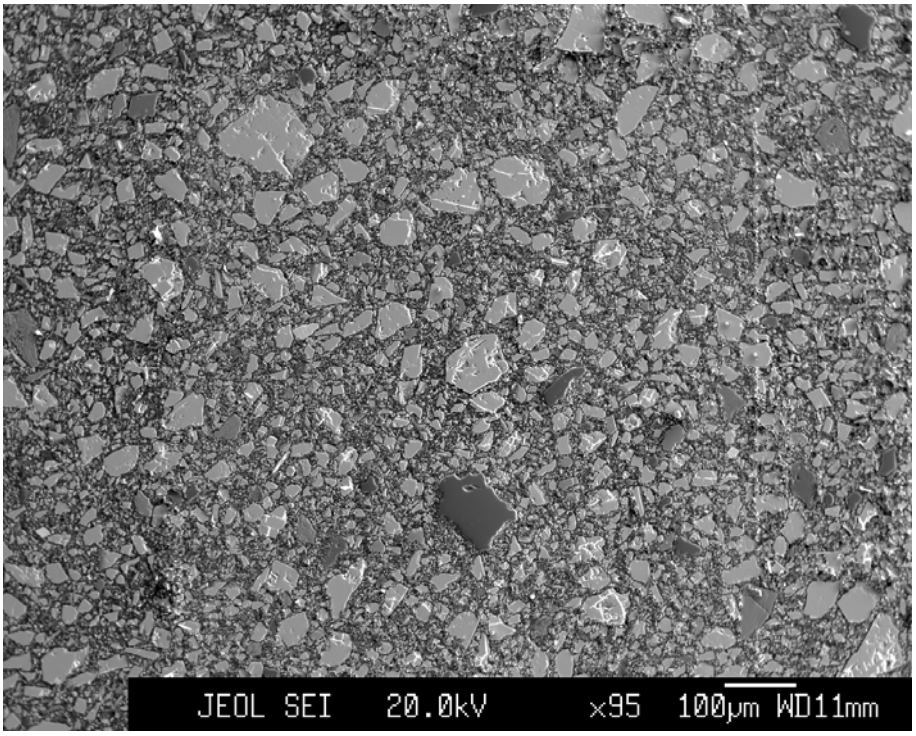

Figure A-1: Backscattered electron (BSE) image of untreated sample FIT-Blend. BSE images recorded atomic-number contrast, with 'heavier' materials showing brighter signals. Area that was examined using X-ray mapping is in the approximate center of this image. Pale grey (most abundant) clasts are barite. Dark, large clast, lower center, is quartz. Other, intermediate gray shades are Fe oxides, Fe, Zn, and Mn sulfides, and silicates and phosphate minerals.

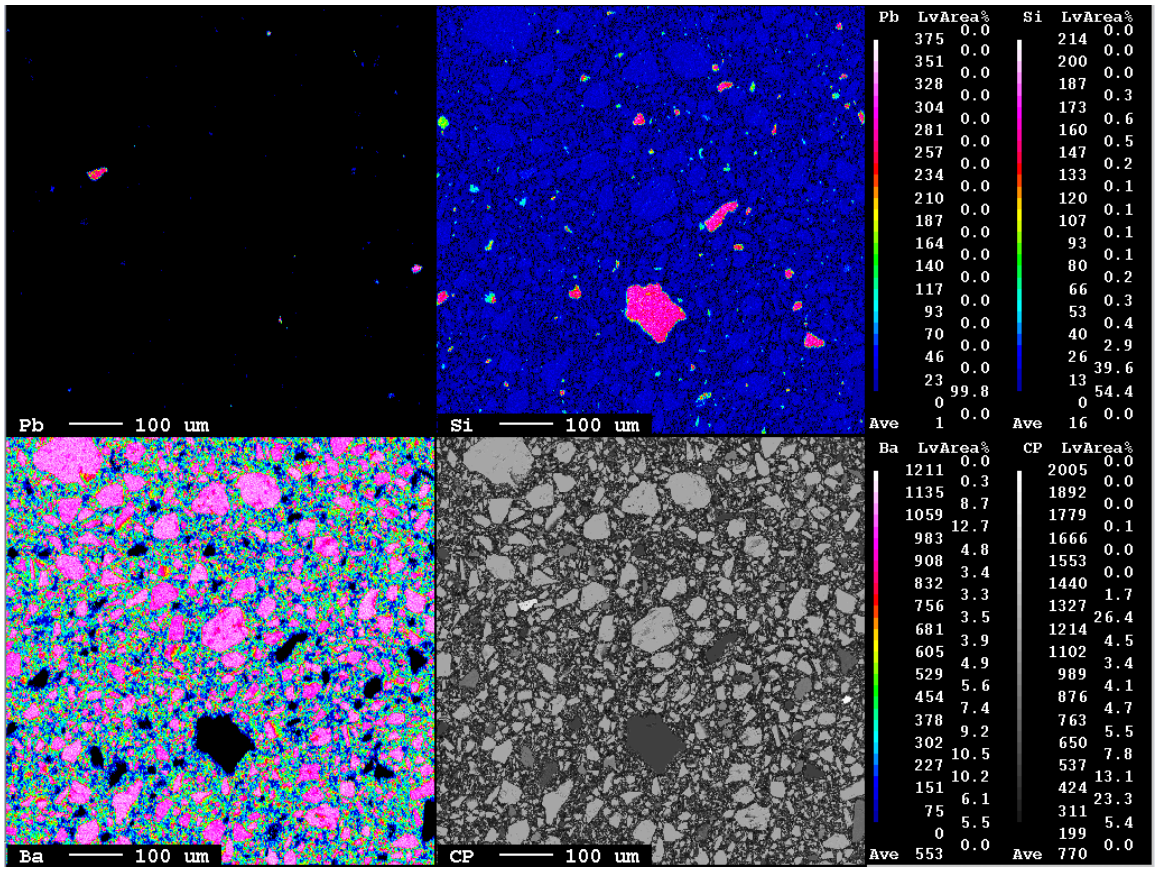

Figure A-2: Elemental abundance maps of an area included in Figure A-1, for Pb, Si, and Ba. Lead was detected in a few clasts; Si is representative of quartz and other silicate minerals, and Ba represents barite.

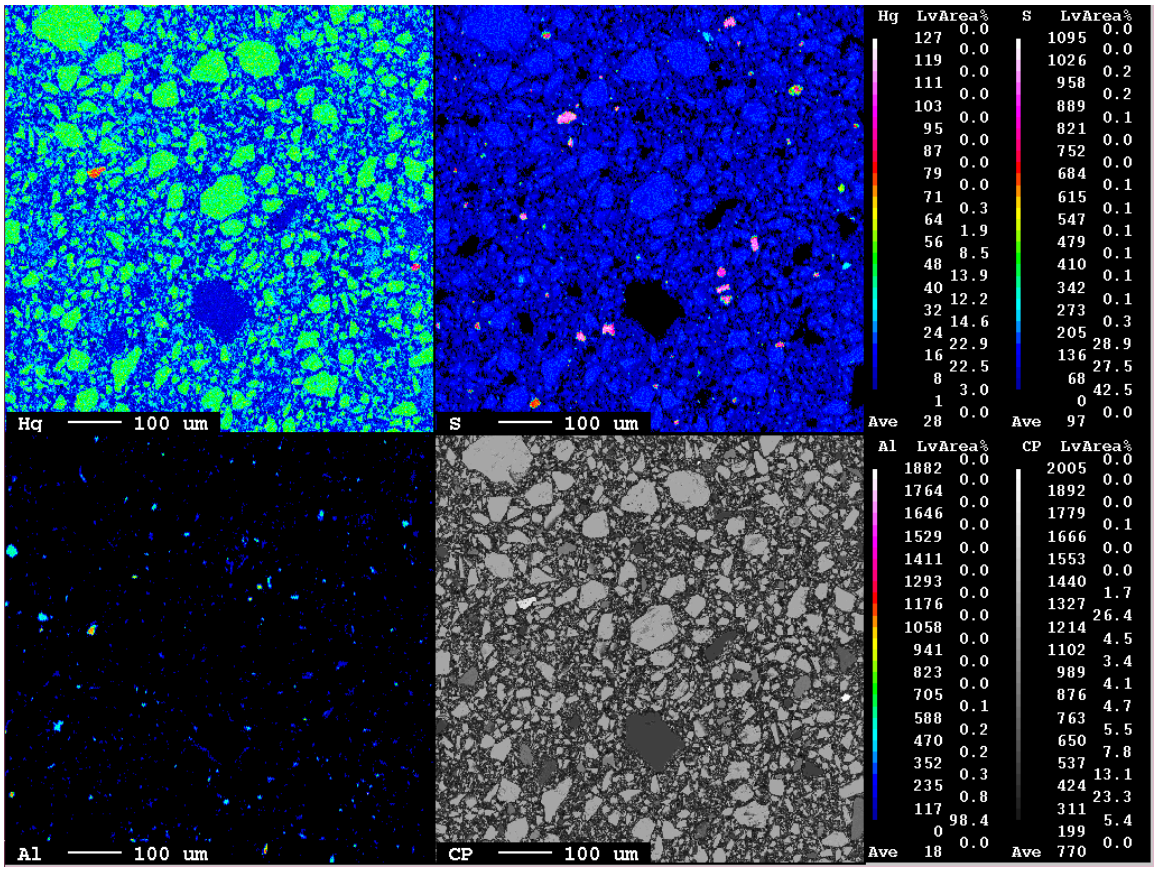

Figure A-3: Elemental abundance maps of an area included in Figure A-1, for Hg, S, and Al. Mercury was present in clasts identified in Figure A-2 as containing Pb. Sulfur represented sulfides, and Al silicates containing Al as a component.

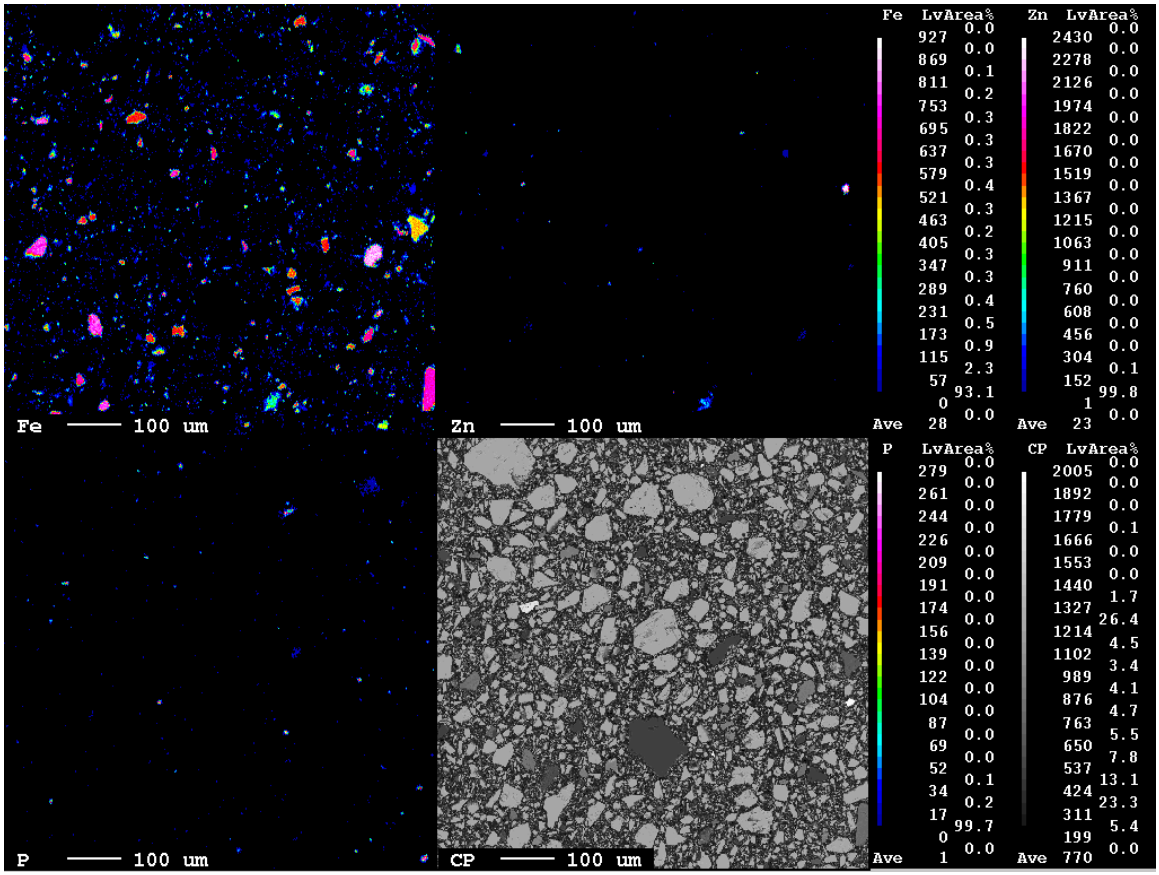

Figure A-4: Elemental abundance maps of an area included in Figure A-1, for Fe, Zn, and P. Iron was present as oxides and sulfides; Zn was either an oxide or a sulfide, and P represented phosphate minerals.

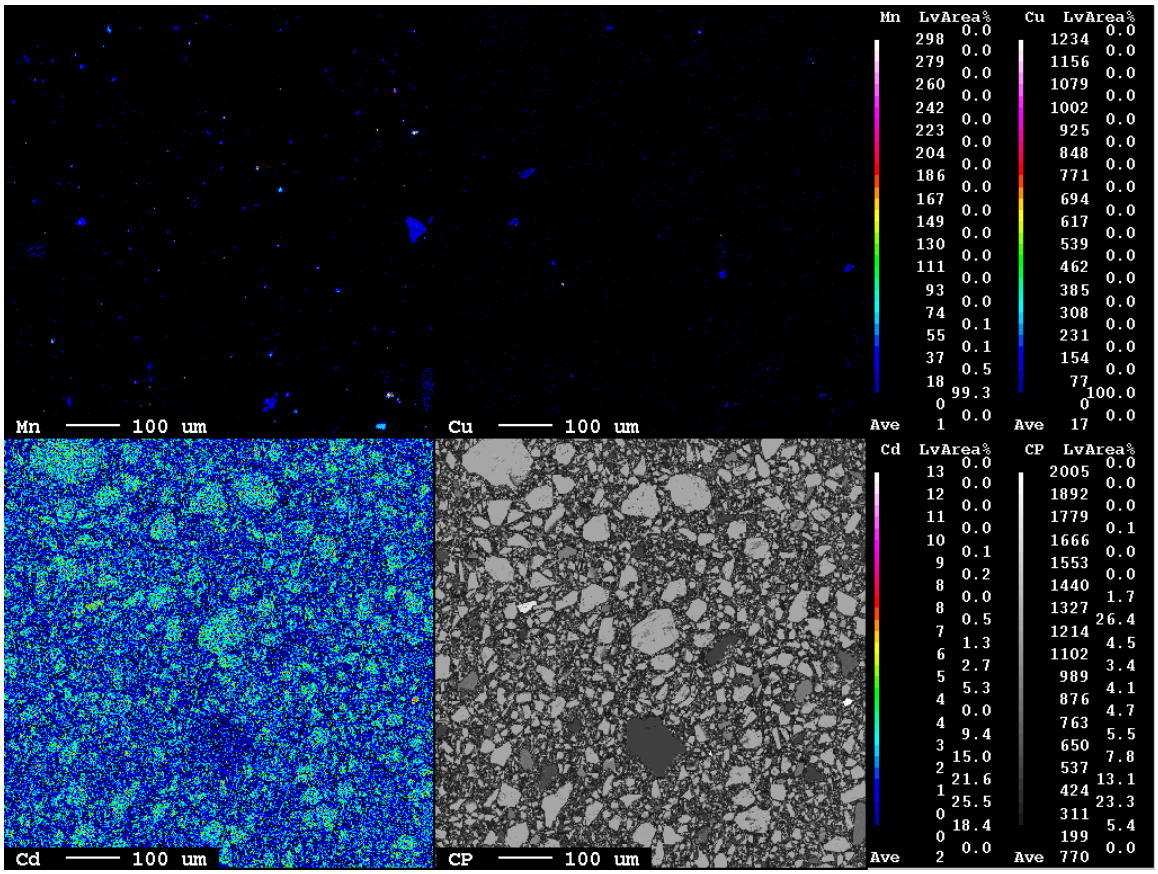

Figure A-5: Elemental abundance maps of an area included in Figure A-1, for Mn, Cu, and Cd. Manganese and Cu were present as minute inclusions, Mn associated with Fe, and Cu with Pb or in isolation. Cadmium was not detected.

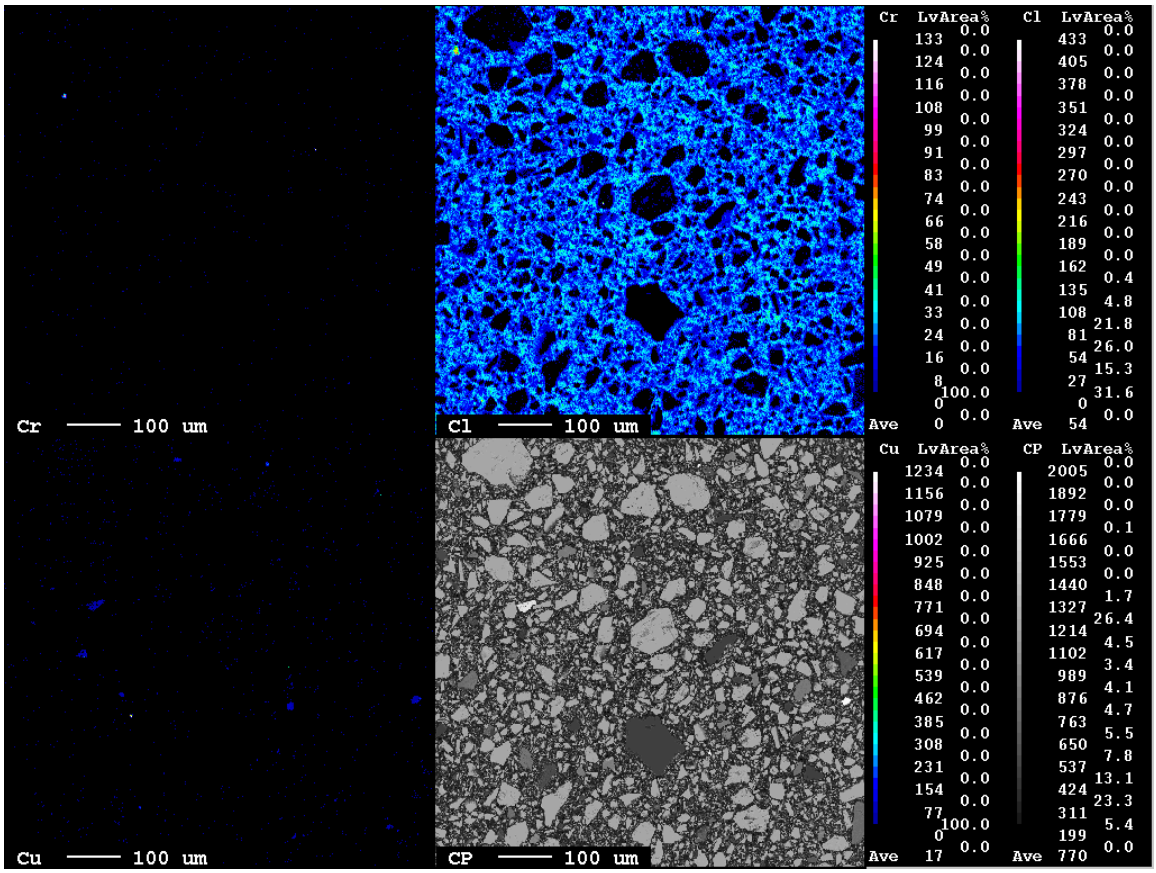

Figure A-6: Elemental abundance maps of an area included in Figure A-1, for Cr, Cl, and Cu (again). A few minute Cr inclusions were present. Chlorine was contained within the epoxy.

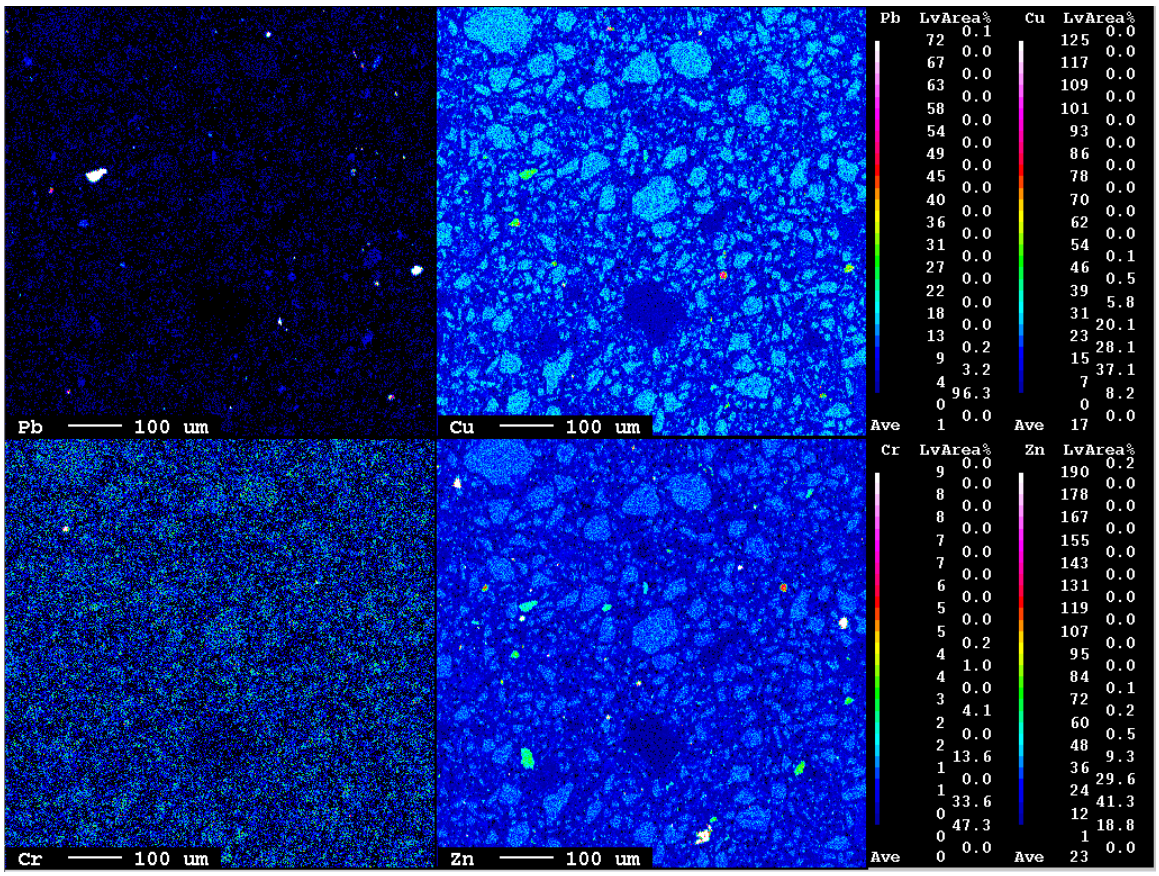

Figure A-7: Elemental abundance maps of an area included in Figure A-1, for Pb, Cu, Cr, and Zn. The false-color spectrum was compressed to include a lower flux at the spectral maximum (white). In each map, blue was at or below detection, and represents background. For Pb, the number of detected particles increased, and they were of similar composition (all were white). For Cu, the detected particles were more apparent, and may have had a more varied composition (clasts were white, red, and green). Chromium was apparently present only as the previously detected minute particles, and Zn was present over a range of compositions (white, red, green false colors).

APPENDIX B

BSE images and EDS spectra of eight single particles of untreated FIT-Blend

Figures B-1 through B-12 show individual areas or particles from FIT-Blend for which spectral analysis was done; all particles are included in an area of Figure A-1. Each BSE image from FIT-Blend is followed by the spectra for the indicated point.

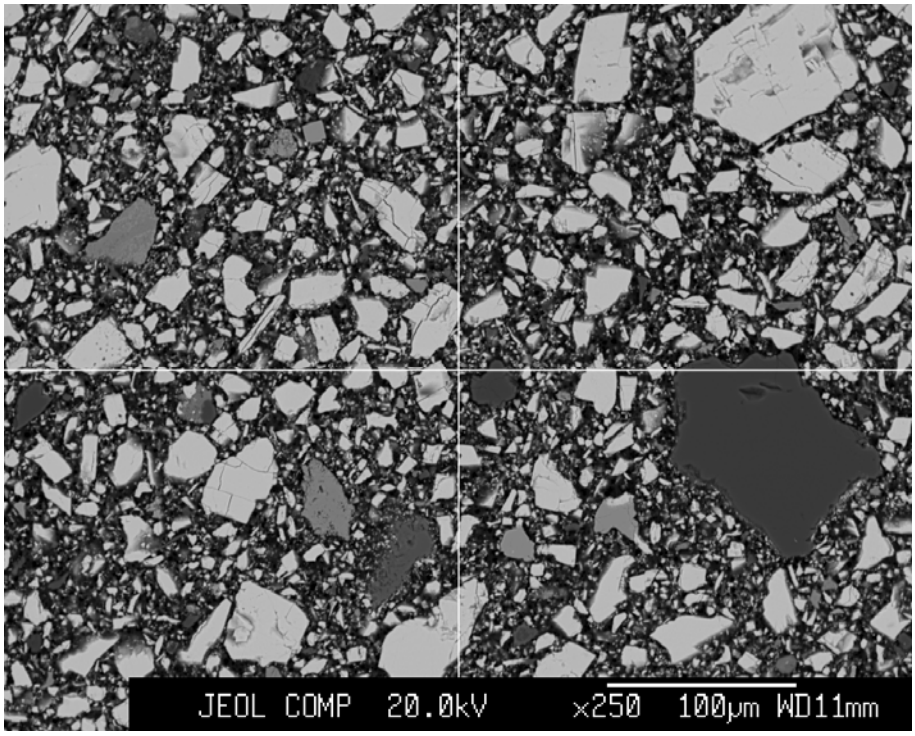

Figure B-1. The particle under the cross hairs (particle # 1) was analyzed and the spectra is shown in Figure B-2.

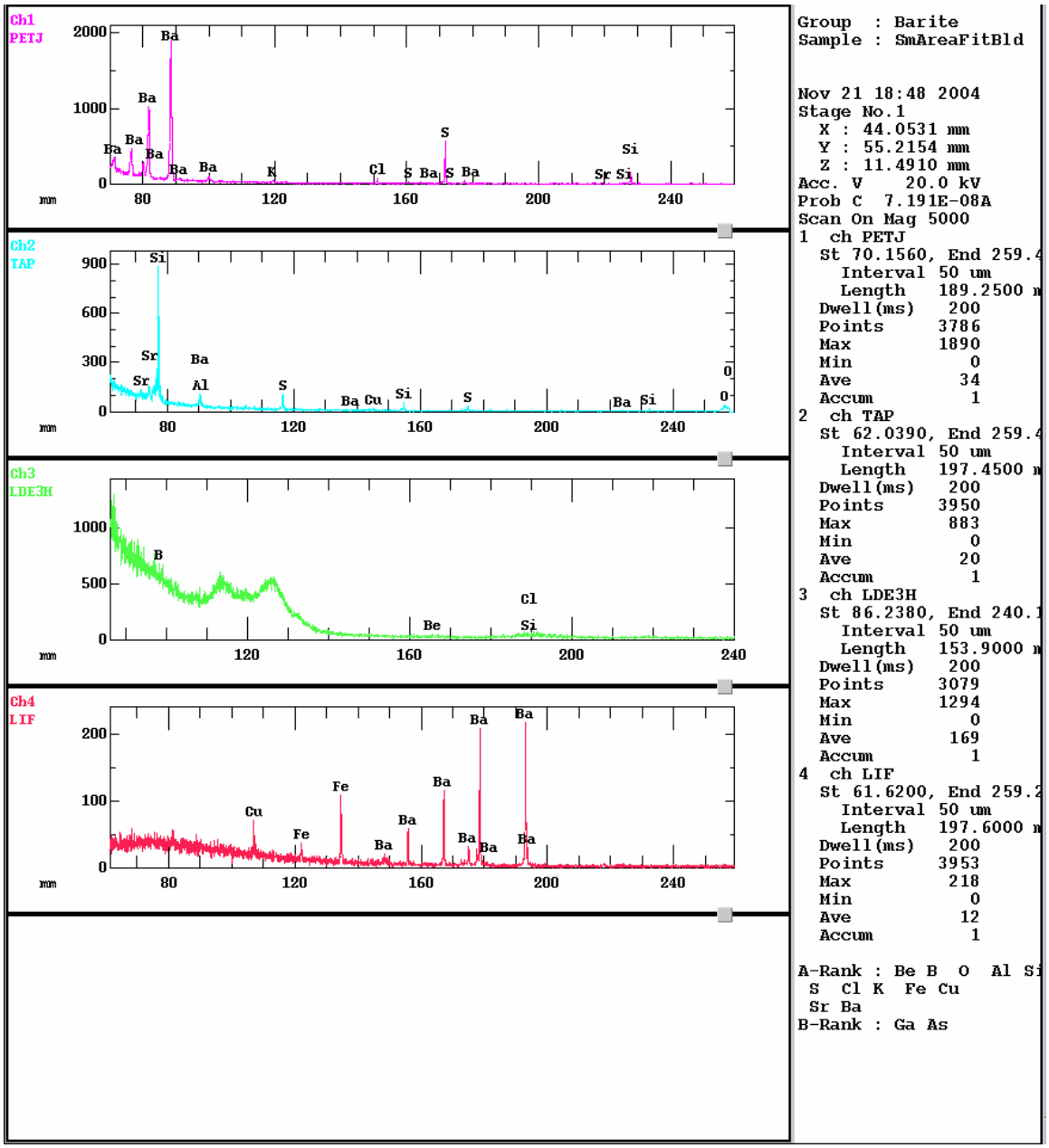

Figure B-2: Spectra for Particle #1. The clast was barite, but included Si and Cu also.

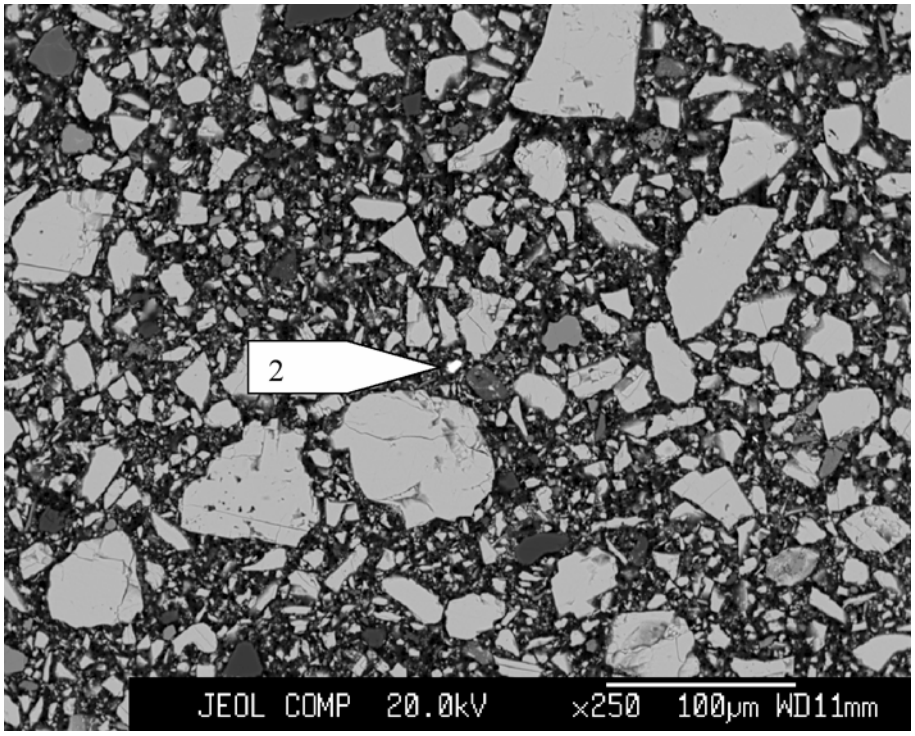

Figure B-3: Particle #2 location.

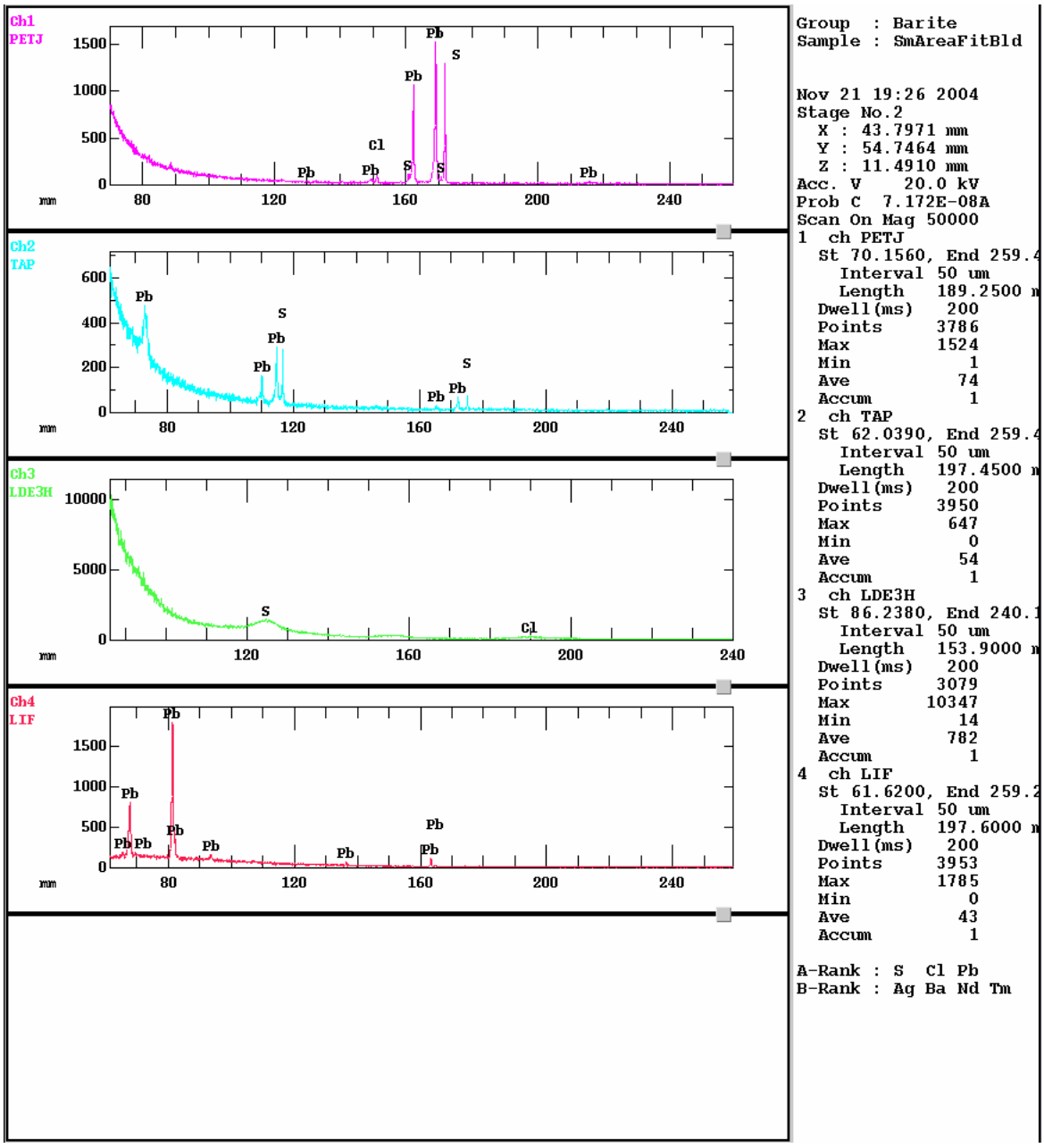

Figure B-4: Spectra for Particle #2. The particle was a Pb sulfide.

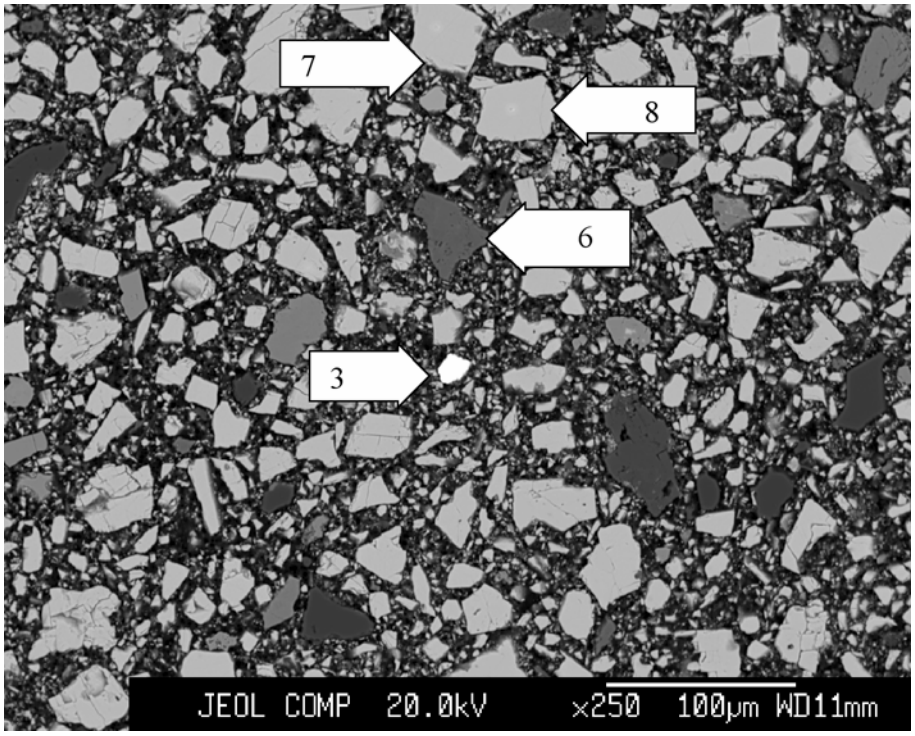

Figure B-5: Location of Particles #3, #6, #7, and #8.

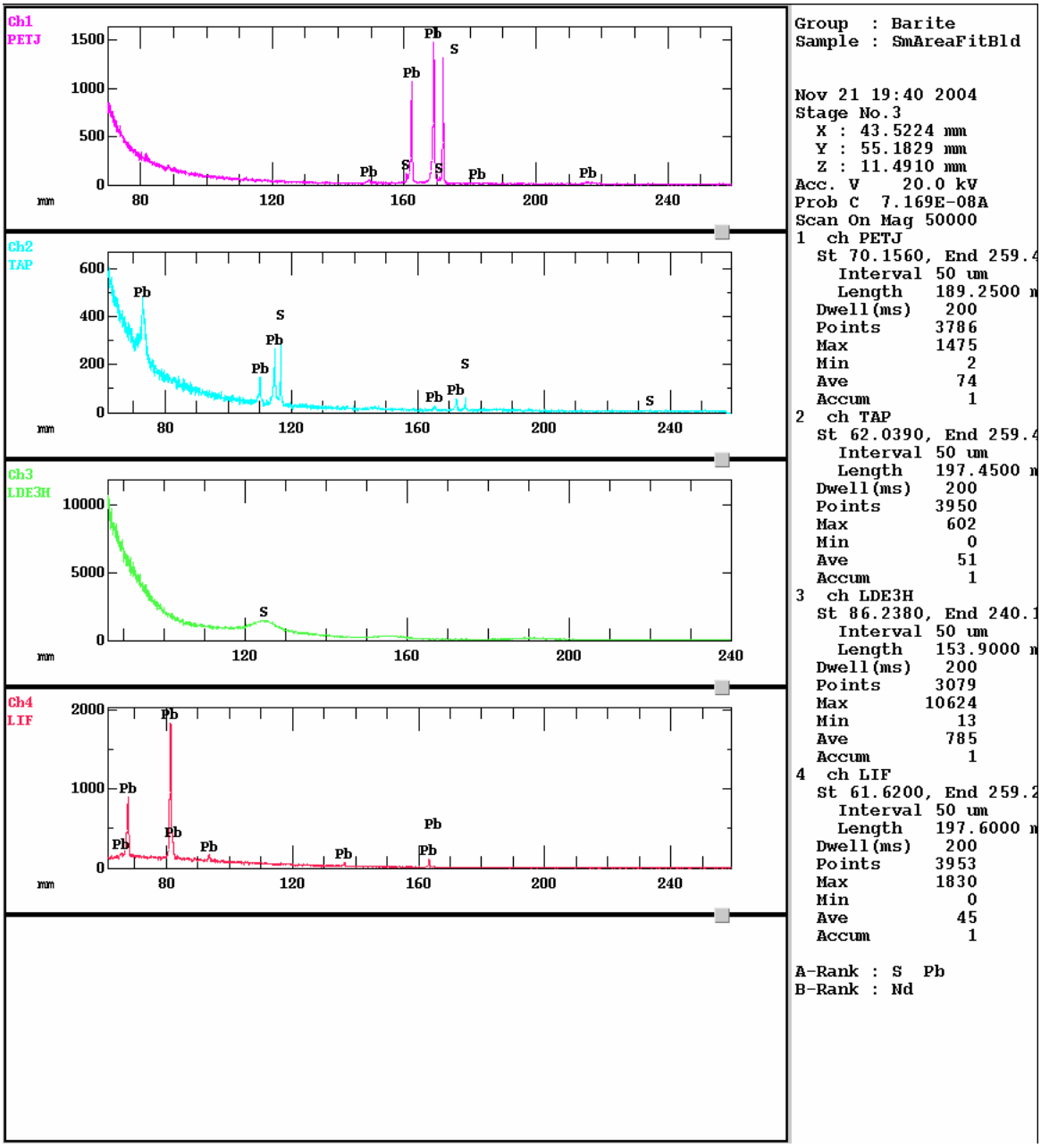

Figure B-6: Spectra for Particle #3. The particle was a Pb sulfide.

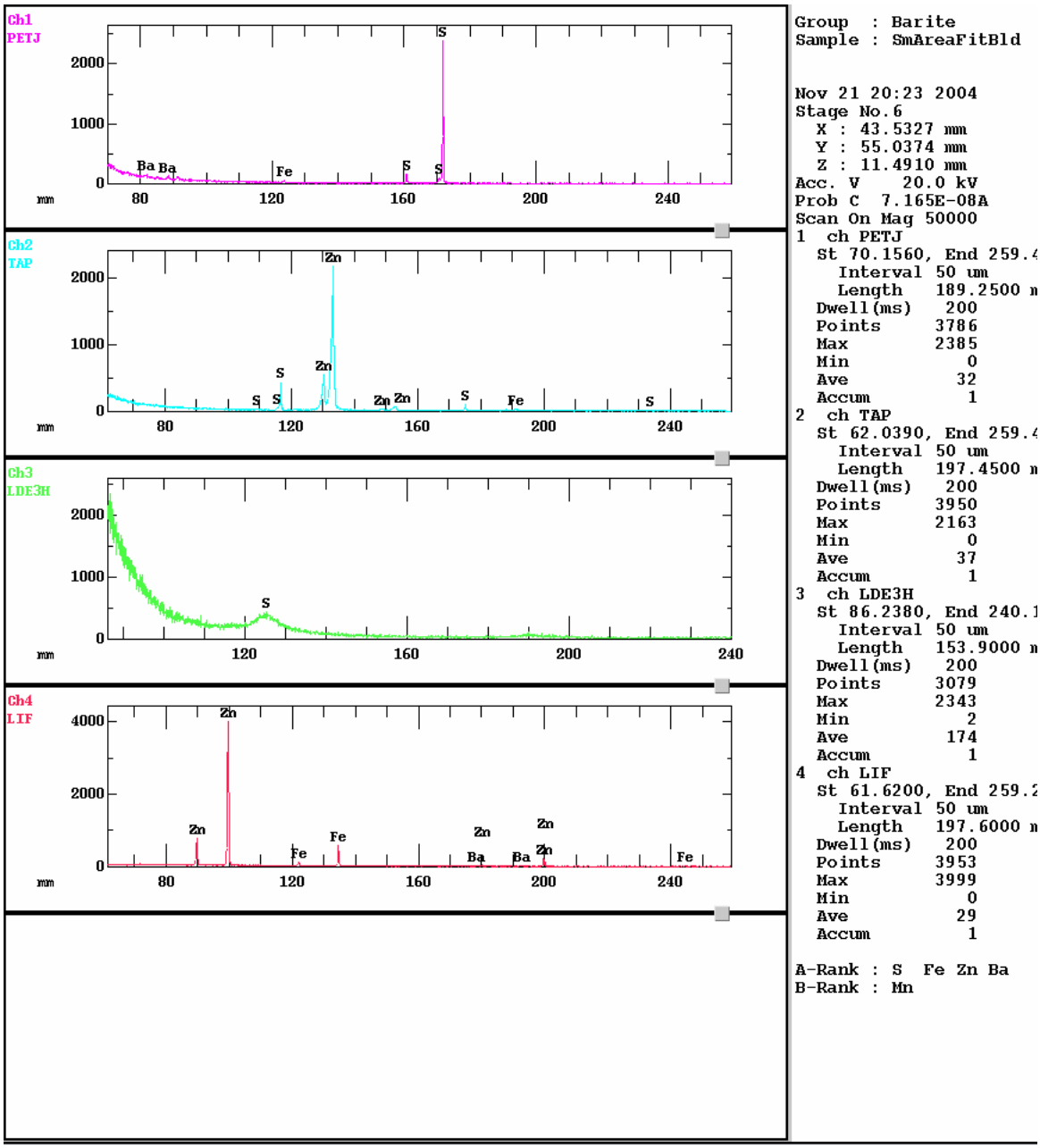

Figure B-7: The spectra for Particle #6. The particle was a Zn sulfide, and included Fe.

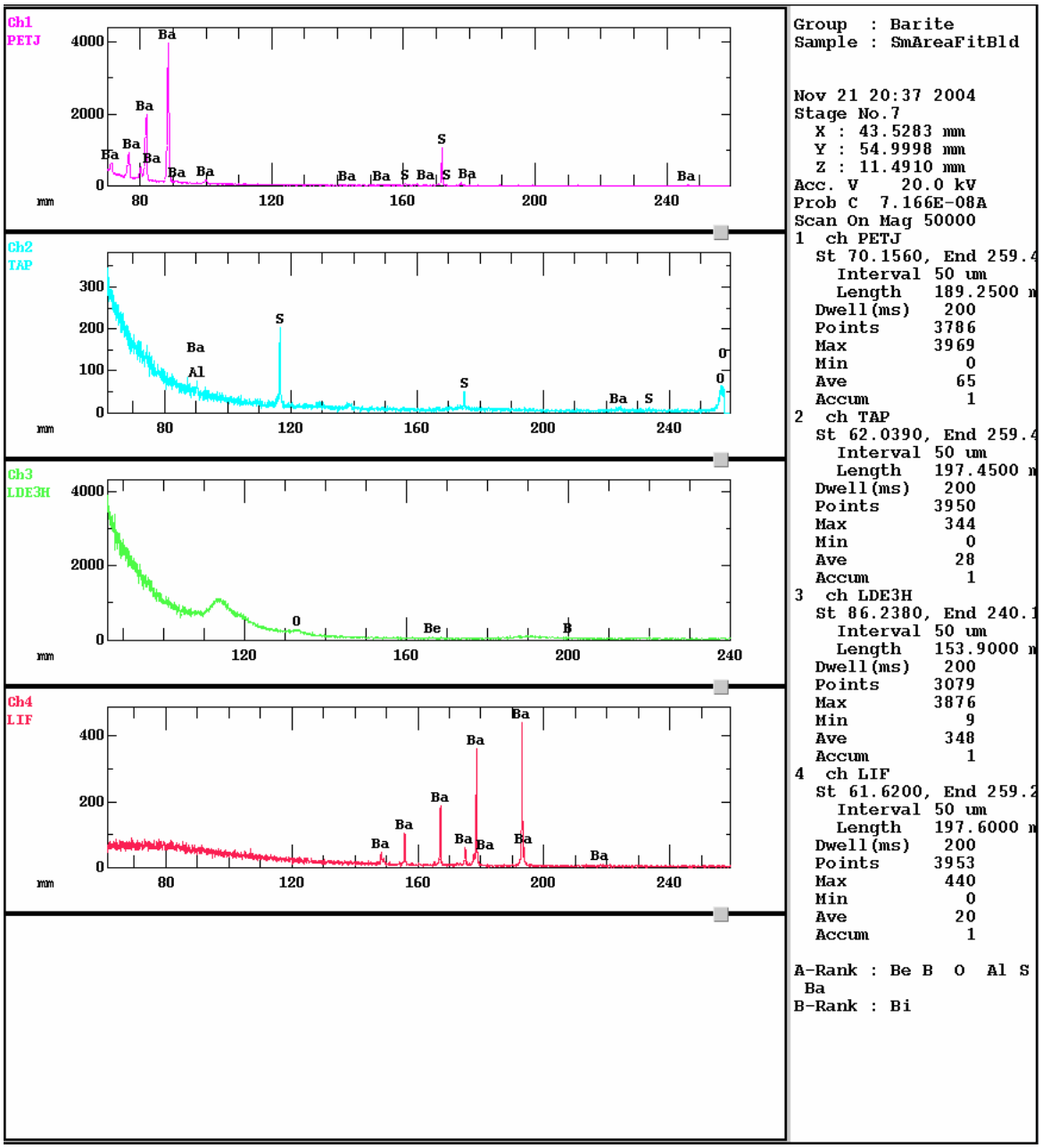

Figure B-8: The spectra for Particle #7. The particle was barite.

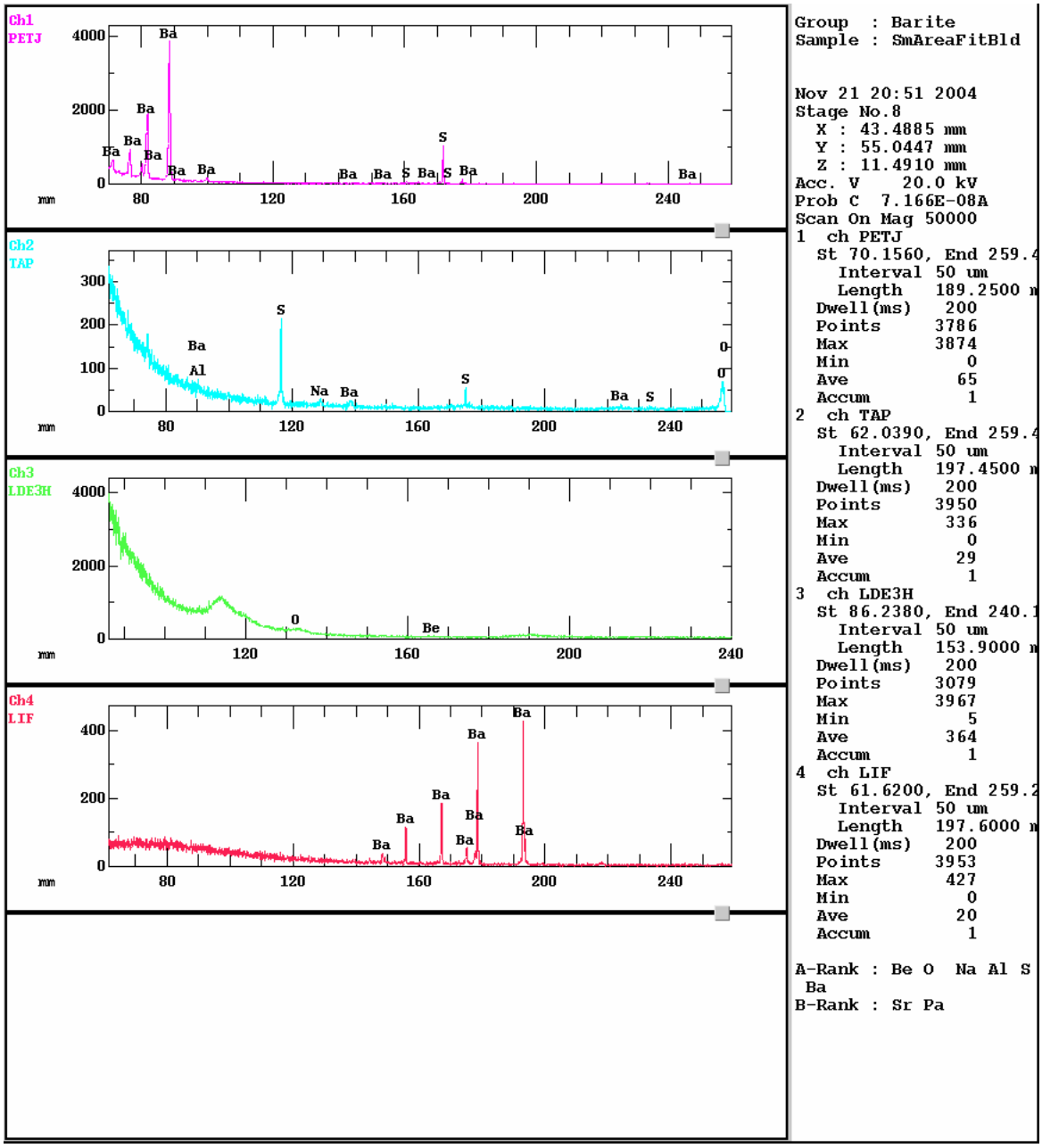

Figure B-9: The spectra for Particle #8. The particle was barite.

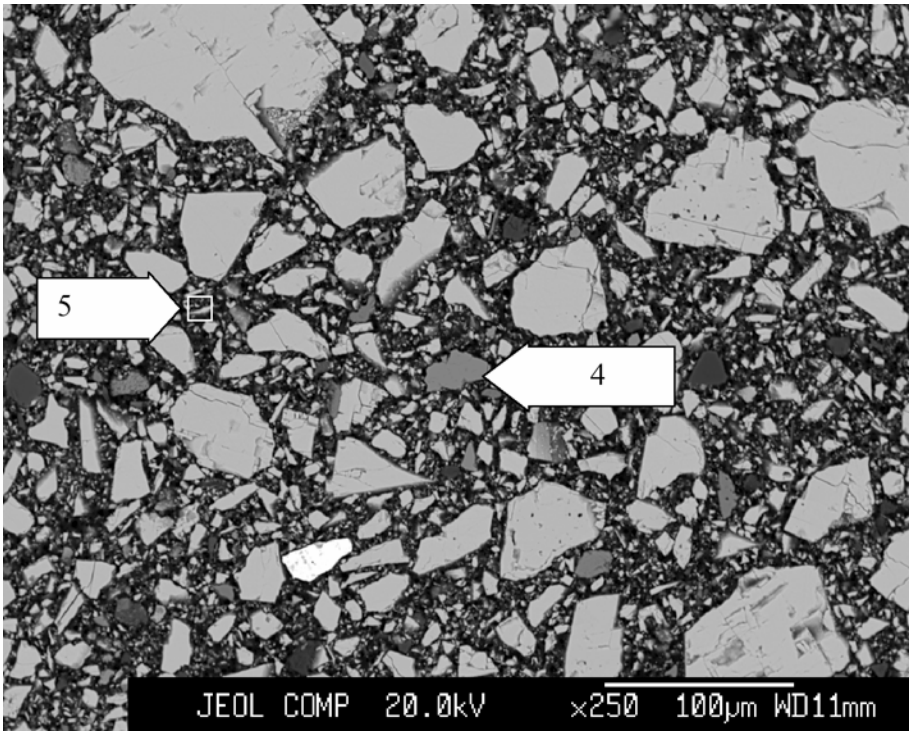

Figure B-10: Location of Particles #4 and #5. Particle #5 was a small area indicated by the box.

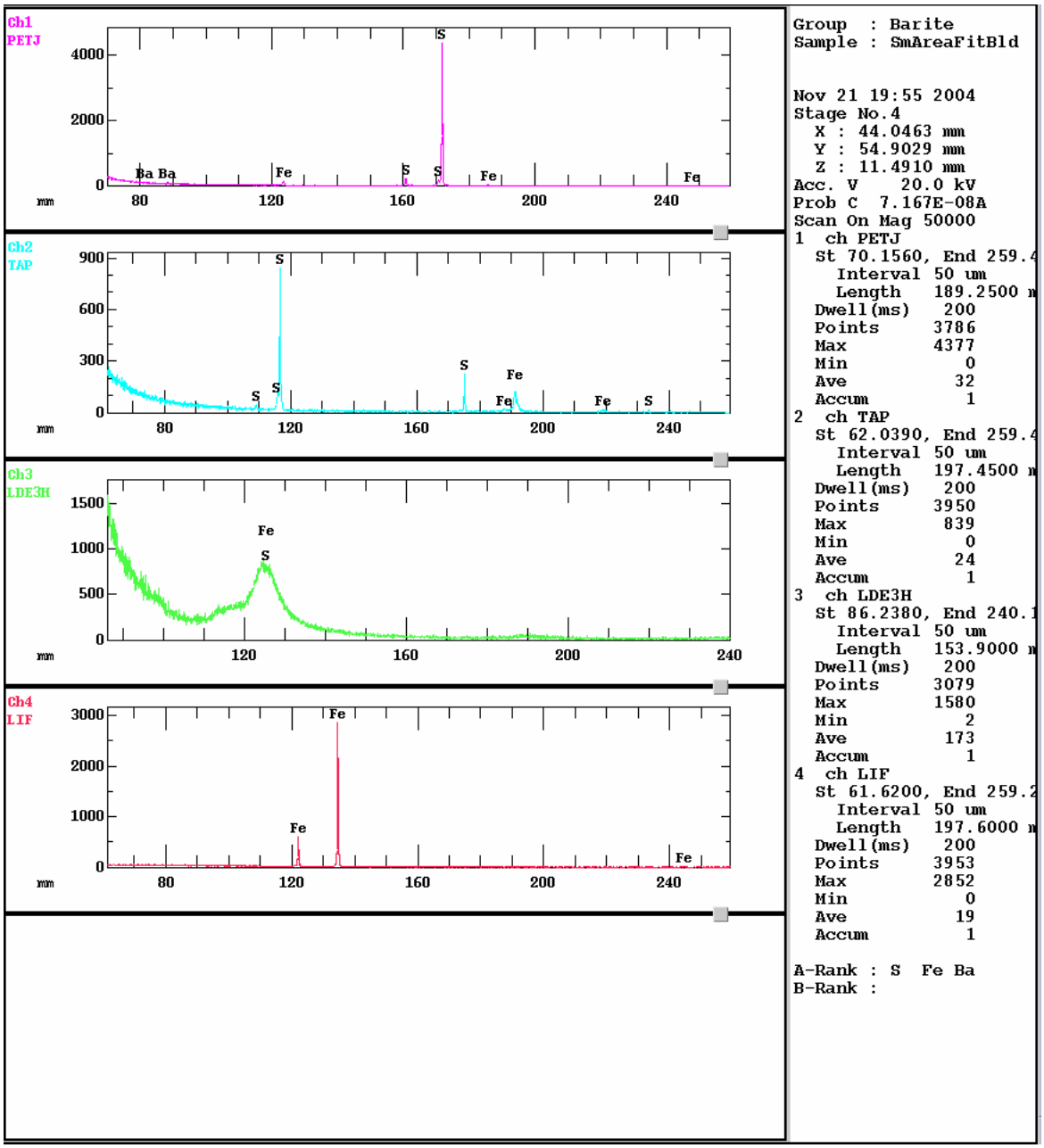

Figure B-11: Spectra for Particle #4. The particle was an Fe sulfide.

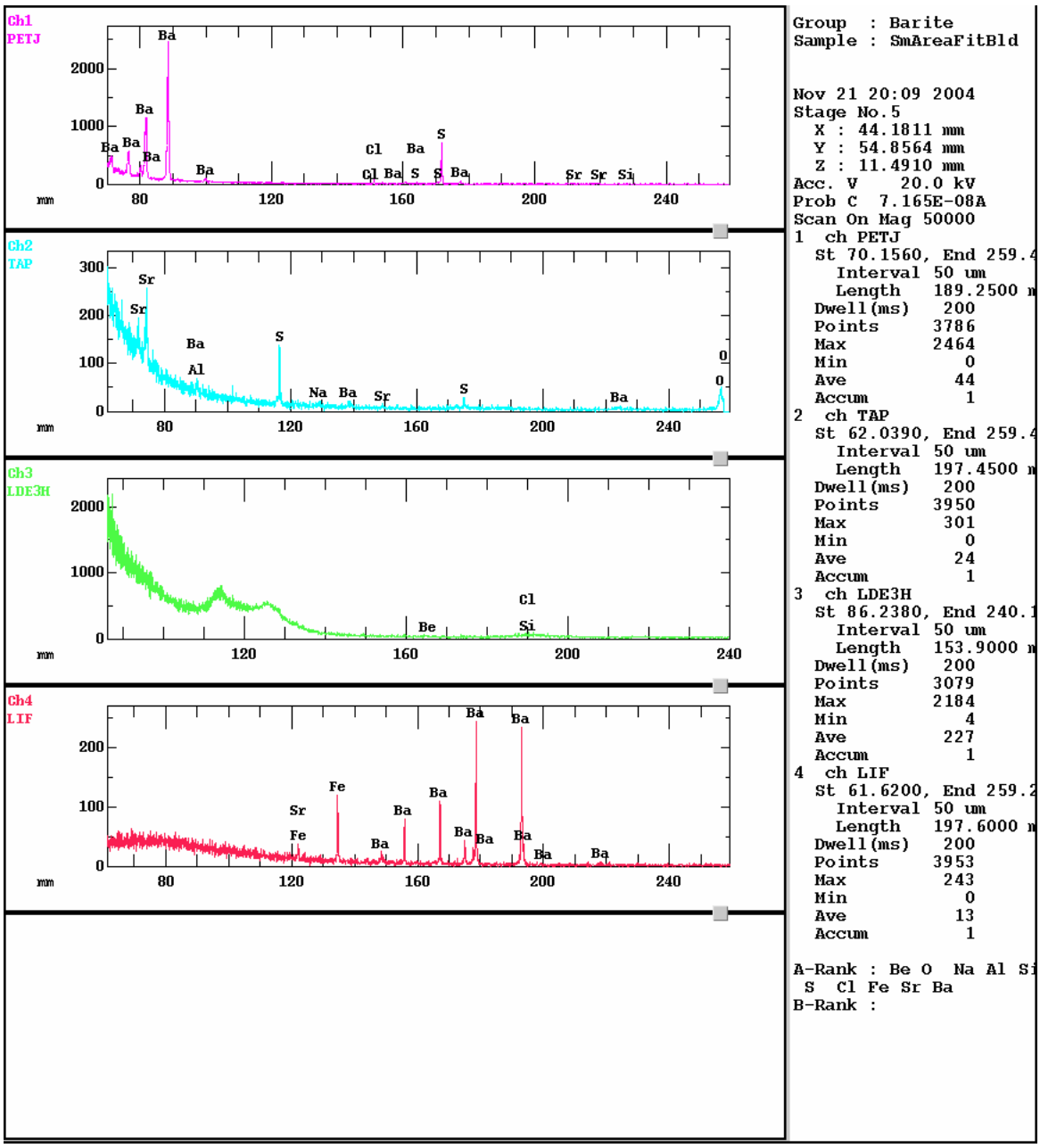

Figure B-12: Spectra for Particle #5. The area was occupied by barite, but included Sr.

APPENDIX C

EMP analysis elemental abundance maps of barite particles from samples MI-High, MI-Low, acid-leached MI-High (AMIH) and acid-leached FIT-Blend (AFIT)

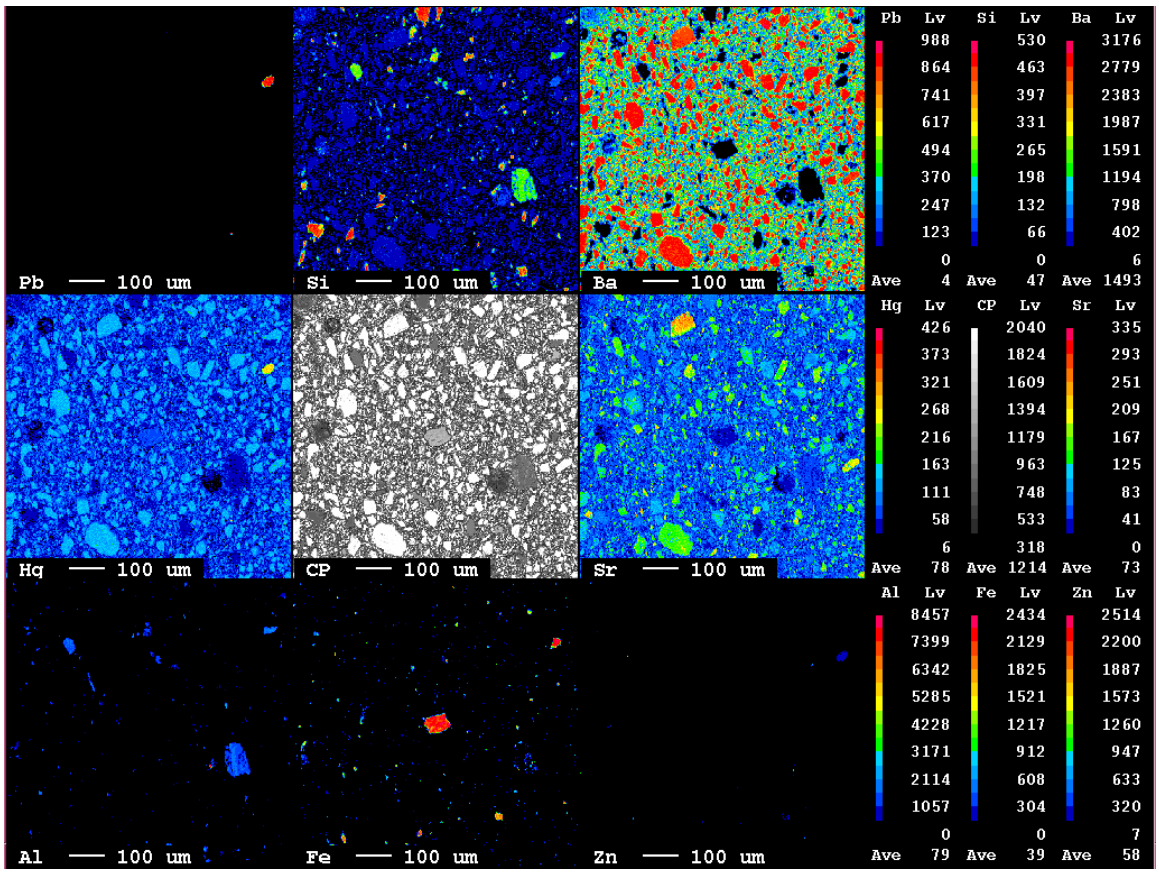

Figure C-1: Elemental Abundance maps for Sample MI-HIGH.

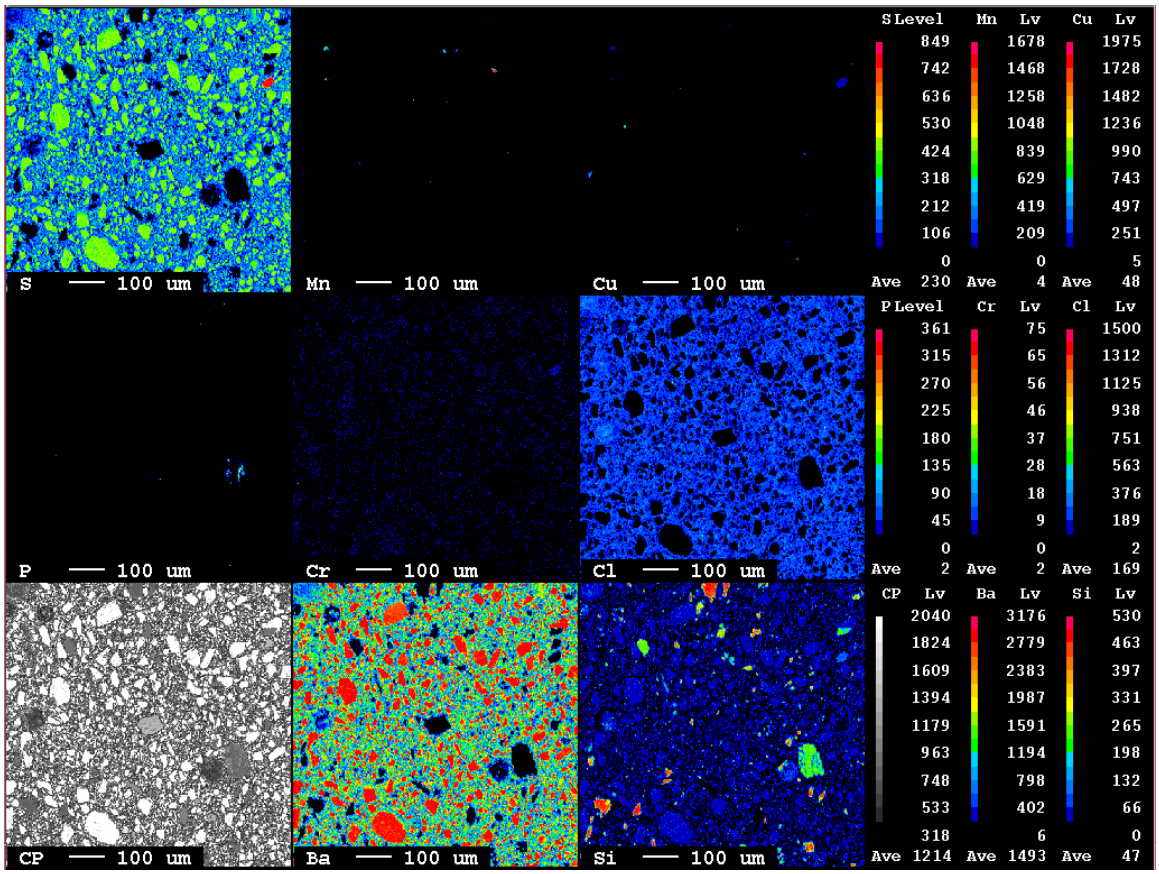

Figure C-2: Elemental Abundance maps for Sample MI-HIGH.

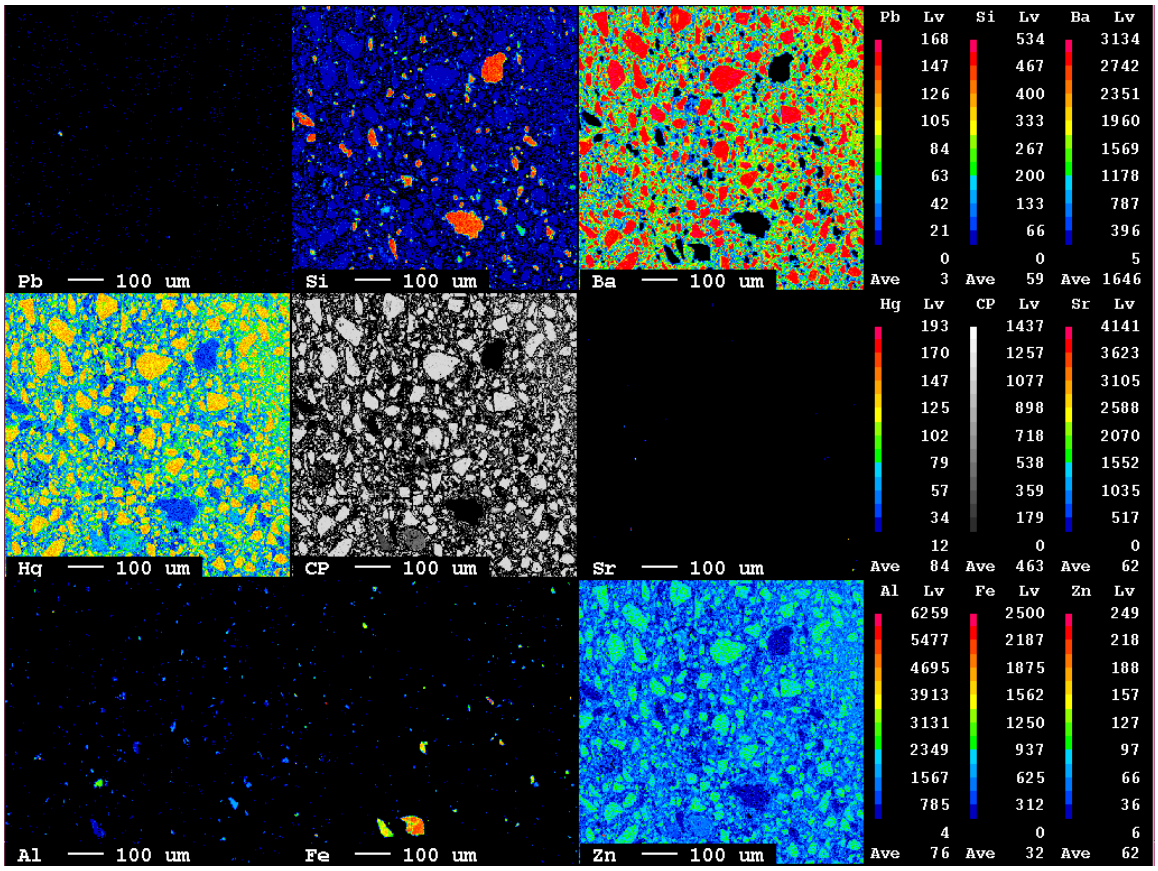

Figure C-3: Elemental Abundance maps for Sample MI-LOW.

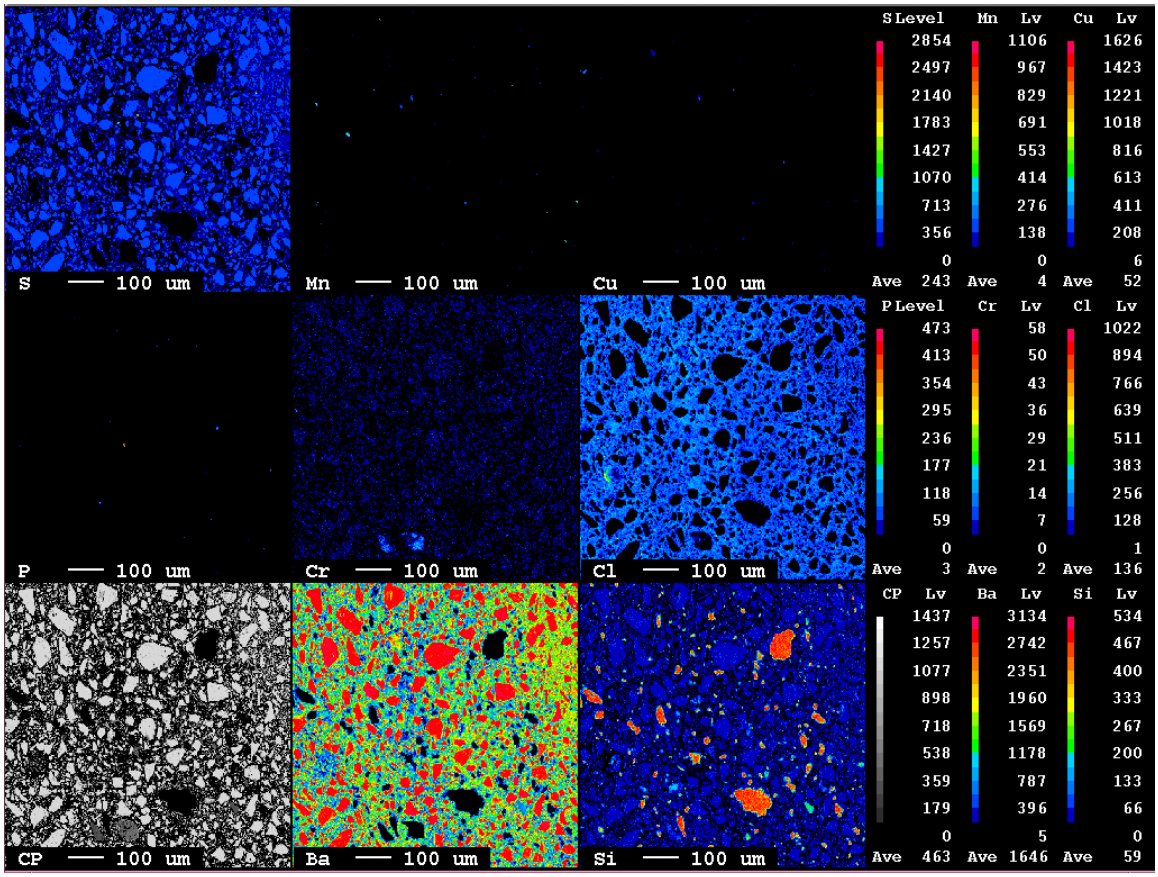

Figure C-4: Elemental Abundance maps for Sample MI-LOW.

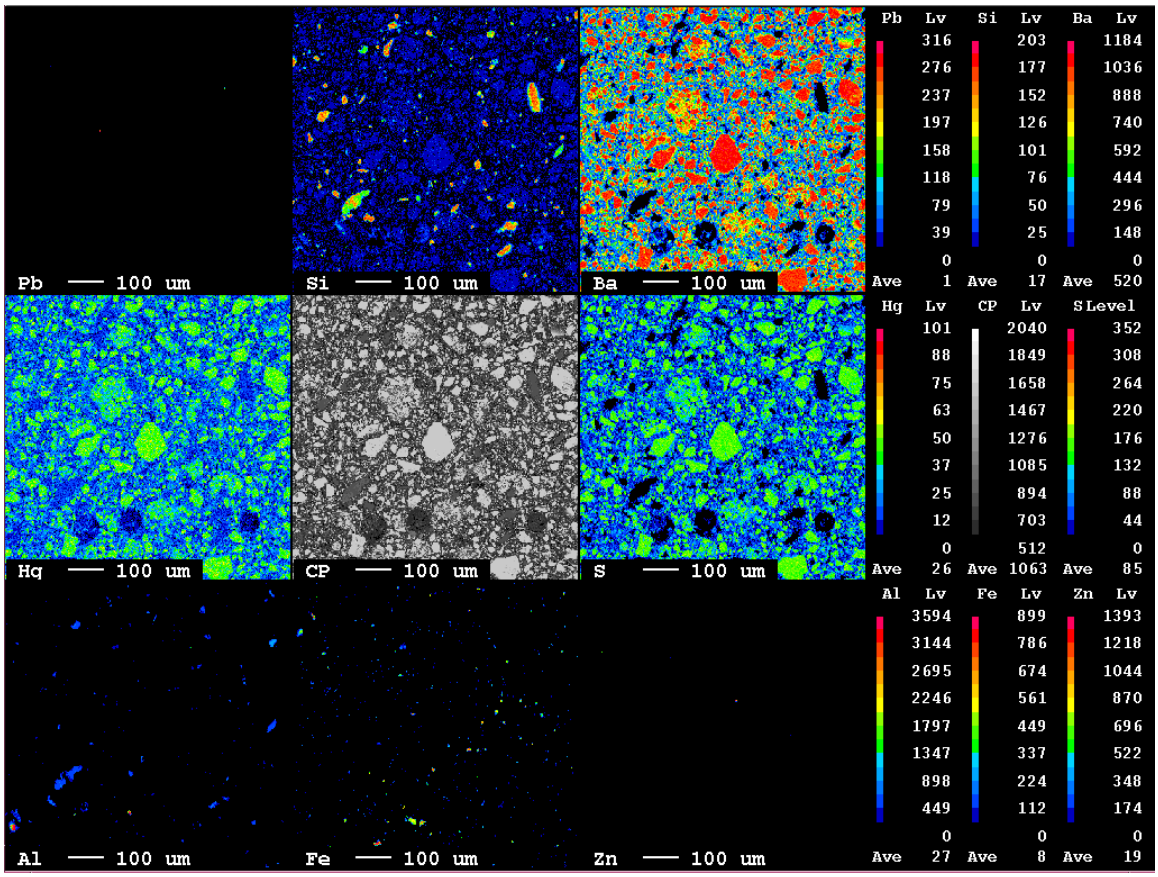

Figure C-5: Elemental Abundance maps for the acid-leached sample MI-HIGH: Sample AMIH.

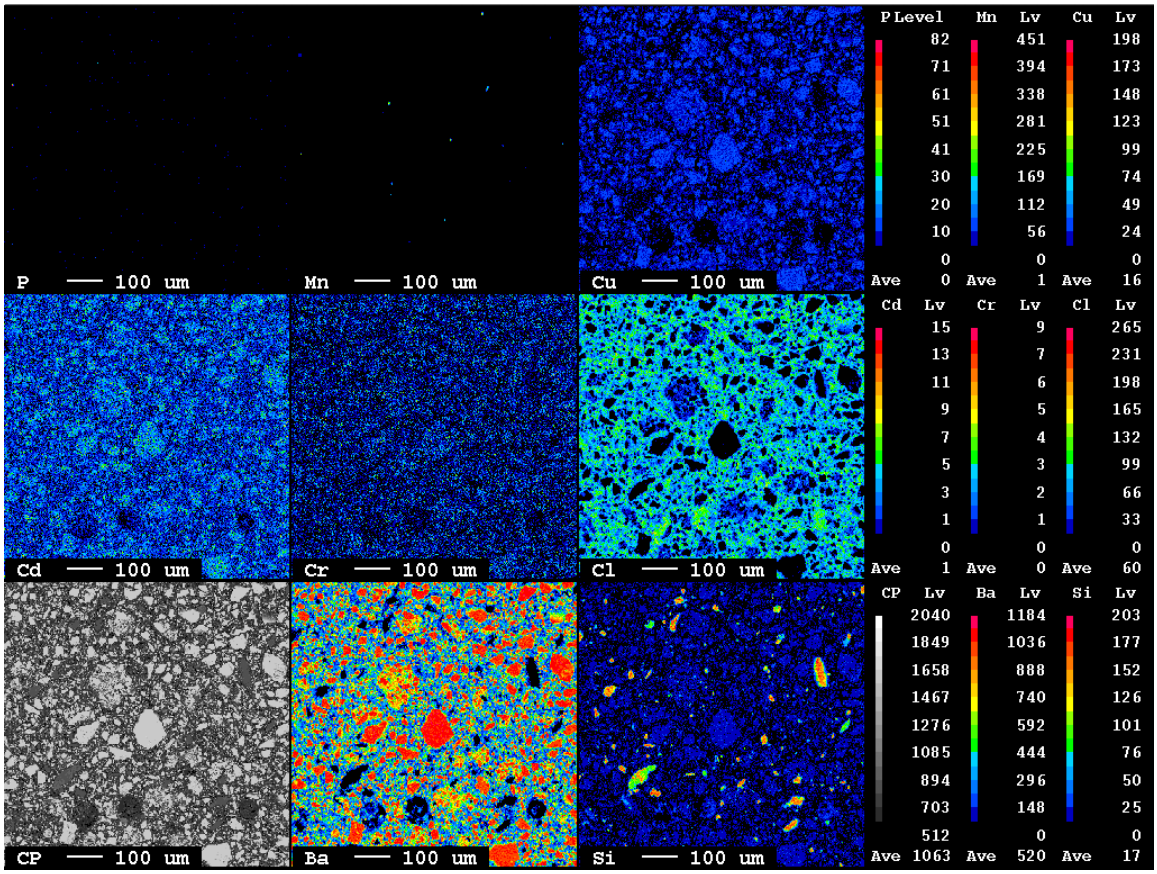

Figure C-6: Elemental Abundance maps for the acid-leached sample MI-HIGH: Sample AMIH.

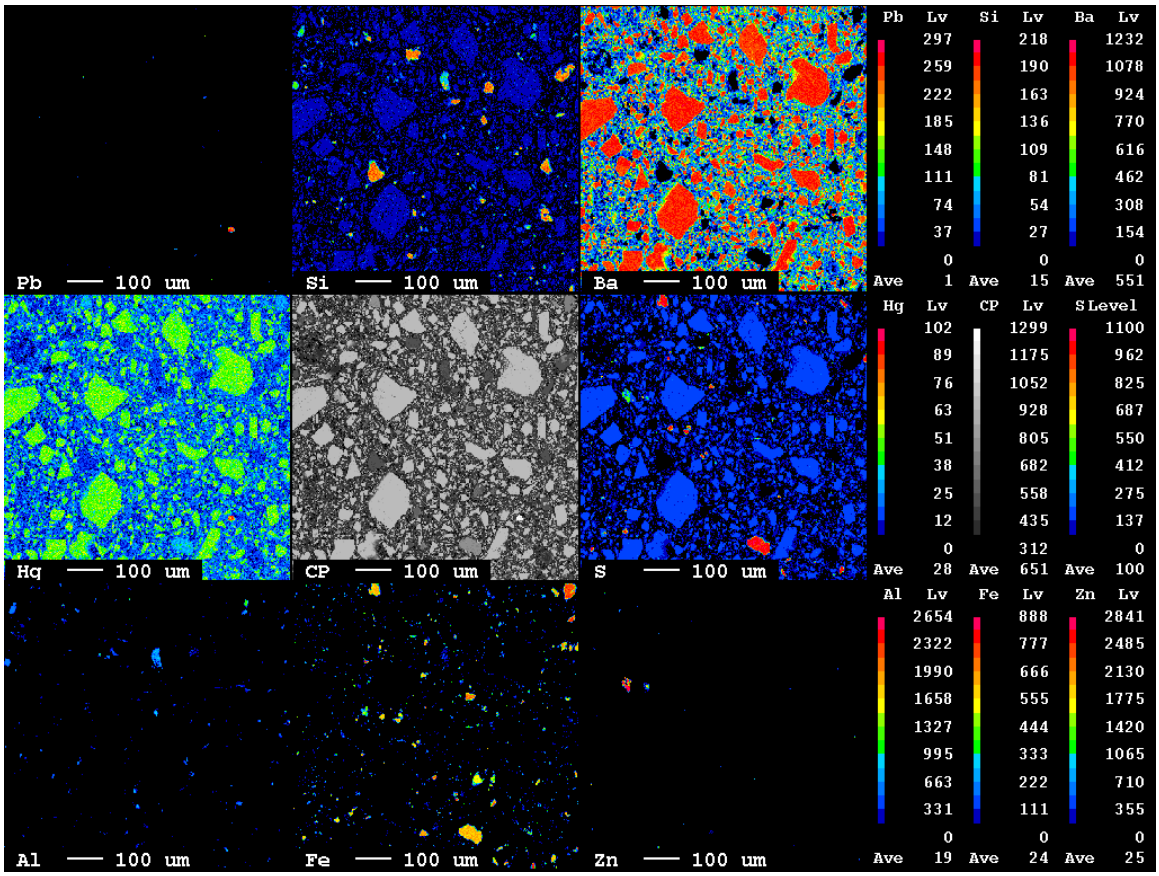

Figure C-7: Elemental Abundance maps for the acid-leached sample FIT-Blend: Sample AFIT.

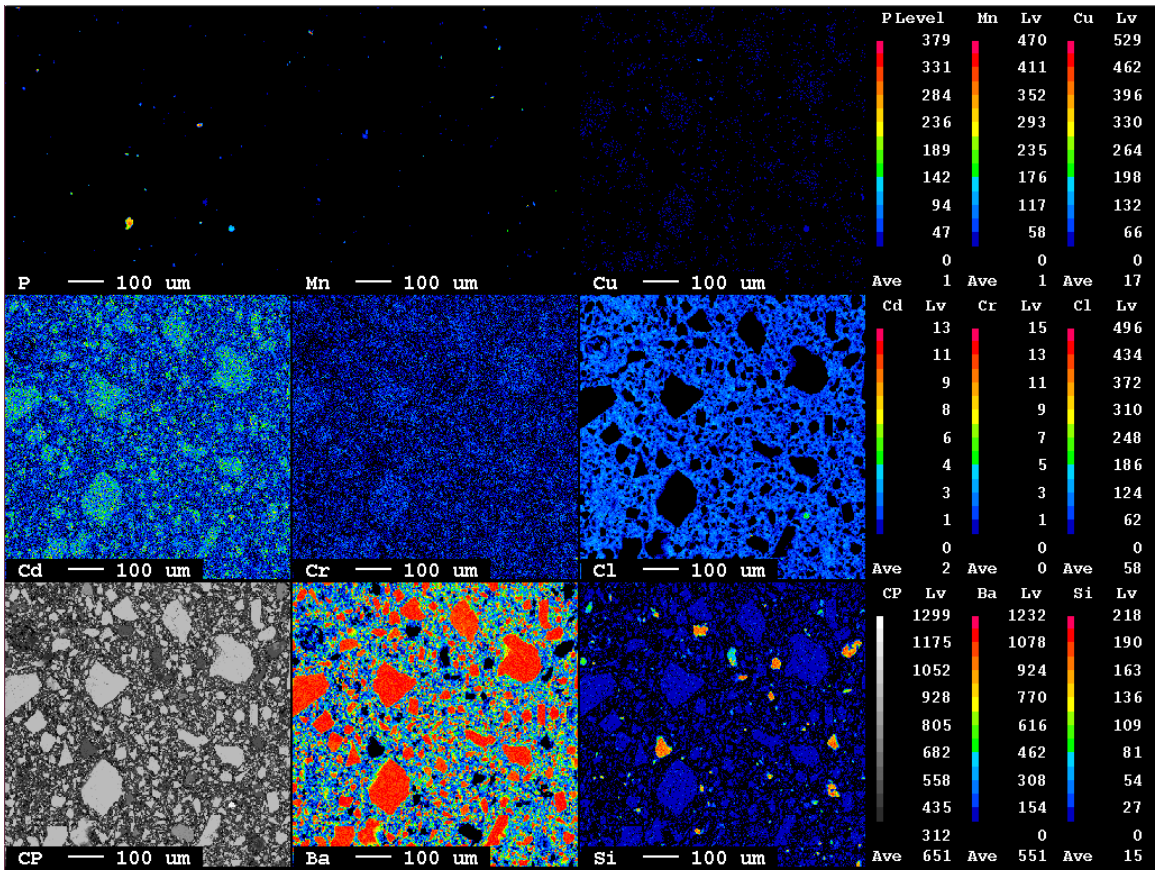

Figure C-8: Elemental Abundance maps for the acid-leached sample FIT-Blend: Sample AFIT.

APPENDIX D

BSE images of FIT-Blend overlain by XMP analysis elemental abundance maps

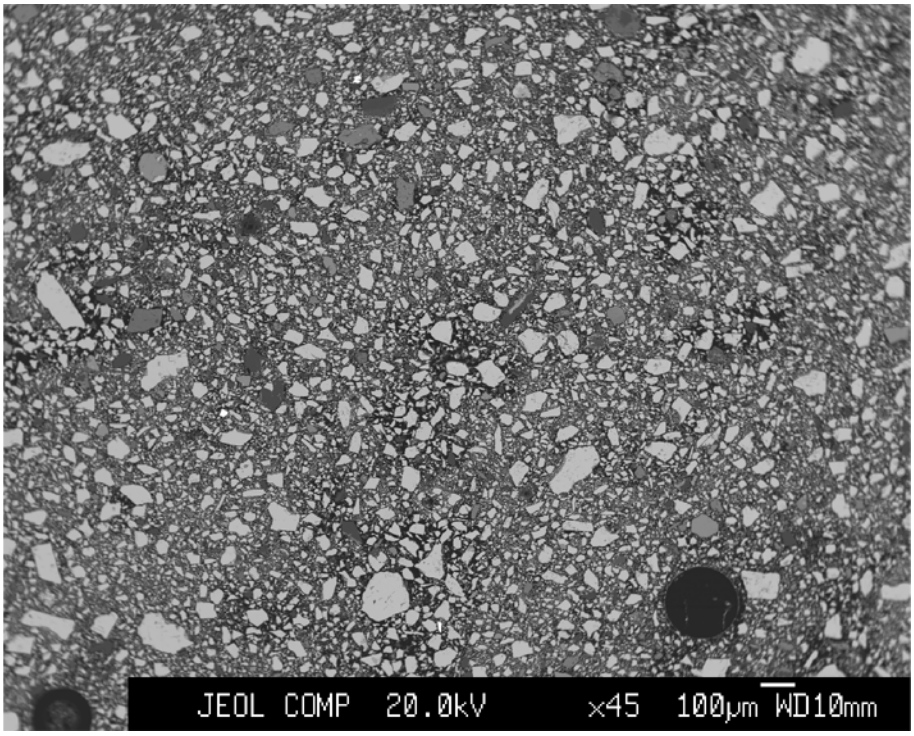

Figure D-1: BSE Image.

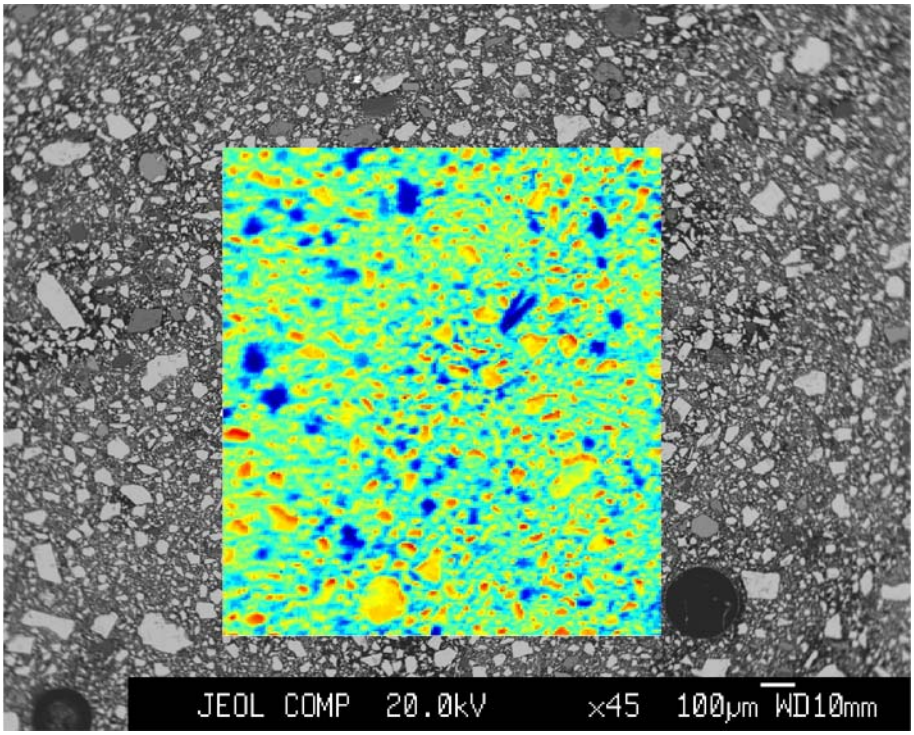

Figure D-2: Ba Overlay.

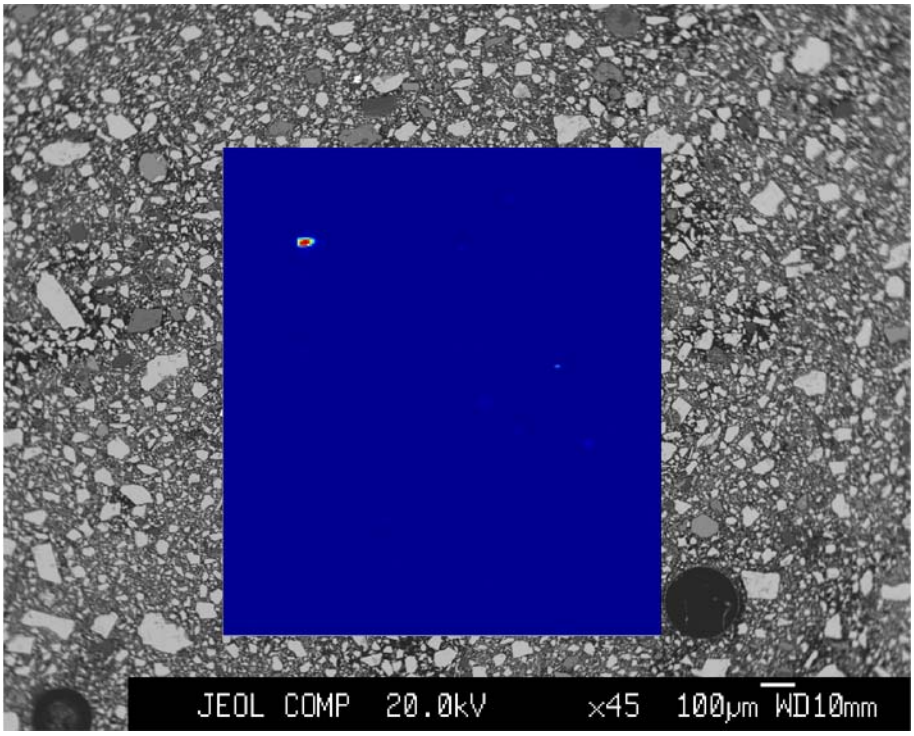

Figure D-3: Hg Overlay.

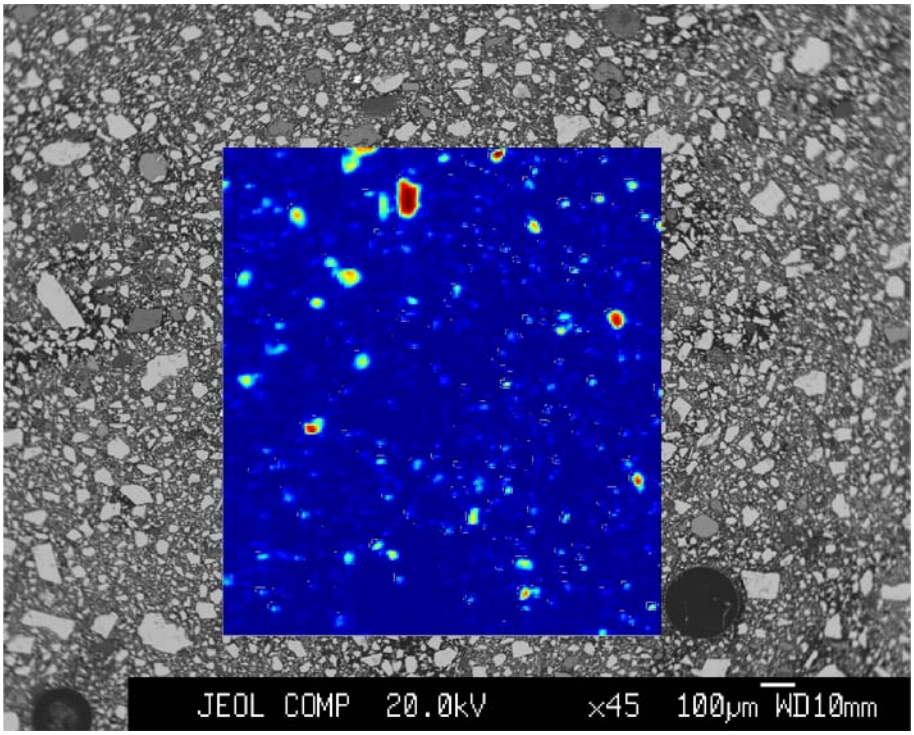

Figure D-4: Fe Overlay.

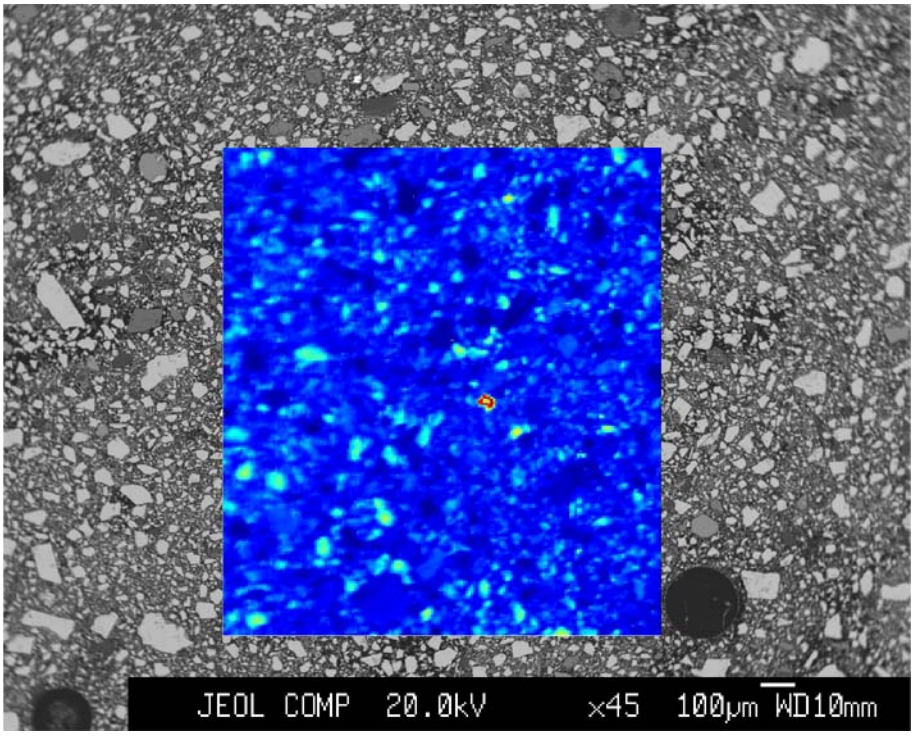

Figure D-5: Sr Overlay.

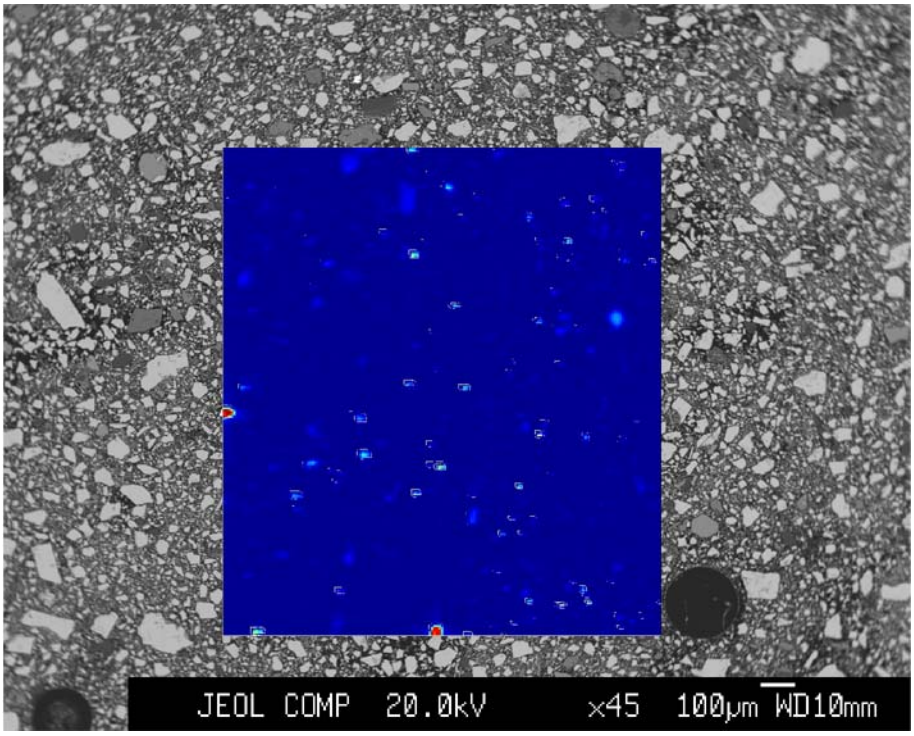

Figure D-6: Pb Overlay.

APPENDIX E

Location photo of QGZ-1 and XMP analysis elemental abundance maps for MI-High barite

QGZ1 (MI-HIGH):
Origin (0,0)

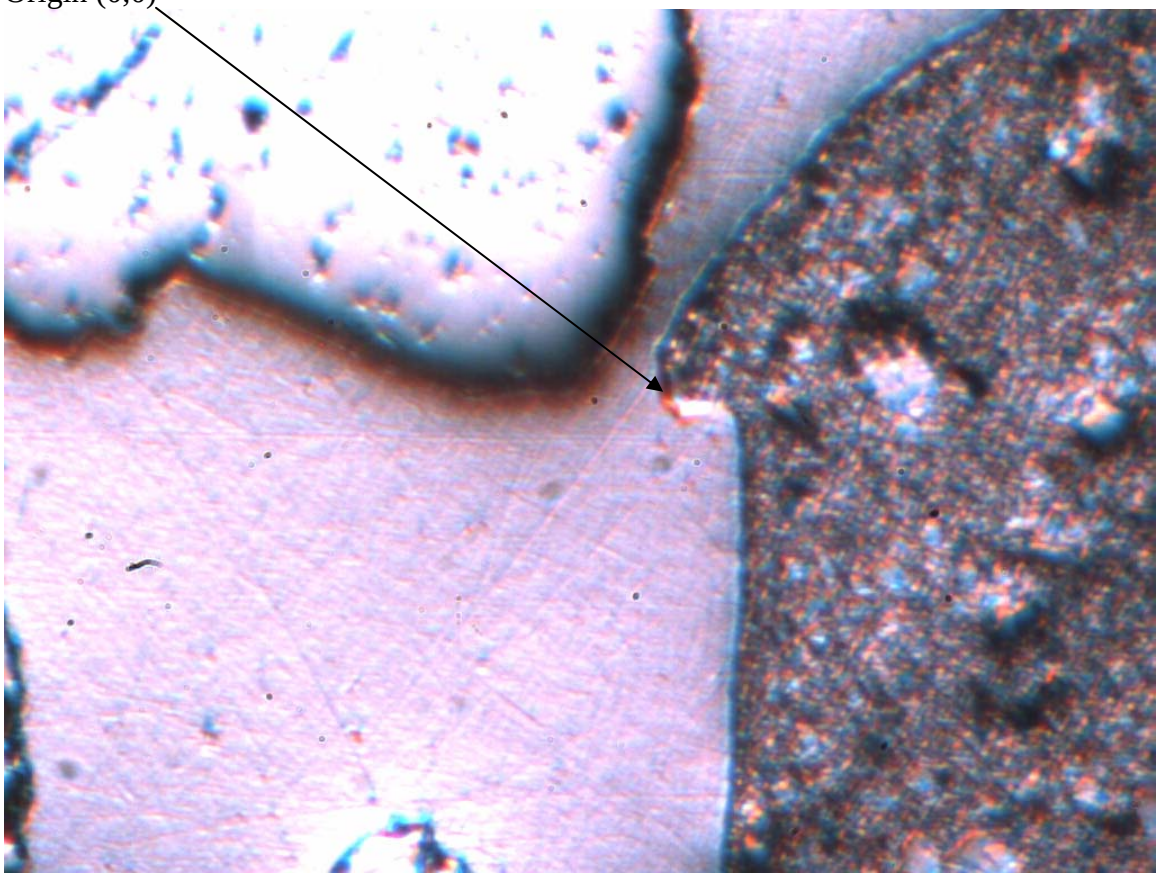

Figure E-1: XMP Abundance Maps with Location Photos for QGZ1.

Analyst's Notes:
There was strong overlap of Cr and Ba. Basically the Cr could not be imaged except at very strong hotspots. There was As in the glass substrate.

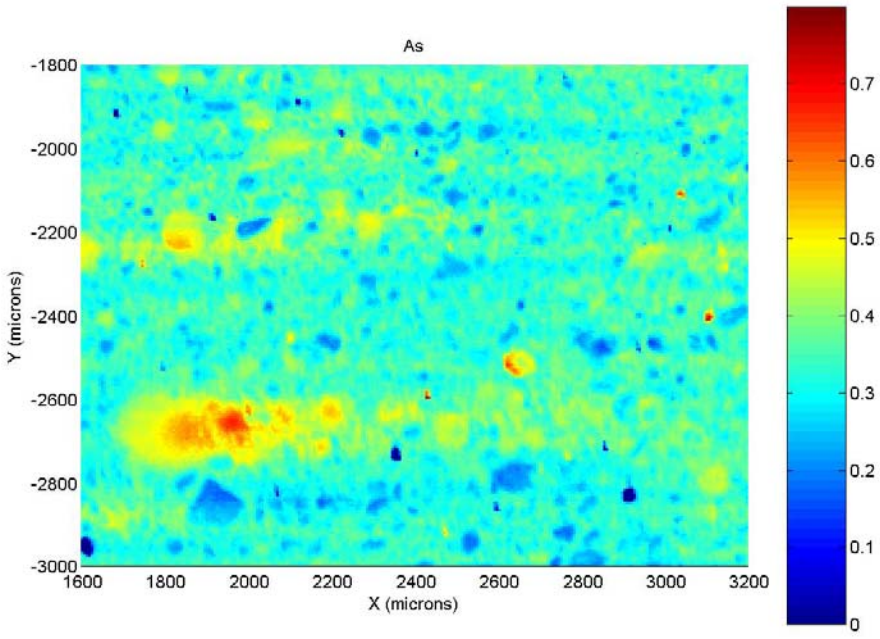

Figures E-2: XMP analysis elemental abundance map of As.

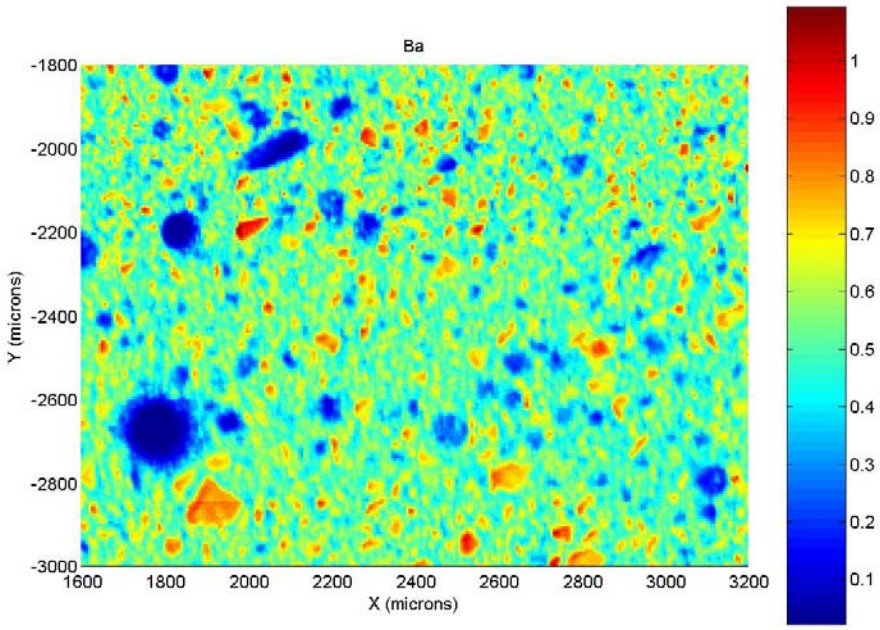

Figures E-3: XMP analysis elemental abundance map of Ba.

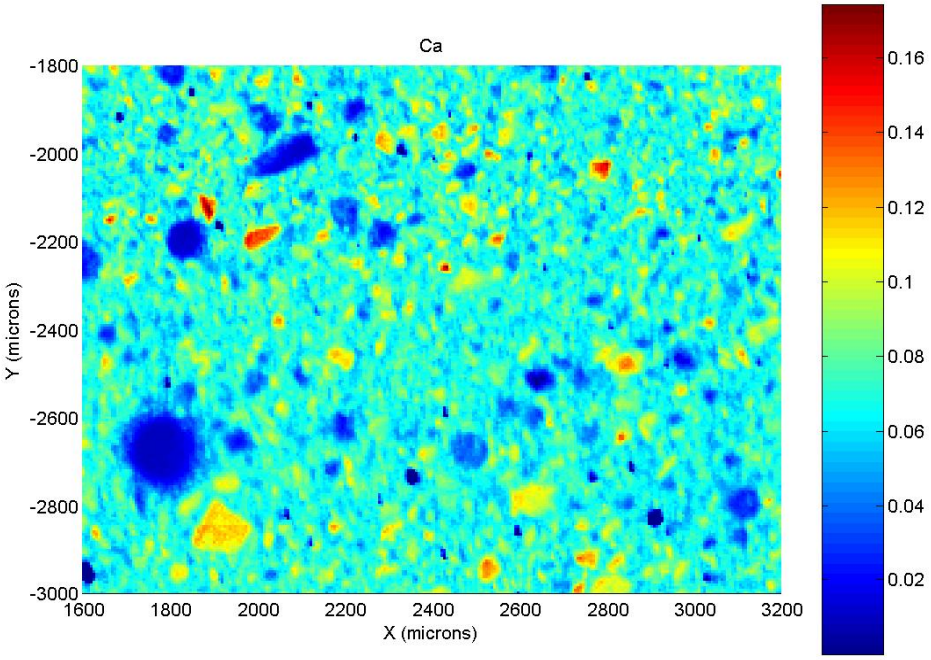

Figures E-4: XMP analysis elemental abundance map of Ca.

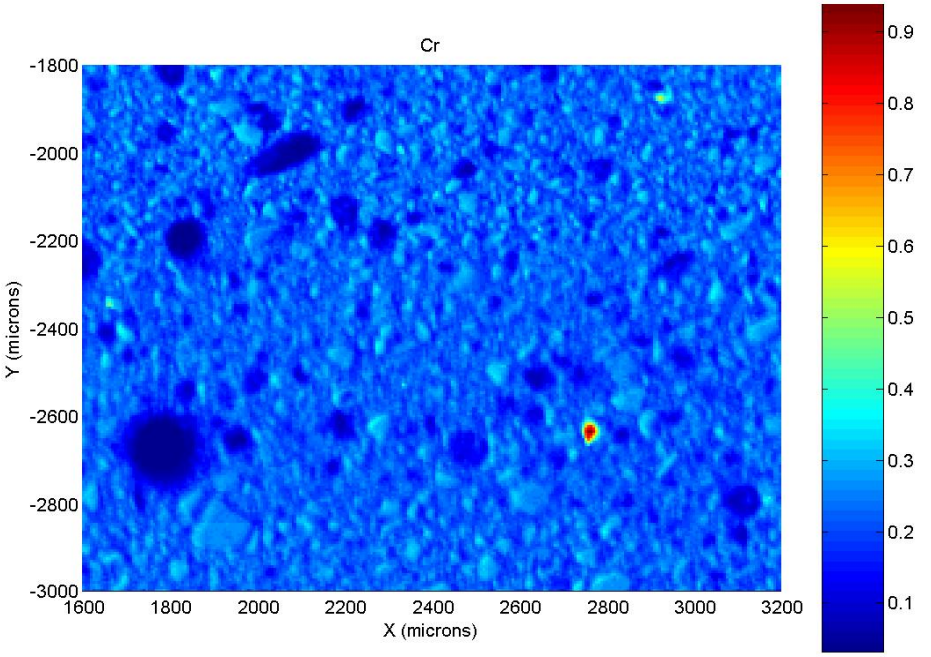

Figures E-5: XMP analysis elemental abundance map of Cr.

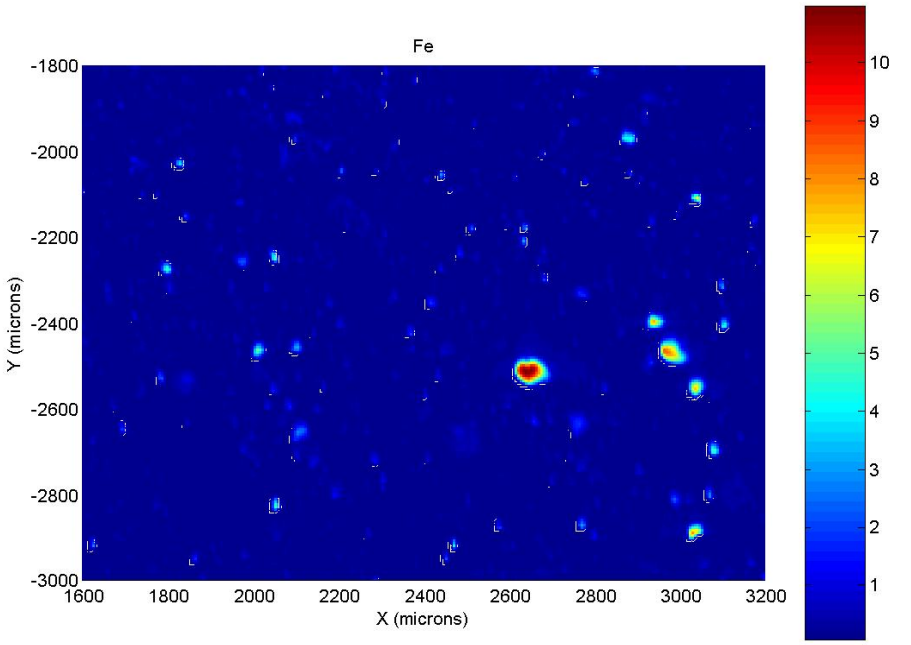

Figures E-6: XMP analysis elemental abundance map of Fe.

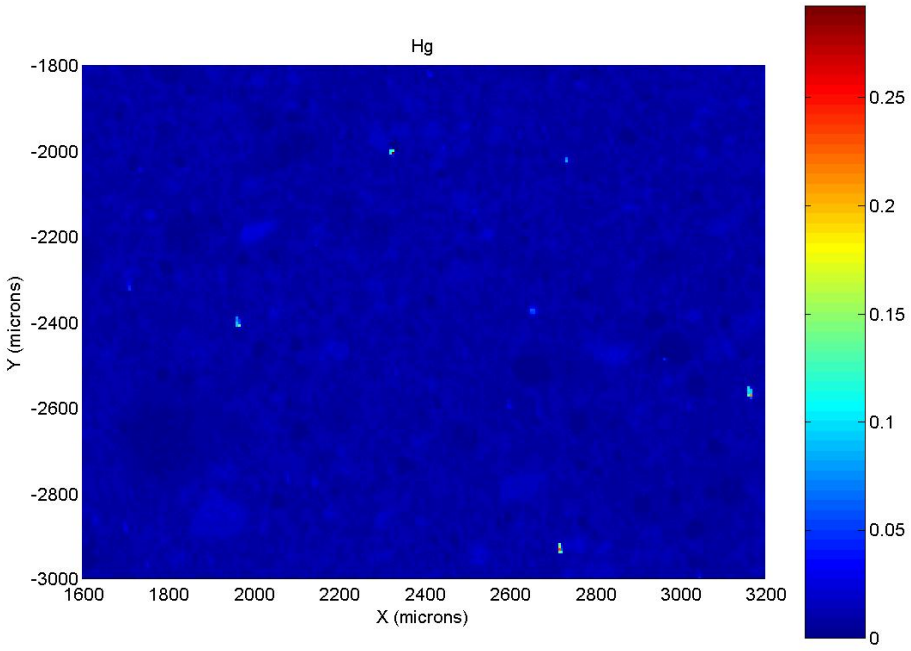

Figures E-7: XMP analysis elemental abundance map of Hg.

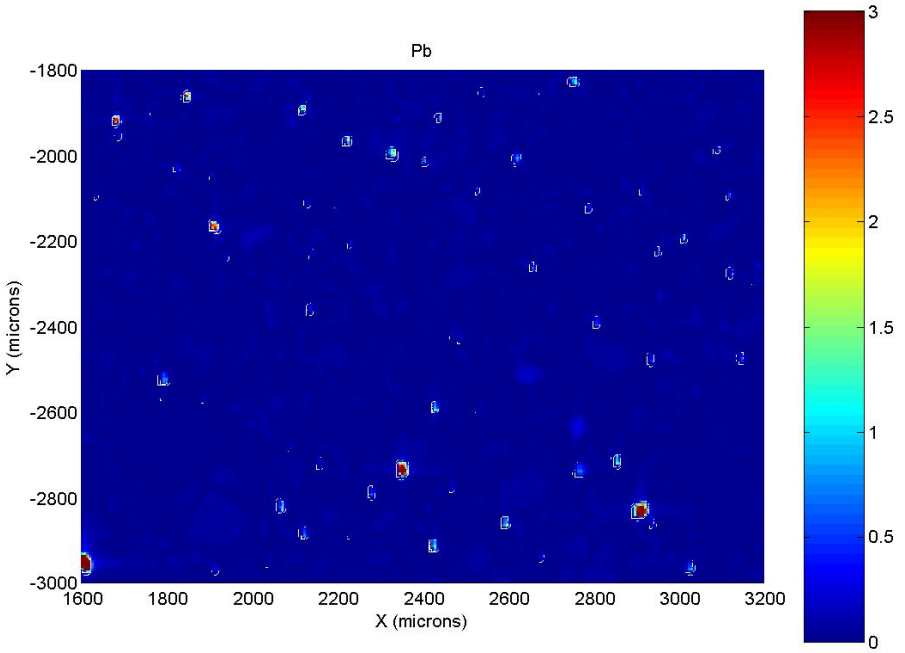

Figures E-8: XMP analysis elemental abundance map of Pb.

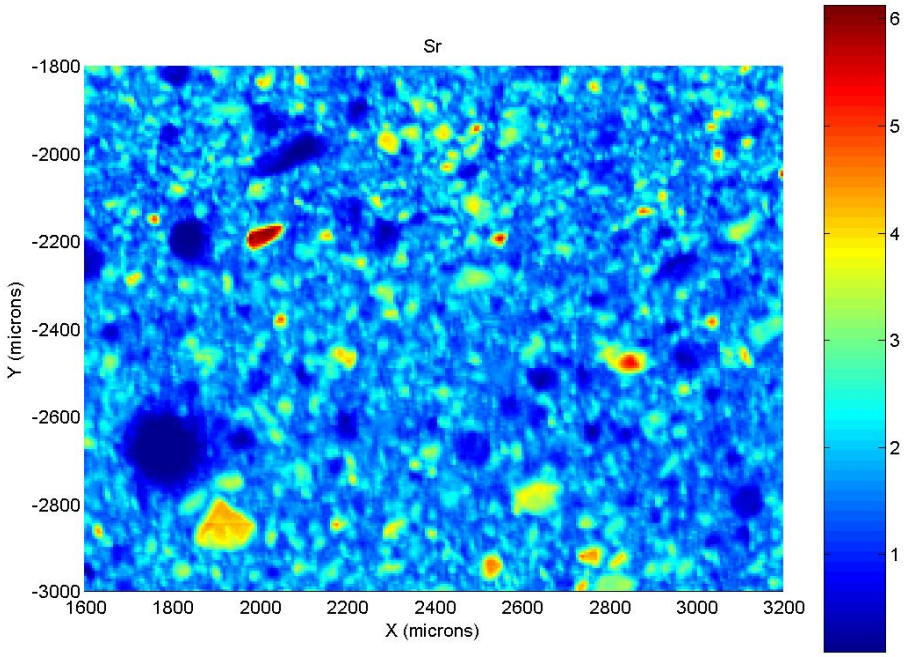

Figures E-9: XMP analysis elemental abundance map of Sr.

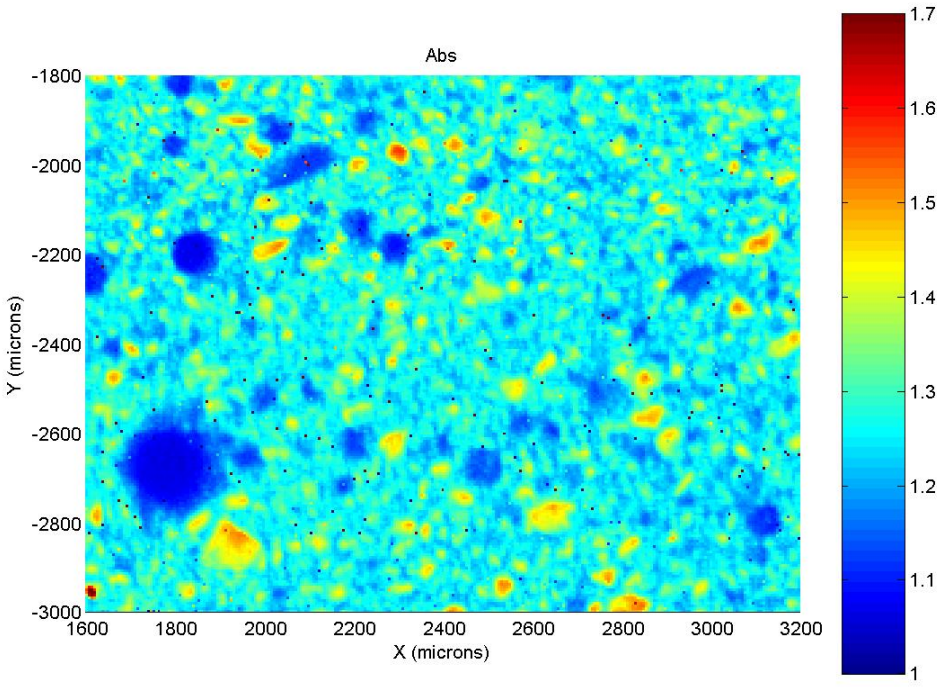

Figures E-10: XMP analysis elemental abundance map of background absorbance.

APPENDIX F

Location photos of QGZ-3 and XMP analysis elemental abundance maps for FIT-Blend barite.

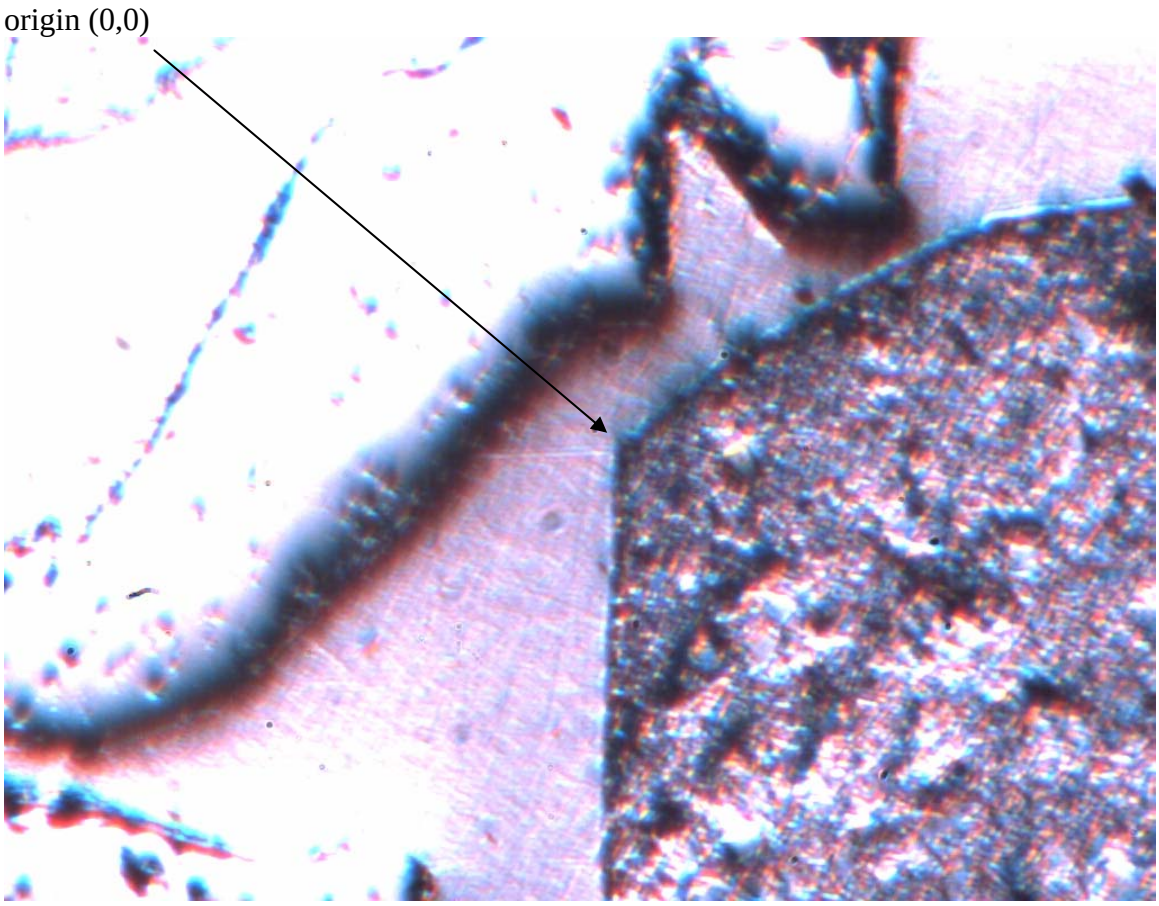

Figure F-1: Location photo of position QGZ-3 for thin section of sample FIT-Blend barite.

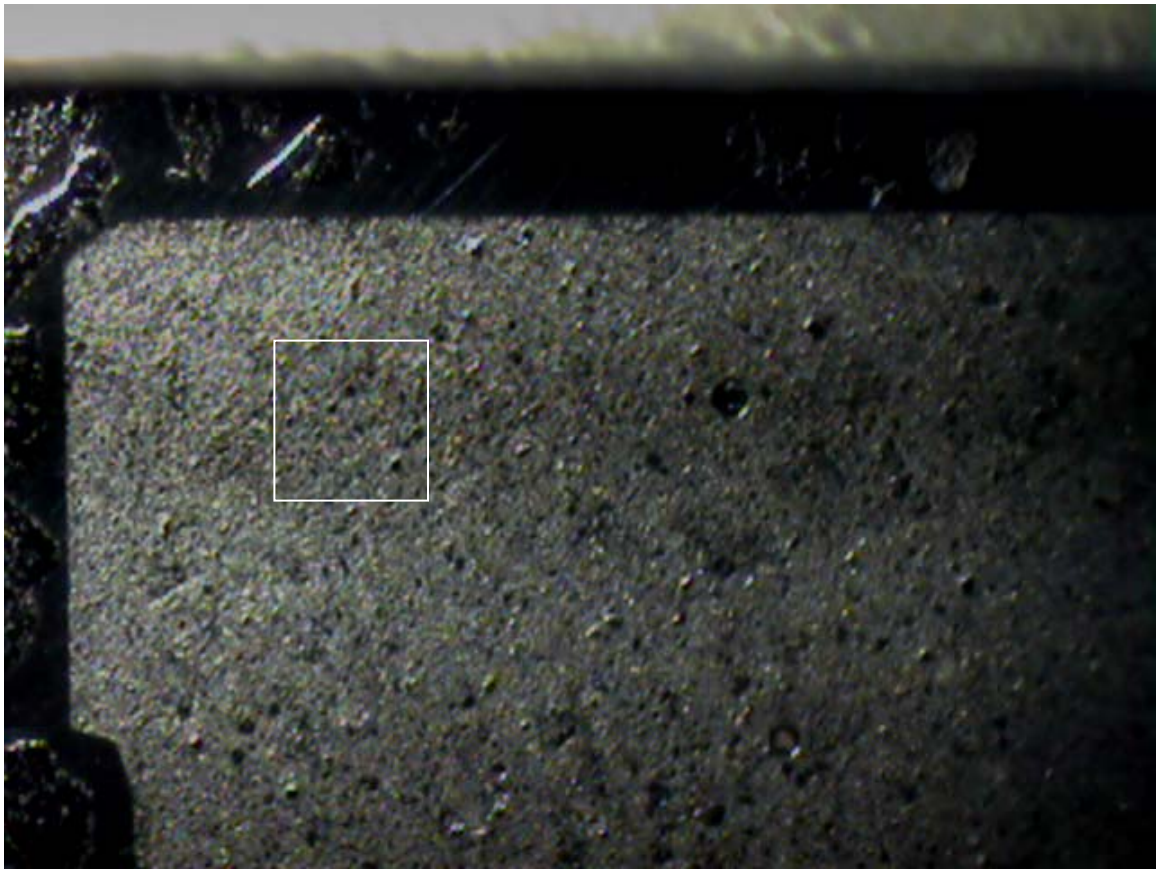

Figure F-2: Approximate scan area.

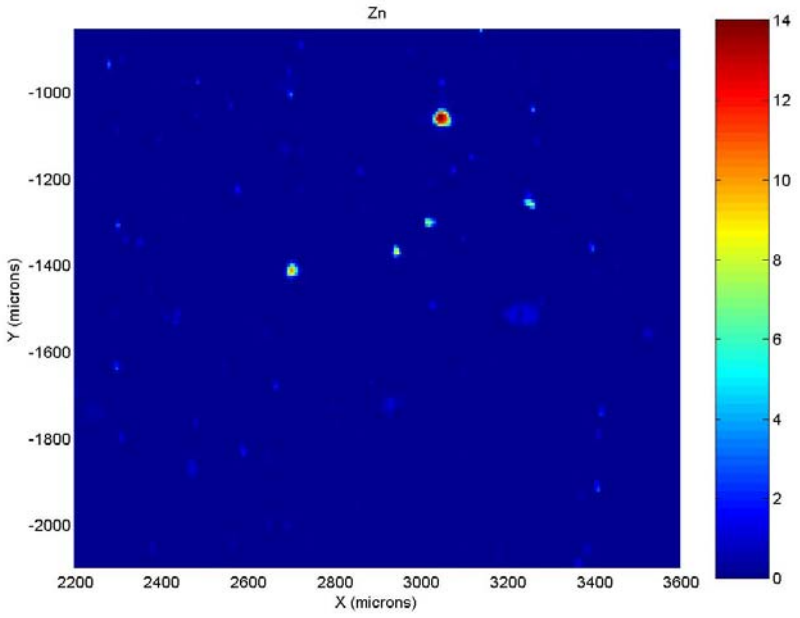

Figures F-3: Elemental abundance map for Zn in FIT-Blend.

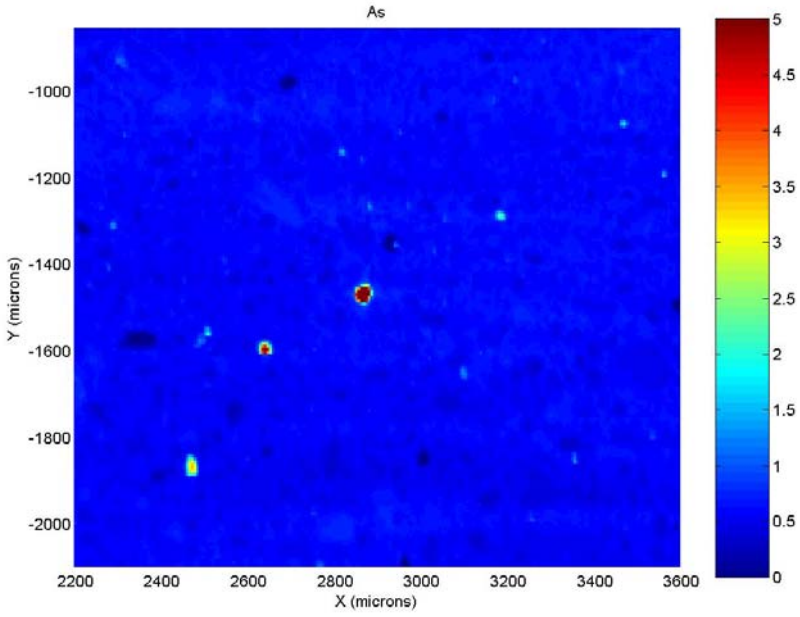

Figures F-4: Elemental abundance map for As in FIT-Blend.

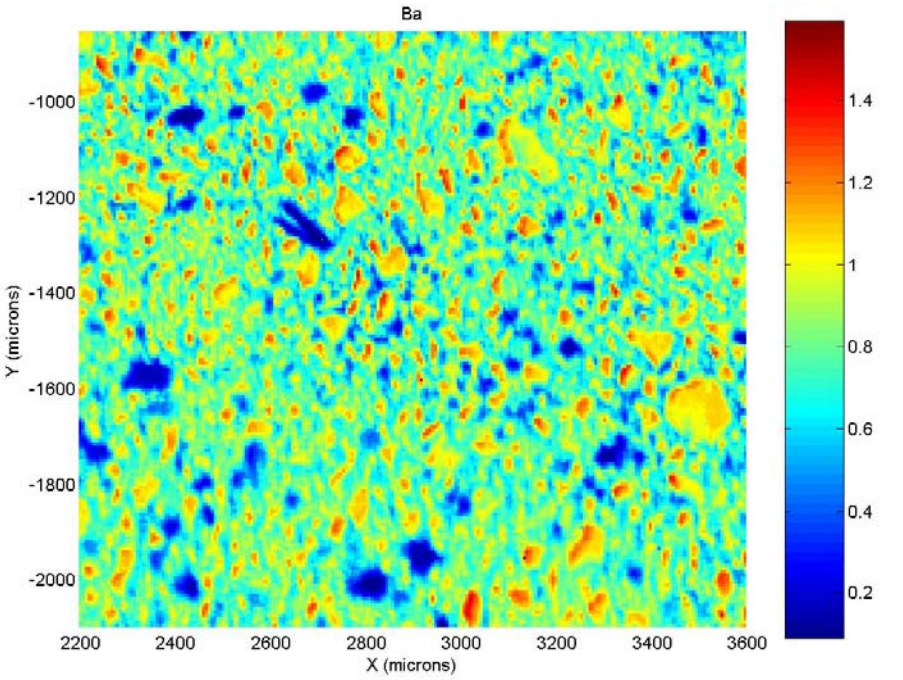

Figures F-5: Elemental abundance map for Ba in FIT-Blend.

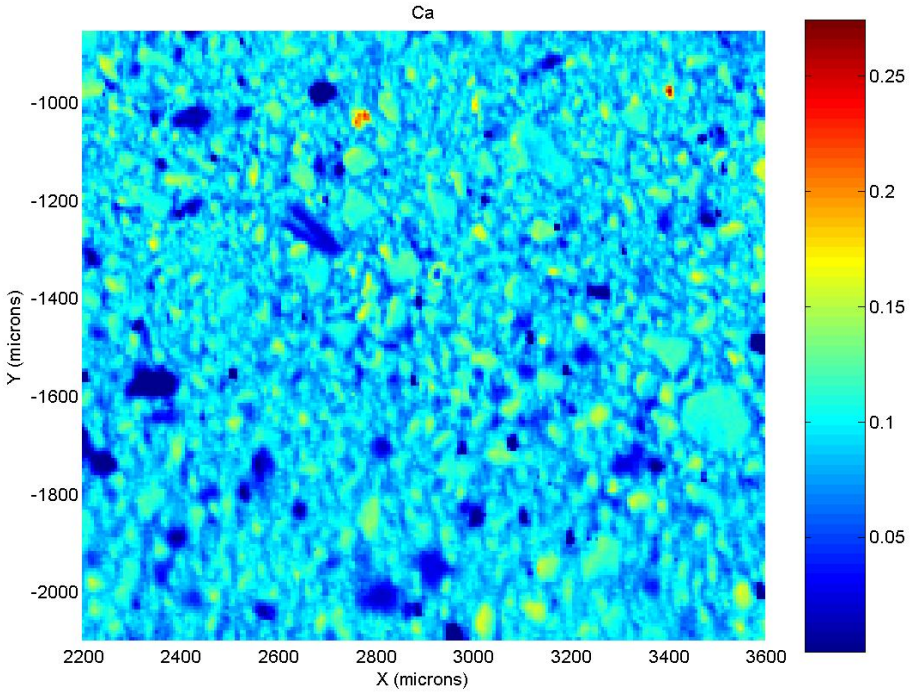

Figures F-6: Elemental abundance map for Ca in FIT-Blend.

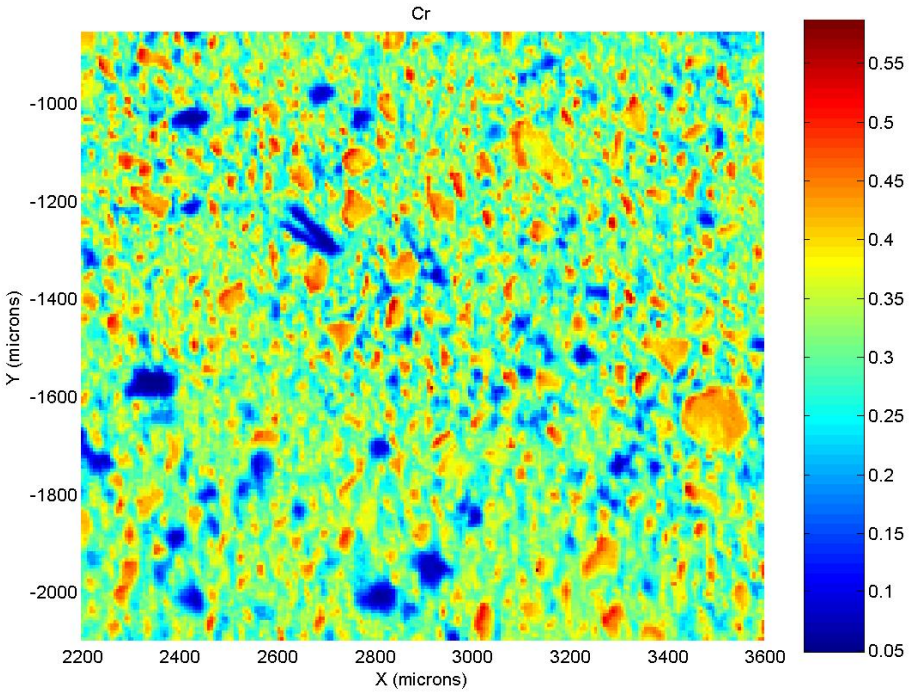

Figures F-7: Elemental abundance map for Cr in FIT-Blend.

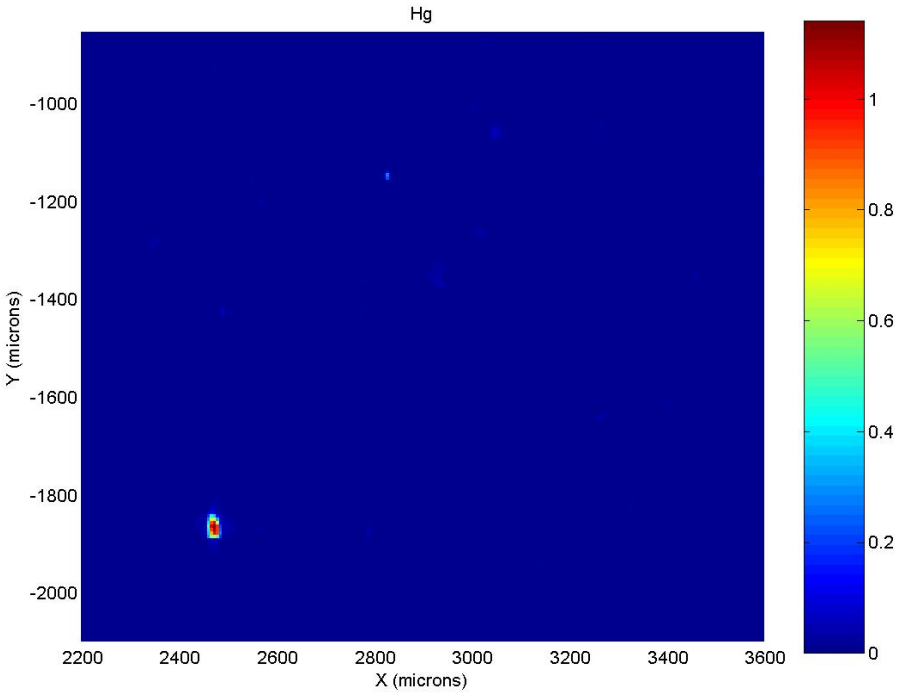

Figures F-8: Elemental abundance map for Hg in FIT-Blend.

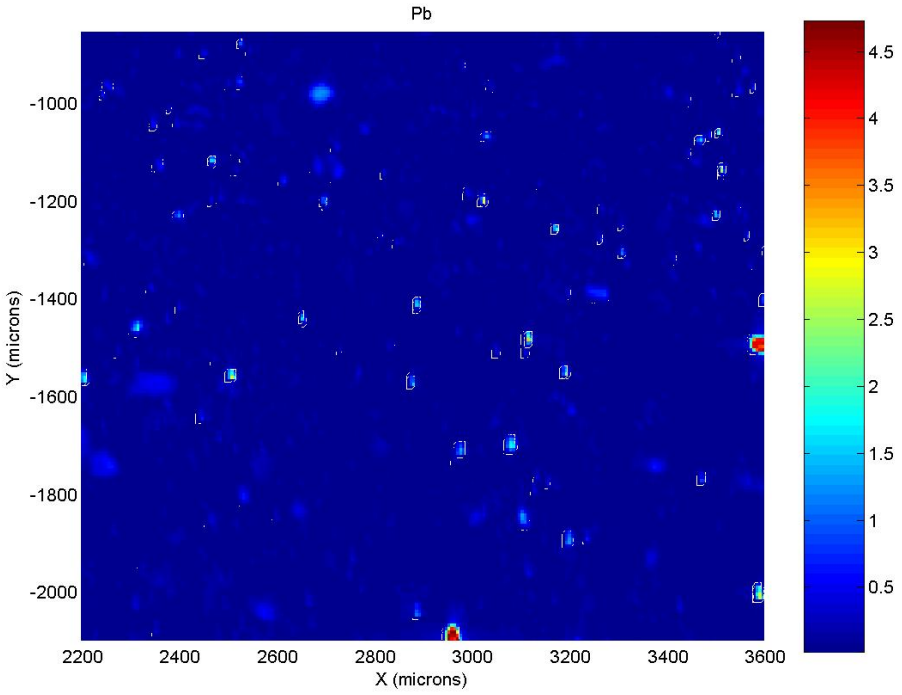

Figures F-9: Elemental abundance map for Pb in FIT-Blend.

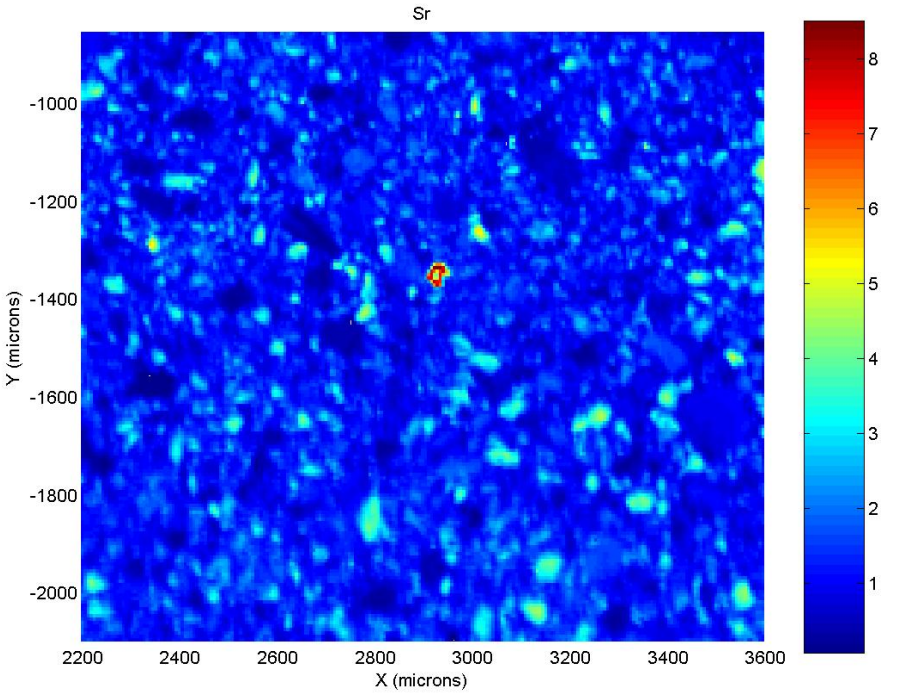

Figures F-10: Elemental abundance map for Sr in FIT-Blend.

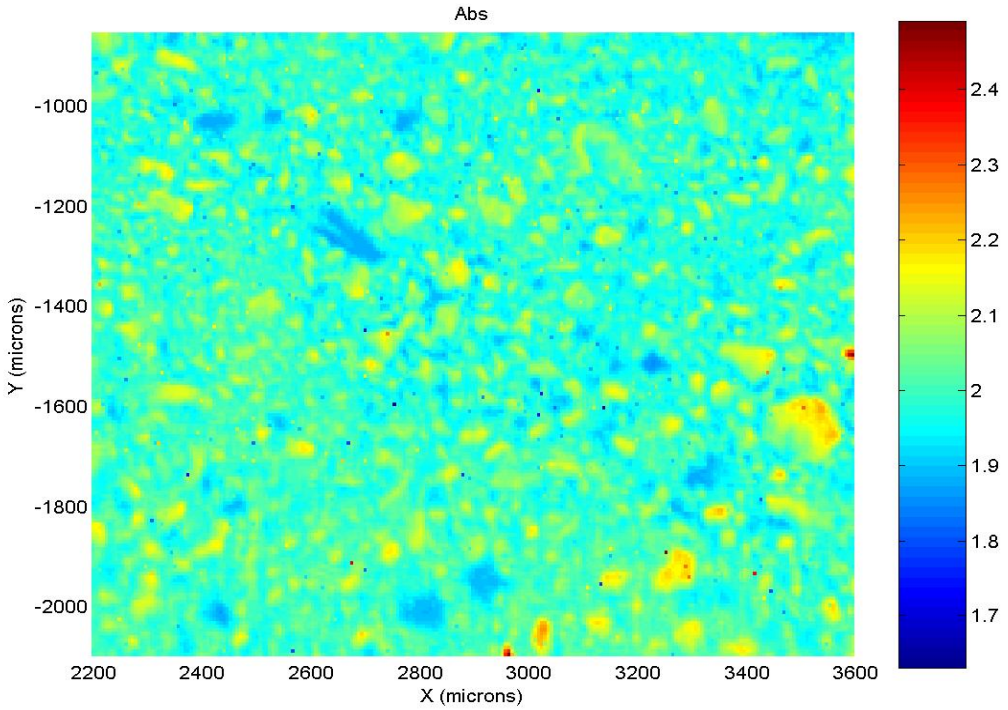

Figures F-11: Elemental abundance map for background absorbance in FIT-Blend.

The Department of the Interior Mission

As the Nation's principal conservation agency, the Department of the Interior has responsibility for most of our nationally owned public lands and natural resources. This includes fostering sound use of our land and water resources; protecting our fish, wildlife, and biological diversity; preserving the environmental and cultural values of our national parks and historical places; and providing for the enjoyment of life through outdoor recreation. The Department assesses our energy and mineral resources and works to ensure that their development is in the best interests of all our people by encouraging stewardship and citizen participation in their care. The Department also has a major responsibility for American Indian reservation communities and for people who live in island territories under U.S. administration.

The Minerals Management Service Mission

As a bureau of the Department of the Interior, the Minerals Management Service's (MMS) primary responsibilities are to manage the mineral resources located on the Nation's Outer Continental Shelf (OCS), collect revenue from the Federal OCS and onshore Federal and Indian lands, and distribute those revenues.

Moreover, in working to meet its responsibilities, the **Offshore Minerals Management Program** administers the OCS competitive leasing program and oversees the safe and environmentally sound exploration and production of our Nation's offshore natural gas, oil and other mineral resources. The MMS **Minerals Revenue Management** meets its responsibilities by ensuring the efficient, timely and accurate collection and disbursement of revenue from mineral leasing and production due to Indian tribes and allottees, States and the U.S. Treasury.

The MMS strives to fulfill its responsibilities through the general guiding principles of: (1) being responsive to the public's concerns and interests by maintaining a dialogue with all potentially affected parties and (2) carrying out its programs with an emphasis on working to enhance the quality of life for all Americans by lending MMS assistance and expertise to economic development and environmental protection.